National Library of Canada
Canadian Theses Service
Ottawa, Canada
K1A 0N4

Bibliothèque nationale du Canada
Services des thèses canadiennes

CANADIAN THESES

THÈSES CANADIENNES

NOTICE

The quality of this microfiche is heavily dependent upon the quality of the original thesis submitted for microfilming. Every effort has been made to ensure the highest quality of reproduction possible.

If pages are missing, contact the university which granted the degree.

Some pages may have indistinct print especially if the original pages were typed with a poor typewriter ribbon or if the university sent us an inferior photocopy.

Previously copyrighted materials (journal articles, published tests, etc.) are not filmed.

Reproduction in full or in part of this film is governed by the Canadian Copyright Act, R.S.C. 1970, c. C-30.

AVIS

La qualité de cette microfiche dépend grandement de la qualité de la thèse soumise au microfilmage. Nous avons tout fait pour assurer une qualité supérieure de reproduction.

S'il manque des pages, veuillez communiquer avec l'université qui a conféré le grade.

La qualité d'impression de certaines pages peut laisser à désirer, surtout si les pages originales ont été dactylographiées à l'aide d'un ruban usé ou si l'université nous a fait parvenir une photocopie de qualité inférieure.

Les documents qui font déjà l'objet d'un droit d'auteur (articles de revue, examens publiés, etc.) ne sont pas microfilmés.

La reproduction, même partielle, de ce microfilm est soumise à la Loi canadienne sur le droit d'auteur, SRC 1970, c. C-30.

THIS DISSERTATION
HAS BEEN MICROFILMED
EXACTLY AS RECEIVED

LA THÈSE A ÉTÉ
MICROFILMÉE TELLE QUE
NOUS L'AVONS REÇUE

Canada

A New Three-Parameter Volume-Cubic Equation Of State

by

Jin-Min Yu

A thesis
presented to the University of Ottawa
in fulfillment of the
thesis requirement for the degree of
DOCTOR of PHILOSOPHY
in
Chemical Engineering

Ottawa, Ontario, 1985

© Jin-Min Yu, Ottawa, Canada, 1986.

Permission has been granted to the National Library of Canada to microfilm this thesis and to lend or sell copies of the film.

The author (copyright owner) has reserved other publication rights, and neither the thesis nor extensive extracts from it may be printed or otherwise reproduced without his/her written permission.

L'autorisation a été accordée à la Bibliothèque nationale du Canada de microfilmer cette thèse et de prêter ou de vendre des exemplaires du film.

L'auteur (titulaire du droit d'auteur) se réserve les autres droits de publication; ni la thèse ni de longs extraits de celle-ci ne doivent être imprimés ou autrement reproduits sans son autorisation écrite.

ISBN 0-315-30966-0

ACKNOWLEDGMENT

Many people made the completion of this thesis possible; I would like to thank specifically the following people:

First of all, Dr. Benjamin C.-Y. Lu, Professor of Chemical Engineering, whose counsel and advice guided me through all phases of this work. He provided invaluable moral assistance through difficult periods in my graduate career.

Dr. W.K. Chung whose advice on the computer programing helped overcome many computational difficulties.

Mr. Y. Adachi whose suggestions were helpful in the early part of this work.

Ms. Diane M. Hull who patiently read through the rough draft and provided helpful suggestions on the organization of this thesis.

Miss Michele Choulguine whose help in using IBM6670 laser printer for printing this manuscript.

Finally, my parents whose love and support have sustained me to take the final step of completing this work.

ABSTRACT

Fourteen well-known volume-cubic equations of state of the van der Waals type,

$$P = \frac{RT}{(v - b)} - \frac{a}{(v^2+ubv+wb^2)}$$

were evaluated by calculating eight physical properties of normal alkanes. A new design procedure based on deviation contours was developed to determine the roles of u and w in this equation. Based upon these results the relationship u-w=3 was proposed for the new equation as it provides a balanced representation of the volumetric properties of pure normal fluids while emphasizing state conditions of practical importance. Only the pure-component parameter a is treated as temperature dependent. The three parameters of the proposed equation were generalized in terms of the critical pressure and temperature and the acentric factor. The new equation of state was extended to mixtures using both random and local composition mixing rules for the parameters in the equation. Calculation of the vapor-liquid equilibria and volumetric properties of normal fluid mixtures and the vapor-liquid equilibria of complex mixtures indicated that the random mixing rules containing up to two adjustable empirical coefficients are the most suitable for the new equation.

Comparison of the new equation with the Soave-Redlich-Kwong, the Peng-Robinson and the Schmidt-Wenzel equations of state showed the new equation to have better overall performance for both pure and mixture volumetric calculations.

NOMENCLATURE

List of Symbols

$\underline{A}$	Helmholtz free energy
A	Molar Helmholtz free energy
A_0, A_1, A_2	Constants in Eq.(4.16)
C_0, C_1, C_2	Constants in Eq.(4.17)
D_0, D_1, D_2	Constants in Eq.(4.18)
E_{ji}	Boltzmann's factor
G	Gibbs free energy
N	Number of molecules
Na	Avogadro's number
ND	Number of data points
NS	Number of substances
P	Pressure
$\underline{P}$	Parachor
Q	Canonical partition function
R	Gas constant
V	Total volume
V_f	Free volume
T	Absolute temperature
Z	Compressibility factor
b	Co-volume of a mole of molecules
a, c, e, u, w	Equation of state parameters

$\hat{\phi}_i$	Fugacity coefficient of component i in the mixture
f	Fugacity
$\hat{f}_i$	Fugacity of component i in the mixture
$g(r)$	Radial distribution function
h	Planck's constant
k	Boltzmann's constant
k_{ij}	Binary interaction coefficient in the mixing rule
ℓ_{ij}	Binary interaction coefficient in the mixing rule
m	Mass of a molecule
n	Number of moles
$q_{r,v}$	Rotational and vibrational partition function
v	Molar volume
v_c	Experimental critical molar volume
v_c^*	Calculated critical molar volume
x	Liquid mole fraction
y	Vapor mole fraction
z	Mole fraction
z_{ji}	Local composition of molecules i around molecule j

Greek Symbols

α	Quantity represents the temperature dependence of parameter a
α_{ji}	Nonrandomness parameter
β	Quantity represents the temperature dependence of parameter b
β_c	Reduces quantity related to parameter b
β_c^*	Quantity β_c obtained from experimental values

ϕ	Fugacity coefficient
Φ	Potential energy of a pair of molecules
κ	Constant in Eq.(4.16)
Λ	DeBroglie wave length
ω	Acentric factor
Ω_{ac} Ω_{bc}	Dimensionless quantities in Eqs(2.32,33)
μ	Chemical potential or internal energy
γ	Constant in Eq.(4.16)
Γ	Pair potential function
σ	Diameter of hard-sphere molecule

Superscripts

E	Excess property
RES	Residual property
a	Property due to attractive force
hs	Hard sphere property
id	Ideal gas property
rep	Property due to repulsive force
sup	Property at supercritical temperature
∞	Property at infinite pressure
ℓ	Liquid property
v	Vapor property

Subscripts

c	Property at the critical point
i, j	Component index in the mixture
ij, ji	Pertaining to the binary pair of molecules i and j

m	Mixture property
r	Reduced property
tri	Property at the triple point

TABLE OF CONTENTS

FIGURES

TABLES

Chapter I

INTRODUCTION

Reliable methods for predicting physical properties of pure substances and their mixtures (such as single and two-phase properties and vapor-liquid equilibria) are frequently required in process design and material handling. In view of the wide range of conditions found in practical applications, the required data may not always be available, and hence considerable attention has been paid to the development of these methods. In particular, a number of equations of state (EOS) have been proposed to meet this demand.

Among the many types of equations of state the extended virial equations and the volume-cubic equations are the most frequently used for vapor-liquid equilibrium (VLE) and volumetric calculations of pure fluids and their mixtures. These equations are usually expressed in pressure-explicit form,

$$P = f(V,T) \qquad (1.1)$$

where P, V and T are the pressure, volume and temperature, respectively. Generally, these equations are developed based on pure fluid properties and application to mixture calculations requires proper mixing rules which relate the mixture parameters to the pure-component parameters and mixture composition.

The extended virial equations, such as the modified Benedict-Webb-Rubin (BWR) equation by Lee and Kesler [66], are in general quite complex in structure, and contain at least eight parameters. These parameters must be determined through the multiproperty regression method [67]. Such an approach is quite time consuming, and does not always guarantee success. Usually, values of the parameters are only available for limited number of substances and cannot be accurately generalized. Moreover, when solved with respect to volume, the solution can only be obtained by use of a trial-and-error procedure. During the iteration roots are chosen ambiguously which not only requires longer computation time, especially for multicomponent calculations [16], but also can easily give rise to convergence problems [124] in the critical region. Although these equations have proven to be more accurate for calculating volumetric properties of pure fluids and their mixtures, they require a mixing rule for each parameter which makes their application to mixture calculations tedious. For routine calculations, these shortcomings are highly undesirable.

However, a volume-cubic equation can be solved with respect to volume by a straightforward analytical method [28] which is fast and accurate. The parameters are easily attainable, and application to mixtures is much simpler as it requires fewer mixing rules. Also, because the root solving procedure is simpler, computational problems in the mixture critical point region can be easily avoided with the help of a carefully designed algorithm [10,51,75]. However, the volume-cubic equations have their shortcomings. They are fundamentally inadequate for calculating volumes in the vicinity of the critical point [116]. For-

tunately, in order to maintain flow stability process designers generally avoid such conditions [49,58]. In the compromise between simplicity, generality and accuracy volume-cubic equations are preferred over complex multi-parameter equations for routine VLE and volumetric calculations.

The oldest, simplest and best known volume-cubic equation is the one proposed by van der Waals (VDW) in 1873 [133]

$$P = \frac{RT}{(v - b)} - \frac{a}{v^2} \qquad (1.2)$$

in which R is the gas constant and v is the molar volume. The first term on the right hand side of the equation accounts for the molecular repulsive interaction while the second term accounts for the molecular attraction. The parameters a and b are characteristic of the fluid. Despite the simplicity of the VDW EOS, the equation can give qualitative representation of the PVT behavior of real fluids. As a result, much effort has been made to improve the accuracy of this equation. A generic expression of the currently popular volume-cubic equations of state may be represented in the form of an extended vān der Waals equation,

$$P = \frac{RT}{(v - b)} - \frac{a}{v^2 + ubv + wb^2} \qquad (1.3)$$

The quadratic expression in volume ($v^2 + ubv + wb^2$) replaces v^2 in the denominator of the attractive term of the original VDW equation. Some general features of Eq.(1.3) are discussed by Abbott [1-3].

When the parameters u and w are assigned particular values, Eq.(1.3) reduces to the original VDW equation (u=0,w=0), the Redlich-

Kwong (RK) equation (u=1,w=0) [103] and its various modifications, the Peng-Robinson (PR) equation (u=2,w=-1) [88], the Schmidt-Wenzel (SW) equation (u+w=1) [112], the Harmens-Knapp equation (HK) (u+w=1) [49] and a number of other equations.

The success of the currently popular volume-cubic EOS is due to their ability to represent VLE values (P-T-composition). These equations include the PR and the Soave [119] modified Redlich-Kwong (SRK) equations which have attained wide popularity in the natural gas and petroleum industries.

There is evidence in the literature [5,27,68] that volume-cubic EOS containing two to four parameters can give virtually identical VLE values to those obtained from more complex multi-parameter EOS. On the other hand, the capabilities of the available volume-cubic EOS for representing volumetric properties vary from equation to equation, especially in the calculation of liquid volumes.

Therefore, it is desirable to modify the available equations or to develop new equations to improve volumetric calculations. Very often, EOS are developed to represent volumetric properties in a specific PVT region without paying attention to other regions. However, in view of the wide range of conditions found in practical applications, it would be advantageous if the EOS had a balanced representation of the volumetric properties over an extensive PVT range.

Before developing a new EOS it is beneficial to evaluate, in a systematic manner, the performance of the available volume-cubic equations

in the representation of the PVT properties of pure fluids. For mixture calculations, several studies [50,90,142] have indicated that the accuracy of the EOS is sometimes affected by the choice of mixing rules for its parameters and therefore special attention must be paid when selecting mixing rules for the parameters.

The purpose of this study is to evaluate the available volume-cubic equations of the VDW-type as represented by Eq.(1.3) to identify their advantages and limitations and the methods used to formulate them. Based on this evaluation a new volume-cubic equation of the VDW-type is developed that can represent the volumetric properties of pure normal fluids over an extensive PVT range. The new EOS is extended to mixtures by selecting mixing rules for its parameters that are appropriate for calculating volumetric properties and VLE of normal fluid mixtures as well as complex mixtures.

Chapter II

THEORETICAL CONSIDERATION

The purpose of this chapter is first of all to review the theoretical background of Eq.(1.3) in terms of the partition function and the virial expansion approaches. The physical meaning and characteristics of Eq.(1.3) and its parameters can be interpreted by means of these two approaches which are often used for deriving theoretical equations of state. Secondly, use of a volume-cubic equation for VLE and volumetric calculations of pure fluid is presented. Finally, use of the corresponding states principle [89] for the generalization of EOS parameters is discussed.

2.1 The Partition Function Approach

As shown in any statistical thermodynamic text (e.g., Hill [54]) the Helmholtz energy, $\underline{A}$, is directly related to the canonical partition function, Q(N,V,T)., by

$$\underline{A}(N,V,T) = -kT \ln Q(N,V,T) \qquad (2.1)$$

where k is the Boltzmann constant and N is the number of molecules. From Eq.(2.1), an equation of state can be obtained using the following thermodynamic relationship:

$$P = kT(\partial \ln Q/\partial V)_{N,T} \qquad (2.2)$$

The partition function approach leads to the classic van der Waals interpretation of the molecular behavior of a real fluid -- the van der Waals fluid theory. This theory resulted in a modification of the ideal gas equation -- the well-known van der Waals equation. Based on the fundamental ideas of van der Waals, several authors [42,43,93,108,135] have discussed the van der Waals fluid theory in a more general fashion using the statistical mechanics argument. Among them, Vera and Prausnitz [135] have shown that several volume-cubic equations of state could be derived from a simple partition function. However, their approach can also be used to derive other volume-cubic equations of a form similar to Eq.(1.3).

The main assumption of the generalized van der Waals theory proposed by Vera and Prausnitz was to assume that for a pure fluid, the partition function, Q, can be expressed as:

$$Q(N,V,T) = (1/N!)\,[V/\Lambda^3]^N\,[V_f/V]^N\,[\exp(-\phi/2kT)]^N\,[q_{r,v}]^N \qquad (2.3a)$$

where the thermal DeBroglie wave length, Λ, is:

$$\Lambda = (h^2/2\pi mkT)^{\frac{1}{2}}$$

and h is Planck's constant and m is the molecular mass.

Eq.(2.3a) refers to N molecules occupying a total volume V. Since real molecules have a finite volume, the free volume V_f represents the space available in a container of volume V for the molecules to move about in. The term $(1/N!)(V/\Lambda^3)^N$ correspond to the translational contribution of an ideal gas to the partition function. The second and third

bracketed terms account for the repulsive and attractive forces between molecules, respectively. The quantity, $\phi/2$, is the attractive potential energy associated with one molecule and ϕ is the sum of the two-body (pair) interactions between any molecule and those around it and is given by:

$$\phi = (Na/v) \int_0^\infty \Gamma(r)\, g(r)\, 4\pi r^2\, dr^2 \qquad (2.3b)$$

where $g(r)$ is the radial distribution function to account for the random distribution of molecules, $\Gamma(r)$ is the pair potential function and r is the radial coordinate located on a particular molecular center. The last term in Eq.(2.3a) represents the contribution of the rotational and vibrational degrees of freedom. The quantity, $q_{r,v}$ is assumed to be a function of temperature only. Thus, as indicated by Eqs(2.1,2), $q_{r,v}$ contributes nothing to the configurational properties which are reflected in the equation of state.

When Eqs(2.3a,b) are substituted into Eq.(2.1), the molar Helmholtz energy, A, is given by the sum of three terms: that of the ideal gas, A^{id}, that of the hard-sphere (hs) repulsive forces, A^{hs} and that of the attractive forces, A^a, as follows:

$$A = A^{id} + A^{hs} + A^a \qquad (2.4a)$$

$$A^{id} = -RT \ln [v/(N\Lambda^3)] - RT - RT \ln(q_{r,v}) \qquad (2.4b)$$

$$A^{hs} = - RT \ln(v_f/v) \qquad (2.4c)$$

$$A^a = \frac{Na\phi}{2} \qquad (2.4d)$$

In deriving Eq.(2.4b) Stirling's approximation ($N!=N^N e^{-N}$) and the identities $v=V(Na/N)$ and $R=Na\,k$ were used and Na is Avogadro's number. In turn, substituting Eq.(2.4) into Eq.(2.2), the equation of state is given by the sum of the three contributions from the ideal gas, the hard-sphere repulsive forces and attractive forces:

$$P = P^{id} + P^{hs} + P^{a} \tag{2.5a}$$

$$P^{id} = RT/v \tag{2.5b}$$

$$P^{hs} = RT\frac{\partial}{\partial V}[\,\ell n(\,v_f/v)]_{T,N} \tag{2.5c}$$

$$P^{a} = -\frac{N}{2}\left(\frac{\partial \Phi}{\partial V}\right)_{T,N} \tag{2.5d}$$

In practice, although it's a misconception, the sum of P^{id} and P^{hs} is considered as the overall repulsive force contribution to the total pressure P i.e., $P^{rep} = P^{id} + P^{hs}$. Thus this results in a two-term expression for P:

$$P = P^{rep} + P^{a}. \tag{2.6}$$

To complete the above equation of state, the expressions for V_f and Φ are required.

To find an expression for V_f, van der Waals assumed that:

1. each molecule has a hard core of radius $\sigma/2$,
2. there is no overlap of the hard cores when two body collisions occur.

Consequently, the smallest possible distance between the two molecular centers is σ. Based on these assumptions, the free volume was then

calculated by subtracting from the total volume the part called the exclusive or co-volume which is not accessible for a particular molecule to move about. For a two body collision the free volume V_f becomes,

$$V_f = V - \frac{N}{Na} b \qquad (2.7)$$

where $b = 4b_o$ and the actual volume of one mole of hard-sphere molecules is $b_o = Na(\pi/6)\,\sigma^3$. The co-volume b is assumed to be independent of temperature due to the fact that the molecular size does not change significantly with temperature.

To find ϕ, van der Waals assumed that the radial distribution function g(r) is independent of temperature and volume for all r. As a result, the integral in Eq.(2.3b) is a constant which was expressed as $-(2\,a/Na^2)$. Then

$$\phi = -(2\bar{a}N/VNa^2) \qquad (2.8)$$

where the constant a should be positive since the attractive potential energy is always negative. Substituting Eqs(2.7,8) to Eqs(2.5,c,d) yields:

$$P^{hs} = (RT\,b)/[v\,(v-b)] \qquad (2.9)$$

$$P^{a} = -a/v^2 \qquad (2.10)$$

From Eqs(2.5,6,9,10) the famous VDW equation is obtained,

$$P = RT/(v-b) - a/v^2 \qquad (2.11)$$

With reference to the above derivation, it is clear that parameter a is related to the attractive potential energy, $\phi/2$, sometimes called the internal energy. Values of a should always be positive. Both parameters a and b are assumed temperature independent. The VDW equation can only illustrate the volume behavior of real fluids qualitatively.

Many authors [18,44,52,115,122] have noted that the non-overlap assumption implies the additivity of the co-volumes which is only correct at low densities. At densities close to those of liquid, the molecules are closely packed and the three-body, four-body, etc. collisions become important, as a result the overlap situation occurs. Therefore, the co-volumes estimated on the basis of two-body collisions alone are too large. Also, the radial distribution function cannot be assumed constant and should vary with temperature and volume. In accordance with the above discussion, efforts were made to improve the original VDW equation as well as his fluid theory by

1. developing an expression for V_f which takes into account the overlapping effect at high densities,
2. allowing the radial distribution function to vary with temperature and volume.

Either one of these methods or both are, in effect, used as the basis for developing empirical equations of state. The ideas involved in them are explained below.

2.1.1 Expressions for Free Volume

By failing to account for overlap, the free volume of van der Waals becomes too small as the density rises. At very high densities, the free

volume of van der Waals becomes negative and therefore meaningless. Meanwhile negative pressures may be predicted by the VDW EOS.

Many efforts have been made to obtain theoretical expressions for free volume, which began with the development of a theoretical equation of state for hard sphere molecules without any attractive forces existing among them i.e., $P^a=0$. Hence the equation of state depends solely on the free volume, $P = P^{rep}$. The progress of this development is thoroughly reviewed by Scott [115]. Several important results for P^{rep} and the corresponding v_f are summarized in Table 2.1. All the hard sphere models for P^{rep} in Table 2.1 are assumed to be funotions only of volume.. The co-volume retains the definition given earlier and is temperature independent. Of all the models, that proposed by Carnaham-Starling (CS) [18] is considered the most accurate with the VDW model the least accurate for calculating the hard sphere compressibility factor when compared to the 'exact' molecular dynamic results of Alder et al. [8]. However, it should be noted that all these models, except the VDW and the S1 models, yield, after rearrangement, an expression in volume of an order higher than cubic. Therefore, in the framework of developing volume-cubic equation of state, only the VDW and the S1 models can be considered as the repulsive term for the equation. This further implies that the counter-part of P^{rep} in the equation, the attractive term, P^a, should be chosen in such a way so as to compensate for the shortcomings in P^{rep} while maintaining the volume-cubic expression. In other words, when taken separately each part of the equation (P^{rep} and P^a) may be incorrect but their combination may cancel out errors and thus give good prediction of the total

pressure. The following generalized expression for P^a is adopted to couple with the VDW hard sphere model

$$P^a = - [a/(v^2+ubv+wb^2)] \qquad (2.12)$$

A similar approach can be used with the S1 model.

Table 2.1: Analytical expressions for hard sphere models (repulsive pressures and free volumes)

name	P^{rep}	v_f	ref.
VDW	$\frac{RT}{(v-b)}$	$(v-b)$	133
PYF	$\frac{4RT\ (16v^2+4bv+b^2)}{(4v-b)^3}$	$(v-\frac{b}{4})\ \exp[\frac{3b(b-8v)}{2(4v-b)}]$	52
PYT	$\frac{RT\ (16v^2+8bv+3b^2)}{v\qquad(4v-b)^2}$	$\frac{16v^3}{(4v-b)^2}\ \exp[-\frac{6b}{(4v-b)}]$	128
G	$\frac{256RTv^3}{(4v-b)^4}$	$(v-\frac{b}{4})\ \exp[\frac{3b(b-8v)}{2(4v-b)^2}-\frac{b^3}{3(4v-b)^3}]$	44
S1	$\frac{RT\ (2v+b)}{v\ (2v-b)}$	$\frac{1}{4v}\ (2v-b)^2$	115
S2	$\frac{2RT\ (4v^2+3bv+b^2)}{v\ (4v+b)(2v-b)}$	$\frac{1}{v^2}\ (v-\frac{b}{2})^{7/3}\ (v+\frac{b}{4})^{2/3}$	115
CS	$\frac{RT\ (64v^3+16bv^2+4b^2v-b^3)}{v\qquad(4v-b)^3}$	$v\ \exp[\frac{b(3b-16v)}{(4v-b)^2}]$	18

It should be noted that the reappearance of the co-volume, b, in Eq.(2.12) can be considered as compensation for the inadequacy inherent in the hard sphere model. As will be explained from the virial expansion approach (section 2.2), the parameters u and w can be considered as correction factors to the co-volume b to account for overlapping at high densities and the non-spherical nature of the molecules.

2.1.2 Temperature and Volume Dependence of the Radial Distribution Function

Examination of the temperature and volume dependence of the radial distribution function in the expression for Φ can reveal which of the parameters a, b, u and w should be temperature dependent and which should not. Since P^a is closely related to Φ (Eq.(2.5d)) it can be shown that

for $u^2-4w > 0$,

$$\frac{\Phi}{2} = -\frac{1}{Na}\left[\frac{a}{b\,(u^2-4w)^{0.5}}\right] \ln\left\{\frac{[2v+ub+b\,(u^2-4w)^{0.5}]}{[2v+ub-b\,(u^2-4w)^{0.5}]}\right\}, \qquad (2.13a)$$

for $u^2-4w = 0$,

$$\frac{\Phi}{2} = -\frac{1}{Na}\,[a/(v+ub/2)]. \qquad (2.13b)$$

Also Eq.(2.3,b) can be rewritten as

$$\Phi = \left(\frac{4\pi N}{V}\right) I(T,V) \qquad (2.14)$$

where

$$I(T,V) = \int_\sigma^\infty r(r)\, g(T,V,r)\, r^2\, dr, \quad r > \sigma \qquad (2.15a)$$

$$I(T,V) = 0, \quad r \le \sigma. \qquad (2.15b)$$

Generally, there are two approaches for treating the temperature and volume dependence of I(T,V):

1. To assume the temperature and volume effects can be separated completely as

$$I(T,V) = H(T)\ F(V) \qquad (2.16)$$

where H(T) is a function of temperature and F(V) is a function of volume.

2. To assume I(T,V) depends on T and V according to

$$I(T,V) = L(T)\ G(V,T) \qquad (2.17)$$

where L(T) is a function of temperature and G(V,T) is a function of volume and temperature.

These approaches give different interpretations of the characteristics of the parameters b, u and w but identical interpretation of the parameter a. Through Eqs(2.5d, 2.14) H(T), F(V), L(T) and G(V,T) can be related to P^a. For Approach 1, the expression for P^a becomes

$$P^a = (2\pi Na^2/v^2)\ H(T)\ [V\frac{dF(V)}{dV} - F(V)] \qquad (2.18)$$

By equating Eq.(2.18) and Eq.(2.12), the analytical expressions for H(T) and F(V) can be obtain by integration

for $u^2-4w > 0$,

$$F(V) = -\frac{1}{Na}\left[\frac{1}{b\ (u^2-4w)^{0.5}}\right] \ln\left\{\frac{[2v+ub+b\ (u^2-4w)^{0.5}]}{[2v+ub-b\ (u^2-4w)^{0.5}]}\right\} \qquad (2.19a)$$

for $u^2-4w = 0$,

$$F(V) = a\, v/(v+ub/2) \qquad (2.19b)$$

with

$$H(T) = a(T)/(2\pi Na) \qquad (2.20)$$

From Eqs(2.19,20) Approach 1 indicates that among the four parameters in Eq.(1.3), only parameter a should be treated as temperature dependent. As for Approach 2, the same expressions for F(V) and H(T) can be found for G(V,T) and L(T), respectively. However, this leads to the interpretation that not only parameter a but also at least one of the three parameters b, u and w should be temperature dependent. It is not possible to justify which assumption is more correct. According to the results of some theoretical studies [104] the radial distribution function depends strongly on density and to a small extent on temperature. On the other hand, the molecular size is a weak function of temperature. This indicates that:

1. In both approaches, the parameter a should depend on temperature.
2. The presence of u, w and b is important for adjusting the density dependence of F(V) or G(V,T).
3. It is not necessary for the parameters b, u and w to depend on temperature strongly.

The necessity of introducing temperature dependence to a, b, u and w and the importance of the presence of b, u and w in P^a can be further understood by applying the virial expansion approach to Eq.(1.3).

2.2 The Virial Expansion Approach

The virial equation of state which was proposed by Kamerlingh Onnes [61] in 1901 is theoretically sound and can be derived from kinetic theory [104]. When written as a serial expansion in volume the equation is as follows:

$$Z = 1 + \frac{B}{v} + \frac{C}{v^2} + \frac{D}{v^3} + \ldots \qquad (2.21)$$

where B, C, D etc. correspond to the 2nd, 3rd and 4th virial coefficients respectively.

Virial coefficients are functions of temperature and can be related to molecular interactions. The second virial coefficient corresponds to two-body (pair) interactions, the third to three-body interactions and so on. It has been found [124] that the virial equation of state truncated after the 2nd virial coefficient is valid for densities less than one half the critical density. For vapor-liquid equilibria, this condition is usually satisfied when calculating vapor densities of most of pure fluids for T_r ($=T/T_c$) < 0.9. However to calculate liquid densities requires more virial coefficients, since higher-order interactions start to occur as density increases.

Eq.(1.3) can be considered as a finite approximation of the infinite virial expansion. Rearranging Eq.(1.3) in the form of the virial expansion yields:

$$Z = 1 + [b-a/RT]/v + [b+au/RT]\, b/v^2 + [b-a\,(u^2-w)/RT]\, b^2/v^3 + \ldots \qquad (2.22)$$

Eq.(2.22) is derived by means of the binomial expansion technique [132]. The coefficient of each term corresponds to a virial coefficient

$$B = b - a/RT \tag{2.23}$$

$$C = (b + au/RT)\, b \tag{2.24}$$

$$D = [b - a(u^2 - w)/RT]\, b^2 \tag{2.25}$$

As can be seen the 2nd virial coefficient contains only the parameters a and b. However, the higher order virial coefficients require the parameters u and w in addition to a and b. Also the higher the order in volume becomes, the more the parameters are required. This indicates that only parameters a and b are required to calculate vapor phase behavior, whereas the additional parameters u and w are needed to describe liquid phase behavior. As a result, u and w could be considered as correction factors to the co-volume b, especially at high densities. On the other hand, the temperature dependence of all the virial coefficients suggests that any one of the parameters a, b, u and w can be temperature dependent. Thus the two approaches previously used to represent the radial distribution function do not conflict with each other.

In developing an EOS of the form of Eq.(1.3) for representing real fluid volumetric behavior, the remaining issues are (i) how to introduce the temperature dependence to parameter a and (ii) is it beneficial to also consider molecular parameters b, u and w as temperature dependent? Some answers can be found by examining the performance of dif-

ferent volume-cubic equations of state that conform to the two approaches for treating I(T,V) and thus a, b, u and w. Consequently, in Chapter III, several well-known volume-cubic equations are reviewed and their performance is evaluated on the basis of their ability to predict several volumetric and thermodynamic properties over a wide PVT range.

2.3 Use of a Volume-Cubic Equation of State for the Calculation of Pure Fluid Properties

In this section, Eq.(1.3) is used as a generalized example in the discussion of how to use volume-cubic EOS for calculating VLE and volumetric properties in different fluid phase regions on the P-V surface. The discussion is divided into two parts according to the phase regions which exist on the P-V surface,

1. The two-phase (saturated liquid and vapor) coexisting region.
2. The single phase region (liquid or gas).

2.3.1 Two-Phase Coexisting Region

The thermodynamic treatment of phase equilibrium introduced by Gibbs [36], is based on the concept of chemical potential, μ. The vapor phase (superscript v) and the liquid phase (superscript ℓ) of a pure fluid are in thermodynamic equilibrium when the temperature (T), the pressure (P), and the chemical potential (μ) are the same in both phases. The chemical potential is often replaced by an equivalent quantity, the fugacity (f), since the fugacity can be easily evaluated by an EOS through a thermodynamic relationship. Thus, the phase equilibrium criteria can be expressed as follows:

$$P^v = P^\ell \ (= P) \tag{2.26a}$$

$$T^v = T^\ell \ (= T) \tag{2.26b}$$

$$f^v(P^v, v^v, T^v) = f^\ell(P^\ell, v^\ell, T^\ell) \tag{2.26c}$$

or

$$\mu^v = \mu^\ell. \tag{2.26d}$$

The thermodynamic relationship between the fugacity (f) and P, v and T is:

$$\ln\left(\frac{f}{P}\right) = \int_v^\infty \left(\frac{P}{RT} - \frac{1}{v}\right) dv - \ln\left(\frac{Pv}{RT}\right) + \frac{Pv}{RT} - 1. \tag{2.27}$$

Substituting Eq.(1.3) to Eq.(2.27) one obtains the following expression for f,

$$\ln\left(\frac{f}{P}\right) = \frac{Pv}{RT} - 1 - \ln\left(\frac{Pv}{RT}\right) + \ln[v/(v-b)] + RS,$$

for $u^2-4w > 0$,

$$RS = -\frac{1}{RT}\left[\frac{a}{b\,(u^2-4w)^{0.5}}\right] \ln\left\{\frac{[2v+ub+b\,(u^2-4w)^{0.5}]}{[2v+ub-b\,(u^2-4w)^{0.5}]}\right\} \tag{2.28a}$$

for $u^2-4w = 0$,

$$RS = -\frac{1}{RT}\,[a/(v+ub/2)]. \tag{2.28b}$$

Eq.(2.28) can apply to both vapor and liquid phases when v is replaced by v^v and v^ℓ, respectively. The saturated liquid and vapor molar volumes, (v^ℓ, v^v) at any given T are obtained by solving Eq.(1.3) while satisfying Eq.(2.26),

$$v^3+[(u-1)b-RT/P)]\ v^2+[(w-u)b^2-(ubRT/P)+a/P]\ v$$

$$-[wb^2+wbRT+a]\,(b/P) = 0. \qquad (2.29)$$

Eq.(2.29) can be solved analytically by means of the Cardano method [28]. There are three roots in which the largest corresponds to the saturated vapor molar volume and the smallest to the saturated liquid molar volume. The computational procedure for obtaining v^{ℓ} and v^{ν} at any given T is described by the following algorithm:

1. Assume P (i.e., $P^{\ell} = P^{\nu}$)
2. Solve Eq.(2.29) to obtain v^{ℓ} and v^{ν}
3. Calculate f^{ℓ} and f^{ν} using Eq.(2.28)
4. Check if $f^{\ell} = f^{\nu}$, otherwise repeat steps (1)-(3)

The physical meaning of the above computational procedure can be interpreted through the Maxwell theorem [94]. As shown in Figure 2.1, the cubic isotherm, curve II, is generated by a volume-cubic EOS. The sum of the two shaded areas on either side of the line ACB can be obtained by integrating v dP along the curve ADCEB. According to the Maxwell theorem the liquid at point A is in true equilibrium with the vapor at point B when the two shaded areas are equal. This is because

$$\mu^{\ell} - \mu^{\nu} = \int_{ADCEB} \left(\frac{\partial \mu}{\partial P}\right)_T dP = \int_{ADCEB} v\, dP. \qquad (2.30)$$

At equilibrium, $\mu^{\ell} - \mu^{\nu} = 0 = \int v\, dP$, the two conditions of equilibrium, namely $P^{\ell} = P^{\nu}$ and $\mu^{\ell} = \mu^{\nu}$ (thus $f^{\ell} = f^{\nu}$) are therefore satisfied. Subsequently the above computational procedure can be explained as follows

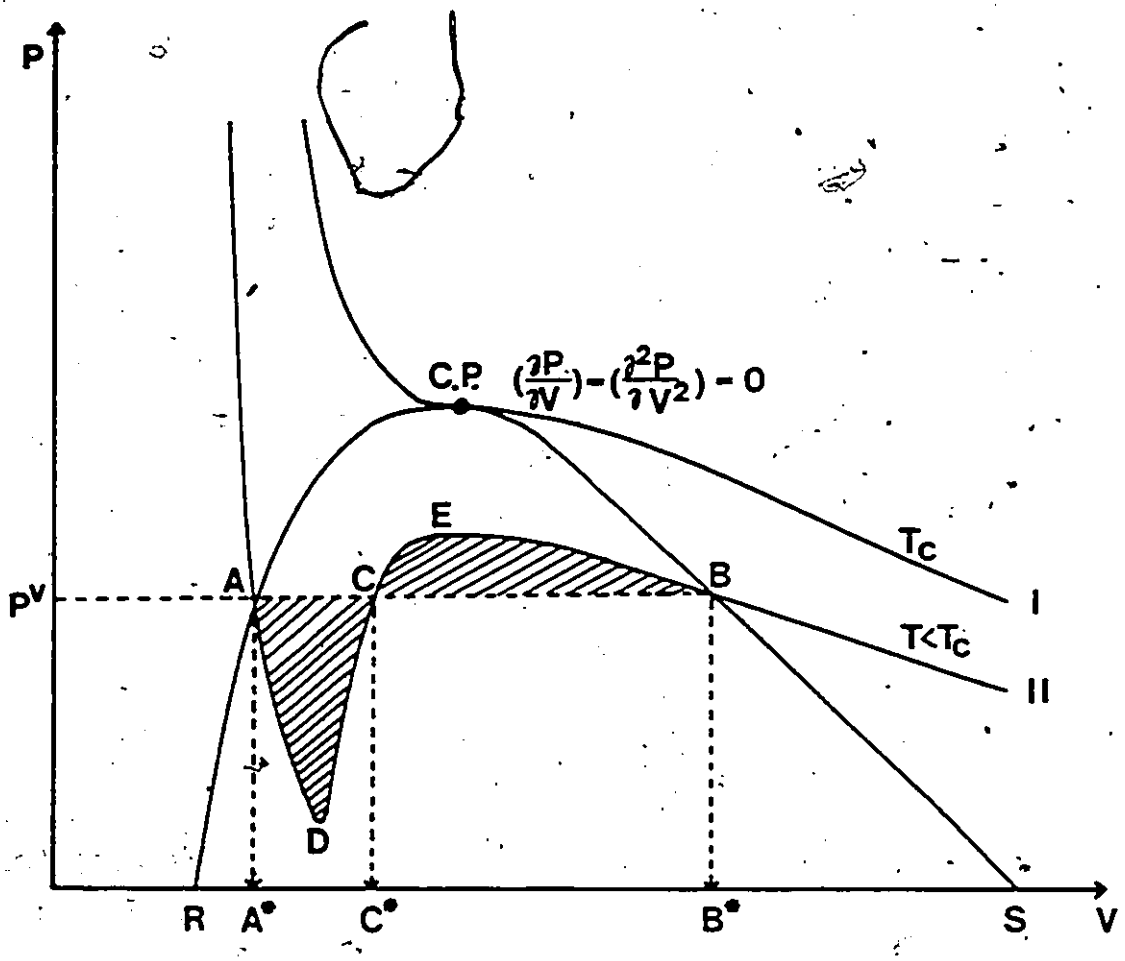

Figure 2.1: Illustration of the Maxwell theorem on a P-V surface.

1. Adjusting the pressure corresponds to the adjustment of the line ACB along the P axis.
2. The three roots A, B, C obtained from the EOS are equivalent to the points A^*, B^* and C^* which are the projections of the three points on the V-axis. When the shaded areas are equal, A^* corresponds to v^{ℓ} and B^* to v^{v}. However, C^*, the intermediate root of the EOS, has no physical meaning.
3. The quantity, $f^{\ell}-f^{v}$, is a measure of the sum of the two shaded areas.

The points A and B coincide with each other at the critical point (C.P.) where the EOS yields three identical roots. The point C^*, is physically insignificant because the condition for stability of an equilibrium state i.e., $(dP/dV)_T \leq 0$ is not met at the point C where $(dP/dV)_T > 0$ [94]. The saturation curve which defines the phase boundary on the P-V surface consists of the locus of all points A and points B for temperatures from the triple point to the critical. At the critical point, three conditions [132] are imposed on the equation of state, namely

$$\left(\frac{\partial P}{\partial V}\right)_T = 0 \qquad (2.31a)$$

$$\left(\frac{\partial^2 P}{\partial V^2}\right)_T = 0 \qquad (2.31b)$$

$$v^{\ell} = v^{v} = v_c^*, \text{ at } T = T_c,\ P = P_c \qquad (2.31c)$$

where v_c^* represents the predicted critical molar volume. The last condition ensures that the EOS yields three identical roots at the critical point. Generally at the critical point, the parameters a and b can be expressed by

$$a_c = \Omega_{ac} R^2 T_c^2 / P_c \qquad (2.32)$$

$$b_c = \Omega_{bc} R T_c / P_c \qquad (2.33)$$

The quantities Ω_{ac} and Ω_{bc} are dimensionless and the subscript, c, denotes the quantity at the critical point.

It should be noted that points A and B along the saturation curve of the P-V surface correspond to the intersection between line ACB and the cubic isotherm. In order to produce loci of A and B close to the actual (experimental) saturation curve, the EOS not only has to generate the correct shape of cubic isotherm under the two-phase coexisting dome, but also calculate P^ν correctly. The former is closely related to the structure of the EOS considered while the latter corresponds to the predictivity of P^ν from the EOS. However the predicted value of P^ν results directly from satisfaction of the equal-fugacity condition as described earlier. Therefore, we can say that the accurate representation of P^ν is the necessary condition for an EOS to adequately describe pure fluid VLE. In principle, as will be discussed in Chapter IV, the structure of Eq.(1.3) is largely determined by the choice of parameters u and w which contribute to the density dependence of the equation. On the other hand, the predictivity of P^ν can be related to the method of introducing temperature dependence to the EOS.

In a recent review article entitled 'Critical Phenomenon with Classical Fluids', Sengers and Levelt-Sengers [116] concluded that volume-cubic EOS are fundamentally inadequate to give good account of volume in the vicinity of the critical point. They stated that "... it becomes

evident that equations of van der Waals' type did not predict correctly (the critical point region) the asymptotic shape of the coexistence (saturation) curve and the critical isotherm of real fluids." This statement stems from the results of their experimental studies and analysis of other related studies on the critical exponents which are commonly used to characterize critical behavior of fluids. It has been known for a long time [58] that fluids exhibit exceptional thermodynamic and volumetric behavior in the vicinity of the critical point, not only when the point is approached from within the two-phase region, but also from the single phase regions. Fluids in these regions are usually referred to as near-critical fluids. The physical and transport properties of near-critical fluids are extremely variable which result in unstable heat transfer and fluid flow processes. In order to keep fluid systems stable, process designers try to avoid these conditions. Therefore, the inherent inadequacy of volume-cubic equations of state in the critical region does not affect its applicability to process design.

It should be noted that the anomalous behavior of the near-critical fluid depends, to a large extent, on how near the fluid is to the critical point. However, this critical region cannot be defined precisely. For single phase regions (liquid or gas), Hsu and Graham [58] suggested that the critical region for hydrogen be considered in the reduced temperature ($T_r = T/T_c$) range of $0.95 \leq T_r \leq 1.30$, and the reduced pressure ($P_r = P/P_c$) range of $0.80 \leq P_r \leq 1.30$. For the two-phase coexisting region Spencer and Alder [120] suggested that for most fluids the critical region be in the range of $0.85 \leq T_r \leq 1.0$, because of the smooth, almost linear behavior of the density at temperature below $T_r = 0.85$.

2.3.2 Single Phase Region

In principle, volume-cubic EOS yield only one real positive root (the other two are imaginary) outside the two-phase coexisting region. This root corresponds to either liquid-like volume or gas-like volume depending on the temperature and pressure considered.

In order to give good account of liquid volumes over a wide range of pressures the three-root oscillation of the cubic isotherm in the two-phase coexisting region should rise sharply outside the saturation curve. This is because the actual liquid isotherms have steep slopes due to the small effect of pressure on volume.

2.4 The Corresponding States Principle

One of the important results of the VDW fluid theory is the corresponding states principle (CSP). To date, this principle is largely used to generalize fluid properties as well as equation of state parameters.

The idea was first explored by van der Waals [133]. He defined reduced variables by

$$P_r = P/P_c,\ T_r = T/T_c,\ v_r = v/v_c. \qquad (2.34)$$

and noted that different fluids at the same P_r and T_r have approximately the same v_r. Therefore, he concluded that all fluids should obey, approximately, the same EOS when written in terms of reduced parameters.

A two-parameter (usually T_c, P_c) CSP can be represented in the functional form

$$Z = J(T_r, P_r) \tag{2.35}$$

where Z (=Pv/RT) is the compressibility factor and the function, J, refers to a universal EOS for all fluids of interest. An important consequence of the two-parameter CSP is that the parameters in any empirical two-parameter EOS can always be characterized in terms of the critical constants. For example, any two-parameter volume-cubic EOS (u and w are fixed) may be represented by:

$$Z = J(T,v,a,b) \tag{2.36}$$

Solving Eq.(2.36) simultaneously with Eqs(2.31,a,b,c) will give the quantities Ω_{ac} and Ω_{bc} in Eqs(2.32,33). In addition, a universal critical compressibility factor, ζ_c, will be obtained.

About thirty years ago Pitzer and co-workers [89] observed that the departure from the two-parameter CSP by fluids of non-spherical molecules was neither large nor random, and could be characterized by a new, small empirical parameter for each fluid. The acentric factor, ω, as its name implies, was introduced to account for the non-spherical nature of the molecules and is defined below

$$\omega \equiv -1 - \log_{10}(P_r)_{Tr=0.7} \tag{2.37}$$

where $(P_r)_{Tr=0.7}$ is the reduced vapor pressure evaluated at T_r=0.7. Using this additional parameter, Pitzer and co-workers have successfully extended the two-parameter (T_c, P_c) CSP to nonpolar and slightly

polar fluids. The above three-parameter (T_c, P_c, ω) CSP can be expressed by

$$Z = J(T_r, P_r, \omega). \qquad (2.38)$$

At the critical point, Eq.(2.38) gives a critical compressibility factor for each fluid considered which can be correlated in terms of ω.

Applying the three-parameter CSP to an EOS of more than two parameters, such as the four-parameter volume-cubic EOS given by Eq.(2.39)

$$Z=J(T,v,a,b,u,w) \qquad (2.39)$$

implies that the parameters a, b , u and w can be characterized in terms of T_c, P_c and the acentric factor, ω. In addition, the critical compressibility factor predicted by the EOS is a function of ω. This further suggests that if the EOS parameters are generalized in terms of T_c, P_c and ω, it can be easily applied to any fluid provided its T_c, P_c and ω are known. In other words, only the (volumetric) data of a few fluids which conform well to the three-parameter CSP are needed to evaluate the EOS parameters. After generalizing the parameters using the selected fluids, the EOS should be able to represent, with similar accuracy, any other fluids whose volumetric properties also conform well to the three-parameter CSP. In general, the volumetric and thermodynamic properties of normal fluids (non-polar and slightly polar fluids) can be represented by the three-parameter (T_c, P_c, ω) CSP quite accurately.

Chapter III

CRITICAL LITERATURE REVIEW

Many variants of the van der Waals (VDW) equation of state have been proposed. It would be prohibitively long to review all the work reported in the literature. Therefore the purpose of this chapter is, first, to review the most recently proposed volume-cubic equations of state of the van der Waals type. Emphasis is placed on those equations which represent different approaches to the development of volume-cubic equations from the VDW EOS to the more complex equations. Secondly, the performance of these equations is evaluated in terms of their accuracy in calculating volumetric and thermodynamic properties of the first ten normal alkanes (C1-C10). Hence the merits as well as the shortcomings of each approach to developing the equations are identified.

3.1 Review of the Well-Known Volume-Cubic Equations of State

There are two important factors involved in the development of an EOS. The first is to choose a form (or mathematical model) as the basis of development. The second is to decide which physical properties will be used to determine the parameters in the model. As mentioned previously, the volume-cubic equations of the VDW type commonly used can be expressed in the form like Eq.(1.3) which contains the four

parameters a, b, u and w. At the critical point parameters a and b are generally expressed by Eqs(2.32,33) in which Ω_{ac} and Ω_{bc} can be universal constants or substance dependent.

The VDW equation is the simplest volume-cubic equation in which the two adjustable parameters a and b are characterized by T_c and P_c as given by Eqs(2.32,33). The VDW equation can only represent the volumetric behavior of real fluids qualitatively since it predicts a critical compressibility factor (ζ_c) of 0.375 for all substances. However most real fluids have critical compressibility factors in the range of 0.20 to 0.29. Thus various modifications to the VDW EOS have been proposed. The main reasons for developing these equations were:

1. to change the density dependence of the attractive term (P^a) in the VDW EOS so that the predicted critical compressibility factors ζ_c are closer to the actual values,
2. to force the equation to fit certain volumetric and/or thermodynamic properties of pure fluids.

The treatment of the four parameters a, b, u and w are generally classified into six types:

(1) 2 adjustable 1 temperature dependent parameter (2P1T) EOS;
(2) 3 adjustable 1 temperature dependent parameter (3P1T) EOS,
(3) 4 adjustable 1 temperature dependent parameter (4P1T) EOS,
(4) 2 adjustable 2 temperature dependent parameter (2P2T) EOS,
(5) 3 adjustable 2 temperature dependent parameter (3P2T) EOS,
(6) 3 adjustable 3 temperature dependent parameter (3P3T) EOS.

The notation 2 adjustable 1 temperature dependent parameter EOS denotes an equation containing only two substance dependent parameters in which one of them is also temperature dependent. Details of these equations are presented in Tables 3.1 and 3.3. It should be noted that the types (1) to (3) are related to the first approach (Approach 1) to the treatment of the temperature dependence of the radial distribution function as mentioned in Chapter II. On the other hand, types (4) to (6) are related to the second approach (Approach 2). The six types of equations are discussed separately as follows.

3.1.1 Two Adjustable One Temperature Dependent Parameter Equations of State

When the parameters u and w are treated as universal constants Eq.(1.3) reduces to a two-parameter (a,b) equation. The first widely used variation of the VDW equation of the 2P1T type was that proposed by Redlich and Kwong (RK) in 1949 [105]. They introduced a simple temperature function to the parameter a and changed the form of the volume dependence in the denominator by assuming u=1,w=0. The temperature function of the parameter a is $a = a_c/T^{\frac{1}{2}}$. The RK equation predicts a ζ_c, equal to 1/3. As a result the accuracy of the volumetric calculations was improved. However the RK equation can only predict gas phase volumes with reasonable accuracy and yields very large errors in liquid compressibility factors as well as in the saturation properties i.e., vapor pressure, saturated liquid and vapor molar volumes.

Table 3.1: Summary of the 2P1T, 3P1T and 4P1T types of equations

1. SRK (1972,1980)

$$P = \frac{RT}{v-b} - \frac{a}{v(v+b)}$$

$$a = \frac{\alpha(T_r)\,\Omega_{ac}\,R^2T_c^2}{P_c}$$

$$b = \frac{\Omega_{bc}\,R\,T_c}{P_c}$$

$$\zeta_c = 1/3$$

$$\Omega_{ac} = 0.42747$$

$$\Omega_{bc} = 0.08664$$

$$\alpha(T_r) = [1 + m(\omega)\,(1 - T_r^{1/2})]^2$$

$$m(\omega) = 0.480+1.574\omega-0.176\omega^2, \quad \omega<0.5$$

$$m(\omega) = 0.47978+1.57624\omega-0.19394\omega^2+0.02779\omega^3 -0.0016577\omega^4-0.00013153\omega^5, \quad \omega>0.5$$

2. PR (1976,1984)

$$P = \frac{RT}{v-b} - \frac{a}{v^2+2bv-b^2}$$

$$a = \frac{\alpha(T_r)\,\Omega_{ac}\,R^2T_c^2}{P_c}$$

$$b = \frac{\Omega_{bc}\,R\,T_c}{P_c}$$

$$\zeta_c = 0.307$$

$$\Omega_{ac} = 0.45724$$

$$\Omega_{bc} = 0.07780$$

$$\alpha(T_r) = [1 + m(\omega)\,(1 - T_r^{1/2})]^2$$

$$m(\omega) = 0.37464+1.54226\omega-0.26992\omega^2, \quad \omega<0.5$$

$$m(\omega) = 0.37964+1.48503\omega-0.16442\omega^2+0.01667\omega^3, \quad 0.2\leq\omega\leq2.0$$

3. HK (1980)

$$P = \frac{RT}{v-b} - \frac{a}{v^2+cbv-(c-1)b^2}$$

$$a = \frac{\alpha(T_r)\,\Omega_{ac}\,R^2T_c^2}{P_c}$$

$$b = \frac{\Omega_{bc}\,R\,T_c}{P_c}$$

$$\Omega_{ac} = 0.44131+0.09168\omega-0.03651\omega^2-0.03651\omega^2-0.00558\omega^3$$

$$\Omega_{bc} = 0.082442-0.0273\omega-0.014048\omega^2+0.000707\omega^3$$

$$c = 1.44515+3.0587\omega-0.4563\omega^2-0.714\omega^3$$

$T_r<1$

$$\alpha(T_r) = [1+A(1 - T_r^{1/2})-B(1 - 1/T_r)]^2$$

$\omega\leq0.2$

$$A = 0.50+0.27767\omega+2.17225\omega^2$$

$$B = -0.022+0.338\omega-0.845\omega^2$$

$\omega>0.2$

$$A = 0.41311+1.14657\omega$$

$$B = 0.0118$$

$T_r>1$

$$\alpha(T_r) = 1-A\,\ln(T_r) +B\,(\ln(T_r))^2$$

$$A = 0.6258+1.5227\omega$$

$$B = 0.1533+0.41\omega$$

$$\zeta_c = 0.3211-0.080\omega+0.0384\omega^2$$

cont'd.

4. SW
(1980,1982)

$$P = \frac{RT}{v - b} - \frac{a}{v^2+(1-c)bv+cb^2}$$

$$a = \frac{\alpha(T_r)\ \Omega_{ac}\ R^2T_c^{\,2}}{P_c}$$

$$b = \frac{\Omega_{bc}\ R\ T_c}{P_c}$$

$\Omega_{ac} = [1 - \zeta_c\ (1 - \beta_c)]^3$

$\Omega_{bc} = \beta_c\ \zeta_c$

$\zeta_c = 1/[3\ (1+\beta_c\ \omega)]$

$\beta_c = 0.25989-0.0217\omega+0.0375\omega^2$

$c = -3\ \omega$

$\alpha(T_r) = [1 + \kappa(T_r,\omega)(1 - T_r^{\frac{1}{2}})]^2$

$T_r \leq 1$

$\omega \leq 0.4$ $\quad \kappa = \kappa_1$

$\omega \leq 0.55$ $\quad \kappa = \kappa_2$

$0.4 \leq \omega \leq 0.55$ $\quad \kappa = \frac{\omega-0.4}{0.15}\ \kappa_1 + \frac{0.55-\omega}{0.15}\ \kappa_2$

$\kappa_1 = \kappa_0 + (5T_r-3\kappa_0-1)^2/70$

$\kappa_2 = \kappa_0 + 0.71\ (T_r - 0.779)^2$

$\omega \leq 0.3671$ $\quad \kappa_0 = 0.465+1.347\omega-0.528\omega^2$

$\omega > 0.3671$ $\quad \kappa_0 = 0.5361+0.9593\omega$

$T_r > 1$

$\kappa(T_r,\omega) = \kappa(1,\omega)$

5. PT
(1982)

$$P = \frac{RT}{v - b} - \frac{a}{v(v+b)+c(v-b)}$$

$$a = \frac{\alpha(T_r)\ \Omega_{ac}\ R^2T_c^{\,2}}{P_c}$$

$$b = \frac{\Omega_{bc}\ R\ T_c}{P_c}$$

$$c = \frac{\Omega_{cc}\ R\ T_c}{P_c}$$

$\Omega_{ac} = 3\zeta_c^{\,2}+3(1-2\zeta_c)\ \Omega_{bc}+\Omega_{bc}^{\,2}+1-3\zeta_c$

$\Omega_{bc}^{\,3}+(2-3\zeta_c)\ \Omega_{bc}^{\,2}+3\zeta_c^{\,2}\ \Omega_{bc}-\zeta_c^{\,3} = 0$

$\Omega_{cc} = 1-3\zeta_c$

$\zeta_c = 0.329032-0.076799\omega+0.0211947\omega^2$

$\alpha(T_r) = [1+m(\omega)\ (1-T_r^{\frac{1}{2}})]^2$

$m(\omega) = 0.452413+1.30982\omega-0.295937\omega^2$

6. TSRK
(1982)

$$P = \frac{RT}{v - b} - \frac{a}{v\ (v+b)}$$

$$a = \frac{\alpha(T_r)\ \Omega_{ac}\ R^2T_c^{\,2}}{P_c}$$

$$b = \frac{\Omega_{bc}\ R\ T_c}{P_c}$$

$v' = v - c$

$b' = b - c$

$$c = \frac{\Omega_{cc}\ R\ T_c}{P_c}$$

$\Omega_{ac} = 0.42747$

$\Omega_{bc} = 0.08664$

$\Omega_{cc} = 0.40768\ (0.29441-Z_{RA})$

$Z_{RA} = 0.00385+0.08775\omega$

$\alpha(T_r) = [1+m(\omega)\ (1-T_r^{\frac{1}{2}})]^2$

$m(\omega) = 0.480+1.574\omega-0.176\omega^2$

cont'd.

7. 3RK
(1983)

$$P = \frac{RT}{v - b} - \frac{a}{v\,(v+c)}$$

$$a = \frac{\alpha(T_r)\,\Omega_{ac}\,R^2T_c^2}{P_c}$$

$$b = \frac{\Omega_{bc}\,R\,T_c}{P_c}$$

$$c = \frac{\Omega_{cc}\,R\,T_c}{P_c}$$

$\beta_c = 0.260796-0.0682692\omega-0.0367338\omega^2$

$C = \{[(4/\beta_c)-3]^{1/2} - 3\}/2$

$A_0 = \beta_c\,(1+C)^3/(1-\beta_c)^3$

$\zeta_c = [1/(1-\beta_c)] - [A_0/(1+C)]$

$\Omega_{ac} = A_0\,\zeta_c$

$\Omega_{bc} = \beta_c\,\zeta_c$

$\Omega_{cc} = C\,\zeta_c$

$\alpha(T_r) = [1+m(\omega)\,(1-T_r^{1/2})]^2$

$m(\omega) = 0.479817+1.55553\omega-0.287787\omega^2$

8. MMC
(1979)

$$P = \frac{RT}{v - b} - \frac{a}{(v^2+c)^2}$$

$$a = \frac{\alpha(T_r)\,\Omega_{ac}\,R^2T_c^2}{P_c}$$

$$b = \frac{\Omega_{bc}\,R\,T_c}{P_c}$$

$$c = \frac{\Omega_{cc}\,R\,T_c}{P_c}$$

$\Omega_{ac} = 27/64$

$\Omega_{bc} = 0.857Z_c-0.1674$

$\Omega_{cc} = -0.857Z_c+0.2924$

$Z_c = 0.291-0.08\omega$

$\alpha(T_r) = [1+m(\omega)\,(1-T_r^{1/2})]^2$

$m(\omega) = 0.499932+1.78183\omega-1.17231\omega^2+1.42463\omega^3$

$\zeta_c = 0.857Z_c+0.0826$

9. Cl
(1983)

$$P = \frac{RT}{v - b} - \frac{a}{(v - d1)\,(v - d2)}$$

$$a = \frac{\alpha(T_r)\,\Omega_{ac}\,R^2T_c^2}{P_c}$$

$$b = \frac{\Omega_{bc}\,R\,T_c}{P_c}$$

$$d1 = \frac{\Omega_{d1}\,R\,T_c}{P_c}$$

$$d2 = \frac{\Omega_{d2}\,R\,T_c}{P_c}$$

$v' = v - c$

$$c = \frac{\Omega_c\,R\,T_c}{P_c}$$

$\Omega_{ac} = 0.456533$

$\Omega_{bc} = \zeta_c - 0.23$

$\Omega_{d1} = \zeta_c - 0.276106$

$\Omega_{d2} = \zeta_c - 0.493894$

$\omega \leq 0.090$

$\zeta_c = 0.319$

$\omega > 0.090$

$\zeta_c = 0.2910+0.04421\,\exp(-6.46361\omega)$

$\Omega_c = 0.02802-0.02787\,\omega - 0.04421\,\exp(-6.46361\omega)$

cont'd.

10. ALS (1982)

$$P = \frac{RT}{v - b} - \frac{a}{(v-d1)\,(v-d2)}$$

$$a = \frac{\alpha(T_r)\,\Omega_{ac}\,R^2T_c^{\,2}}{P_c}$$

$$b = \frac{\Omega_{bc}\,R\,T_c}{P_c}$$

$$d1 = \frac{\Omega_{d1}\,R\,T_c}{P_c}$$

$$d2 = \frac{\Omega_{d2}\,R\,T_c}{P_c}$$

$$\Omega_{ac} = 0.44869+0.04024\omega+0.01111\omega^2-0.00576\omega^3$$

$$\Omega_{bc} = 0.08974-0.03452\omega+0.00330\omega^2$$

$$\Omega_{d1} = 0.03686+0.00405\omega-0.01073\omega^2+0.00157\omega^3$$

$$\Omega_{d2} = 0.15400+0.14122\omega-0.00272\omega^2-0.00484\omega^3$$

$$\alpha(T_r) = [1+m(\omega)\,(1-T_r^{0.5})]^2$$

$$m(\omega) = 0.4070+1.3787\omega-0.2933\omega^2$$

Many attempts (see for example [57]) were made to improve the RK equation. One of the modifications of the RK equation for mixture VLE calculations which has received extensive testing is that proposed by Soave [119]. The Soave-Redlich-Kwong (SRK) equation has acquired wide popularity in the hydrocarbon industries and has proven to be one of the most successful equations proposed to date. He fitted the parameter a directly to the vapor pressures of pure nonpolar substances, and correlated it by a simple function of T_r as shown below

$$a = [1+m(\omega)\cdot(1-T_r^{\frac{1}{2}})]^2 a_c \qquad (3.1)$$

where $m(\omega)$ is a function of the acentric factor ω.

Since the basic mathematical model of the original RK equation is not changed, the SRK equation has the same shortcomings as the RK equation. It is still unable to generate satisfactorily the saturated liquid molar volumes for large molecules, even though the calculated saturated vapor volumes are generally acceptable. In the prediction of liquid or saturated liquid volumes the SRK equation is only suitable for small molecules like nitrogen or methane.

In 1976, Peng and Robinson (PR) [88] proposed another equation to improve the VDW EOS by assuming u=2,w=-1. In a short time, the PR equation has found wide application in natural gas and petroleum technology. Following the same approach as Soave, the parameter a in the PR equation was fitted to pure-component vapor pressures and the same expression for the temperature function was retained. However, it gives a more realistic ζ_c (=0.307). The PR equation shows a significant

improvement over the SRK equation in the prediction of volumetric properties, especially saturated liquid volumes for molecules larger than nitrogen and methane. Nevertheless, for accurate calculation of (saturated) liquid volumes the PR equation is only suitable for molecules whose size is close to that of n-hexane.

To date, among the available volume-cubic equations, the SRK and the PR equations are the most widely used for fluid phase equilibrium calculations. These two equations though derived only for subcritical conditions are extrapolated in practice above the critical temperature.

3.1.2 Three Adjustable One Temperature Dependent Parameter Equations of State

It was often thought [2] that the ability of an EOS to yield substance-dependent critical compressibility factor was a necessary condition for better performance, especially in the representation of (saturated) liquid molar volumes. To obtain substance dependent ζ_c, the EOS must contain more than two substance dependent parameters while satisfying the two derivatives at the critical point (Eqs(2.31a,31b)).

In the development of the 3P1T EOS the forms of the VDW, the RK and the PR equations were often used as building blocks in order to reduce Eq.(1.3) to a three-parameter equation. With a third adjustable parameter in addition to a and b, Eq.(1.3) gives a value of ζ_c which is substance dependent. Again, only the parameter a is temperature dependent while the remaining two parameters depend on substance only.

Using the RK and the PR equations as building blocks, Schmidt and Wenzel (SW) in 1980 [114], Harmens and Knapp (HK) in 1980 [49] and Patel and Teja (PT) in 1982 [89] proposed equations, which after rearrangement, are of identical mathematical form. The form was found by assuming $u*w=1$ so that Eq.(1.3) becomes

$$P = \frac{RT}{v - b} - \frac{a}{v^2+(1-c)bv+cb^2} \qquad (3.2)$$

where the parameter c is equivalent to the parameter w. It should be noted that the line $u*w=1$ contains the points (u,w) that correspond to those of the SRK and the PR equations. This can be seen from a u-w diagram as shown in Figure 3.1.

Although the equations are of the same mathematical form, these authors established different procedures to determine the three parameters for each substance considered. Schmidt and Wenzel adjusted the parameters so as to fit saturated liquid molar volumes at $T_r=0.7$. Instead of fitting saturated liquid molar volumes at a single point, Patel and Teja used the temperature range from the normal boiling point to the critical to determine their three parameters. As for the HK equation, the three parameters were adjusted so that Eq.(3.2) gave a 'compromise' fit along the critical isotherms up to $P_r=5$. At subcritical temperatures, all these equations had temperature dependence introduced to the parameter a by fitting the vapor pressures using the procedure proposed by Soave [119]. The correlations were of a form similar to that of Eq.(3.1). At supercritical temperatures, values of the parameter a in the SW and the PT equations were usually estimated by extrapolating the subcritical temperature function. However, in the HK

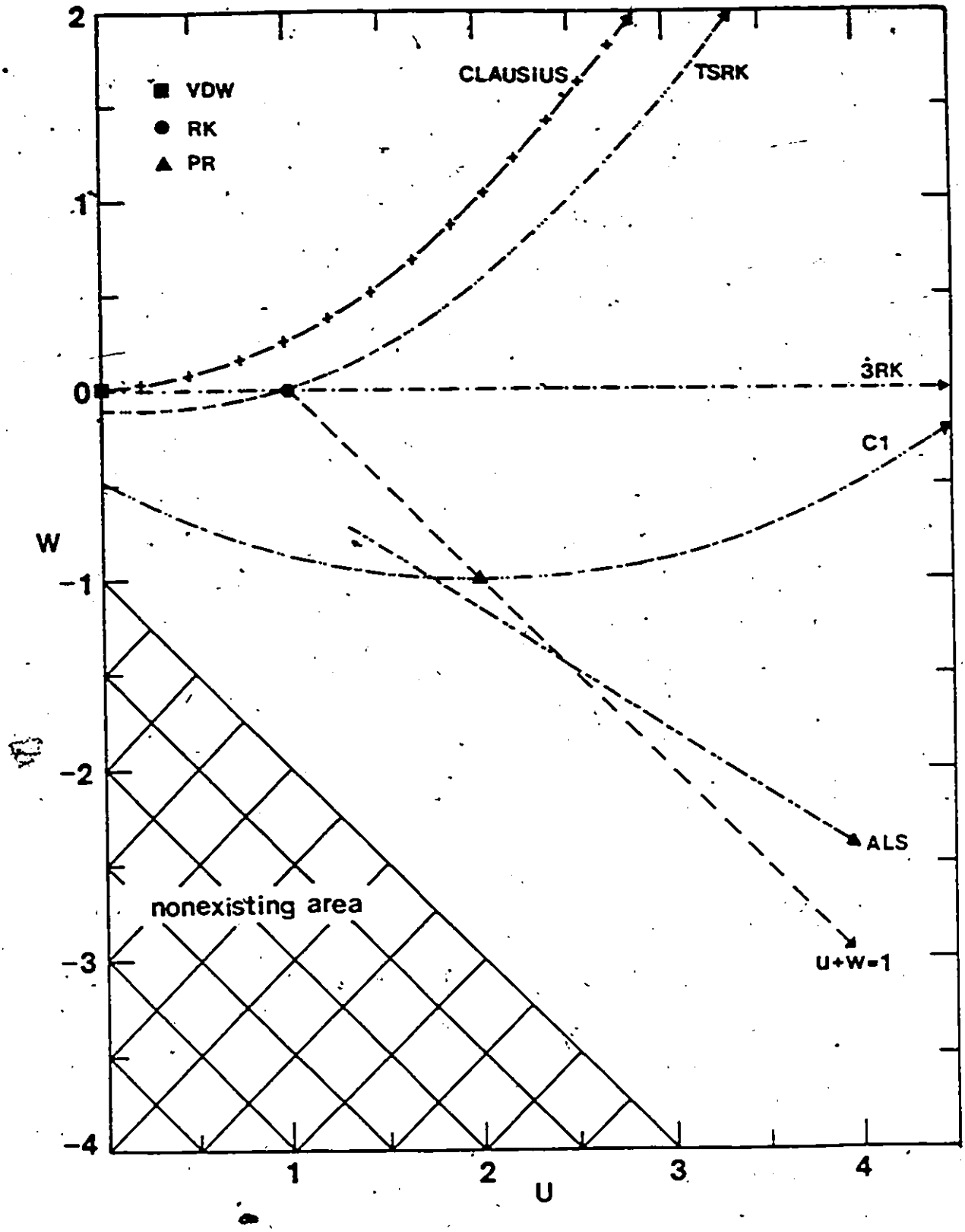

Figure 3.1: Loci of (u,w) of the well-known equations of state

EOS the temperature function for the parameter a was based on the isochor data at $P_r=1$, for $T_r>1$. Details of this function are presented in Table 3.1. Of the three equations, the SW equation was the most extensively tested [40,112,113].

Another approach to formulating the 3P1T equation requires only one two-parameter equation to serve as the building block. This corresponds to the volume-translation method proposed by Peneloux, Rauzy and Freze in 1982 [87]. The basic idea behind this method was to introduce a third substance dependent parameter, c, that would correct the volume predicted by the selected two-parameter equation without changing the equilibrium condition originally predicted. From a physical point of view, this is simply translating along the V-axis the saturation dome or the isotherms on the P-V surface generated by the two-parameter EOS without changing their original shape. In so doing the equal-fugacity condition at each temperature will not be affected. Thus, the predictions of the equilibrium conditions and of the vapor pressures are never affected by the translation. The relationship between the volume before translation and the volume after translation (designated as v') is

$$v'=v-c \tag{3.3a}$$

$$b'=b-c \tag{3.3b}$$

and the corresponding relation for the fugacity is:

$$\ln\left(\frac{f'}{P}\right) = \ln\left(\frac{f}{P}\right) - \left(\frac{cP}{RT}\right). \tag{3.4}$$

where f' is the fugacity after translation. At the equal-fugacity condition, the term cP/RT in Eq.(3.4) is cancelled out.

Peneloux, Rauzy and Freze [87] applied this method to the SRK equation in order to correct its predicted saturated liquid molar volumes. The SRK equation was chosen due to its ability in predicting mixture VLE (P-T-composition) with reasonable accuracy. Substituting Eq.(3.3) into the SRK EOS, the translated equation, (TSRK) has the form

$$P = \frac{RT}{v' - b'} - \frac{a}{(v'+c)(v'+b'+2c)} \qquad (3.5)$$

Rearranging Eq.(3.5) to a form of Eq.(1.3) gives

$$P = \frac{RT}{v - b} - \frac{a}{v^2+[1+(3c/b)]bv+[(c/b)+(2c^2/b^2)]b^2} \qquad (3.6)$$

where u and w are related by $w=(2u^2-u-1)/9$ with $u = (1+3c/b)$. Thus Eq.(3.6) is a three-parameter equation. It should be noted that whatever temperature function is adopted in the SRK EOS for the parameter a Eq.(3.6) will yield exactly the same vapor pressures as those obtained from the SRK equation. This implies that the quantity Ω_{ac} in Eq.(2.31) remains unchanged since the parameter a can be expressed as

$$a = \alpha(T_r)\, a_c \qquad (3.7)$$

where $\alpha(T_r)$ remains the same as in the original equation in which Ω_{ac} is a universal constant. The most obvious characteristic of a three-parameter EOS obtained by a volume-translation is that the equation has a constant Ω_{ac}. Other types of three-parameter EOS have substance dependent Ω_{ac}. To illustrate, the locus of (u,w) given by the TSRK

equation is depicted on a u-w diagram as shown in Figure 3.1. The loci of (u,w) for the SW, the HK and the PT equations are also shown in Figure 3.1 as indicated by the line u+w=1. Also indicated in Figure 3.1 are the locations of the SRK and the PR equations. As will be seen in Chapter IV, the locus of (u,w) for the TSRK equation is a typical example of the constant-Ω_{ac} curve on the u-w diagram. In fact, constant-Ω_{ac} curve represents a family of EOS which result from the volume translation of a two-parameter EOS with the same Ω_{ac}.

Another example of this idea is the three-parameter equation proposed by Clausius in 1880 [21]

$$P = RT/(v-b) - [a/(v+c)^2] \qquad (3.8)$$

where c is the third parameter. The Clausius equation is the simplest three-parameter EOS. When Eq.(3.8) is rearranged into the form of Eq.(1.3), parameters u and w are related by $w = u^2/4$. Eq.(3.8) results from a volume translation of the VDW equation. Both these equations have identical values of Ω_{ac} (=27/64). The Clausius equation is depicted in Figure 3.1. Its locus of (u,w) passes through the point for the VDW EOS. The original Clausius equation contains no temperature function and therefore is of no practical use when representing fluid properties. Martin in 1979 [70] modified the Clausius equation by adjusting the parameter c to fit vapor molar volumes and introduced a temperature function to the parameter a based on the slopes of the critical isochor and the vapor pressure curve at the critical point. Martin claimed this form of the Clausius equation to be the 'best' volume-cubic equation for representing volumetric properties. The

temperature function was subsequently modified by Adachi and Lu in 1983 [6] by adopting the expression in Eq.(3.1) for the parameter a and thereby calculated it using vapor pressure data. This modified version, designated as the MMC equation in Table 3.1, thus became suitable for VLE calculations.

As shown in the Appendix A, any equation in which u and w are related by the following expression is merely a volume translation of any two-parameter EOS with the same Ω_{ac}

$$w' = w+[(4w-u^2)/(2+u)^2]\,u' + [(1+u+w)/(2+u)^2]\,u'^2$$

$$- [(u+2w)/(2+u)]\,u'+ [(1+u+w)/(2+u)^2]\,u^2 \qquad (3.9)$$

in which u' and w' are the parameters u and w of the volume-translated EOS. Eq.(3.9) can be used to represent all the constant-Ω_{ac} curves on the u-w diagram. Assigning particular values to u and w in Eq.(3.9) for a given u' and substituting into Eq.(1.3) reduces it to a three-parameter volume-translated equation. As examples, Table 3.2 presents three cases of volume translation involving the VDW, the SRK and the PR equations.

The volume-translated EOS corresponding to the PR equation closely resembles the C1 equation developed by Freze, Chevalier, Peneloux and Rauzy in 1983 [33]. The C1 equation has a constant Ω_{ac} (=0.45653) close to that of the PR equation in which Ω_{ac}=0.45724. It was developed first from binary VLE data (P-T-composition) and then translated for the calculation of liquid compressibility factors for normal hydrocarbons. Details of the C1 equation are included in Table 3.1 and

Table 3.2: The volume-translated VDW, SRK and PR equations of state.

EOS	u	w	Ω_{ac}	Translated EOS	
VDW	0	0	27/64	$w = u^2/4$	Clausius
SRK	1	0	0.42747	$w = (2u^2-u-1)/9$	TSRK
PR	2	-1	0.45724	$w = (u^2-4u-4)/8$	TPR (= C1)

its locus of (u,w) is plotted in Figure 3.1. It should be noted that the C1 EOS was originally developed as a four-parameter equation of the form

$$P = \frac{RT}{v - b} - \frac{a}{(v-d1)(v-d2)} \qquad (3.10)$$

where a, b, d1 and d2 are the four parameters. Eq.(3.10) is equivalent to Eq.(1.3) since its parameters d1 and d2 correspond to the two roots of $v^2+ubv+wb^2=0$. Based on the above discussion, the C1 equation could also have been developed from a two-parameter EOS together with the volume-translation relation in Eq.(3.9).

It is worth noting that the three-parameter equation proposed by Usdin and McAuliffe in 1976 [131] is another example in which a single two-parameter EOS was used as a building block. The equation, based on the RK equation, is

$$P = \frac{RT}{v - b} - \frac{a}{v^2+ubv} \qquad (3.11)$$

The parameter u was obtained by fitting saturated liquid molar volumes, while the parameter a was determined using the vapor pressure data. Unfortunately, this equation is inconvenient to use since its parameters are not generalized. Eq.(3.11) was also studied by Fuller in 1978 [34] who treated all the three parameters as function of temperature.

If c = ub, Eq.(3.11) assumes a form as

$$P = \frac{RT}{v - b} - \frac{a}{v\,(v+c)} \qquad (3.12)$$

where c is the third parameter. Harmens in 1980 [48] pointed out that Eq.(3.4) may be of a better form than Eq.(3.12) for representing saturation properties. In 1983, Adachi and Lu [6] reworked Eq.(3.12). They adopted the same approach for treating the parameters as Usdin and McAuliffe but were able to provide a complete generalization of the three parameters, a, b and c. The resulting equation designated as 3RK, is presented in Table 3.1 and its locus is plotted in Figure 3.1.

3.1.3 Four Adjustable One Temperature Dependent Parameter Equations of State

In 1982, Adachi, Lu and Sugie (ALS) [5] proposed a four-parameter equation of the form of Eq.(3.10). Similar to Harmens and Knapp [50] they optimized the four parameters (a, b, d1, d2) by fitting the critical isotherms of normal fluids generated from the tabulated Pitzer's correlation [90]. Temperature dependence was introduced to the parameter a using Soave's correlation in Eq.(3.1). The locus of (u,w) for the ALS equation is depicted in Figure 3.1. As can be seen, it goes in approximately the same direction as those of the SW, the HK and the PT

equations. It appears that its locus could be approximated by a simple mathematical relationship such as a straight line and therefore the ALS EOS could be reduced to a three-parameter equation.

In summary, the parameters of all the 2P1T, 3P1T and 4P1T equations described in Table 3.1 were generalized quite well by means of the three-parameter (T_c, P_c, ω) corresponding states principle. Temperature dependence was introduced to the parameter a by fitting it to vapor pressures. In most cases, the temperature functions were extrapolated for calculations at supercritical temperatures. Using one or two parameters in addition to a and b enables the equations to predict substance dependent critical compressibility factors.

3.1.4 Two Adjustable Two Temperature dependent Parameter Equations of State

In the 2P2T type equations the parameters a and b are considered as functions of temperature, while the parameters u and w are kept as universal constants. The RK equation has been used extensively as the basis for the development of this type of equation.

At each given temperature, the parameters a and b are either fitted to PVT data outside the saturation dome, or are fitted simultaneously to the vapor pressure and saturated liquid molar volume. The former case was adopted by Chaudron and Renon [20]. But the resulting EOS is not suitable for VLE calculations, since the equal-fugacity condition is not satisfied.

Table 3.3: Summary of the 2P2T, 3P2T and 3P3T types of equations

11. HCL (1977)

$$P = \frac{RT}{v - b} - \frac{a/T^{1/2}}{v\,(v+b)}$$

$$a = \frac{\Omega_a(T_r)\, R^2 T_c^{2.5}}{P_c}$$

$$b = \frac{\Omega_b(T_r)\, R\, T_c}{P_c}$$

$0.85 \le T_r \le 1.0$

$$\Omega_a = a_0 + a_1 (1-T_r) + a_2 (1-T_r)^{1/2} + a_3 (1-T_r)^{3/2}$$

$$\Omega_b = c_0 + c_1 (1-T_r) + c_2 (1-T_r)^{1/2} + c_3 (1-T_r)^{3/2}$$

$$a_i = \sum_{j=0}^{2} (a_{ij}\, \omega^j), \quad c_i = \sum_{j=2}^{2} (d_{ij}\, \omega^j) \quad (i = 0,1,2,3)$$

$T_r \le 0.85$

$$\Omega_a = \sum_{i=0}^{2} (b_i\, T_r^{\,i}), \quad \Omega_b = \sum_{i=0}^{2} (d_i\, T_r^{\,i})$$

$$b_i = \sum_{j=0}^{2} (b_{ij}\, \omega^j), \quad d_i = \sum_{j=2}^{2} (d_{ij}\, \omega^j) \quad (i = 0,1,2)$$

12. H (1983)

$$P = \frac{RT}{v - b} - \frac{a}{v^2 + (b+e)v - eb}$$

$$a = \frac{\alpha(T_r)\, \Omega_{ac}\, R^2 T_c^{\,2}}{P_c}$$

$$b = \frac{\beta(T_r)\, \Omega_{bc}\, R\, T_c}{P_c}$$

$$e = \frac{\Omega_e\, R\, T_c}{P_c}$$

$$\Omega_{ac} = 3 Z_c^{\,2} + 2 \Omega_{bc} \Omega_c + \Omega_{bc} + \Omega_c + \Omega_{bc}^2$$

$$\Omega_{bc} = 0.32429\, Z_c - 0.022005$$

$$\Omega_e = 1 - 3 Z_c$$

$$Z_c = 0.2905 - 0.0085\omega$$

$$\alpha(T_r) = \exp[\, \kappa(\omega)\, (1 - T_r^{\,n(\omega)})]$$

$$\kappa(\omega) = 0.49164 + 0.43882\omega - 0.08821\omega^2$$

$$n(\omega) = 1.637 + 1.389\omega$$

$$\beta(T_r) = 1 - m(\omega)\, \tanh[\frac{\theta(\omega)}{2}\, (T_r - 1)]$$

$$m(\omega) = 0.23333 - 0.06737\omega + 0.49110\omega^2$$

$$\theta(\omega) = 7.2562 + 14.153\omega + 1.33137\omega^2$$

cont'd.

13. KMC (1982)

$$P = \frac{RT}{v - b} - \frac{a}{(v+c)^2}$$

$$a = \frac{\alpha(T_r)\ \Omega_{ac}\ R\ T_c}{P_c}$$

$$b = \frac{\Omega_{ac}\ R\ T_c}{P_c}$$

$$c = \frac{\Omega_c(T_r)\ R\ T_c}{P_c}$$

$\Omega_{ac} = 27/64$

$\Omega_{bc} = 0.082 - 0.0713\omega^*$

$\alpha(T_r) = \alpha_0(T_r) + \omega^* \alpha_1(T_r)$

$\alpha_0(T_r) = -0.1514\ T_r + 0.7895 + 0.3314/T_r + 0.029/T_r^2 + 0.0015/T_r^7$

$\alpha_1(T_r) = -0.237\ T_r - 0.7846/T_r + 1.0026/T_r^2 + 0.019/T_r^7$

$\Omega_c(T_r) = 0.043\ \gamma_0(T_r) + 0.0713\omega^*\ \gamma_1(T_r)$

$\gamma_0(T_r) = 4.275051 - 0.878889/T_r + 8.508932/T_r^2 - 3.481498/T_r^3 + 0.576312/T_r^4$

$\gamma_1(T_r) = 12.856404 - 34.744125/T_r + 37.433095/T_r^2 - 18.059421/T_r^3 + 3.514050/T_r^4$

$\omega^* = 0.000756 + 0.90984\omega + 0.16226\omega^2 + 0.14549\omega^3$

$\zeta_c = 0.291 - 0.083\omega$

14. F (1976)

$$P = \frac{RT}{v - b} - \frac{a}{v\,(v+cb)}$$

$$a = \frac{\alpha(T_r)\ \Omega_a\ R^2 T_c^2}{P_c}$$

$$b = \frac{\Omega_b(T_r)\ R\ T_c}{P_c}$$

$$c = [(\frac{1}{\beta} - \frac{3}{4}) - \frac{3}{2}]/\beta$$

$\Omega_a = [(1+c\ \beta)^2\ \Omega_b]/[\beta\ (1-\beta)^2\ (2+c\ \beta)]$

$\Omega_b = \beta\ [(1-\beta)(2+c\ \beta) - (1+c\ \beta)]/[(2+c\ \beta)(1-\beta)^2]$

$\beta = \beta_c\ [1 + (\frac{\beta_0}{\beta_c} - 1)[\frac{2}{1+[\exp(\theta\ (T_r - 1))]} - 1\ ]$

$\beta_0 = \beta_c\ [7.7880 - 36.8316 Z_c + 50.7061 Z_c^2]$

$\zeta_c = \dfrac{(1-\beta_c)(2+c_c\ \beta_c) - (1+c_c\ \beta_c)}{(2+c_c\ \beta_c)(1-\beta_c^2)}$

$c_c = [(\frac{1}{\beta_c} - \frac{3}{4}) - \frac{3}{2}]/\beta_c$

$\theta = 10.9356 + 0.0285\ P$ (P -- parachor)

$Z_c = 0.290 - 0.085\omega$

$\alpha(T_r) = [1 + q(\beta)\ (1 - T_r^{1/2})]^2$

$q(\beta) = (\beta/0.26)^{1/2}\ m(\omega)$

$m(\omega) = 0.480 + 1.5740\omega - 0.176\omega^2$

As for the latter case, both parameters a and b show strong minima with temperature as the the critical point is approached. Consequently, generalization of the temperature dependence of parameters a and b in the vicinity of the critical point becomes very difficult. Several authors [45,46,144] have tried to tackle this problem. In 1977, Hamam, Chung and Lu (HCL) [45] used two equations to represent the temperature dependence of each parameter in the two temperature ranges of $0.60 \leq T_r \leq 0.85$ and $0.85 \leq T_r \leq 1.0$. However the temperature functions used in the HCL equation are limited to subcritical temperatures. For supercritical temperatures, values of the parameters a and b must be those at the critical point. Also the two temperature functions used for the parameters are not continuous at $T_r=0.85$, and may give inconsistent predictions of the saturation dome in the vicinity of this temperature.

3.1.5 Three Adjustable Two Temperature Dependent Parameter Equations of State

Compared to the 2P2T type of equation, the main advantage of the 3P2T equation is that the predicted ζ_c is substance dependent. Therefore it is expected that these equations will perform better in the vicinity of the critical point. Two equations of this type worth noting are the Heyen (H) equation [53] and the Kubic (KMC) equation [65]. Both equations are summarized in Table 3.3.

The H equation has the following form

$$P = \frac{RT}{v - b} - \frac{a}{v^2+(b+e)v-eb} \qquad (3.13)$$

where both parameters a and b are functions of temperature, and were determined using vapor pressures and saturated liquid molar volumes. When Eq.(3.13) is rearranged into the form of Eq.(1.3), it is then of a form identical to that of the SW, the HK and the PT equations, i.e., Eq.(3.2). In this case, the parameter c in Eq.(3.2) is defined as c=-e/b. It should be noted that at the critical point values of a, b and e were adjusted so that the predicted ζ_c be identical with the experimental one. In order to generalize the parameters the experimental compressibility Z_c, is required in addition to T_c, P_c and ω.

Kubic developed his equation based on the Martin's [70] modified version of the Clausius equation. He determined the temperature functions for the parameters a and c using second virial coefficients and vapor pressures respectively. All the parameters in the KMC equation can be generalized in terms of T_c, P_c and ω. At the critical point, Kubic retained the generalized correlations proposed by Martin [70] for the parameters a, b and c (designed a_c, b_c and c_c, respectively).

All temperature functions in both the H and the KMC equations can be extrapolated for calculations at supercritical temperatures.

3.1.6 Three Adjustable Three Temperature Dependent Parameter Equations of State

It is possible when all the parameters of a three-parameter equation are temperature dependent to represent accurately all three saturation properties i.e., the vapor pressure and the saturated liquid and vapor molar volumes. A typical example is the equation proposed by Fuller

[34]. As mentioned earlier, Fuller's equation, summarized as the F equation in Table 3.3, was developed from the form of Eq.(3.11). The three parameters (a, b and c) were fitted along the saturation curve.. It was found, as shown in the original paper, that correlations of the temperature dependence of the three parameters are very complex. Also generalization of the parameters at the critical point requires four characteristic constants, T_c, P_c, Z_c and the Parachor (P) [95]. Values of the Parachor may not be available for all substances of interest. Thus this reduces the application of the equation. In addition, the temperature functions used in the F equation were found in this study to be unsuitable for supercritical calculations. Extrapolation of these functions led to large errors in predicting the volumetric properties of gases. The calculated results could be improved only if the temperature function for the parameter a was extrapolated while the values of b and c remained those at the critical point.

Summarized in Table 3.4 are features of the equations discussed herein. In general the 2P2T and the 3P2T types of equations have more complicated temperature functions than the 2P1T, the 3P1T and the 4P1T equations whose temperature functions are more easily generalized. Both Abbott [3] and Adachi and Lu [6] have warned that using more temperature functions does not render the equation capable of representing volumetric properties in a PVT range in which the parameters were not adjusted. However it is still not clear which type of equations is more suitable for representing volumetric properties over a wide PVT range. Consequently the fourteen equations in Tables 3.1 and 3.3. were evaluated in calculating several volumetric and thermo-

dynamic properties over a wide range of conditions. These results are presented in the next section.

Table 3.4: Features of the volume-cubic equations of state

$$P = \frac{RT}{v-b} - \frac{a}{v^2+ubv+wb^2}$$

TYPE	EOS	u	w	a	b	Fitted Properties
	VDW	0	0	a_c	b_c	none
2P1T	RK	1	0	$a_c/T^{\frac{1}{2}}$	b_c	none
	SRK	1	0	a(T)	b_c	P^v
	PR	2	-1	a(T)	b_c	P^v
3P1T	HK	1-w	f(ω)	a(T)	b_c	P^v, Critical Isotherm
	SW	1-w	f(ω)	a(T)	b_c	$P^v, v^l (T_r=0.7)$
	PT	1-w	f(ω)	a(T)	b_c	$P^v, v^l (T_r = 0.6$ to $1.0)$
	3RK	f(ω)	0	a(T)	b_c	P^v, v^l
	MMC	f(ω)	$u^2/4$	a(T)	b_c	P^v
	TSRK	f(ω)	$(2u^2-u-1)/9$	a(T)	b_c	P^v, v^l
	C1	f(ω)	$=(u^2-4u-4)/8$	a(T)	b_c	P^v, Z^l
4P1T	ALS	f(ω)	f(ω)	a(T)	b_c	P^v, Critical Isotherm
2P2T	HCL	1	0	a(T)	b(T)	P^v, v^l
3P2T	H	1-w	f(ω,b)	a(T)	b(T)	P^v, v^l
	KMC	f(ω)	$u^2/4$	a(T)	b(T)	P^v,B
3P3T	F	f(T)	0	a(T)	b(T)	p^v, v^l, v^v

3.2 Evaluation of the Well-Known Volume-Cubic Equations

The properties of the first ten normal alkanes (methane to n-decane) obtained from generalized correlations and tabulations available in the literature were used as the basis for comparing the performance of the fourteen equations. The ten normal alkanes were selected because their properties conform well to Pitzer's three-parameter (T_c, P_c ω) corresponding states principle. Also the acentric factors of these fluids range from 0.0 to 0.5. A total of eight properties were considered. Data on these fluids available in the literature were not used for the present purpose due to the fact that they cover limited ranges of pressure and temperature. The vapor pressures, P^v , were obtained from the correlations proposed by Gomez-Nieto and Thodos [39] for nonpolar substances. The saturated liquid molar volumes, v^ℓ, were obtained from a modified Rackett equation using the input parameters suggested by Spencer and Alder [120]. The saturated vapor molar volumes, v^v, were obtained from the correlation of Barile and Thodos [12]. The second virial coefficients, B, were obtained from the correlation of Tsonopoulos [128]. For these four properties, the correlation-generated data points were taken at 0.02 intervals in the T_r range from 0.50 to 0.80 and at T_r equals 0.85, 0.90, 0.95 and 0.98 for a total of twenty T_r values. This range corresponds to a temperature between the triple and the normal boiling points and up to the critical point. The tabulated correlation of Lee and Kesler [66] was used to obtain the values of the liquid compressibility factor, Z^ℓ, ($0.30 \le T_r \le 0.99$, $0.01 \le P_r \le 4.00$ -315 points), vapor compressibility factor, Z^v, ($0.55 \le T_r \le 0.99$, $0.01 \le P_r \le 0.80$ -56 points), gas compressibility factor

above the critical temperature, Z^{sup}, ($1.01 \leq T_r \leq 4.00$, $0.01 \leq P_r \leq 10.0$ -240 points) and compressibility factor along the critical isotherm, Z^c, ($T_r = 1.0$, $0.01 \leq P_r \leq 10.0$ -15 points). For normal alkanes these correlations were shown by the original authors to be accurate with absolute average errors less than 0.5% when compared with data available in the literature.

A summary of the calculated results in terms of the overall average absolute percent deviations is presented in Table 3.5. The average absolute percent deviation (AAPD) is defined as follows:

$$AAPD = \frac{1}{ND}\sum_{1}^{ND} |[(\text{calculated} - \text{actual})/\text{actual}]| \times 100 \qquad (3.14)$$

where ND is the number of data points. It should be noted that the results presented may be slightly different from those obtained using similar calculations but different intervals for T_r and P_r. However as long as the range of T_r and P_r are approximately the same, the same conclusion about the ability of the equations should be obtained.

Upon examining Table 3.5, one can see that almost all equations yield acceptable results in predicting P^v. The only exception is the Heyen equation. Large errors given by this equation are mainly caused by inaccurate generalization of the parameters in the equation. On the other hand, the C1 equation gives the best results. Of the remaining equations the PR, the MMC, the ALS and the KMC equations have relatively larger errors in P^v than the others. For predicting v^l the MMC and the SRK equations yield the largest deviations. Deviations in the calculated v^v values resemble those for P^v, whereas deviations in the Z^l values are similar to those for v^l.

Table 3.5: Summary of overall average absolute percent deviations in the calculated physical properties of ten normal alkanes

Property		SRK	PR	HK	SW	PT	3RK	MMC	TSRK	CI	ALS	HCL	H	KMC	F
P^v	200	1.51	2.55	1.02	1.44	1.95	1.29	2.33	1.51	0.96	2.75	1.88	10.5	3.56	1.8
v^l	200	13.4	5.47	4.37	2.78	2.56	4.00	12.4	3.77	3.65	2.66	0.65	2.26	5.41	2.0
v^v	200	1.23	2.54	1.45	1.22	2.01	1.08	2.51	1.20	1.26	2.59	4.10	10.3	4.01	1.9
Z^l	3150	11.2	4.96	4.14	2.96	3.03	3.37	12.6	3.67	3.93	3.13	2.61	5.53	13.5	5.2
Z^v	560	0.95	0.58	0.55	0.38	0.40	0.56	0.44	0.64	0.49	0.45	2.24	2.24	0.19	0.9
Z^{sup}	2400	2.37	1.54	1.47	1.41	1.28	1.36	1.89	1.35	1.30	1.30	2.98	3.72	2.09	6.1
Z^c	150	8.50	4.68	4.05	4.08	4.13	4.92	5.24	5.42	6.24	4.00	8.37	8.90	5.32	12.6
B	200	17.2	15.5	15.1	15.6	15.4	15.9	15.4	16.1	15.6	15.4	23.2	16.9	1.71	17.4

In predicting Z^v, Z^{sup} and Z^c the results obtained from the equations which contain only one temperature-dependent parameter do not differ from one another and have much smaller deviations than the HCL, the H and the F equations. Since the KMC EOS was fitted to second virial coefficients it therefore has the lowest deviations in the calculated B values. Meanwhile it also has the smallest deviations in the calculated Z^v values. This seems to imply that incorporation of the second virial coefficient in an equation would result in good representation of Z^v. However, the poor predictions of B as given by the other equations tested seem not to have an effect on the representation of Z^v.

Although some of the findings mentioned above could have been deduced from the features of the equations listed in Table 3.4, several additional points revealed by the results in Table 3.5 are

1. The currently popular equations (SRK and PR) do not give the best results.
2. The inferior overall performance of the equations containing more than one temperature dependent parameter indicates that these equations are only suitable for representing the properties used in the fitting procedure.
3. The equations of the Clausius type that were tested do not appear to be 'the best' as Martin had claimed.
4. The equations containing only one temperature dependent parameter have better overall performance in the representation of volumetric properties (v^l, v^v, Z^l, Z^v, Z^{sup}, Z^c). Among them, the 3P1T and the 4P1T equations are usually better than the 2P1T equations. Although the ALS EOS has four adjustable

parameters it did not exhibit distinct superiority over some of the 3P1T equations. The performance of the six 3P1T equations (SW, HK, PT, 3RK, TSRK, C1) seems to be adequate.

Further examination of the deviations of the 2P1T and the 3P1T equations for individual alkanes (as shown in Table 3.6) reveals that

1. The ability to predict P^v has little to do with number of adjustable parameters in the equation. The accuracy in predicting P^v largely attributes to the accuracy in the generalization of the temperature dependence of parameter a which was obtained from the P^v values. Errors in P^v will generally increase with increasing molecular size of the fluid.
2. The PR EOS will yield larger deviations in P^v for larger molecules, and deviations in v^l will increase with increasing molecular size of the alkane.
3. For the SRK EOS, the deviations in v^l will also increase with increasing molecular size of the alkane.
4. All the equations have large deviations in B, and these increase with the molecular size of the alkane.
5. The TSRK EOS yields deviations in P^v identical to those of the SRK equation indicating that the volume-translation method does not affect the calculation of P^v.
6. As far as the deviations in v^l and Z^l are concerned, the PT and the SW equations appear to be comparable to or better than the HK equation, while all three equations fall into the same family represented by the u+w=1 relationship. Among the equations which result from a volume-translation (MMC, TSRK, C1),

the performance of the TSRK EOS is considered the best because the deviations for all the alkanes are about the same. The deviations of the C1 EOS tend to increase with molecular size. A comparison of the SW, the PT, the TSRK and the C1 equations reveals that equations with substance dependent Ω_{ac} give better representation of v^{ℓ} and Z^{ℓ}. In general, if an equation is able to represent one of these properties, it can also represent the other with the same degree of accuracy.

7. Although nearly all the equations have small deviations in the calculated Z^{v} and Z^{sup} values, there is a tendency to have larger deviations for alkanes with larger molecules. It is interesting to note that although the HK equation has a temperature function for the parameter a specially developed for calculations at supercritical temperatures it does not show any superiority in predicting Z^{sup}.

8. The family of equations represented by the u+w=1 relationship has smaller deviations in the Z^{c} values than the equations obtained from the volume-translation method. In addition, the individual deviations obtained from the former equations are about the same for each of the ten alkanes.

For the 2P2T, the 3P2T and the 3P3T types of equations, the results shown in Table 3.6 indicate that forcing the parameters of the equations to fit properties in a limited PVT range, may result in undesirable errors in other PVT regions. Comparison of the performance of the HCL and the F equations with the SRK equation demonstrates this problem. Fitting the parameters a and b in the RK EOS to both P^{v} and

Table 3.6: Average absolute percent deviations of the eight physical properties for ten normal alkanes.

	SRK	PR	MK	SW	PT	3RK	MMC	TSRK	CI	ALS	HCL	H	KMC	F
							Vapor Pressure, p^v ($0.50 < T_r < 0.98$)							
C_1	1.64	1.15	1.00	0.37	1.32	1.60	2.06	1.64	0.97	0.47	0.89	3.44	1.85	1.55
C_2	1.12	2.51	0.67	1.73	2.73	1.01	1.60	1.12	0.66	2.23	0.64	2.32	3.61	1.04
C_3	1.42	2.61	0.85	1.88	2.72	1.21	1.55	1.42	0.78	2.70	0.70	4.02	4.30	1.42
C_4	1.31	2.42	0.75	1.69	2.35	1.04	1.55	1.31	0.79	2.77	0.76	5.93	4.55	1.44
C_5	1.49	0.94	1.00	0.39	0.64	1.54	2.80	1.49	0.69	1.46	1.78	6.70	5.28	1.10
C_6	1.08	2.35	0.68	1.57	1.64	0.88	1.90	1.08	0.96	2.95	0.76	10.3	4.04	1.60
C_7	1.63	1.28	1.41	0.54	1.08	1.73	2.86	1.63	1.13	1.82	0.99	11.5	3.46	0.90
C_8	0.85	2.19	1.37	1.48	1.58	0.95	2.38	0.85	1.18	2.72	1.08	15.0	1.50	1.38
C_9	1.71	4.16	1.10	2.19	2.10	1.11	2.89	1.71	1.02	4.44	3.82	20.0	1.85	3.19
C_{10}	2.81	5.94	1.42	2.59	3.36	1.80	3.66	2.81	1.41	5.94	7.42	25.3	5.15	4.72
							Saturated Liquid Volume, V^l ($0.50 < T_r < 0.98$)							
C_1	3.99	9.25	5.11	3.56	3.50	4.13	5.39	3.69	2.33	2.83	0.97	1.42	3.92	0.58
C_2	7.08	7.04	4.97	3.28	3.10	4.60	5.22	3.69	2.14	3.09	0.32	1.15	3.12	0.76
C_3	8.92	5.83	4.96	2.97	2.88	4.49	6.24	3.68	2.47	2.98	0.16	1.49	2.70	1.20
C_4	10.2	4.97	5.13	2.50	2.83	3.93	9.49	3.67	2.55	2.50	0.71	0.84	3.14	1.27
C_5	12.4	3.55	4.89	2.37	2.56	3.62	16.0	3.69	3.45	2.43	0.75	2.18	3.92	1.76
C_6	15.1	2.28	4.00	3.21	2.36	4.22	13.2	3.74	4.66	3.28	0.31	1.53	4.29	3.02
C_7	16.2	2.95	4.26	2.34	2.26	3.32	13.4	3.75	4.46	2.30	0.43	2.71	5.98	2.49
C_8	18.5	4.99	3.57	2.83	2.32	3.33	15.1	3.74	5.12	2.58	0.60	3.74	6.94	3.23
C_9	19.5	5.85	3.74	2.25	2.30	4.00	17.1	4.04	4.34	2.28	0.85	4.17	9.26	2.63
C_{10}	21.8	7.96	3.05	2.46	2.42	4.35	23.0	4.05	4.98	2.35	1.36	3.38	10.8	3.18

cont'd.

Table 3.8 Continued

	SRK	PR	HX	SW	PT	3RK	MMC	TSRK	C1	ALS	HCL	H	KMC	F
							Saturated Vapor Volume, V^v ($0.50 < T_r < 0.98$)							
C_1	1.86	2.11	1.36	0.49	1.51	1.80	2.42	1.91	1.47	0.92	2.41	4.14	2.17	2.46
C_2	0.87	3.09	1.10	1.60	2.85	0.86	1.86	1.04	1.07	2.45	2.01	3.95	4.46	1.52
C_3	1.03	2.97	1.19	1.73	2.77	0.98	1.76	1.24	1.18	2.81	2.32	5.83	5.36	1.87
C_4	0.90	2.53	1.01	1.52	2.26	0.67	1.74	0.96	1.13	2.70	2.83	8.16	5.57	1.71
C_5	1.43	1.08	1.40	0.39	0.77	1.54	3.11	1.33	0.89	1.31	4.93	10.8	6.31	1.30
C_6	0.56	2.05	1.11	1.22	1.53	0.52	1.92	0.50	1.19	2.61	3.37	11.5	4.56	1.60
C_7	1.57	1.42	1.96	0.38	1.47	1.72	3.09	1.42	1.30	1.94	4.22	11.0	3.72	1.11
C_8	0.97	2.11	1.93	1.25	2.03	1.15	2.58	0.68	1.63	2.72	4.47	12.9	1.62	1.16
C_9	1.09	3.35	1.60	1.78	2.12	0.57	2.88	1.00	1.22	3.74	5.89	15.6	1.80	2.92
C_{10}	2.04	4.70	1.87	1.87	2.80	0.95	3.77	1.93	1.52	4.70	8.58	19.4	4.55	4.02
							Liquid Compressibility Factor, Z^l ($0.30 < T_r < 0.99$, $0.01 < P_r < 10.0$)							
C_1	3.67	8.35	4.21	3.44	3.16	3.78	3.72	3.58	3.25	3.64	3.60	5.09	5.85	5.12
C_2	5.30	6.64	4.53	3.02	3.11	3.34	5.82	3.43	3.17	3.29	2.26	5.01	7.57	5.19
C_3	6.83	5.46	4.65	2.93	3.09	3.14	7.69	3.40	3.20	3.17	2.23	5.00	9.07	5.13
C_4	8.27	4.52	4.66	2.90	3.06	3.01	9.40	3.38	3.34	3.11	2.76	5.02	10.5	5.09
C_5	10.2	3.52	4.55	2.86	3.02	2.91	11.6	3.43	3.75	3.06	3.09	5.08	12.4	5.12
C_6	11.7	3.03	4.37	2.86	2.99	2.88	13.3	3.46	3.96	3.03	3.09	5.21	13.9	5.17
C_7	13.7	2.96	4.12	2.85	2.92	2.95	15.6	3.81	4.47	3.00	2.77	5.44	16.0	5.36
C_8	15.5	3.52	3.74	2.87	2.94	3.25	17.5	3.85	4.59	2.99	2.26	5.78	17.8	5.40
C_9	17.6	4.97	3.41	2.91	2.98	3.88	19.7	4.08	4.69	2.99	1.83	6.42	20.1	5.57
C_{10}	19.6	6.65	3.18	3.00	3.09	4.54	21.9	4.28	4.90	2.99	2.26	7.25	22.3	5.74

cont'd.

Table 3.6 Continued

	SRK	PR	HK	SW	PT	3RK	MMC	TSRK	CI	ALS	HCL	H	KMC	F
							Compressibility Factor of Vapour, Z^V ($0.55 < T_r < 0.99$, $0.01 < P_r < 0.8$)							
C_1	0.19	0.88	0.44	0.17	0.20	0.20	0.18	0.18	0.58	0.39	0.76	1.94	0.10	0.95
C_2	0.39	0.71	0.48	0.23	0.27	0.31	0.25	0.29	0.49	0.38	1.20	2.00	0.13	0.95
C_3	0.56	0.60	0.51	0.28	0.31	0.39	0.31	0.38	0.43	0.39	1.50	2.05	0.16	0.95
C_4	0.71	0.52	0.53	0.32	0.35	0.46	0.36	0.47	0.39	0.40	1.78	2.11	0.18	0.95
C_5	0.89	0.45	0.55	0.37	0.39	0.55	0.42	0.60	0.40	0.43	2.12	2.18	0.20	0.96
C_6	1.04	0.43	0.56	0.40	0.42	0.61	0.47	0.68	0.42	0.45	2.39	2.24	0.21	0.98
C_7	1.21	0.45	0.58	0.45	0.46	0.68	0.53	0.80	0.47	0.48	2.72	2.33	0.22	1.01
C_8	1.35	0.49	0.59	0.49	0.49	0.74	0.58	0.89	0.51	0.50	3.00	2.41	0.23	1.03
C_9	1.52	0.57	0.61	0.52	0.52	0.80	0.62	1.00	0.56	0.53	3.32	2.50	0.23	1.06
C_{10}	1.67	0.67	0.62	0.56	0.55	0.84	0.66	1.10	0.63	0.56	3.63	2.60	0.24	1.08
							Compressibility Factor of Gas above the Critical Temperature, Z^{sup} ($1.01 < T_r < 4.00$, $0.01 < P_r < 10.0$)							
C_1	1.14	2.13	1.15	1.71	0.83	1.16	0.98	0.98	0.88	0.84	1.05	3.17	1.22	4.80
C_2	1.55	1.66	1.26	1.36	0.87	1.20	1.08	1.06	0.89	0.86	1.52	3.21	1.23	5.15
C_3	1.83	1.48	1.33	1.18	0.92	1.20	1.18	1.11	0.97	0.93	1.92	3.29	1.29	5.41
C_4	2.05	1.37	1.39	1.09	1.01	1.20	1.32	1.17	1.07	1.01	2.30	3.37	1.49	5.67
C_5	2.32	1.31	1.46	1.08	1.14	1.23	1.57	1.24	1.22	1.15	2.79	3.53	1.79	6.00
C_6	2.51	1.31	1.51	1.16	1.27	1.27	1.84	1.32	1.33	1.27	3.17	3.68	2.08	6.27
C_7	2.75	1.36	1.57	1.35	1.44	1.36	2.21	1.44	1.48	1.45	3.65	3.89	2.45	6.62
C_8	2.94	1.44	1.62	1.52	1.59	1.48	2.52	1.55	1.60	1.62	4.03	4.09	2.76	6.91
C_9	3.17	1.57	1.68	1.73	1.78	1.67	2.89	1.71	1.73	1.82	4.45	4.35	3.15	7.24
C_{10}	3.39	1.73	1.73	1.92	1.96	1.89	3.25	1.89	1.88	2.03	4.88	4.62	3.54	7.57

cont'd.

Table 3.6 Continued

	SRK	PR	HK	SW	PT	3RK	MMC	TSRK	CI	ALS	HCL	H	KMC	F
Compressibility Factor along the Critical Isotherm, Z^c (T_r = 1.0, 0.01 < P_r < 10.0)														
C_1	4.33	4.44	3.31	3.59	4.12	3.99	3.84	4.12	3.15	3.30	2.92	7.27	3.81	9.80
C_2	5.30	4.21	3.50	3.72	3.70	4.35	4.11	4.48	3.92	3.46	5.48	7.77	4.10	10.7
C_3	6.19	4.18	3.64	4.12	3.79	4.46	4.34	4.74	5.06	3.74	6.45	8.19	4.33	11.3
C_4	7.02	4.21	3.77	4.23	4.04	4.68	4.65	4.98	5.77	3.71	7.19	8.49	4.61	11.8
C_5	8.07	4.26	3.94	4.32	3.93	4.81	5.01	5.28	6.50	4.00	6.19	8.85	4.99	12.4
C_6	8.89	4.46	4.12	4.21	4.03	4.94	5.29	5.53	6.96	3.98	8.96	9.12	5.30	12.9
C_7	9.93	4.72	4.36	4.09	4.34	5.34	5.66	5.84	7.40	4.31	9.91	9.45	5.70	13.5
C_8	10.8	4.94	4.47	4.12	4.24	5.49	6.06	6.10	7.67	4.45	10.7	9.68	6.20	14.0
C_9	11.8	5.43	4.59	4.19	4.61	5.47	6.50	6.40	7.89	4.37	11.5	9.98	6.78	14.5
C_{10}	12.7	5.99	4.70	4.26	4.49	5.68	6.98	6.69	8.05	4.67	12.4	10.2	7.34	15.0
Second Virial Coefficient, B (0.50 < T_r < 0.98)														
C_1	7.73	7.83	7.16	7.81	7.63	7.77	7.49	7.59	7.59	7.26	8.54	13.4	1.09	8.81
C_2	11.8	10.9	10.6	11.2	11.1	11.4	11.1	11.4	11.1	10.8	14.7	13.7	0.77	12.6
C_3	14.0	12.6	12.4	13.0	12.9	13.3	12.9	13.3	12.9	12.7	18.1	14.6	0.87	14.6
C_4	15.7	14.0	13.8	14.3	14.2	14.7	14.2	14.8	14.3	14.2	20.7	15.5	1.00	16.0
C_5	17.5	15.6	15.54	15.8	15.7	16.2	15.5	16.4	15.7	15.7	23.5	16.5	1.20	17.7
C_6	18.8	16.7	16.4	16.8	16.7	17.3	16.7	17.5	16.9	16.7	25.5	17.4	1.43	18.8
C_7	20.2	18.0	17.5	18.0	17.8	18.4	18.0	18.6	18.0	17.9	27.3	18.3	1.88	20.0
C_8	21.2	18.9	18.4	18.8	18.6	19.1	18.7	19.5	19.0	18.8	29.4	19.0	2.34	20.8
C_9	22.2	19.9	19.2	19.6	19.5	20.0	19.5	20.4	20.0	19.7	31.1	19.8	2.93	21.7
C_{10}	23.1	20.7	19.9	20.3	20.2	20.6	19.9	21.2	20.7	20.4	32.7	20.5	3.56	22.5

v^{ℓ} causes the HCL equation to yield rather large errors in v^{v} and Z^{v} when compared to the SRK equation in which only the parameter a is fitted to P^{v}. On the other hand, forcing the three parameters (a, b and c) in the F equation, which is a modified form of the RK EOS, to fit P^{v}, v^{ℓ} and v^{v} results in larger errors in Z^{ℓ} and Z^{sup} than those obtained from the HCL equation. To illustrate, the percent deviations in P^{v}, v^{ℓ}, v^{v}, B and Z^{ℓ} for C1, C6 and C10 calculated from the HCL and the F equations are presented in Figures 3.2, 3.3 and 3.4.

As can be seen in Figure 3.2 both equations yield large errors in P^{v} at low temperatures, especially as the size of the molecule increases. Also the HCL equation produces a saturation dome for C10 in the liquid phase which is slightly deformed around T_r=0.85. This is shown by the deviation curve of v^{ℓ} for C10 given by the HCL equation (Figure 3.2). The deformation of the saturation curve in the liquid phase results from the correlation for the parameters in the HCL EOS which are not continuous at T_r=0.85.

Listed below by order of their ability in representing P^{v}, v^{ℓ}, v^{v}, Z^{ℓ}, Z^{v}, Z^{sup} and Z^{c} are the fourteen equations which were evaluated in Table 3.5.

P^{v}	:C1 HK 3RK SW SRK TSRK F HCL PT MMC PR ALS KMC H
v^{ℓ}	:HCL F H PT ALS SW C1 TSRK 3RK HK KMC PR MMC SRK
v^{v}	:3RK TSRK SW SRK C1 HK F PT MMC PR ALS KMC HCL H
Z^{ℓ}	:HCL SW PT ALS 3RK TSRK C1 HK PR F H SRK MMC KMC
Z^{v}	:KMC SW PT MMC ALS C1 HK 3RK PR TSRK SRK F HCL H
Z^{sup}	:PT C1 ALS TSRK 3RK SW HK PR MMC KMC SRK HCL H F
Z^{c}	:ALS HK SW PT PR 3RK MMC KMC TSRK C1 HCL SRK H F

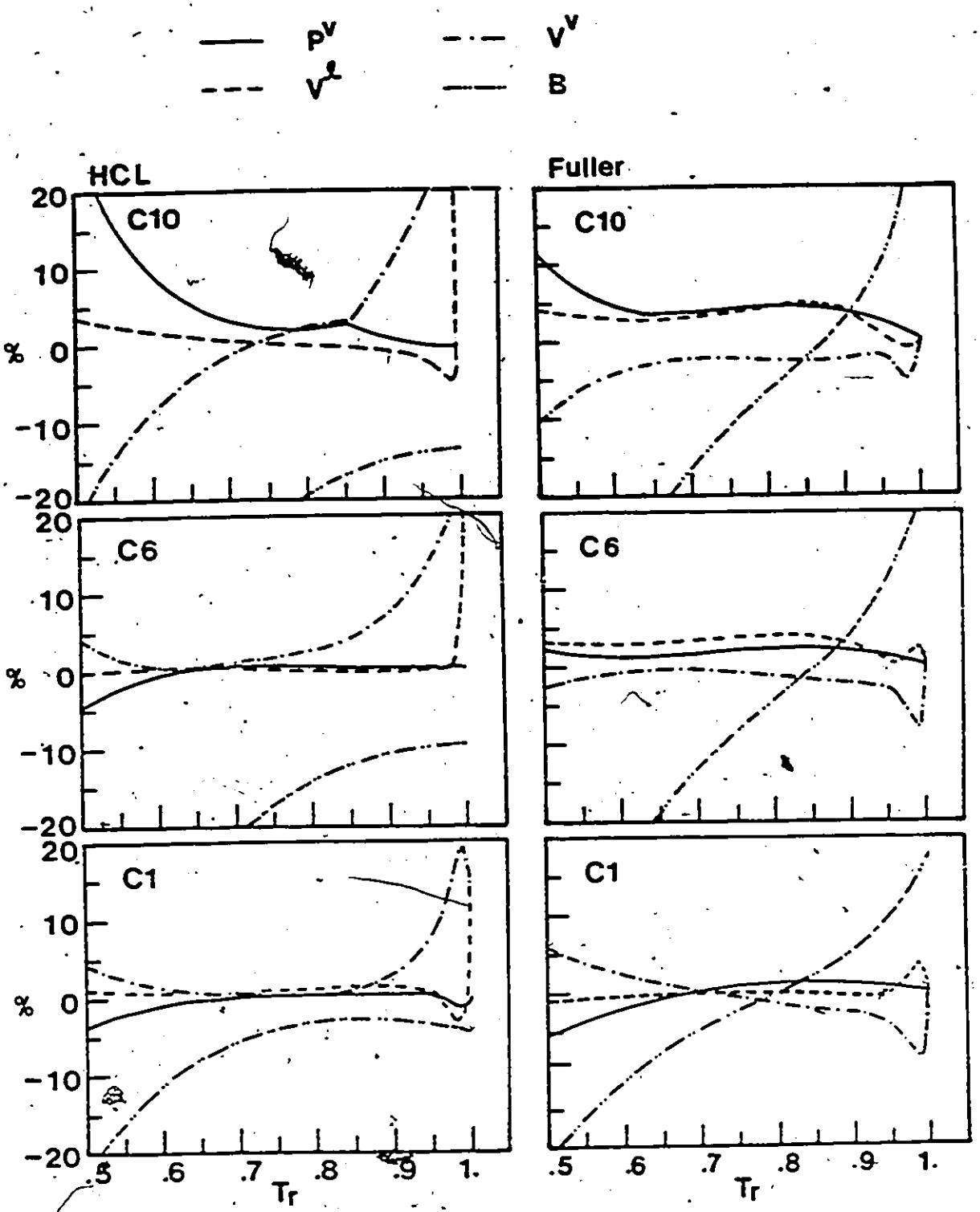

Figure 3.2: Percent deviations of P^v, v^l, v^v and B for C1, C6 and C10 for the HCL and the F equations.

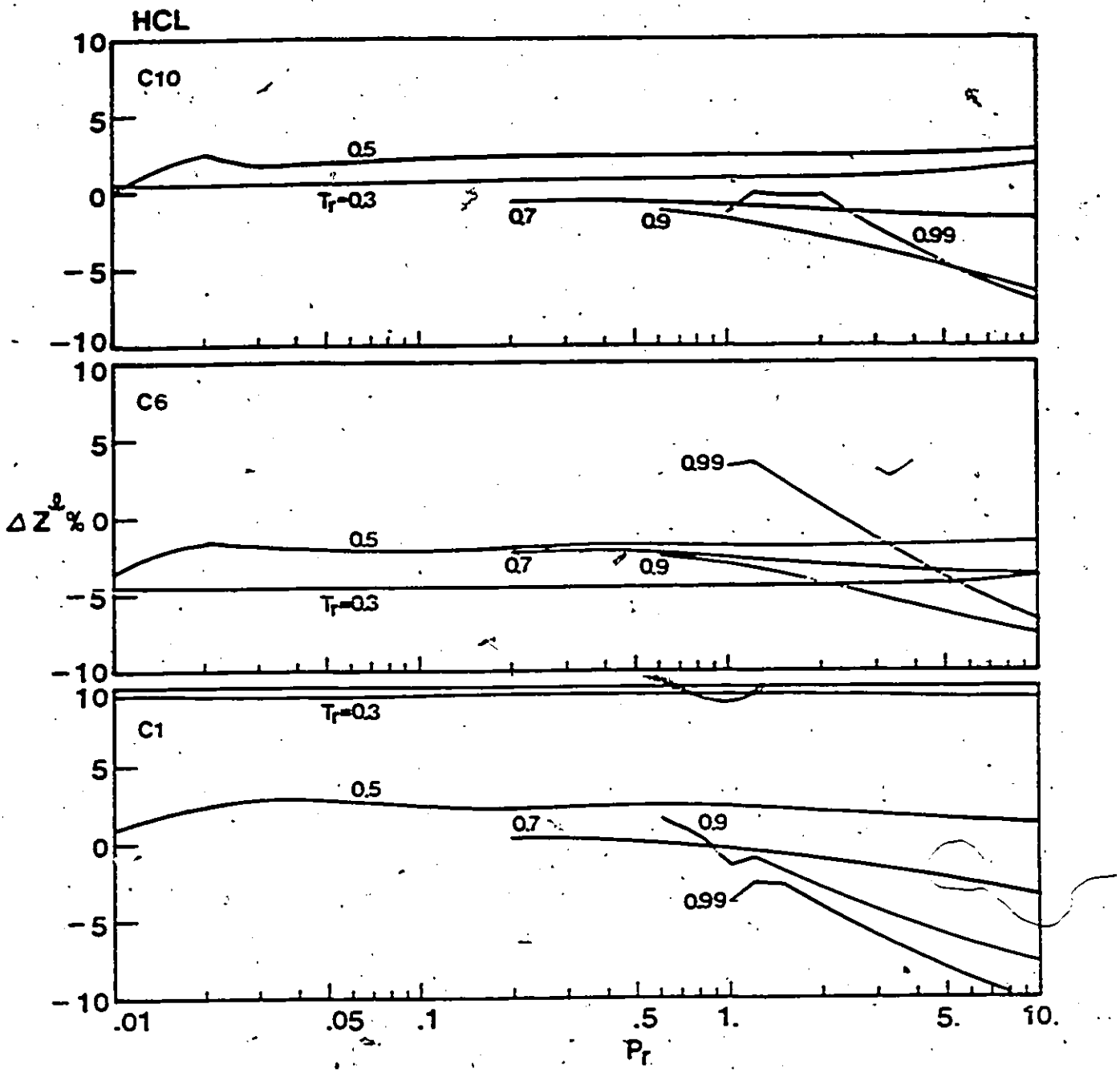

Figure 3.3: Percent deviations of Z^{ℓ} for C1, C6 and C10 for the HCL equation.

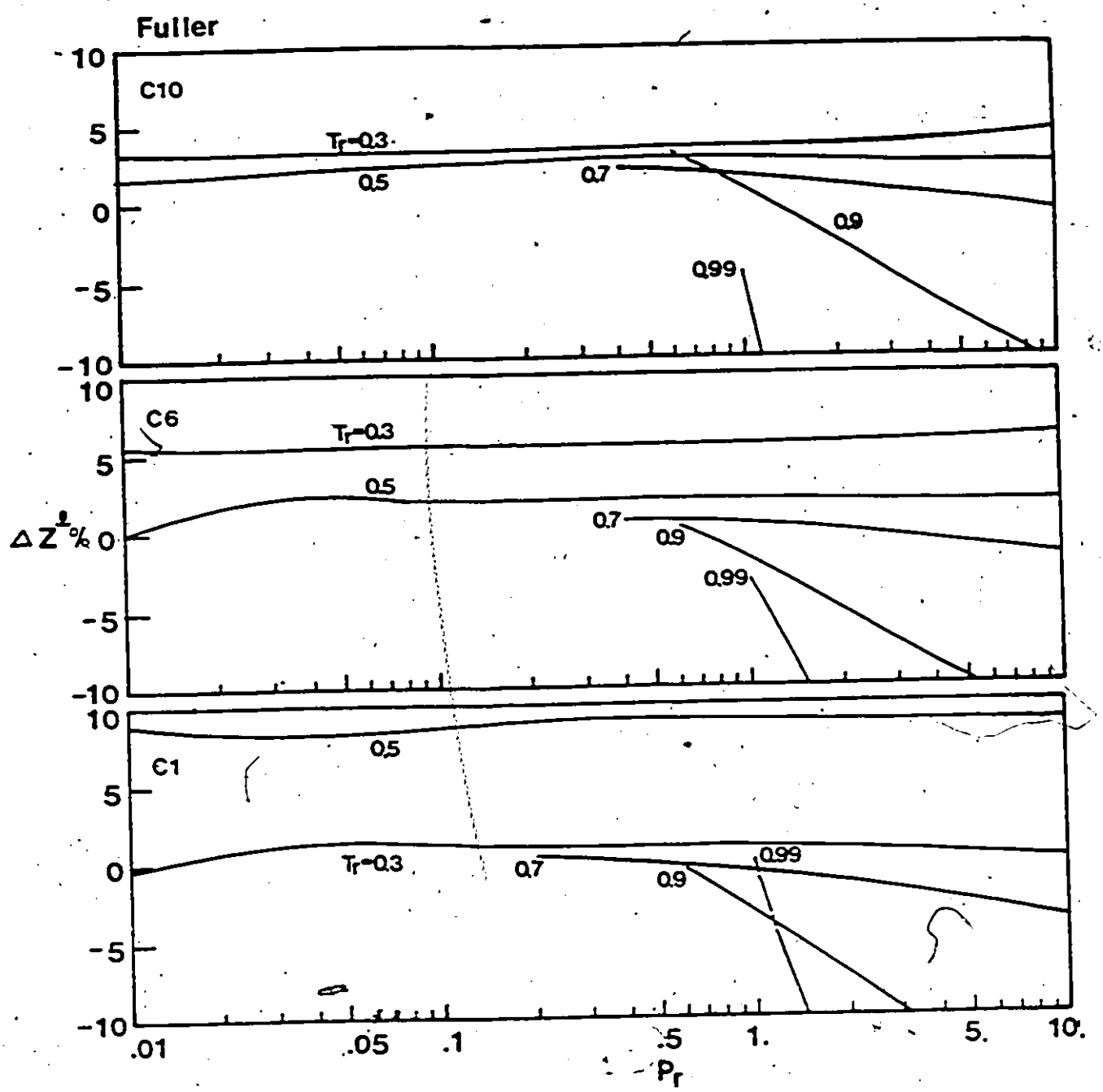

Figure 3.4: Percent deviations of Z^{ℓ} for C1, C6 and C10 for the F equation.

Based on the above listing the SW, the PT and the ALS equations show better overall performance than the others. Of these equation, the SW EOS appears to be slightly better than the PT EOS which in turn appears to be better than the ALS EOS. As mentioned earlier equations with only one temperature dependent parameter appear to be better for predicting physical properties over a wide PVT range. This finding is consistent with the partition function approach presented in Chapter II where it was noted that the temperature dependence of the attractive term reflected in $I(T,V;r)$ should not be too strong.

Figures 3.5, 3.6 and 3.7 depict the percent deviations of P^v, v^ℓ, v^v, B and Z^ℓ for C1, C6 and C10 for the SW and the ALS equations. As can be seen, large errors in P^v result at low temperatures (T_r) which increase with molecular size, particularly for the ALS EOS. At most temperatures the B values were underestimated by both equations. The deviations in v^v appear to be mirror images of those of P^v along the zero deviation line. In the vicinity of the critical point large errors occur in v^ℓ, v^v and Z^ℓ.

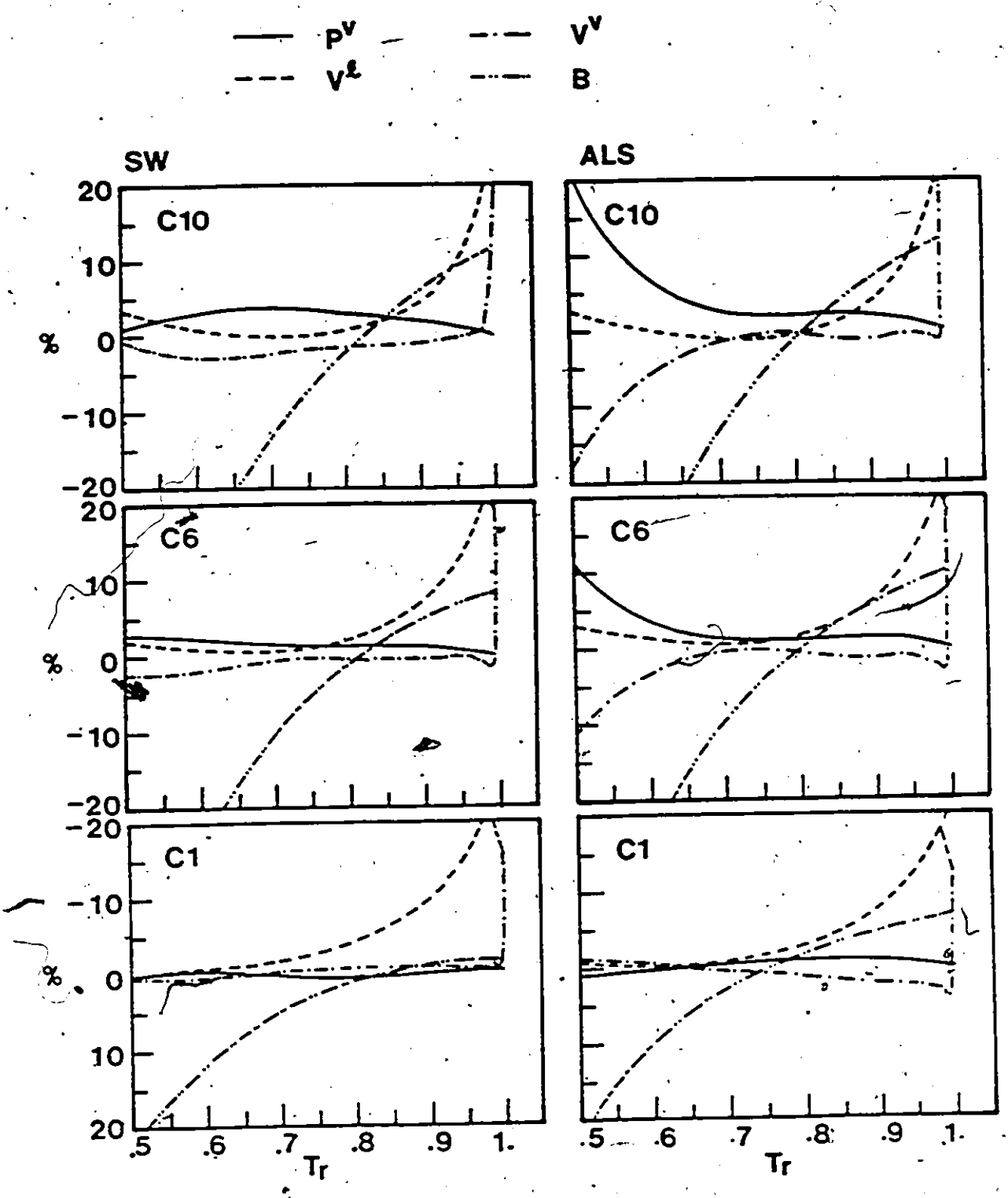

Figure 3.5: Percent deviations of P^v, v^ℓ, v^v and B for C1, C6 and C10 for the SW and the ALS equations.

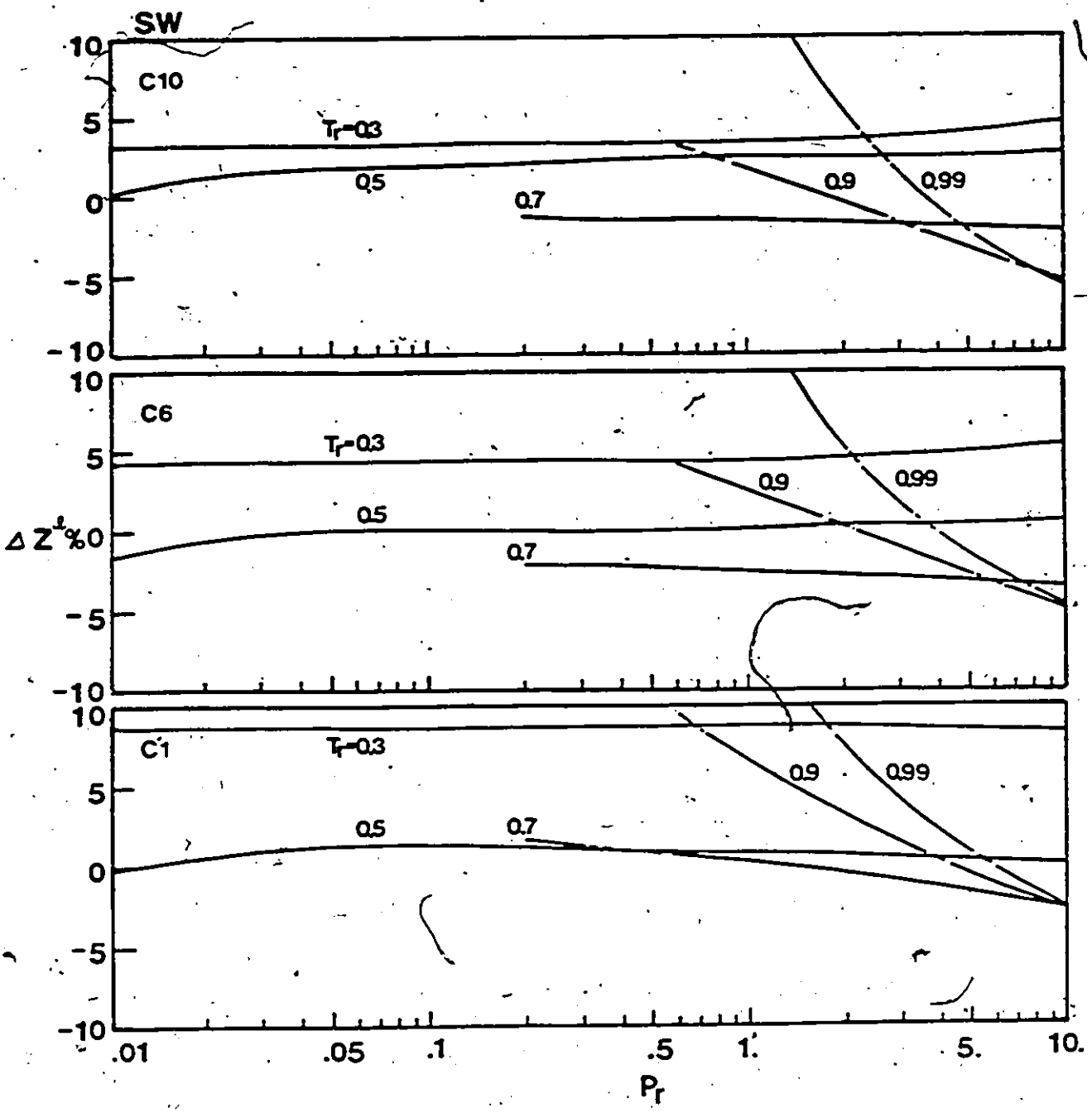

Figure 3.6: Percent deviations of Z^{ℓ} for C1, C6 and C10 for the SW equation.

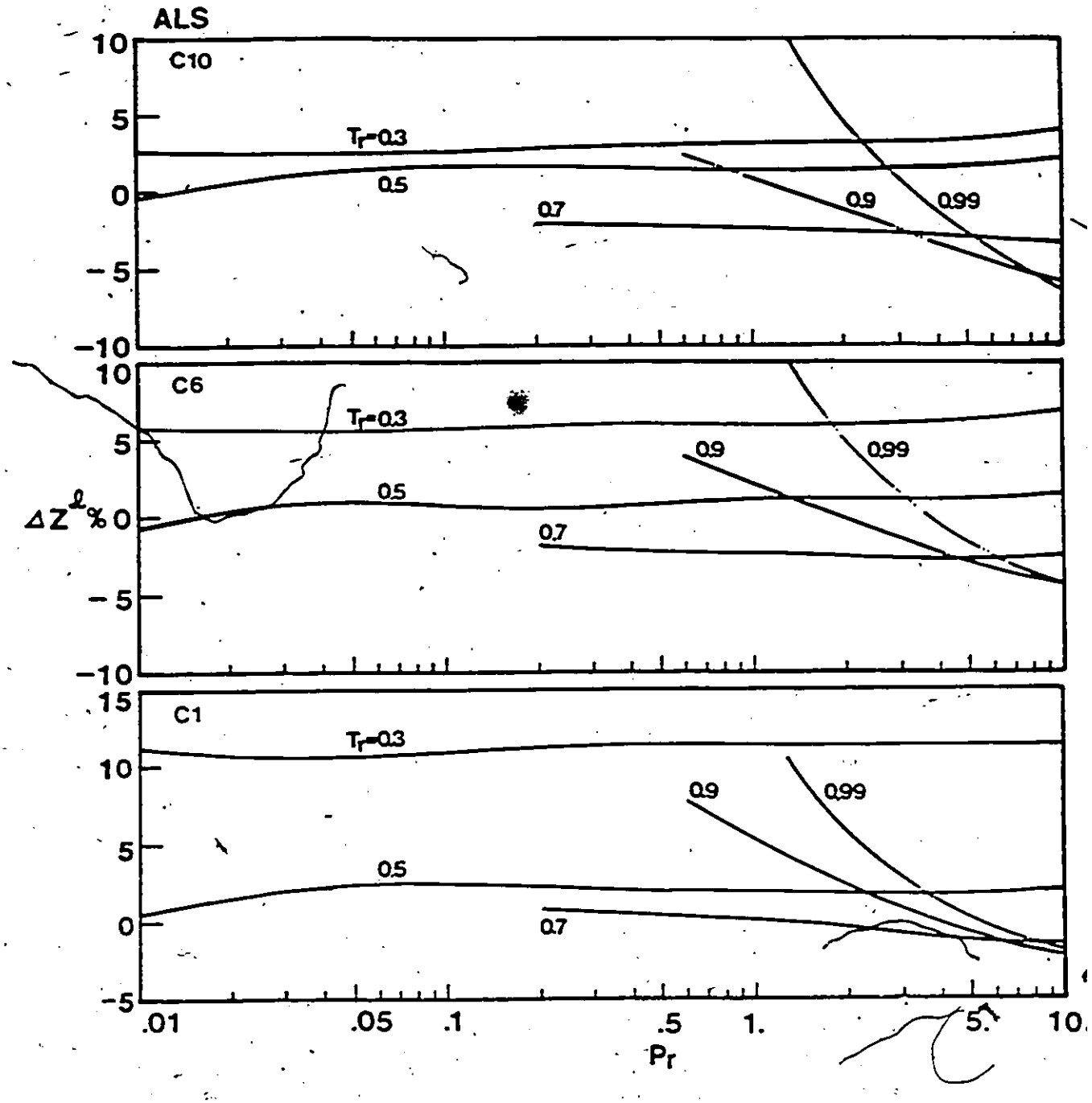

Figure 3.7: Percent deviations of Z^{ℓ} for C1, C6 and C10 for the ALS equation.

Chapter IV

DEVELOPMENT OF A NEW EQUATION OF STATE

In this study, a new equation of state is developed on the basis of a generalized form of the VDW-type volume-cubic EOS as shown by Eq.(1.3)

$$P = \frac{RT}{v - b} - \frac{a}{v^2+ubv+wb^2} \qquad (1.3)$$

As pointed out by Schmidt and Wenzel [112], to avoid the condition where $v^2+ubv+wb^2=0$ for $v>b$, values of the parameters u and w must satisfy the following two constraints

for $u \geq -2$,

$$w > -u-1, \qquad (4.1a)$$

for $u \leq -2$,

$$w > u^2/4. \qquad (4.1b)$$

The first part of the development includes the determination of the parameters (a,b,u,w) in Eq.(1.3) as well as examining their effect on the volumetric behavior of the equation in various PVT region; namely the two-phase coexisting region, the liquid phase region and the supercritical ($T>T_c$) fluid region. From the evaluation of the well-known

equations in Chapter III, this analysis is carried out under the assumption that only the attractive parameter a is temperature dependent. Nevertheless, the advantages and drawbacks of also treating parameter b as a function of temperature are demonstrated by studying the volumetric behavior along the saturation curve. Other regions are not included in the study since, as was shown in Chapter III, volume-cubic equations with one temperature dependent parameter can adequately describe these regions with similar accuracy. The volumetric properties of the first ten normal alkanes (C1-C10) are again used as the basis for the analyses. These properties include the saturated liquid and vapor molar volumes (v^{ℓ} and v^{v}), liquid compressibility factors (Z^{ℓ}) and gas compressibility factors for supercritical temperatures (Z^{sup}). Values of these properties are generated from the same correlations in the same temperature and pressure ranges as were used in Chapter III to evaluate the well-known equations. The second part of the development involves a study of how to design 2P1T, 3P1T and 4P1T equations based on the results obtained from the first part. Finally, a new equation of state will be proposed.

4.1 Determination of Parameters and Analyses of the Volumetric Behavior of Eq.(1.3)

4.1.1 Critical point

At the critical point, the parameters in Eq.(1.3) are related to one another through exact algebraic relations. These relations are derived from the following three critical point conditions,

$$\left(\frac{\partial P}{\partial v}\right)_T = 0 \qquad (2.31a)$$

$$\left(\frac{\partial^2 P}{\partial v^2}\right)_T = 0 \qquad (2.31b)$$

$$v^{\ell} = v^{v} = v_c^*, \text{ at } T = T_c, P = P_c \qquad (2.31c)$$

where Eq.(2.31c) is equivalent to

$$(v - v_c^*)^3 = 0$$

where v_c^* is the critical molar volume predicted by the EOS. From Chapter II, the parameters a and b are defined at the critical point as

$$a_c = \Omega_{ac} R^2 T_c^2 / P_c \qquad (2.32)$$

$$b_c = \Omega_{bc} R T_c / P_c \qquad (2.33)$$

where Ω_{ac} and Ω_{bc} are dimensionless quantities. Applying Eqs(2.31,32,33) to Eq.(1.3), gives the relationship between Ω_{ac}, Ω_{bc}, u, w and the predicted critical compressibility factor ζ_c ($=Pv_c^*/RT$),

$$\zeta_c = [(1-2\beta_c-(u+w)\beta_c^2]/[(1-\beta_c)^2(2+u\beta_c)] \qquad (4.2)$$

$$\Omega_{ac} = [1+u\beta_c+w\beta_c^2]\zeta_c/[(1-\beta_c)^2(2+u\beta_c)] \qquad (4.3)$$

$$\Omega_{bc} = \beta_c \zeta_c \qquad (4.4)$$

where β_c is defined as

$$\beta_c \equiv (b_c/v_c^*) \qquad (4.5)$$

The value of β_c is given by the smallest root of the following cubic equation

$$(w-uw-u^2)\beta_c^3-3(w+u)\beta_c^2-3\beta_c+1=0. \qquad (4.6)$$

There are 10 variables (T_c, P_c, β_c, ζ_c, Ω_{ac}, Ω_{bc}, a_c, b_c, u and w) to be determined by solving six equations (Eqs(2.32,33,4.2,3,4,6)). Hence, among the 10 variables, four must be specified. In order for the equation of state to conform to the corresponding states principle, T_c and P_c must be chosen as independent variables. Using experimental T_c and P_c as input data, the most sensible choice for the remaining two independent variables would be either the parameters u and w or the parameters β_c and ζ_c. The former pair is more convenient to use for solving the six equations for the remaining variables where it involves only the straightforward substitution of the parameters u and w into the equations. Otherwise, numerical solutions would be required and in some cases two valid solutions for Ω_{ac} and ζ_c are obtained. This complicates the analysis of Eq.(1.3). Nevertheless, the pair (β_c, ζ_c) has clearer physical meaning since they reflect the local volumetric behavior of Eq.(1.3) on the P-V surface. In general, β_c is related to the volumetric properties of incompressible liquid while ζ_c is related to those of a fluid at the critical point. Comparison of β_c and ζ_c obtained from an EOS with experimental values can provide a measure of the behavior of the equation in the (saturated) liquid phase as well as in the vicinity of the critical point. Consequently, throughout this study the pair (u,w) is used as the independent variables while the quantities β_c and ζ_c associated with the resulting equation are used to examine the local behavior of the equation on the P-V surface.

For a two-parameter equation in which u and w are universal constants, the parameters Ω_{ac}, Ω_{bc}, β_c and ζ_c will also be constant for all substances. It is only when parameters u and w are substance dependent that Ω_{ac}, Ω_{bc}, β_c and ζ_c will be substance dependent. In reality, values of β_c and ζ_c should vary with substance, since experimental critical compressibility factors for most substances range from 0.2 to 0.3. As indicated by Eq.(4.5), the reduced quantity, β_c, is related to the van der Waals co-volume, b, which should vary with molecular size. The value of b is in turn close to that of the incompressible liquid molar volume which can be estimated from the saturated liquid molar volume at the triple point, v^{ℓ}_{tri}. Therefore, the value of β_c can be estimated using the ratio between v^{ℓ}_{tri} and the experimental critical molar volume. These estimated values of β_c, designated as β^*_c, along with the experimental critical compressibility factors for the first ten normal alkanes are listed in Table 4.1. Also included are values of T_c, P_c, the acentric factor ω and the corresponding u, w, Ω_{ac} and Ω_{bc} calculated from Eqs(4.2,3,4,5,6). Values of T_c, P_c and Z_c are from the 1977 compilation of Reid, Prausnitz and Sherwood [105]. Values of the acentric factor are adopted from the compilation of Passut and Danner [85].

Values of Z_c for the normal fluids can be related to the acentric factor by a linear equation such as the one given by Lee and Kesler [66]: $Z_c = 0.2905 - 0.08\omega$. The same expression can also be used to approximate β^*_c with average percent deviation less than 7.0%: $\beta^*_c = 0.3331 - 0.07503\omega$.

Table 4.1: Values of the physical constants of the first ten normal alkanes and related equation of state parameters.

	β_c	Z_c	T_c/K	P_c/atm	ω	u	w	Ω_{ac}	Ω_{bc}
C1	0.3565	0.288	190.6	45.43	0.0072	2.325	-2.721	0.54068	0.10267
C2	0.3125	0.285	305.4	48.15	0.0908	2.628	-2.680	0.51984	0.08906
C3	0.3001	0.281	369.8	41.93	0.1454	2.862	-2.792	0.51842	0.08433
C4	0.3148	0.274	425.2	37.46	0.1928	3.064	-3.174	0.53590	0.08626
C5	0.3273	0.262	469.6	33.24	0.2510	3.495	-3.751	0.55897	0.08575
C6	0.3136	0.260	507.4	29.72	0.2957	3.698	-3.843	0.55447	0.08154
C7	0.3003	0.263	540.2	26.99	0.3506	3.671	-3.673	0.54330	0.07898
C8	0.3048	0.259	568.8	24.53	0.3942	3.825	-3.888	0.55126	0.07894
C9	0.2950	0.260	594.6	22.59	0.4437	3.868	-3.821	0.54474	0.07670
C10	0.3060	0.247	617.6	20.68	0.4902	4.426	-4.545	0.56891	0.07561

The relationship between both $(\Omega_{ac},\Omega_{bc})$ and (β_c,ζ_c) and (u,w) are presented in Figures 4.1 and 4.2, respectively. The shaded areas on the diagrams correspond to the constraints (Eqs(4.1,2)) imposed on u and w. Shown in Figures 4.1 and 4.2 are constant Ω_{ac} and Ω_{bc} curves and constant β_c and ζ_c curves, respectively. As can be seen in Table 8, values of β_c^* and ζ_c have a tendency to decrease with increasing molecular size. The locus of (β_c^*,ζ_c) from C1 to C10 is plotted in Figure 4.2.

Comparing Figure 4.2 to Figure 3.1, which presents the loci of (u,w) for several well-known equations of state, shows that only those equations whose loci of (u,w) follow closely to that of the family of equations represented by u+w=1 can produce loci of (β_c,ζ_c) in a direction similar to that of (β_c^*,ζ_c). As for the volume-translated equations the loci of (β_c,ζ_c) deviate from that of (β_c^*,ζ_c). However, it should be noted that not all three-parameter equations which result from the volume-translation method will produce such loci. As pointed out in Chapter III, the locus of (β_c,ζ_c) for this type of equation is in fact

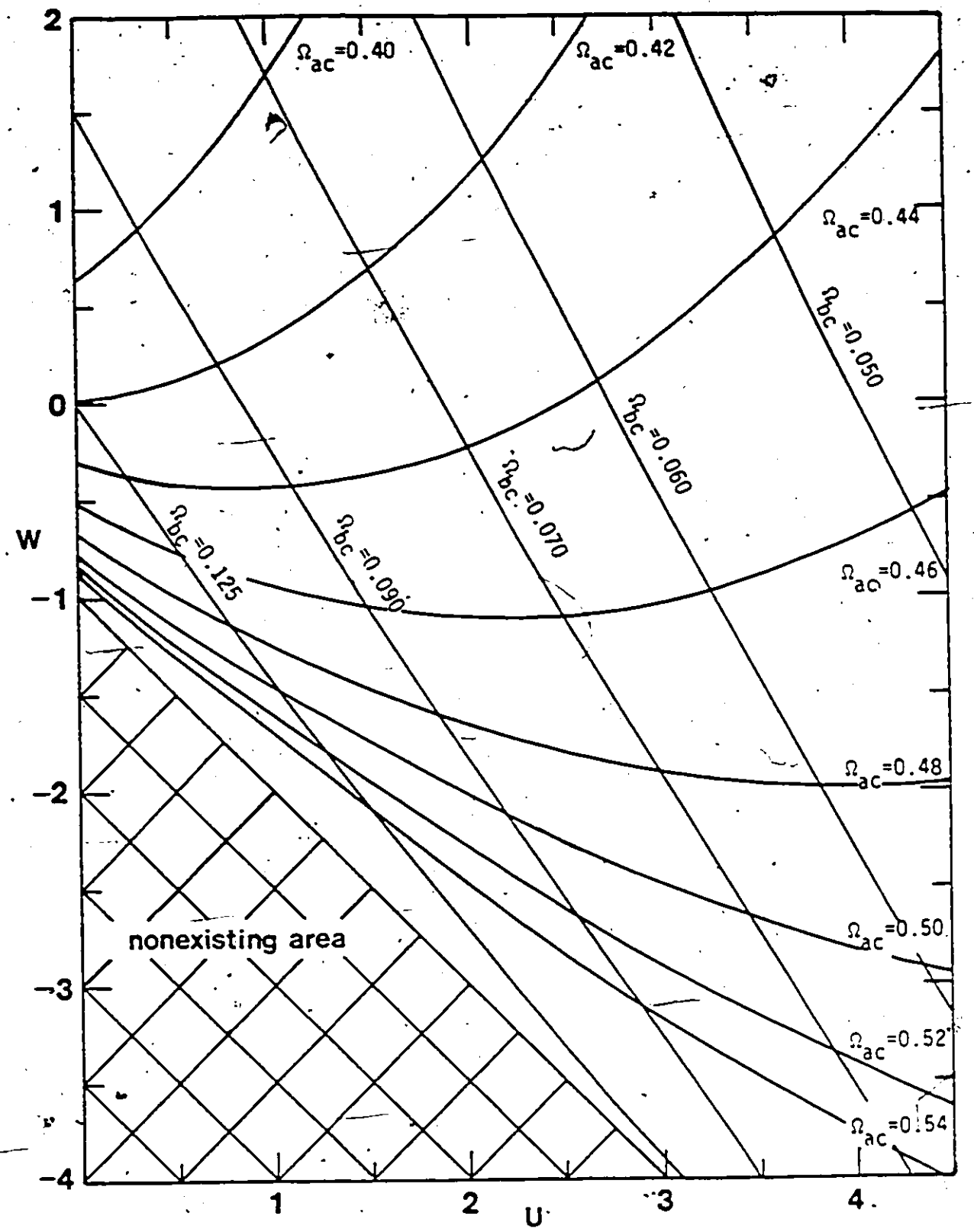

Figure 4.1: Constant Ω_{ac} and Ω_{bc} curves on a u-w diagram.

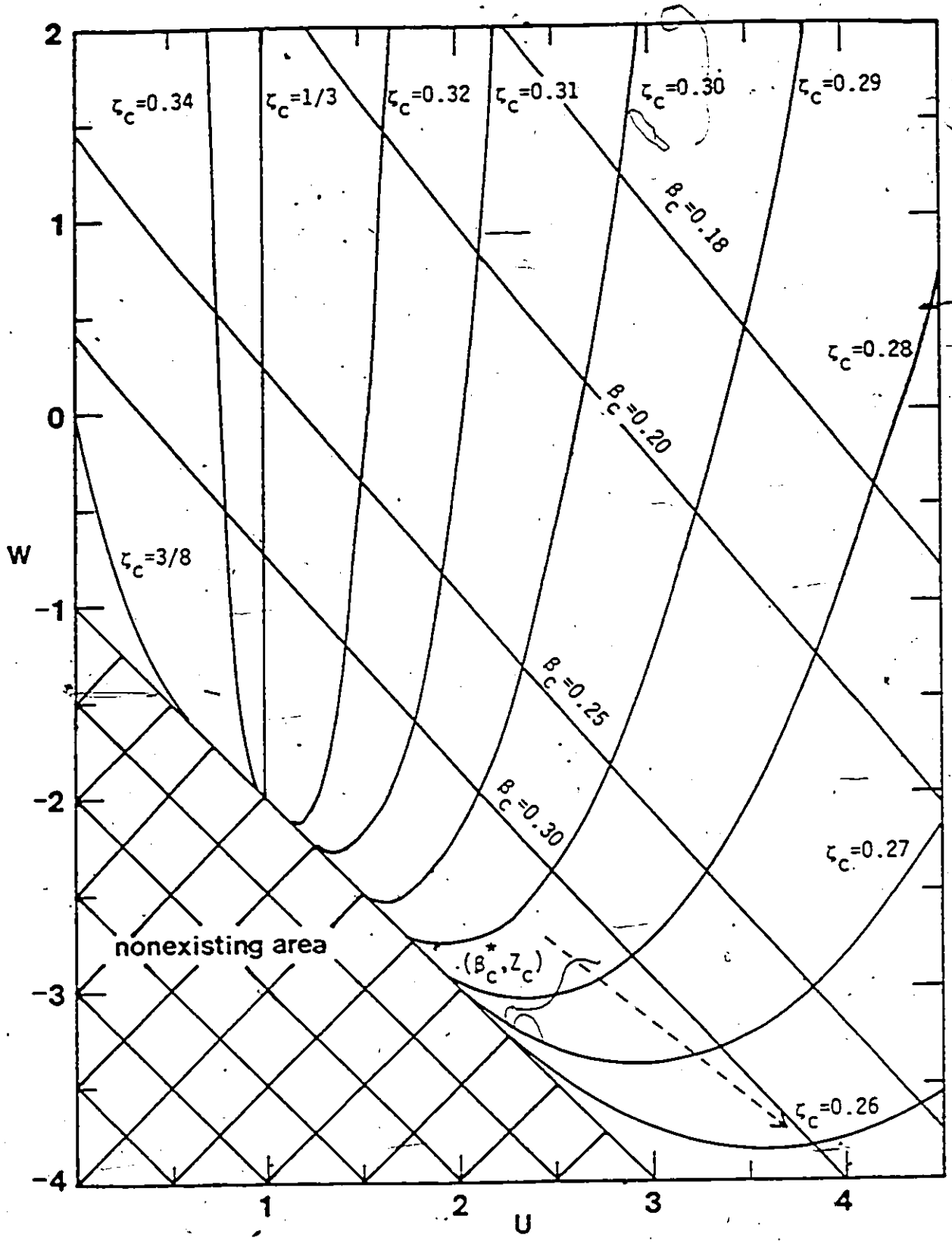

Figure 4.2: Constant β_c and ζ_c curves on a u-w diagram. -----> Locus of (β_c^*, ζ_c).

represented by the constant-Ω_{ac} curve on the u-w diagram. Therefore the location of the locus of (β_c,ζ_c) on the u-w diagram is dependent on the value of Ω_{ac} associated with the equation. By comparing Figure 4.2 to Figure 4.1, one can note that the location of the constant-Ω_{ac} curve approaches that of (β_c^*,ζ_c) as the value of Ω_{ac} increases. For a volume-translated equation with $\Omega_{ac}>0.5$, the locus of (β_c,ζ_c) should be in the same direction as that of (β_c^*,ζ_c). On the other hand, the locus of (β_c,ζ_c) produced by an equation in which w=0 such as the 3RK EOS is somewhere in between those for the line u=w=1 and the Clausius equation.

The above observation results in the question, how does the volumetric behavior of an equation such as Eq.(1.3) relate to the resulting locus of (β_c,ζ_c) when compared to that of (β_c^*,ζ_c), and moreover, to the corresponding locus of (u,w), since (u,w) and (β_c,ζ_c) are interrelated? To address this question, the following analyses were undertaken to determine the effect of the parameters u and w as well as β_c and ζ_c on the volumetric behavior of Eq.(1.3) in different fluid regions.

4.1.2 Saturated Liquid and Vapor Phases

In the study of the pure fluid phase equilibrium behavior of Eq.(1.3) in both liquid and vapor phases, mathematical analysis of the equation is first carried out in order to estimate the parameters (a,b,u,w) along the saturation curve.

In addition to the parameters a, b, u and w, the variables include T and P as well as v and the fugacity f for both saturated vapor and

liquid phases. For pure fluid VLE calculations, Eq.(1.3) must satisfy the three equilibrium conditions of Eqs(2.26a,b,c). Saturated liquid and vapor molar volumes (v^{ℓ} and v^{v}) are calculated from Eq.(2.29) and the fugacities in both phases are calculated from Eq.(2.28). This gives a total of seven equations since Eqs(2.28,29) apply to both phases. However, there are twelve variables of which any five may be specified in order that the remaining seven be obtained by solving the seven equations.

In general, the five independent variables are a, b, u, w and T. Thus, at each temperature the four parameters are adjusted until the calculated P^{v}, v^{ℓ} and v^{v} are close or identical to the experimental values along the saturation curve. However, the process of adjusting these parameters depends on the number of temperature dependent parameters present. Generally, the more temperature dependent parameters there are in Eq.(1.3), the more saturation properties there are which can be fitted exactly. The priority in choosing saturation properties for the determination of the temperature dependence of the parameters should be by order of the vapor pressure, the saturated liquid and vapor molar volumes. This is because, as shown graphically in Chapter II, accurate prediction of P^{v} is necessary for the correct representation of the phase equilibrium condition ($f^{\ell}=f^{v}$). On the other hand, the results in Chapter III of the evaluation of the fourteen equations have shown that it is more difficult for volume-cubic equations to represent v^{ℓ} than v^{v}. In accordance with the discussion presented in Chapter II, the priority in treating the four parameters as functions of temperature should be given to the 'attractive' parameter, a, followed

by the 'molecular' parameters b, u and w. Parameters u and w should have the lowest priority, since they are considered as correction factors for the co-volume, b, which varies only slightly with temperature.

When Eq.(1.3) contains three or four temperature dependent parameters, P^{ν}, v^{ℓ} and v^{ν} can be fitted exactly by adjusting parameters a, b, u and/or w. This results in the formulation of a 3P3T, a 4P3T or a 4P4T type of equation. Mathematically, a 3P3T equation which is the simplest of the three types, should be sufficient to fit P^{ν}, v^{ℓ} and v^{ν} exactly at each given temperature. However, it was noted by Adachi and Lu [6] that the resulting temperature functions for the parameters of the 3P3T equations are rather complex and difficult to correlate and that after generalization some accuracy would be lost. Also the resulting equation is often found unsuitable for predicting properties in other PVT regions.

When Eq.(1.3) contains two temperature dependent parameters, i.e, a and b, the equation can fit P^{ν} and v^{ℓ} exactly if the temperature dependence of the parameters can be generalized accurately. Parameters u and w can be either assumed as universal constants or treated as substance dependent. The former approach results in a 2P2T equation, such as the HCL EOS, while the latter results in a 3P2T or 4P2T equation, such as the H EOS. For an equation of the 3P2T type, either the parameters u and w conform to an exact mathematical relationship or one of them be a universal constant. As noted in Chapter III the HCL and the H equations have some difficulties in calculating v^{ν} and Z^{sup} implying that there are certain drawbacks when using two temperature dependent parameters.

In this part of the study, the cause of these problems is examined. A 2P2T equation for one substance is used as the basis of the investigation. The reason for this being that just as a 3P1T or a 4P1T equation may be considered as a combination of 2P1T equations, each having been obtained for a particular substance, so may a 3P2T or a 4P2T equation be considered as a combination of 2P2T equations with each having been found for a particular substance. Therefore, the volumetric behavior of a 2P2T equation for a selected substance should be representative in a qualitative sense of that of a 3P2T or a 4P2T equation. Naturally, the results of the study should also apply for all substances of interest in a generalized 2P2T equation. However, this is probably limited to those substances with similar PVT behavior such as the normal fluids. Since, as was noted in Chapter III the form of the PR equation is suitable for representing the volumetric properties of n-hexane, this form along with values of P^{ν}, v^{ℓ} and v^{ν} for n-hexane are used as the basis of the investigation. The temperature dependence of parameters a and b are determined by simultaneously fitting a and b to P^{ν} and v^{ℓ} at each given temperature for $0.60 \leq T_r \leq 1.0$. The fitting procedure is presented in Figure 11. The five independent variables selected are u, w, P^{ν}, v^{ℓ} and T with u=2 and w=-1. While parameter b is adjusted based on the co-volume at the critical point, b_c, parameter a is calculated from the following equation

$$a = [\, RT/(v^{\ell}-b)-P^{\nu}][(v^{\ell})^2+ubv^{\ell}+wb^2] \qquad (4.7)$$

Eq.(4.7) is obtained from Eq.(1.3) using P^{ν}, v^{ℓ} and T as input data. The temperature dependence of parameters a and b thus obtained are

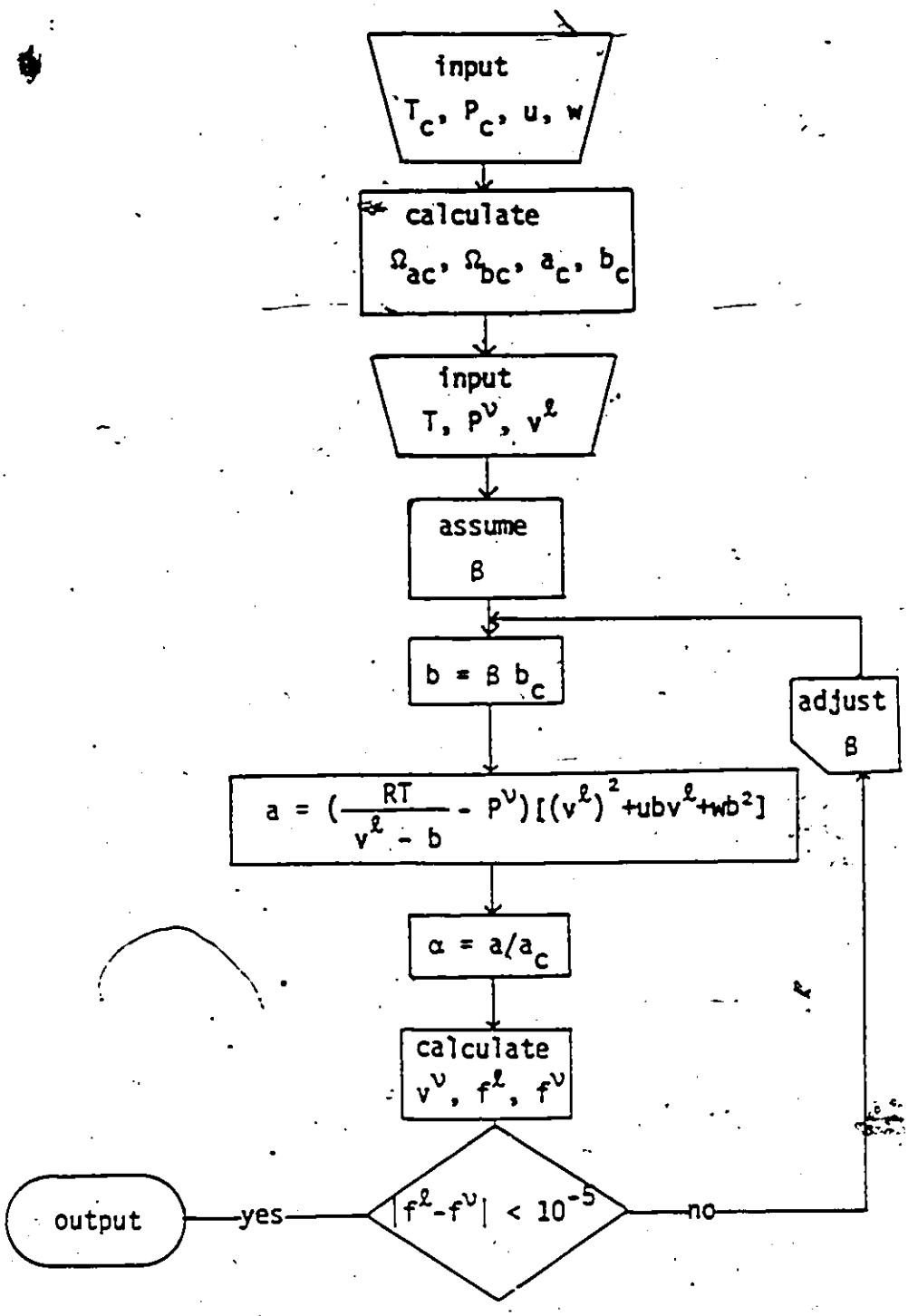

Figure 4.3: Procedure for fitting parameters a and b to vapor pressure and saturated liquid molar volume.

plotted in Figure 4.4, while the calculated P^v, v^l and v^v are compared with those obtained from the HCL and the H equations in Figure 4.5. It should be noted that the temperature dependence of parameters a and b shown in Figure 4.4 are typical for Eq.(1.3) when parameters a and b are fitted to P^v and v^l.

There are three drawbacks in treating parameters a and b as temperature dependent. First, the deep valleys in the temperature functions of parameters a and b (Figure 4.4) at T_r=0.98 cause difficulties when correlating these functions. Second, extrapolation into the temperature functions of parameters a and b to the supercritical region may result in an exponential increase in the values of the two parameters. This is physically unrealistic since as temperature increases, the attractive forces between molecules (thus the attractive term in the equation) should diminish. Also the molecule should not expand indefinitely. As a result large errors are often observed in the calculation of Z^{sup}, especially at temperatures close to T_c. As pointed out earlier in this study, convergence problems can arise during extrapolation. The third drawback can be seen from Figure 4.5. Deviations given by the HCL, the H and the modified PR equations show that forcing the equations to fit v^l results in large errors in v^v, especially as temperatures approach the critical value. In view of these three drawbacks, it appears that it is not promising to be able to develop an equation with two temperature dependent parameters evaluated from P^v and v^l which is simple yet capable of representing the volumetric properties v^l, v^v, Z^l and Z^{sup} with reasonable accuracy. Therefore subsequent analyses are restricted to cases where only parameter a is considered as a function of temperature.

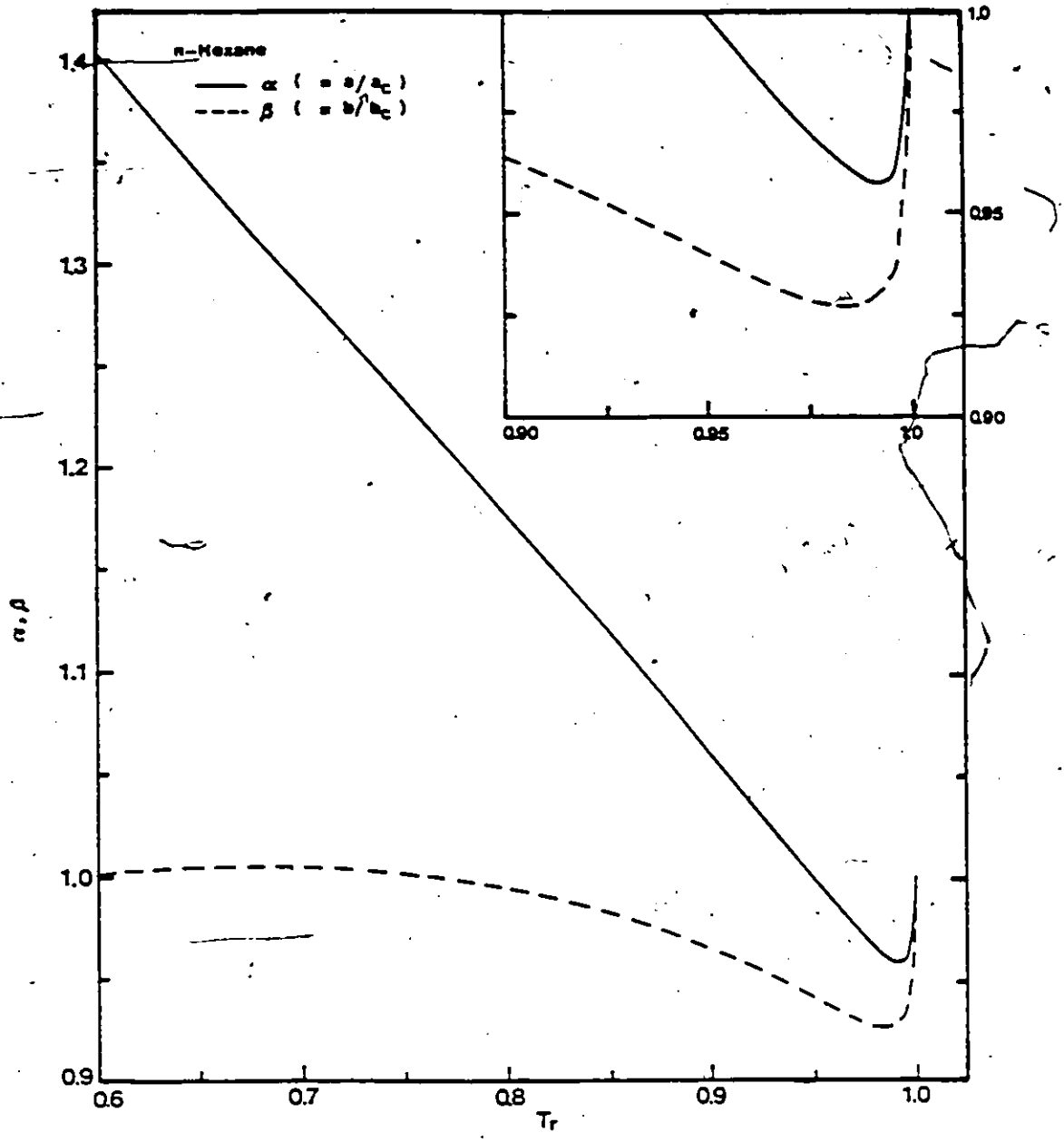

Figure 4.4: Temperature dependence of the parameters a and b in the PR equation for n-hexane.

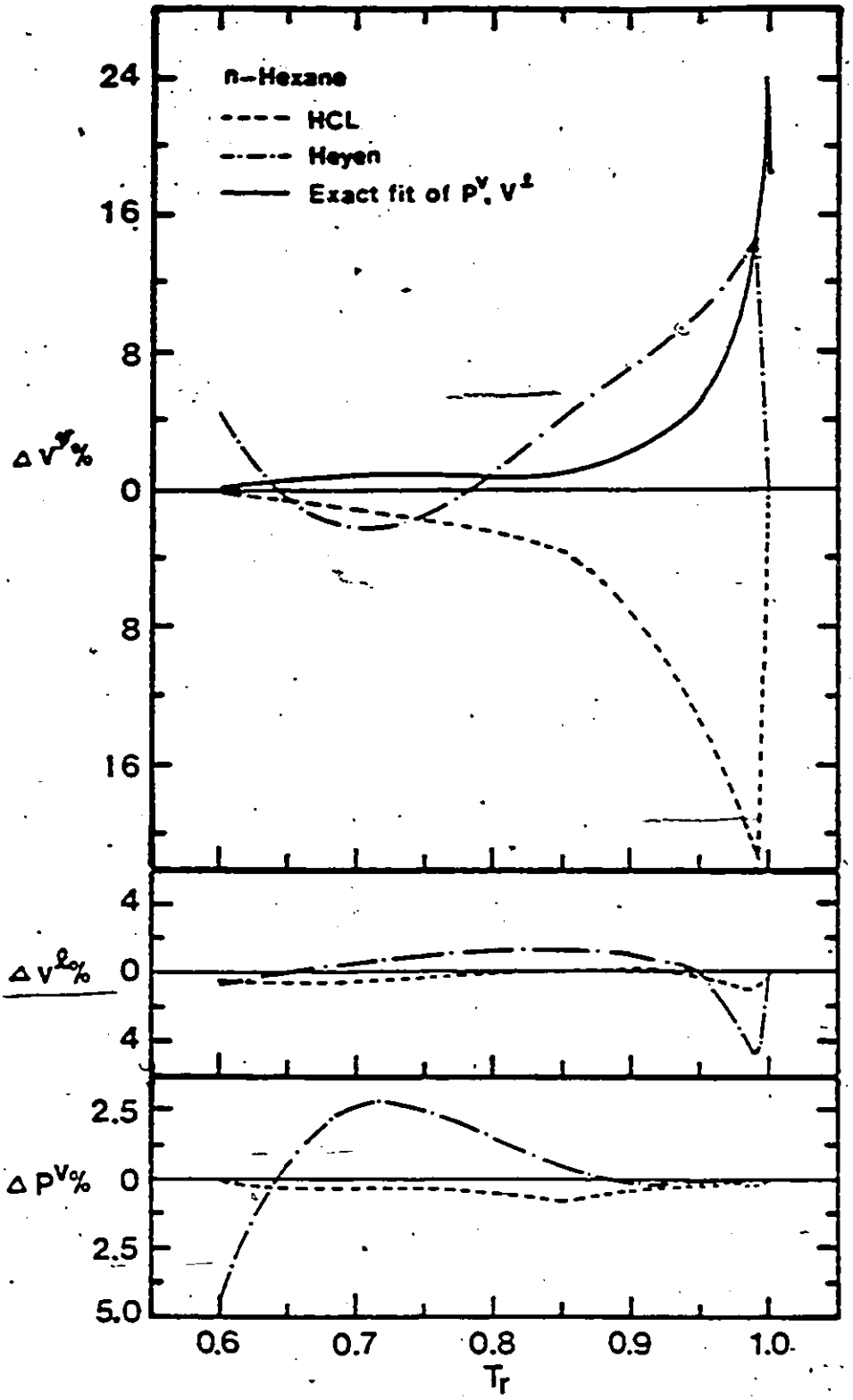

Figure 4.5: Comparison of the HCL, the H and the modified PR equations in calculating three saturation properties for n-hexane.

From theoretical discussion in Chapter II there are two factors that contribute to the correct representation of the saturation dome on the P-V surface. The first is that accurate prediction of P^{ν} is a necessary condition for determining the boundary of the vapor and liquid phases in equilibrium on the P-V surface. In other words, accurate representation of v^{ℓ} and v^{ν} requires accurate representation of P^{ν}. The second is that parameters u and w make important contributions to the volumetric behavior of Eq.(1.3) especially at high densities where multibody interactions are frequent. The former condition suggests that at subcritical temperatures, the temperature dependence of parameter a should be determined from vapor pressure values. The latter implies that parameters u and w should be chosen on the basis of the volumetric behavior of the equation in the saturated liquid or liquid phase. The influence of these two factors on the representation of v^{ℓ} and v^{ν} is further demonstrated based on Eq.(1.3).

For the first factor, the form of the PR equation is once again used to calculate v^{ℓ} and v^{ν} for n-hexane while different temperature functions are assumed for parameter a. These functions are

1. $a = a_c$ (4.8)

2. $a = a_c/T^{\frac{1}{2}}$ (4.9)

3. $a = a_c/T^{s}$, $s=0.697$ (4.10)

4. $a = a_c\,(1+m\,(1-T_r^{\frac{1}{2}}))^2$, $m=0.8085$ (4.11)

5. $a = \alpha(T_r)\,a_c$ (4.12)

The five equations listed above exhibit different degrees of accuracy in the calculation of P^v for n-hexane. In Eq.(4.8) the parameter a is treated as temperature independent. The quantity, s, in Eq.(4.10) is obtained by minimizing the average absolute percent deviation in P^v. Eq.(4.11) is the correlation originally used in the PR equation for the parameter a in which the value of m=0.8085 is obtained for P^v of n-hexane. The quantity, α, in Eq.(4.12) is determined from an exact fit of P^v at each given temperature while satisfying the equal-fugacity equilibrium condition.

Shown in Figure 4.6 is the comparison of the values of P^v, v^ℓ and v^v calculated from Eqs(4.8,9,10,11,12) with the actual values in the reduced temperature range from 0.6 to 1.0. As can be seen the degree of accuracy in predicting v^ℓ and v^v is related to that in predicting P^v. The more accurate the prediction of P^v is, the better the prediction of v^ℓ and v^v will be. Using values of the parameter a calculated from P^v leads to better representation of phase boundary, especially in the saturated vapor phase region. Without a temperature function for the parameter a, the prediction of the phase boundary is out of the question. It is interesting to note that for the first four equations studied the deviations in v^v are almost mirror images of the deviations in P^v along the zero deviation line except around the critical point where the deviations in v^v are very dependent on the error associated with the predicted critical compressibility factor. This indicates that the ability of an EOS to predict v^v depends primarily on its ability to predict P^v. This ability is, to a lesser extent, also necessary for predicting v^ℓ particularly in the region close to the critical point. This is mainly

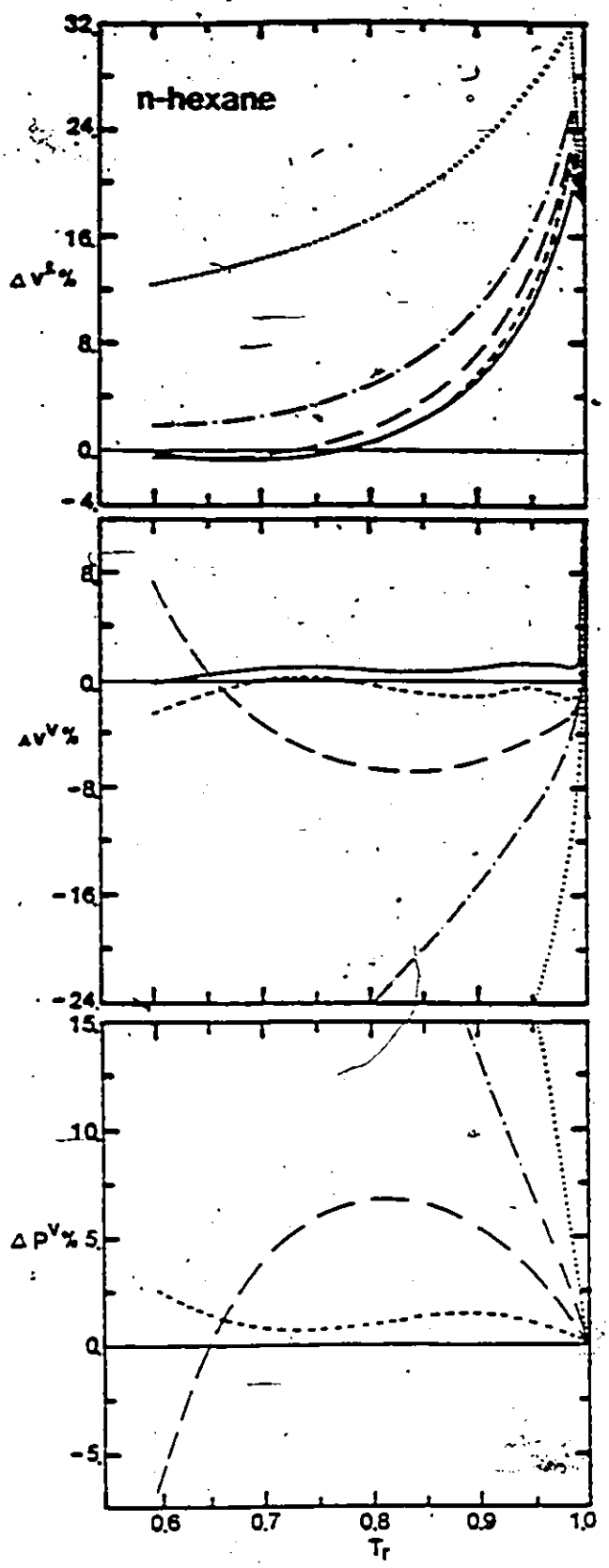

Figure 4.6: Calculated results of three saturation properties obtained from the PR equation together with Eqs(4.8,9,10,11,12).

because at low temperature, saturated liquid molar volumes do not change significantly with vapor pressure. However, overestimation of P^v would shift the saturation dome upwards from its actual position on the P-V surface. It should be noted that the above observations though derived using the form of the PR equation are typical of other VDW-type volume-cubic equations. Thus it would be safe to conclude that for accurate pure fluid VLE calculations, it is essential that Eq.(1.3) represent P^v with reasonable accuracy. By the same token, the temperature dependence of the parameter a determined from P^v values must be correlated and generalized as accurately as possible over the entire temperature range considered.

The second factor which concerns the parameters u and w is examined by assigning three sets of (u,w) values to Eq.(1.3). For each of the resulting equations, values of parameter a obtained by exact fitting of P^v are used. Thus the effect of the accuracy in reproducing P^v on the accuracy in predicting v^ℓ and v^v is eliminated. The three equations considered are the RK, the PR and that proposed by Harmens [47] designated herein as the Ha equation. Values of u, w, β_c, ζ_c, Ω_{ac} and Ω_{bc} for the three equations are given in Table 4.2.

Table 4.2: Values of the parameters in the RK, the PR and the Ha equations at the critical point.

equation	u	w	β_c	ζ_c	Ω_{ac}	Ω_{bc}
RK	1	0	0.260	0.333	0.42747	0.08666
PR	2	-1	0.253	0.307	0.45724	0.07780
Ha	3	-2	0.247	0.286	0.48288	0.07072

Calculation of v^{ℓ} and v^{v} demonstrates that the parameters u and w have greater effect on the representation of v^{ℓ} than on v^{v}. To illustrate, percent deviations in v^{ℓ} and v^{v} given by the three equations for C1, C6 and C10 are depicted in Figures 4.7, 4.8 and 4.9, respectively. As can be seen, by varying u and w, and thus β_c and ζ_c, the ability of Eq.(1.3) to predict v^{ℓ} changes drastically when compared to v^{v}. In the case of C6, the form of the PR equation (u=2,w=-1) appears to be quite suitable for calculating v^{v} and particularly well suited for predicting v^{ℓ}. For C1, v^{ℓ} and v^{v} are best predicted by the RK equation whereas the Ha equation gives the best predictions of v^{ℓ} and v^{v} for C10. It is interesting to note that the deviation curves for C1, C6 and C10 generated by the three equations have similar shapes, but shift up or down depending on the substance. However, this shifting occurs in such a way that does not alter significantly the relative spacing among the three deviations curves for v^{ℓ} and v^{v}. Similarity in the shape of the deviation curves indicates that the VDW-type volume-cubic equations always generate similarly shaped saturation domes no matter how u and w are adjusted. Nevertheless, shifting with substance would suggest that the location of the predicted saturation dome on the P-V surface would depend on the values assigned to u and w in Eq.(1.3). Insignificant changes in the relative spacing between the three deviation curves for v^{ℓ} and v^{v} indicate that there may exist a method for adjusting parameters u and w with substance so that Eq.(1.3) might give good account of the volumetric behavior of fluids, particularly in the saturated liquid phase.

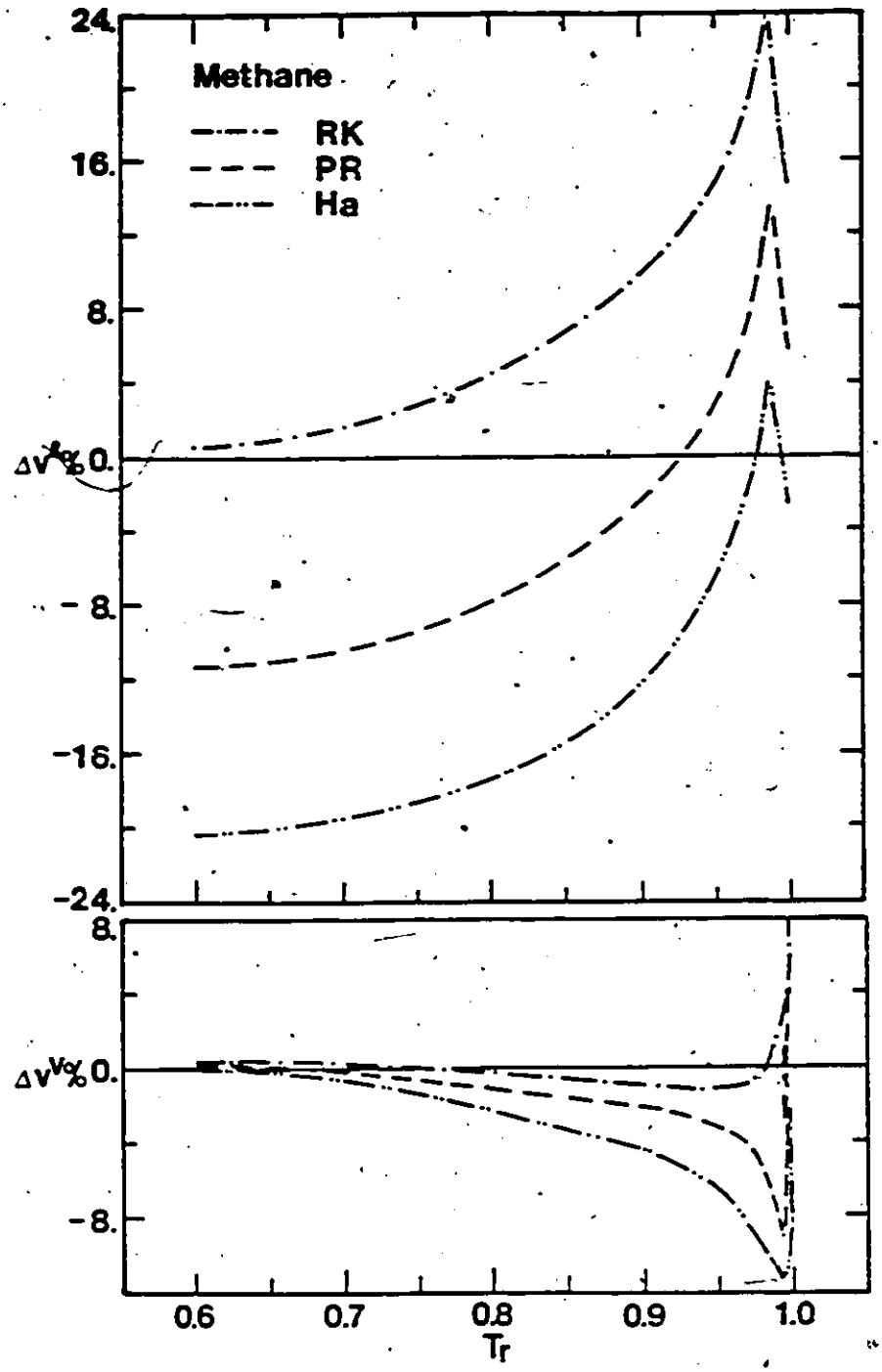

Figure 4.7: Comparison of the RK, the PR and the Ha equations in calculating saturated liquid and vapor molar volumes for methane.

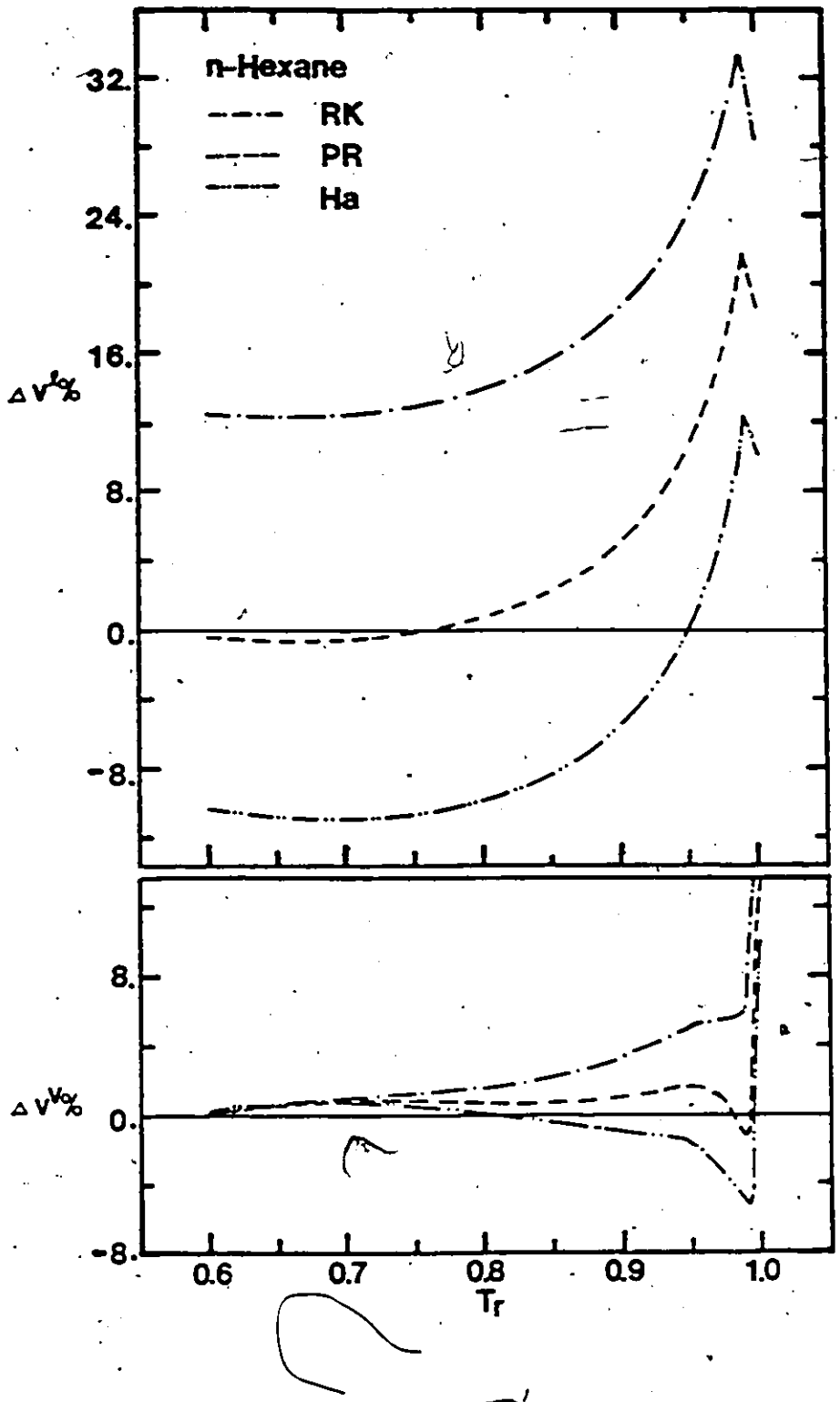

Figure 4.8: Comparison of the RK, the PR and the Ha equations in calculating saturated liquid and vapor molar volumes for n-hexane.

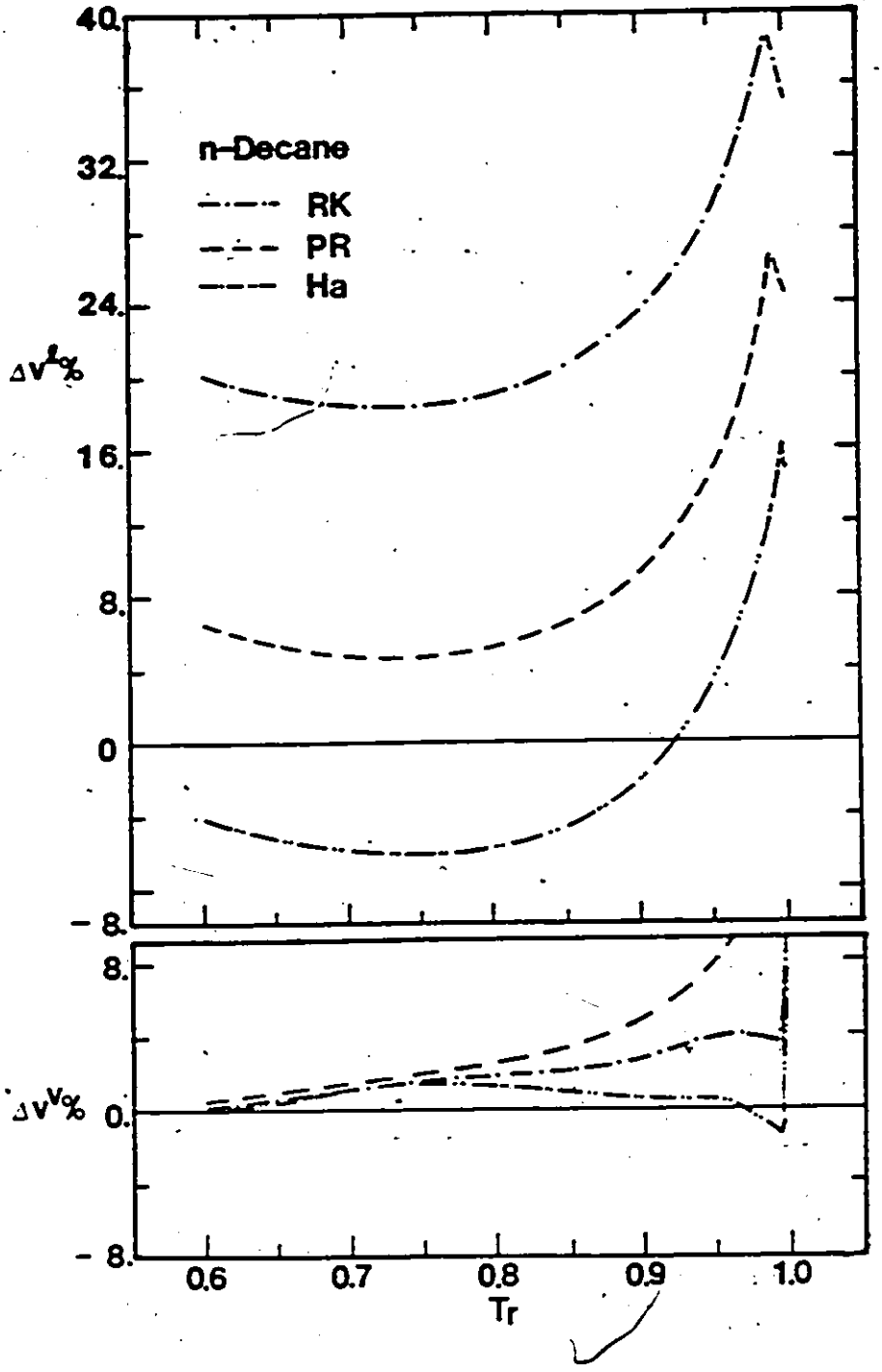

Figure 4.9: Comparison of the RK, the PR and the Ha equations in calculating saturated liquid and vapor molar volumes for n-decane.

The wide separation of the three deviation curves for v^{ℓ} for the alkanes studied indicates that both β_c and ζ_c influence the volumetric behavior of Eq.(1.3) in the saturated liquid phase. While β_c is related to the behavior of Eq.(1.3) at low temperatures, ζ_c affects the behavior in the critical region. On the other hand, the three deviation curves for v^{ν} start to separate significantly only when temperatures approach the critical. This indicates that the influence of u and w on the saturated vapor phase volumetric behavior in Eq.(1.3) is probably limited to the critical region. In addition, ζ_c plays a more important role than β_c in the volumetric behavior of Eq.(1.3) in the saturated vapor phase.

The quantitative effects of u and w on Eq.(1.3) in calculating v^{ℓ} and v^{ν} are investigated by means of deviation contours. Throughout this study, the average absolute percent deviation is chosen as the basis for the investigations. Two temperature ranges are considered. One covers the reduced temperature range from 0.5 to 0.98 and includes the critical region and another covers the reduced temperature range from 0.5 to 0.85 but excludes the critical region.

The computational scheme used to construct the deviation contours and to search for the optimum points $(u,w)_{min}$ related to the minimum average absolute percent deviations in v^{ℓ} and v^{ν} is described by means of the flow diagram in Figure 4.10. The inner loop 1 is used to determine a value of parameter a from the exact fit of P^{ν} for given u and w at each temperature, while satisfying the phase equilibrium condition $f^{\ell}=f^{\nu}$. The inner loop 2 is used to calculate the average absolute per-

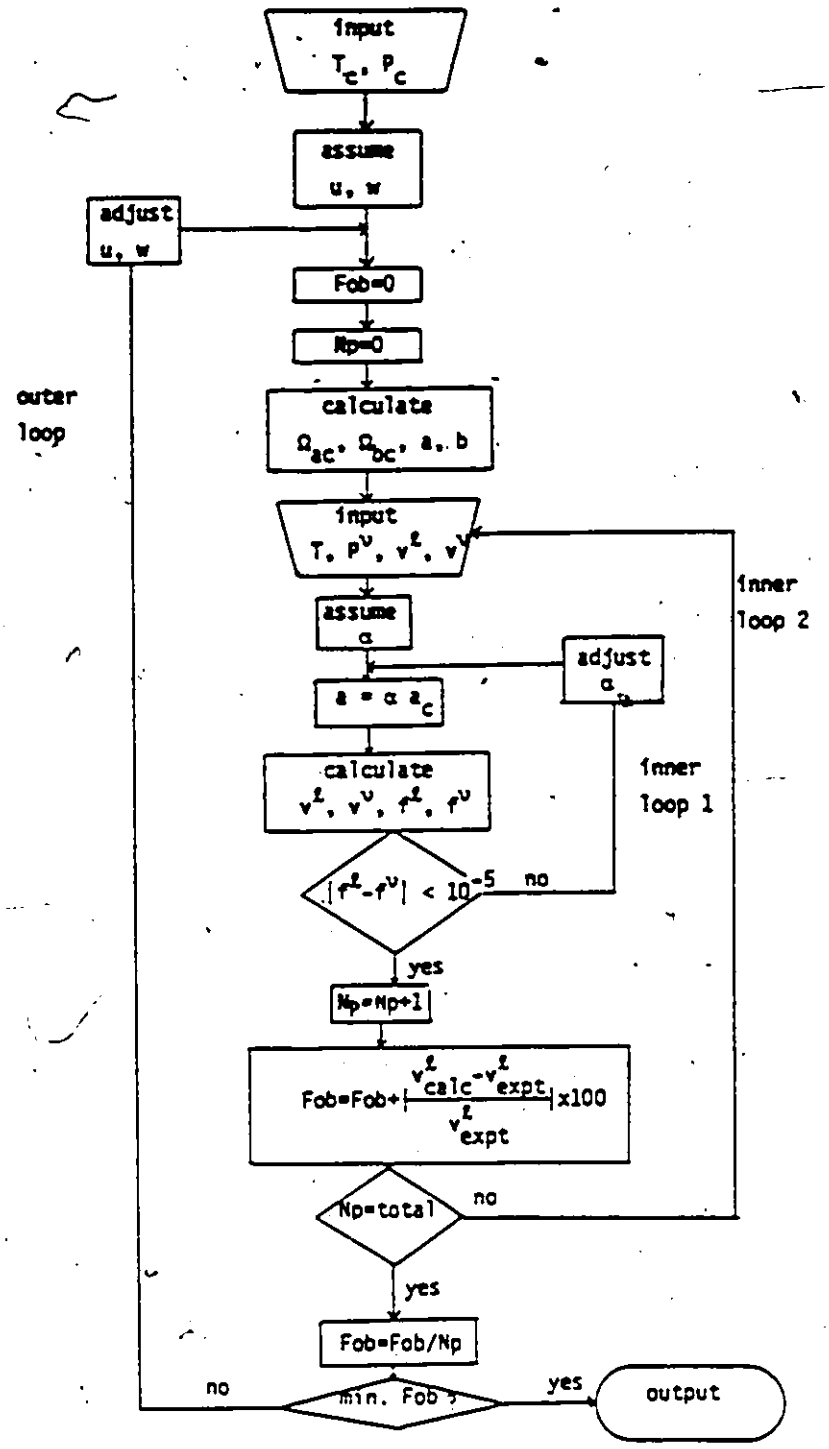

Figure 4.10: Flow diagram to construct deviation contours and to search for optimum u and w for saturated liquid or vapor molar volumes. Np- number of data points

cent deviations in both v^{ℓ} and v^{v} for each normal alkane from C1 to C10. The outer loop has two functions, the first is to assign sequential sets of (u,w) in order to construct contours for designated average absolute percent deviations. The second is to search for optimum values of u and w that will minimize the objective function, FOB, which corresponds to the average absolute percent deviation in v^{ℓ} or v^{v}. The search procedure for optimizing u and w is that of the golden-section optimization method [32].

Presented in Figures 4.11 and 4.12 are contours for 1.0 and 2.5 average absolute percent deviations in v^{v} and v^{ℓ}, respectively, for C1, C6 and C10 in the temperature range of $0.50 \leq T_r \leq 0.98$. Similar contours for the remaining normal alkanes fall between those for C1 and C10 by order of their carbon numbers and overlap with their immediate neighbors. The solid circles in Figure 4.12 indicate the optimum points, $(u,w)_{min}$, for v^{ℓ} from C1 to C10. Values of the optimum points and the corresponding Ω_{ac}, Ω_{bc}, β_c and ζ_c for C1 to C10 are recorded in Table 4.3 along with their respective average absolute percent deviations in v^{ℓ}. It should be noted that the 2.5% average deviation in v^{ℓ} corresponds to an increase in magnitude of the minimum deviations given by $(u,w)_{min}$ of between 0.5 and 1.0%. In view of the relatively large areas covered by the 1.0% deviation contours of v^{v} it would not be necessary to search for optimum values of u and w in Eq.(1.3) for v^{v}. However, it is worth noting that the shifting of the deviation contours of v^{v} for C1 to C10 indicates that the locus of the optimum points for v^{v} would move in a direction away from that of v^{ℓ} and towards that of (β_c^*, ζ_c).

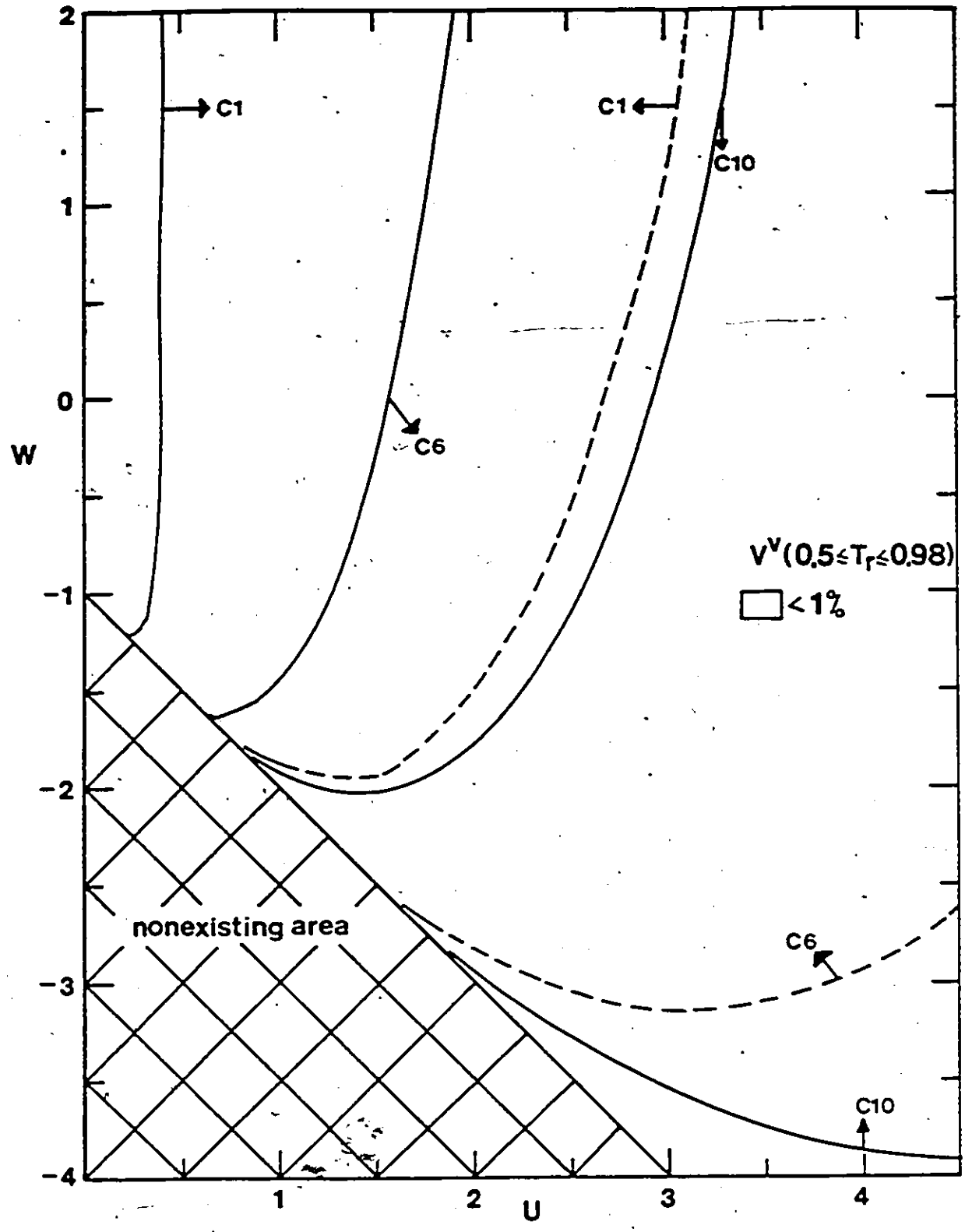

Figure 4.11: 1.0% deviation contours of saturated vapor molar volumes for C1, C6 and C10 for $0.50 \leq T_r \leq 0.98$.

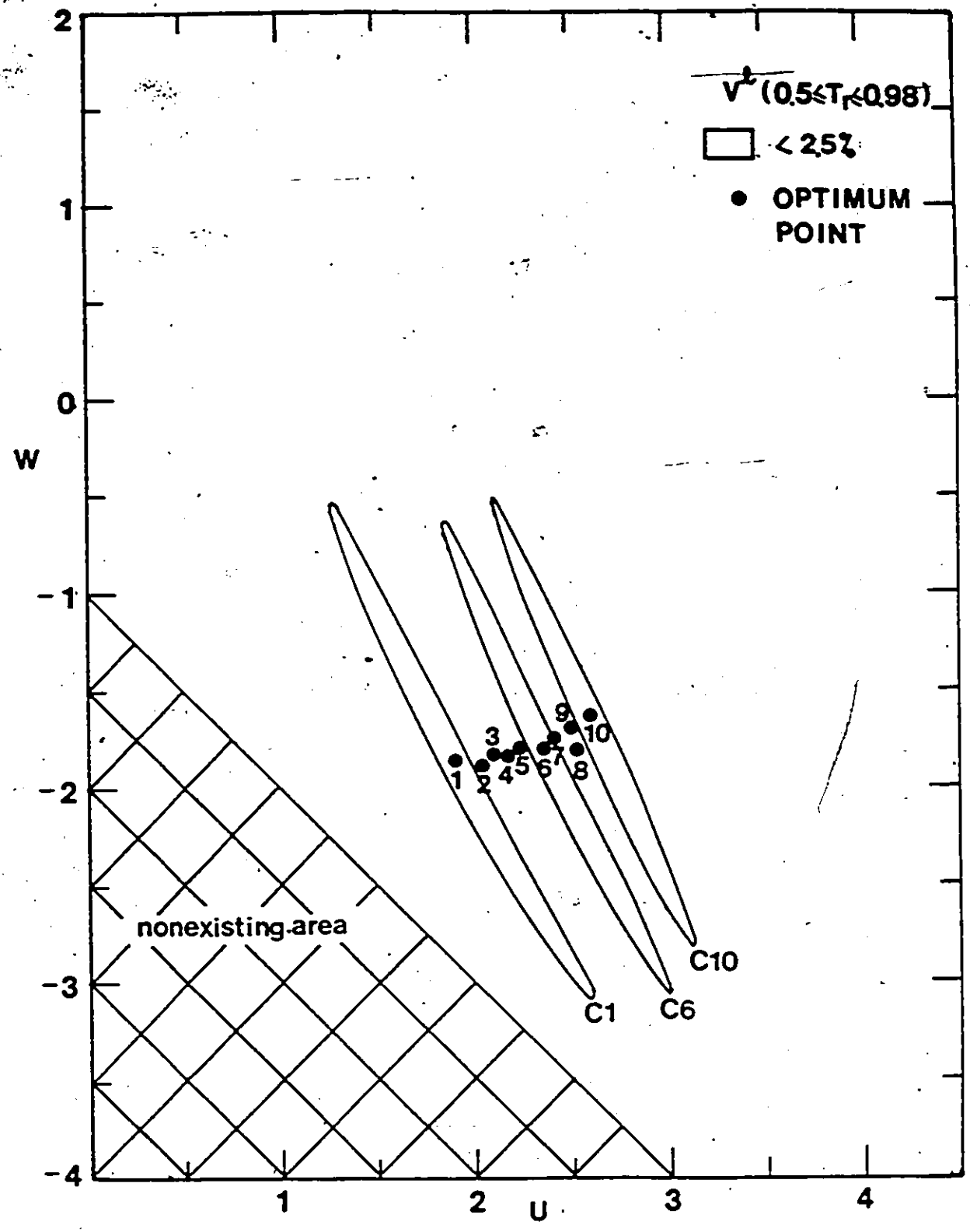

Figure 4.12: 2.5% deviation contours of saturated liquid molar volumes for C1, C6 and C10 for $0.50 \leq Tr \leq 0.98$.

Table 4.3: Results of the minimization of deviations in saturated liquid molar volumes for $0.50 \leq Tr \leq 0.98$.

	u_{min}	w_{min}	β_c	ζ_c	Ω_{ac}	Ω_{bc}	$\lvert\Delta v^{\ell}\rvert$%
C1	1.903	-1.870	0.3108	0.3048	0.49289	0.09747	1.47
C2	2.041	-1.886	0.2997	0.3020	0.49030	0.09048	1.61
C3	2.090	-1.826	0.2913	0.3014	0.48629	0.08781	1.70
C4	2.160	-1.848	0.2875	0.3000	0.48610	0.08625	1.77
C5	2.235	-1.800	0.2793	0.2990	0.48285	0.08349	1.83
C6	2.360	-1.818	0.2723	0.2967	0.48205	0.08079	1.90
C7	2.392	-1.766	0.2676	0.2965	0.47977	0.07935	1.96
C8	2.520	-1.825	0.2633	0.2941	0.48069	0.07744	2.06
C9	2.493	-1.673	0.2577	0.2954	0.47580	0.07613	2.08
C10	2.581	-1.636	0.2518	0.2943	0.47420	0.07490	2.13

Note that all deviation contours of v^{ℓ} and v^{v} for C1 to C10 fall into the same region on the u-w diagram, that is $u > 0$. With reference to Figure 4.2, this region corresponds approximately to $\beta_c < 0.35$ and $\zeta_c < 0.375$. Several characteristics of the deviation contours of v^{ℓ} and v^{v} can be observed from Figures 4.11 and 4.12.

Comparing Figure 4.11 with Figure 4.2 shows that the boundaries of each contour of v^{v} are very close to those outlined by two constant-ζ_c curves on the u-w plot. Also due to their orientation and shape the contours for C1 to C10 have almost the same range of β_c values but a limited range of ζ_c values. These evidently affirm the observation made earlier that the predicted ζ_c dominates the volumetric behavior of Eq.(1.3) in the saturated vapor phase, while the predicted β_c has little influence. It is interesting to note that if 2.5% average absolute deviation is used to define the deviation contour of v^{v}, the area of the resulting contour covers most of the area on the u-w diagram shown in Figure 4.12. Thus for each alkane, any chosen point (u,w) from $0<u<4$, $-4<w<2$, can give an average absolute deviation in v^{v} within 2.5%.

For the same designated deviation, the area occupied by the contour of v^{ℓ} of each alkane is much smaller than that of the corresponding contour of v^{v} on the same u-w plot. It appears that the orientation of the contours of v^{ℓ} is different from that for v^{v} on the u-w diagram. Contrary to the deviation contours of v^{v}, those for v^{ℓ} from C1 to C10 are arranged in sequence with the constant-β_c curves of decreasing magnitude. In this way the elliptical deviation contour of v^{ℓ} for each alkane has relatively limited ranges of β_c and ζ_c values. This indicates that the volumetric behavior of Eq.(1.3) in the saturated liquid phase is sensitive to the variation of u and w as well as β_c and ζ_c.

In this study, it is assumed that 2.5% average absolute deviation would be about the maximum allowance for accepting an equation for the representation of v^{ℓ} and v^{v} at reduced temperatures ranging from 0.5 to 0.98. To satisfy this requirement one should select u and w for each alkane within the area encircled by the 2.5% deviation contour of v^{ℓ}, since a 2.5% deviation contour of v^{v} covers almost the whole area occupied by the corresponding contour of v^{ℓ}.

It should be noted that using the optimum points $(u,w)_{min}$ for v^{ℓ} determined for $0.50 \leq T_r \leq 0.98$ would not result in the the best representation of v^{ℓ} at temperatures away from the critical. This is because the effect of minimization is to dissipate the relatively large errors in v^{ℓ} near the critical point to lower temperatures. While reducing the accuracy in representing v^{ℓ} at low temperatures, the errors near the critical point are still not acceptable.

Following the suggestion of Spencer and Alder [120], the critical point region considered in this study is the temperature range from T_r=0.85 to T_r=1.0. Consequently the optimum points $(u,m)_{min}$ for v^ℓ for $0.50 \leq T_r \leq 0.85$ are obtained by minimizing the average absolute percent deviation in v^ℓ for each individual alkanes. The results of minimization are presented in Table 4.4. The last two columns list the average absolute percent deviations in v^ℓ and v^v calculated for $0.50 \leq T_r \leq 0.98$. It can be seen that the optimum points thus obtained can maintain average deviations in v^ℓ close to those corresponding to the optimum points determined for the entire temperature range of $0.50 \leq T_r \leq 0.98$. It is further observed that these optimum points also enable Eq.(1.3) to represent v^ℓ for $0.50 \leq T_r \leq 0.85$ within $\pm$1.0% compared to $\pm$2.0% given by the optimum points determined for $0.50 \leq T_r \leq 0.98$. In addition, Table 4.4 also shows that for $0.50 \leq T_r \leq 0.98$, these optimum points can predict less than 1.0% average absolute deviations in v^v for all the normal alkanes considered except C10 for which the deviation is slightly higher.

Figure 4.13 presents 1.0% deviation contours of v^ℓ for C1, C6 and C10 for $0.50 \leq T_r \leq 0.85$. The optimum points presented in Table 4.4 are also depicted. Similar contours for other normal alkanes fall between C1 and C10 in sequence of their carbon numbers and overlap with their immediate neighbors. As can be seen these contours have the same characteristics as those obtained for $0.50 \leq T_r \leq 0.98$ as shown in Figure 4.12. It appears that excluding the critical point region results in the contours shifting towards the area of higher values of ζ_c and lower values of β_c. This fact can be further demonstrated by plotting the

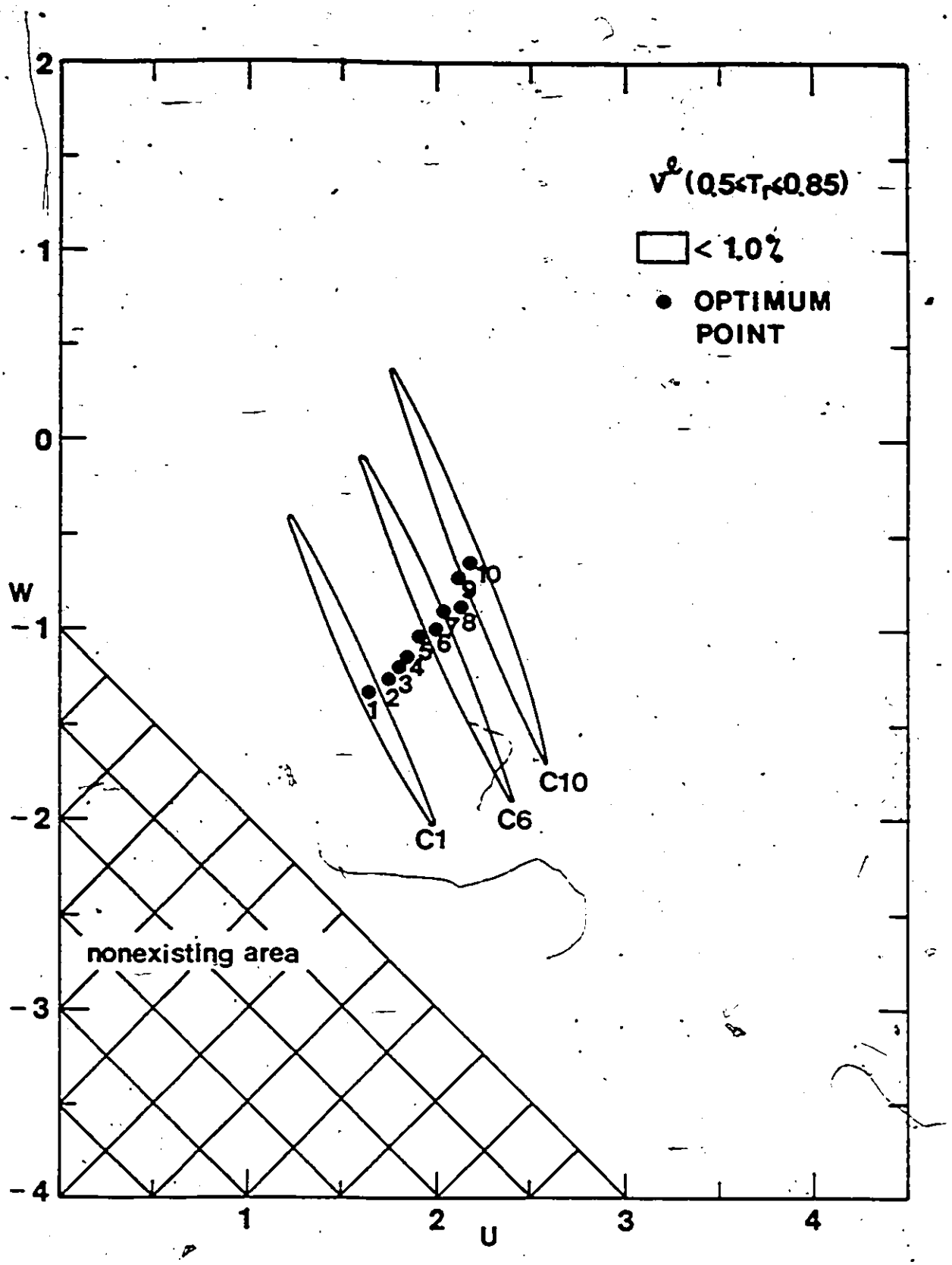

Figure 4.13: 1.0% deviation contours of saturated liquid molar volumes for C1, C6 and C10 for $0.50 \leq T_r \leq 0.85$.

Table 4.4: Results of the minimization of deviations in saturated liquid molar volumes for $0.50 \leq T_r \leq 0.85$.

	u_{min}	w_{min}	β_c	ζ_c	Ω_{ac}	Ω_{bc}	$\lvert\Delta v^{\ell}\rvert\%$	$\lvert\Delta v^{\ell}\rvert\%$ [1]	$\lvert\Delta v^{v}\rvert\%$ [1]
C1	1.636	-1.327	0.2918	0.3139	0.47035	0.09162	0.42	1.63	0.75
C2	1.743	-1.265	0.2803	0.3117	0.46674	0.08738	0.46	1.79	0.61
C3	1.799	-1.201	0.2733	0.3107	0.46400	0.08491	0.48	1.89	0.50
C4	1.826	-1.128	0.2679	0.3104	0.46138	0.08315	0.50	1.98	0.35
C5	1.890	-1.036	0.2601	0.3095	0.45835	0.08047	0.50	2.04	0.47
C6	2.002	-1.008	0.2533	0.3073	0.45745	0.07785	0.52	2.12	0.55
C7	2.019	-0.910	0.2486	0.3074	0.45485	0.07642	0.53	2.19	0.50
C8	2.122	-0.898	0.2438	0.3055	0.45472	0.07447	0.56	2.32	0.61
C9	2.089	-0.717	0.2388	0.3067	0.45036	0.07325	0.55	2.33	0.66
C10	2.169	-0.639	0.2333	0.3056	0.44898	0.07129	0.56	2.39	1.21

1) for $0.50 \leq T_r \leq 0.98$

deviation contours of v^{ℓ} for $0.50 \leq T_r \leq 0.85$ and $0.50 \leq T_r \leq 0.98$ on a β_c-ζ_c diagram. Shown in Figure 4.14 are the deviation contours of v^{ℓ} for C1 and C10 obtained for the two temperature ranges. When the critical point region is excluded, the optimum point shifts to where the corresponding value of β_c decreases by about 15.0% and that of ζ_c increases by about 15.0%. This results in a large amount of error being shifted to the critical point region while the total error for $0.50 \leq T_r \leq 0.98$ remains the same (since the new optimum point is still within the 2.5% deviation contour). It should be noted that the changes in the values of β_c and ζ_c caused by narrowing the temperature range, should occur simultaneously in order that Eq.(1.3) have optimal performance.

It should be noted that for each alkane there exists an overlapping area between the contours of v^{ℓ} obtained for the two temperature ranges considered. In this area each (u,w) enables Eq.(1.3) to predict v^{ℓ} within 1.0% absolute average deviation for $0.50 \leq T_r \leq 0.85$ and within 2.5% for $0.50 \leq T_r \leq 0.98$. If emphasis is placed on representing of v^{ℓ} in the

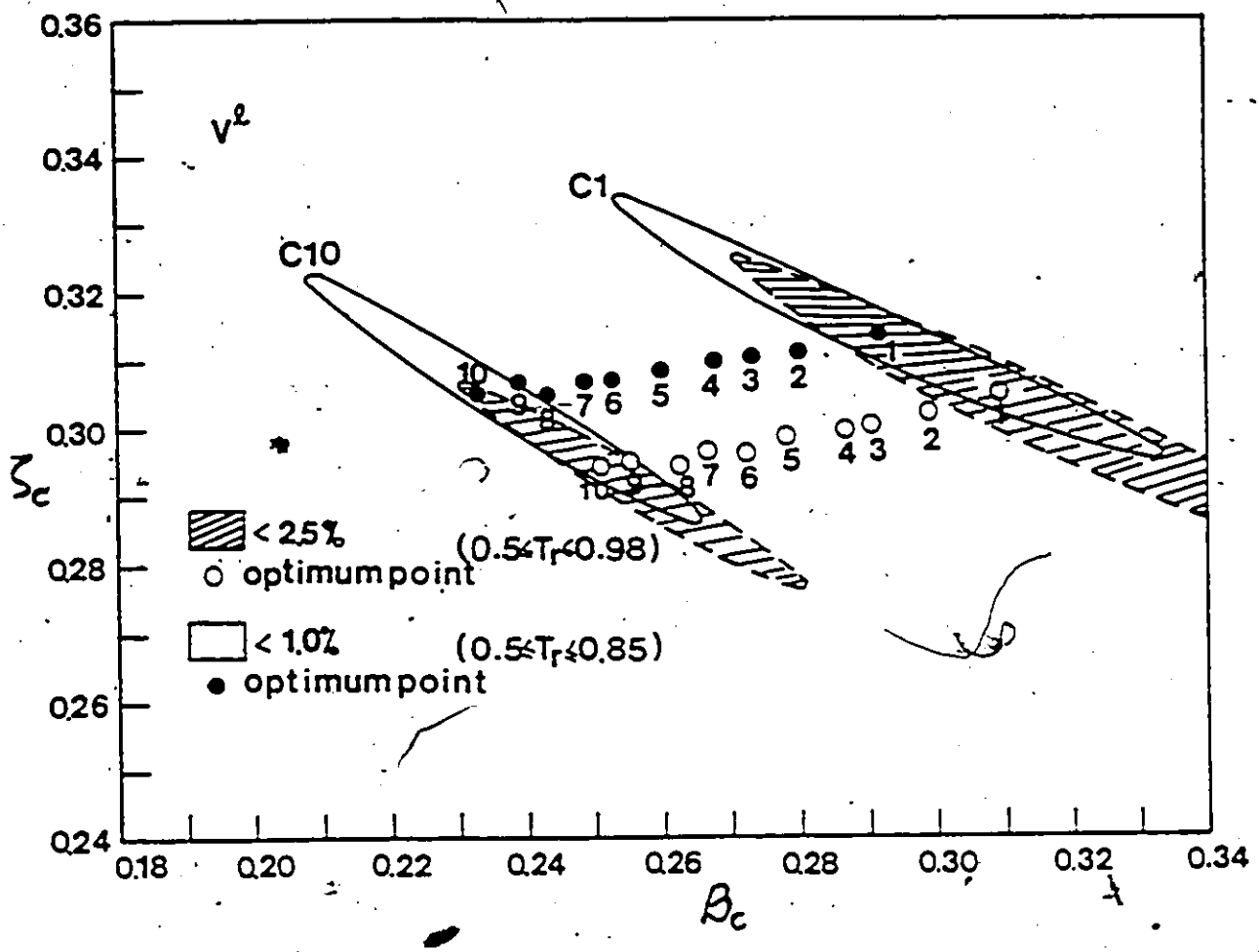

Figure 4.14: 1.0% ($0.50 \leq T_r \leq 0.85$) and 2.5% ($0.50 \leq T_r \leq 0.98$) deviation contours of saturate liquid molar volumes on $\beta_c - \zeta_c$ diagram.

range $0.50 \leq T_r \leq 0.85$ while trying to maintain the average absolute deviation within 2.5% for $0.50 \leq T_r \leq 0.98$, values of the parameters u and w should therefore be chosen from the overlapping area.

4.1.3 Analytical Expression for the Temperature Dependence of Parameter a at Subcritical Conditions

The above analyses were carried out using exact values of parameter a determined from the vapor pressures. Therefore, it is necessary to find an expression that can accurately predict these values. Values of parameter a can be related to that at the critical point by the expression $a = \alpha\, a_c$. The dimensionless quantity, α, is a function of temperature whose values are calculated from the vapor pressures. At $T_r = 1$, the value of α is unity in order to satisfy the critical point conditions.

Figure 4.15 shows a typical plot of α vs. T_r for the ten alkanes. In this study, three analytical expressions are considered to represent the temperature dependence of α shown in Figure 4.15. They are

$$\alpha^{\frac{1}{2}} - 1 = \kappa\,(1 - T_r^{\frac{1}{2}}) \qquad (4.13)$$

$$\log_{10}\alpha = \kappa\,(1 - T_r^{\frac{1}{2}}) \qquad (4.14)$$

$$\log_{10}\alpha = \kappa\,(1 - T_r) \qquad (4.15)$$

Eq.(4.13) was originally proposed by Soave [119] and later on adopted in many equations of state. Eq.(4.14) was suggested by El-Twaty and Prausnitz [29] for calculations at supercritical conditions. Eq.(4.15) retains a form similar to the one proposed by Heyen for his own equa-

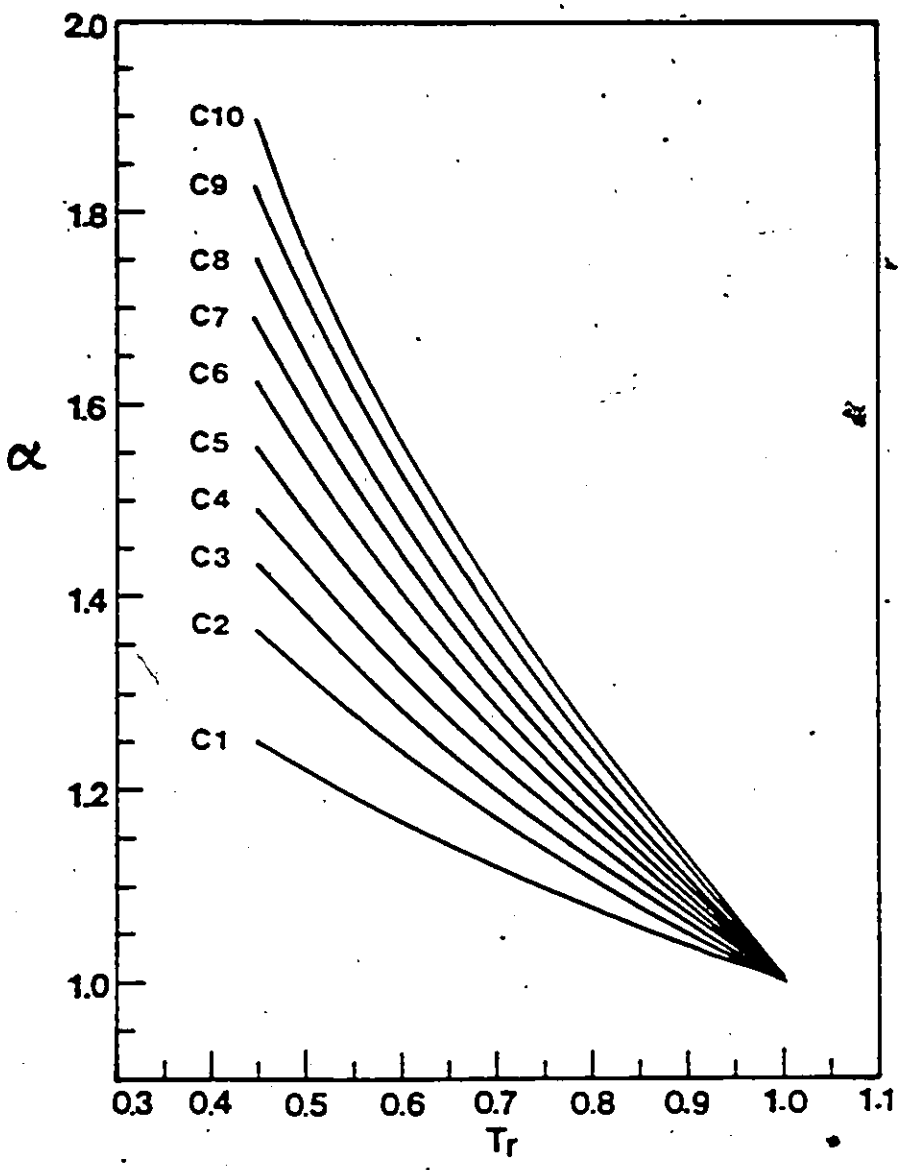

Figure 4.15: Typical temperature dependence of α determined from the vapor pressures.

tion of state [53]. The quantity, κ, in Eqs(4.13,14,15) was originally treated as substance dependent in order to linearize each α-T_r curve in Figure 4.15. At the critical point, all these equations can predict a value of α equal to unity.

The quantity, κ, should be treated as temperature dependent for accurate correlation of α at low temperatures $T_r < 0.60$, particularly for substances with large molecules. It should be noted that the temperature dependence of κ for the three equations is similar. A typical plot of the temperature dependence of κ is illustrated in Figure 4.16. As can be seen it would be a poor approximation to assume κ independent of temperature. Using the κ-T_r curve for C7 as reference, the following expression is adequate for Eqs(4.13,14,15) to represent the temperature dependence of κ for the ten alkanes

$$\kappa(T_r, \omega) = \frac{\gamma(\omega)}{\gamma_0} (A_0 + A_1 T_r + A_2 T_r^2) \qquad (4.16)$$

The quantity γ is substance dependent and is evaluated by averaging κ values at reduced temperatures ranging from 0.45 to 1.0, and is generalized by a simple polynomial in the acentric factor, ω. The quantity, γ_0 corresponds to that of the reference fluid, n-heptane. The constants A_0, A_1 and A_2 are calculated from the values of κ for n-heptane. The result obtained for κ in Eq.(4.13) by means of Eq.(4.16) is presented in Figure 4.16. As can be seen, the temperature dependence of κ can be closely simulated. In general, when incorporating the three equations Eqs(4.13,14,15) with Eq.(4.16) Eq.(1.3) can predict the vapor pressures of normal fluids with similar accuracy. However, these equations exhibit different behavior at

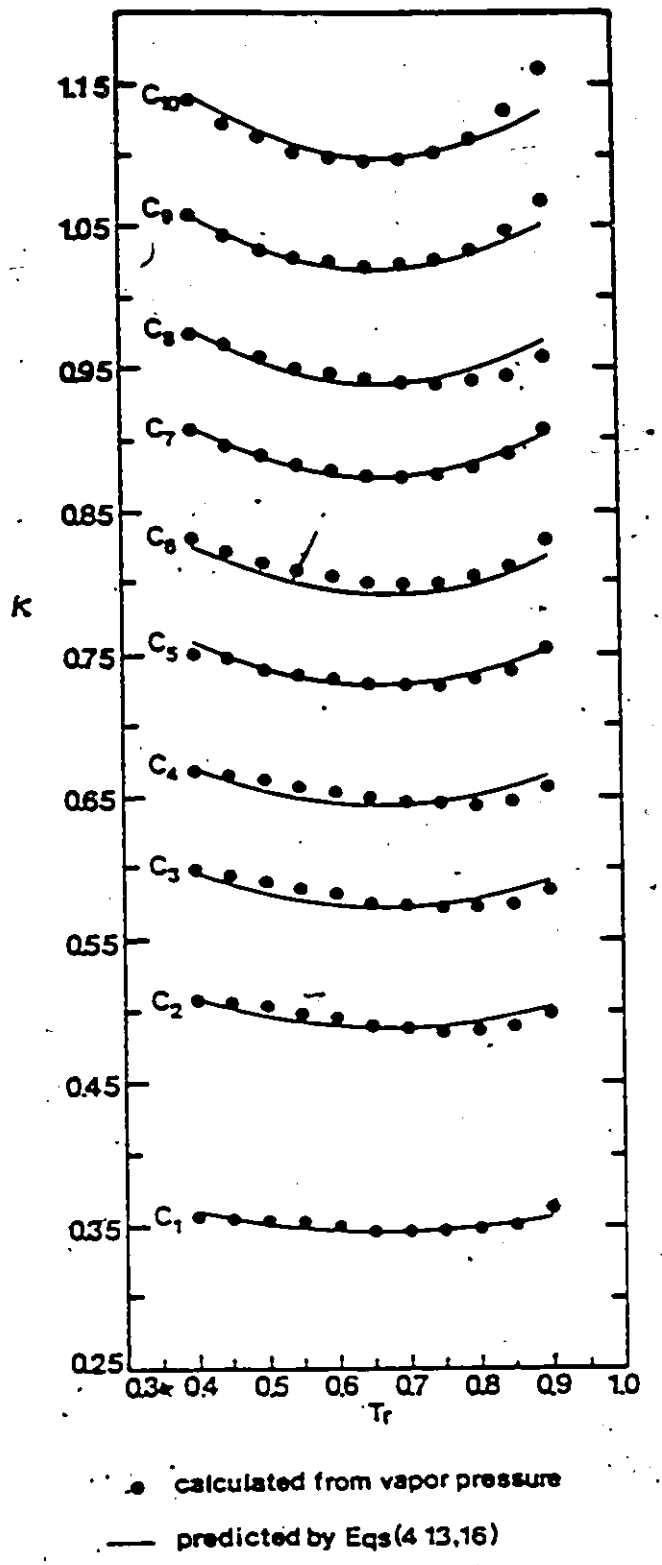

Figure 4.16: Typical temperature dependence of κ in Eq.(4.16).

supercritical temperatures and so their ability to calculate gas compressibility factors at these conditions must be taken into consideration when choosing one as the temperature function for the parameter a.

4.1.4 Supercritical Gas Phase

In the application of Eq.(1.3) at supercritical temperatures, the temperature dependence of parameter a can be estimated either by extrapolating the temperature function for parameter a found at subcritical temperatures, or by using an additional temperature function developed by fitting Z^{sup} values. The former method requires extrapolation of the three equations found in the previous section, i.e., Eqs(4.13,14,15). The latter is related to the use of α to minimize the deviations in the calculated Z^{sup} values for each supercritical isotherm. For the sake of simplicity, it is preferable to use a single temperature function for parameter a for the volumetric calculations at subcritical and supercritical temperatures. Hence, one of the three temperature functions for parameter a is selected on the basis of its accuracy in representing the temperature dependence of the optimum α obtained by minimizing the deviations in Z^{sup}. Typical temperature dependence of the optimum α for the first ten normal alkanes is depicted in Figure 4.17. As can be seen, the optimum α value decreases with increasing reduced temperature and for large molecules, it becomes negative at $T_r > 2$. Negative values of α are not acceptable, since in theory parameter a should be positive. None of the three temperature functions considered yields negative values of α. However for a closer approximation to the optimum α, values of κ in Eqs(4.13,14,15) should

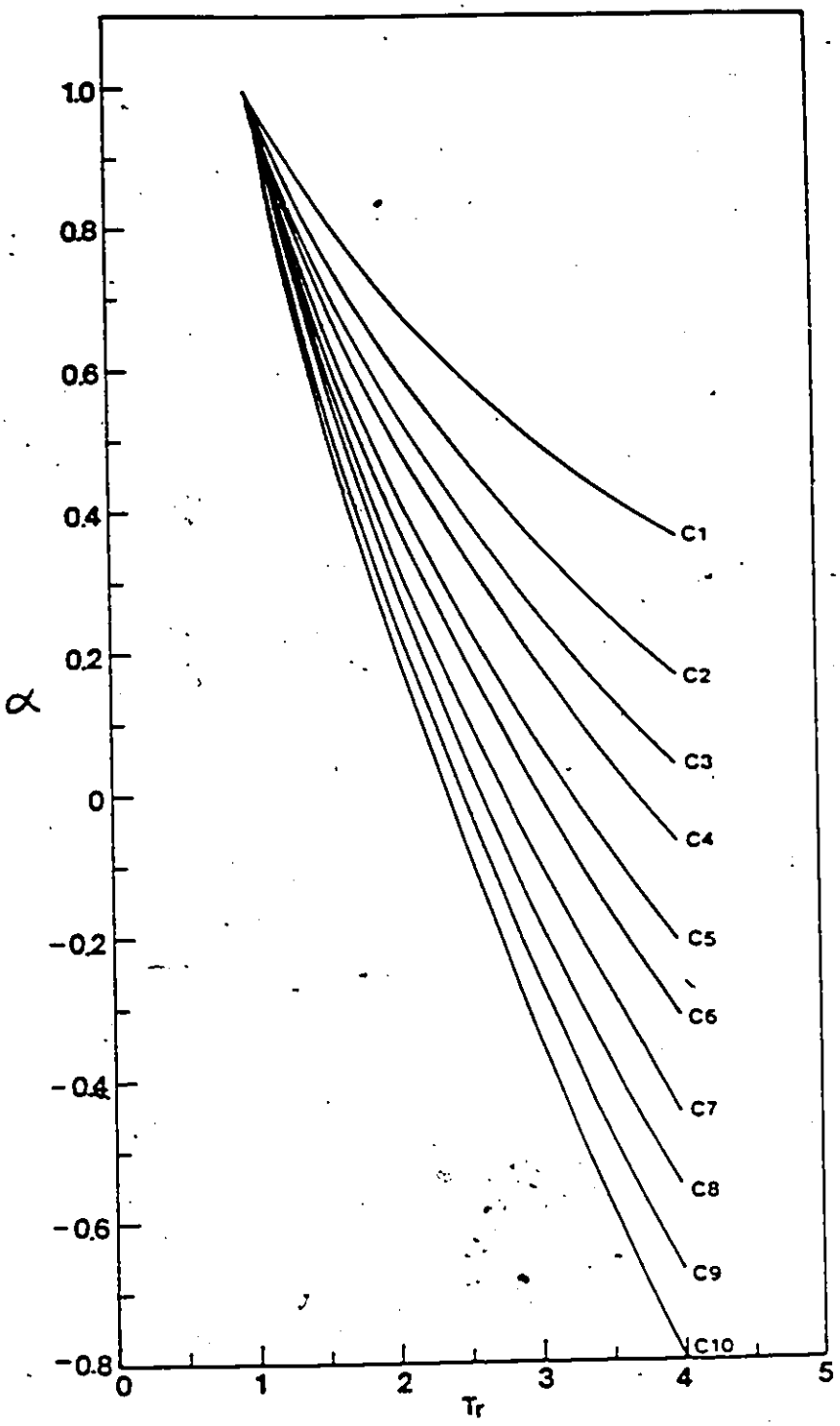

Figure 4.17: Typical temperature dependence of the optimum α determined by minimizing the deviations in Z^{sup}.

be those at the critical temperature i.e., $\kappa(T_r,\omega)=\kappa(1,\omega)$. It should be noted that Eq.(4.13) having the same form as that proposed by Soave [119] can approximate the temperature dependence of the optimum α better than Eqs(4.14,15). To illustrate, Figure 4.18 shows the comparison of α values calculated by the three equations with those of the optimum α for C1 and C10. It is clear that Eq.(4.13) can better represent the temperature dependence of the optimum α than Eqs(4.14,15). Consequently, Eq.(4.13) is chosen to represent the temperature dependence of α, and therefore parameter a, throughout the rest of the study.

In principle, the intermolecular attractive forces should diminish as temperature approaches infinity. Thus the attractive term in Eq.(1.3) must vanish as $T \to \infty$. This further implies that as the temperature approaches infinity, either the predicted α should vanish or the magnitude of the denominator in the attractive term of Eq.(1.3) should increase faster than parameter a. The first condition can be satisfied by Eqs(4.14,15), but not by Eq.(4.13). This is because Eq.(4.13) tends to predict a value for α which increases with temperature at very high T_r. When T_r is very large the second condition will be automatically be satisfied since the volume in the denominator of the attractive term will also be very large.

It is interesting to note that the temperature dependence of α determined from P^v and that of the optimum α determined using Z^{sup} can be represented with deviations of about $\pm$ 1% by a single temperature function of the following form

$$\alpha = 1+C_0(1-T_r^{\frac{1}{2}})+C_1(1-T_r^{\frac{1}{2}})^2+C_2(1-T_r^{\frac{1}{2}})^3 \qquad (4.17)$$

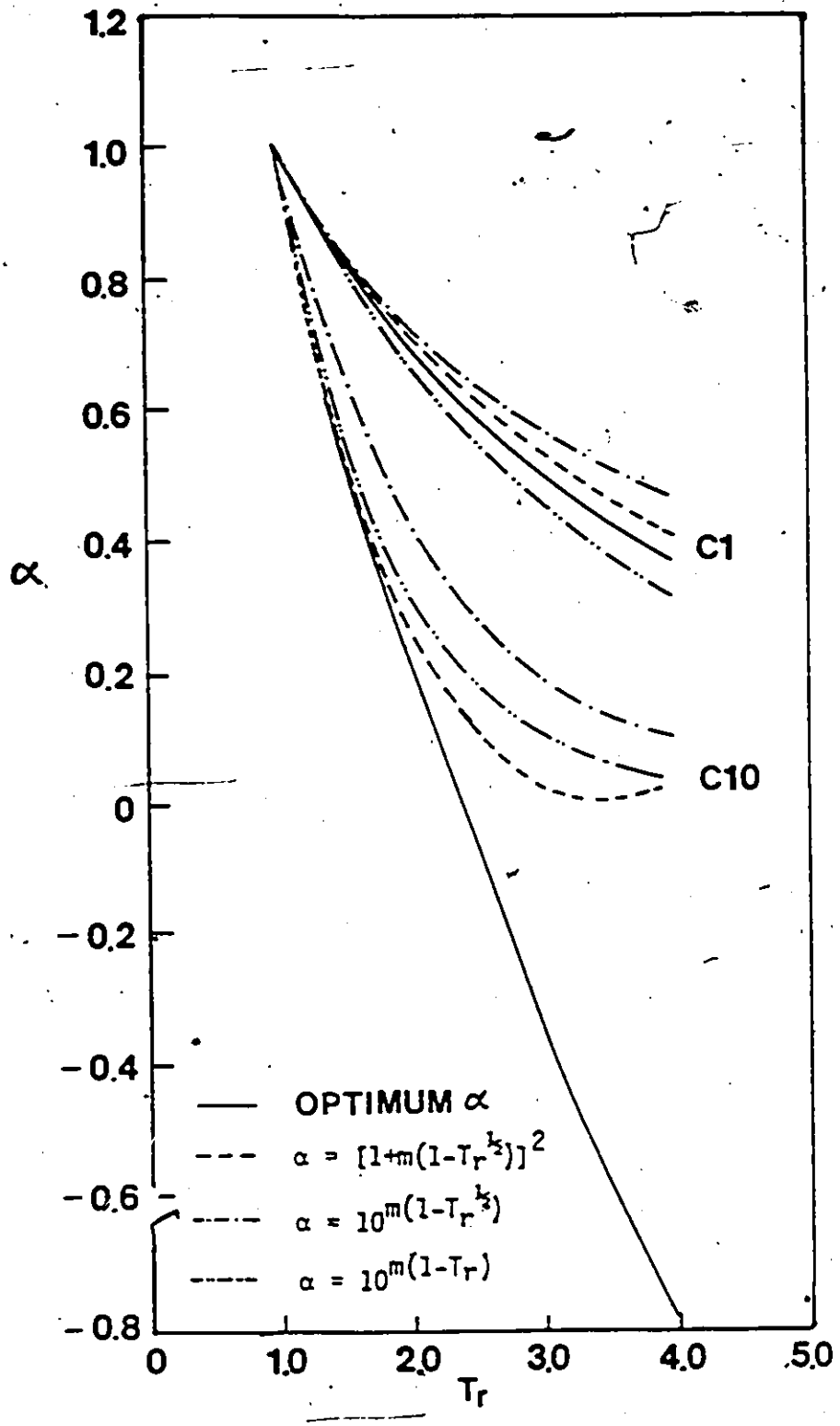

Figure 4.18: Comparison of α calculated from Eqs(4.13,14,15) and the optimum α of Z^{sup} for methane and n-decane.

where the constants C_0, C_1 and C_2 can be accurately generalized using polynomials in the acentric factor. At T_r=1, Eq.(4.17) yields a value of α of unity and negative values of α at $T_r > 2$. Even though negative values of α are theoretically unacceptable, Eq.(4.17) can still be used for such calculations as P^v and Z^{sup}.

Using Eq.(4.13) to represent the temperature dependence of parameter a, the effects of u and w as well as β_c and ζ_c on the volumetric representation of Eq.(1.3) at supercritical temperatures are investigated by means of deviation contours on a u-w diagram. The computational scheme to construct the contours and to search for optimum points $(u,w)_{min}$ for minimizing deviations in Z^{sup} is described in Figure 4.19. For each given (u,w), the temperature dependence of parameter a must be determined using P^v values for C1 to C10 and correlated by means of Eqs(4.13,16). The outer loop in Figure 4.19 is only used to obtain the optimum value of (u,w) for each alkane.

Summarized in Table 4.5 are the results of the minimization of deviations in Z^{sup} for the ten normal alkanes. The optimum points $(u,w)_{min}$ for the first ten alkanes are depicted on the u-w diagram in Figure 4.20. Also shown are the average absolute deviation contours of 1.5% for C1, 2.0% for C6 and 2.5% for C10. Each of the these deviations which are considered acceptable in this study is about a 0.5% increase in magnitude from those calculated using the optimum points. Similar contours for other normal alkanes fall between those for C1 and C10 by order of their carbon numbers and overlap extensively with their neighbors.

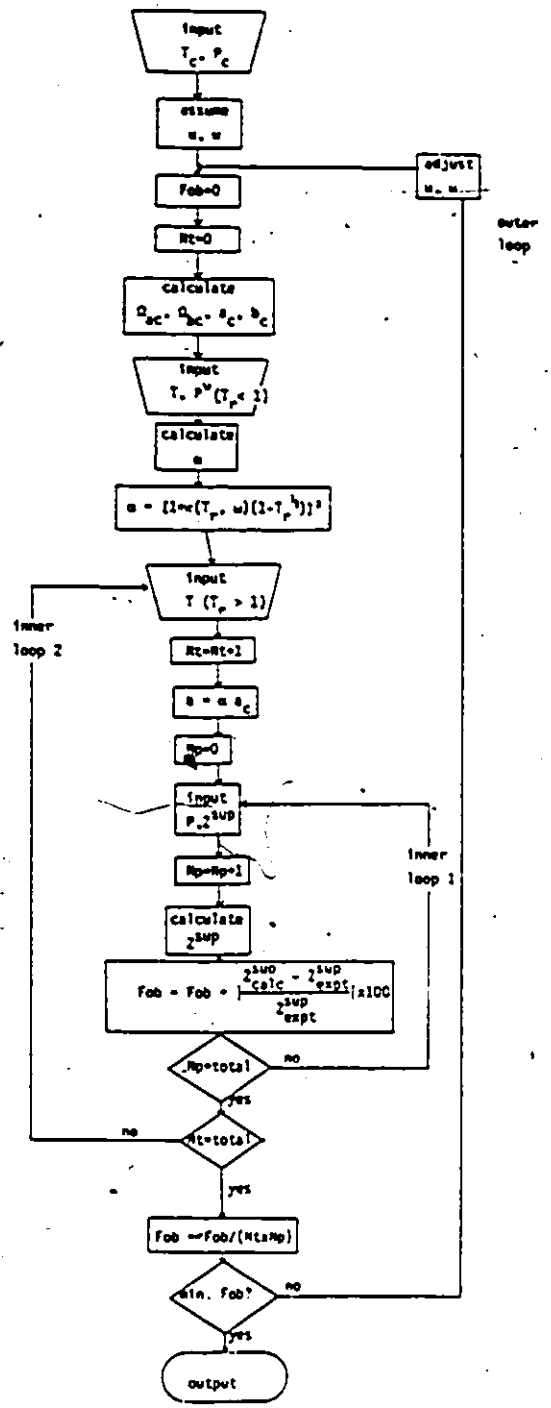

Figure 4.19: Flow diagram to construct deviation contour and to search for optimum u and w for supercritical gas compressibility factors. Nt- number of isotherms.

Table 4.5

Results of the minimization of deviations in supercritical gas compressibility factor.

	u_{min}	w_{min}	β_c	ζ_c	Ω_{ac}	Ω_{bc}	$\lvert\Delta Z^{sup}\rvert$%
C1	1.497	-0.904	0.2757	0.3188	0.45497	0.08789	0.85
C2	1.683	-1.098	0.2748	0.3137	0.46098	0.08621	0.91
C3	1.765	-1.181	0.2742	0.3115	0.46347	0.08543	0.94
C4	1.821	-1.185	0.2710	0.3103	0.46332	0.08411	0.99
C5	1.874	-1.143	0.2659	0.3094	0.46170	0.08227	1.07
C6	1.925	-1.118	0.2619	0.3084	0.46075	0.08079	1.14
C7	1.999	-1.110	0.2578	0.3070	0.46036	0.07914	1.26
C8	2.059	-1.126	0.2555	0.3058	0.46073	0.07812	1.37
C9	2.136	-1.165	0.2534	0.3041	0.46176	0.07708	1.51
C10	2.215	-1.211	0.2515	0.3025	0.46294	0.07609	1.66

As can be seen in Figure 4.20, all the contours on the u-w plot are located where $u > 0$. The locus of the optimum point $(u,w)_{min}$ for C1 to C10 is in a direction similar to that of (β_c^*, ζ_c). The extensive overlapping among the contours indicates that the volumetric behavior of Eq.(1.3) for each substance at supercritical temperatures is not very sensitive to variations in either u and w or β_c and ζ_c. In other words, it is possible to choose a single point (u,w) that would enable Eq.(1.3) to represent Z^{sup} for the ten normal alkanes with an accuracy comparable to that when the individual optimum points are used. Consequently, it may only require a 2P1T type of equation to represent Z^{sup}. This is shown by the fact that the PR equation whose (u,w) = (2,-1) falls in the overlapping area of the contours from C2 to C10.

In general, the supercritical region ($1.01 \leq T_r \leq 4.00$, $0.01 \leq P_r \leq 10.0$) on the P-V surface can be classified into three areas

1. the gas area ($P_r < 0.8$) where the fluid density is very low,

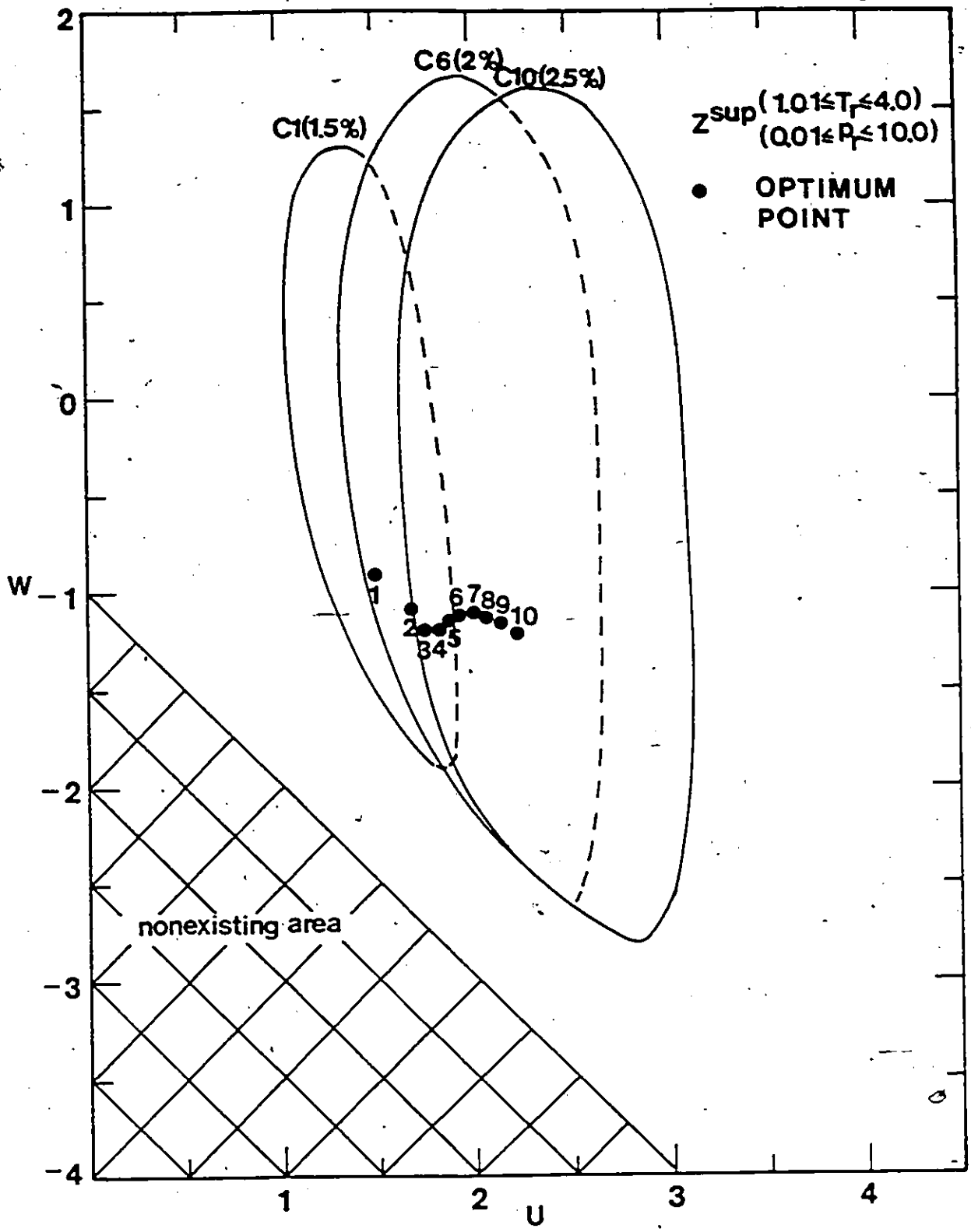

Figure 4.20: Deviation contours for supercritical gas compressibility factors for C1, C6, and C10.

2. the critical point area ($1.01 \leq T_r \leq 1.50$, $0.8 \leq P_r \leq 3.0$) where the isotherms form plateaus above the critical point,

3. the high-pressure area ($T_r > 1.50$, $P_r > 3.0$) where the fluid density is approximately that of liquid.

It is in the last two areas where most of the error in Z^{sup} occurs, particularly in the critical point area where volume-cubic equations are fundamentally inadequate. On the other hand, just as in the saturated vapor phase, Eq.(1.3) can represent the volumetric behavior of fluids in the gas area accurately.

Although the roles of β_c and ζ_c are not very clear in the present case, it is reasonable to assume that ζ_c has a stronger influence on the behavior of Eq.(1.3) in the vicinity of the critical point and the quantity, β_c, is more influential at high pressures where the fluid is as dense as liquid.

Irrespective of the values of u and w, Eq.(1.3) exhibits the same pattern of error distribution for Z^{sup} over the three areas. However, the magnitude of the errors in the vicinity of the critical point and in the high-pressure area vary with the quantities β_c and ζ_c. To illustrate, shown in Figure 4.21 is the typical pattern of error distributions in Z^{sup} for C1, C6 and C10 at four selected isotherms T_r = 1.05, 1.50, 2.00 and 4.00 over the entire P_r range considered. As can be seen, the patterns of error distributions in Z^{sup} for the three substances are very similar. Larger errors occur in the vicinity of the critical point and in the high-temperature, high-pressure regions where errors increase with increasing molecular weight. However, at low pressures

Z^{sup} can be accurately predicted. The error distribution pattern illustrated in Figure 4.21 is not restricted to the present treatment of parameter a in which the temperature dependence is represented by Eq.(4.13). Similar patterns are exhibited by equations with different temperature functions for their parameters. For example, the results obtained from the HK and the KMC equations are plotted in Figures 4.22 and 4.23. As can be seen, the patterns of the error distributions are the same as those shown in Figure 4.21. This would imply that all the VDW-type volume-cubic equations exhibit same limitations in the representation of Z^{sup}, the only difference being in the magnitude of errors.

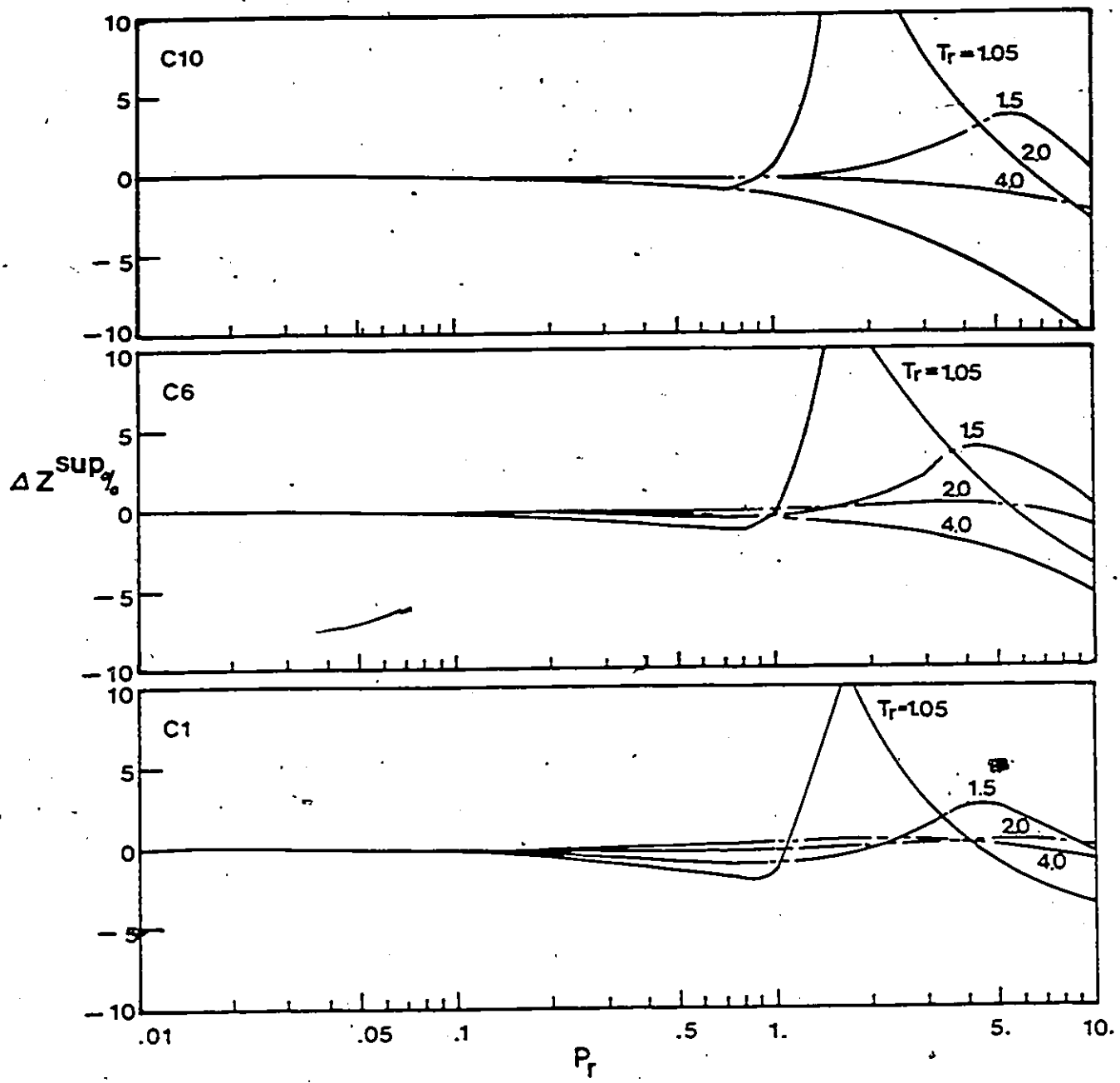

Figure 4.21: General pattern of error distribution for supercritical gas compressibility factors.

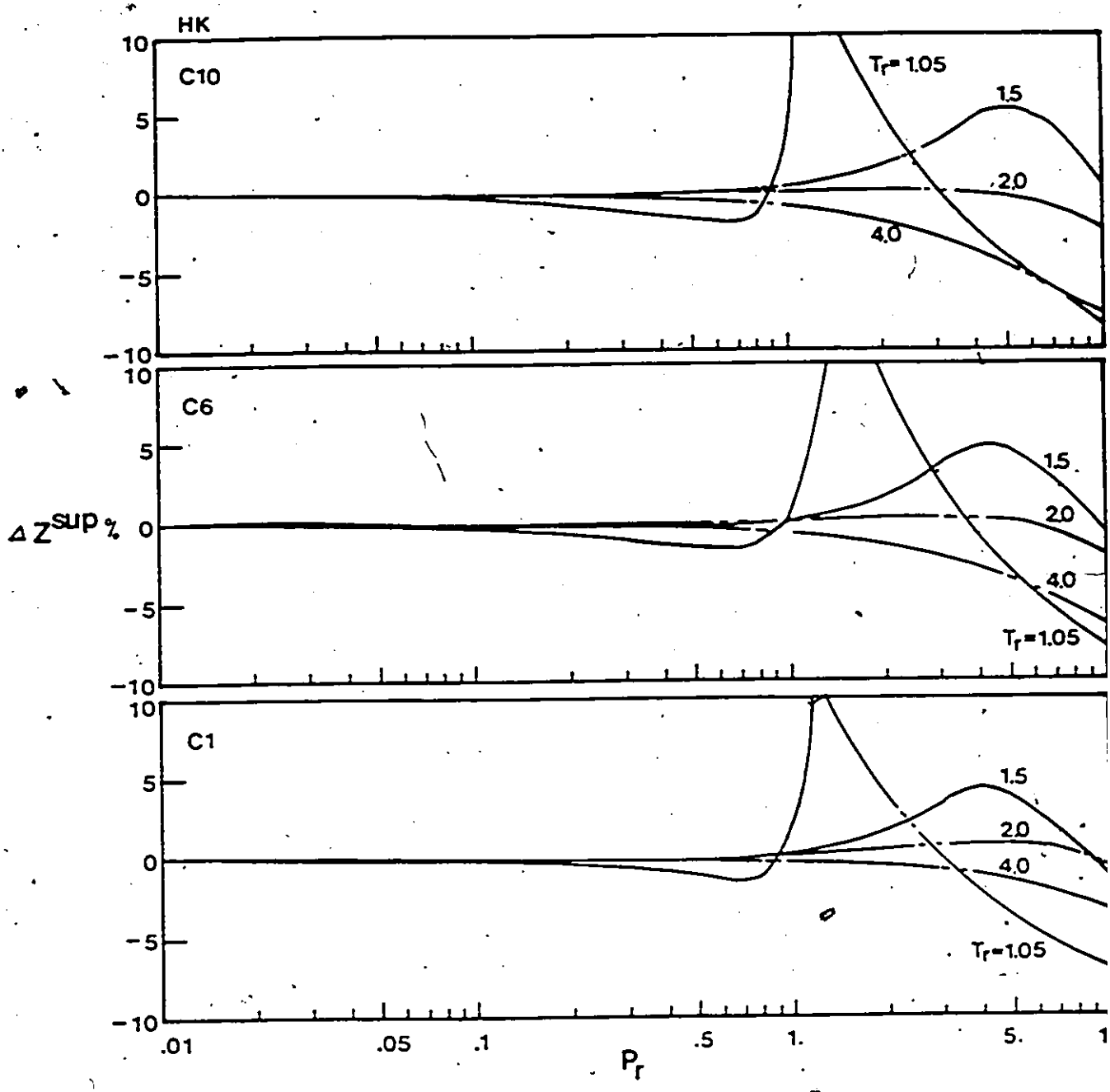

Figure 4.22: Error distributions for supercritical gas compressibility factors predicted by the HK equation.

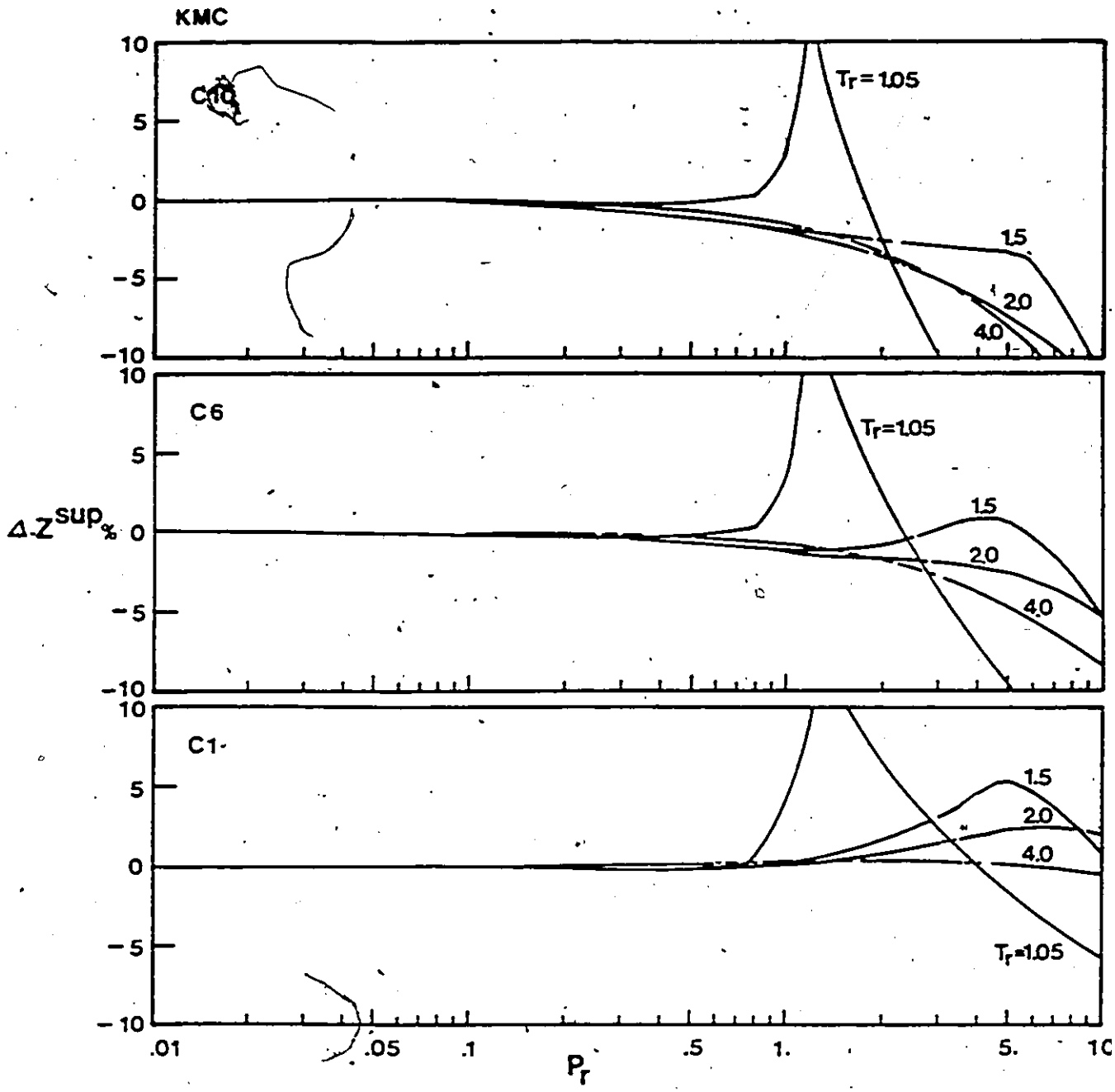

Figure 4.23: Error distributions for supercritical gas compressibility factors predicted by the KMC equation.

4.1.5 Liquid Phase

Following the same procedure used earlier, the quantitative effect of u and w on the volumetric behavior of Eq.(1.3) in the liquid phase is examined by means of the deviation contours for Z^{ℓ} on u-w diagrams. The computational scheme used to construct the contours and to search for the optimum values of u and w is identical to the one in Figure 4.19. Table 4.6 summarizes the results of the minimization and Figure 4.24 presents the 4.0% average absolute deviation contours of Z^{ℓ} for C1, C6 and C10. The optimum points $(u,w)_{min}$ for the first ten normal alkanes are also included. In this study, an average absolute deviation in Z^{ℓ} less than 4% is considered acceptable. Similar contours for the remaining alkanes are between those for C1 and C10 by order of their carbon numbers and overlap slightly with their immediate neighbors. The 4.0% deviation is between a 1.0 and 1.5% increase in magnitude from those obtained at the optimum points.

Table 4.6

Results of the minimization of deviations in liquid compressibility factor.

	u_{min}	w_{min}	β_c	ζ_c	Ω_{ac}	Ω_{bc}	$\lvert\Delta Z^{\ell}\rvert$%
C1	1.234	-0.342	0.2629	0.3266	0.43767	0.08587	3.06
C2	1.314	-0.309	0.2574	0 3246	0 43720	0.08356	2.96
C3	1.353	-0.234	0.2527	0.3237	0.43559	0.08176	2.90
C4	1.415	-0.214	0.2490	0.3222	0.43553	0.08025	2.84
C5	1.478	-0.145	0.2484	0.3209	0.43445	0.07824	2.77
C6	1.561	-0.181	0.2417	0.3189	0.43580	0.07708	2.71
C7	1.630	-0.100	0.2364	0.3176	0.43466	0.07508	2:64
C8	1.687	-0.028	0.2321	0.3165	0.43375	0.07347	2.58
C9	1.771	0.020	0.2279	0.3149	0.43357	0.07177	2.51
C10	1.860	0.020	0.2250	0.3131	0.43433	0.07045	2.50

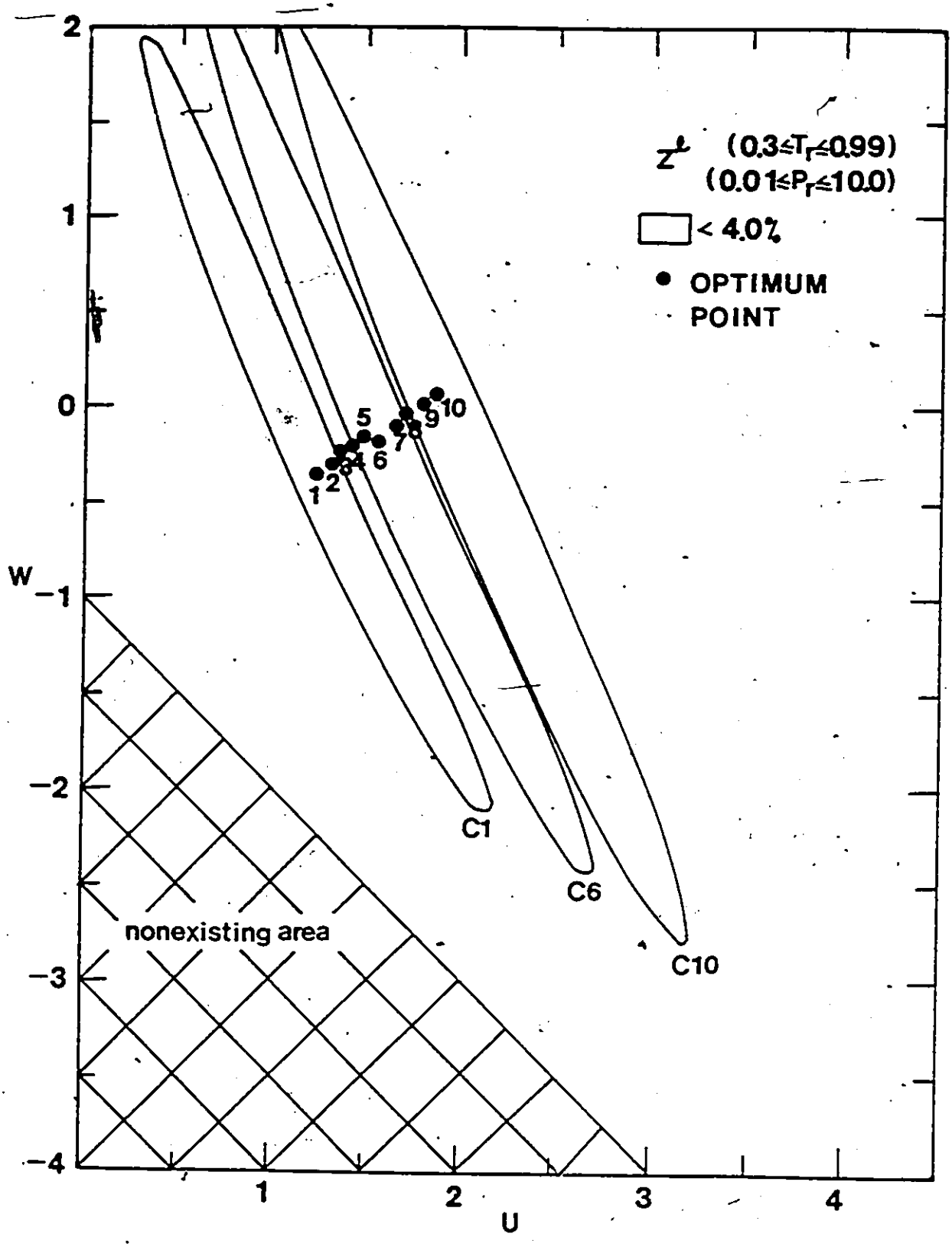

Figure 4.24: Deviation contours of liquid compressibility factors for C1, C6 and C10.

As can be seen in Figure 4.24, the contours are situated on the u-w plot where $u > 0$. The shapes and orientations of the contours are strikingly similar to those for v^{ℓ} and the locus of the optimum points for C1 from C10 is in a direction similar to those for v^{ℓ}. Also, when the critical point region ($0.85 \leq T_r \leq 1.0$) is excluded, shifting of the contours and the optimum points similar to those in Figure 4.14 should occur. Furthermore, when the contours of Z^{ℓ} and v^{ℓ} in Figures 4.12, 4.13 and 4.24 are superimposed the contours for each alkane overlap with one another. These characteristics suggest that the volumetric behavior of Eq.(1.3) in the liquid phase is closely related to that in the saturated liquid phase. Therefore, the results from section 4.2 concerning the effects of u and w and β_c and ζ_c on the volumetric behavior of Eq.(1.3) in the saturated liquid phase also apply to the liquid phase. Namely, there is a limited ranges of u and w values for each fluid for which Eq.(1.3) can give reasonable prediction of Z^{ℓ}, and the predicted β_c and ζ_c affected the behavior of Eq.(1.3) at low temperatures and in the vicinity of the critical point, respectively.

Upon examination of the local behavior of Eq.(1.3), it is found the error distributions for Z^{ℓ} have a general pattern regardless of the values of u and w. However, the magnitude of these errors depends on u and w. To illustrate, a plot of the general pattern of the error distribution in Z^{ℓ} at several temperatures is presented in Figure 4.25. As can be seen for $T_r < 0.7$, the errors associated with the calculated Z^{ℓ} are almost evenly distributed throughout the entire reduced pressure range. This means that when the temperature dependence of parameter a is determined using the vapor pressure values Eq.(1.3) is able to

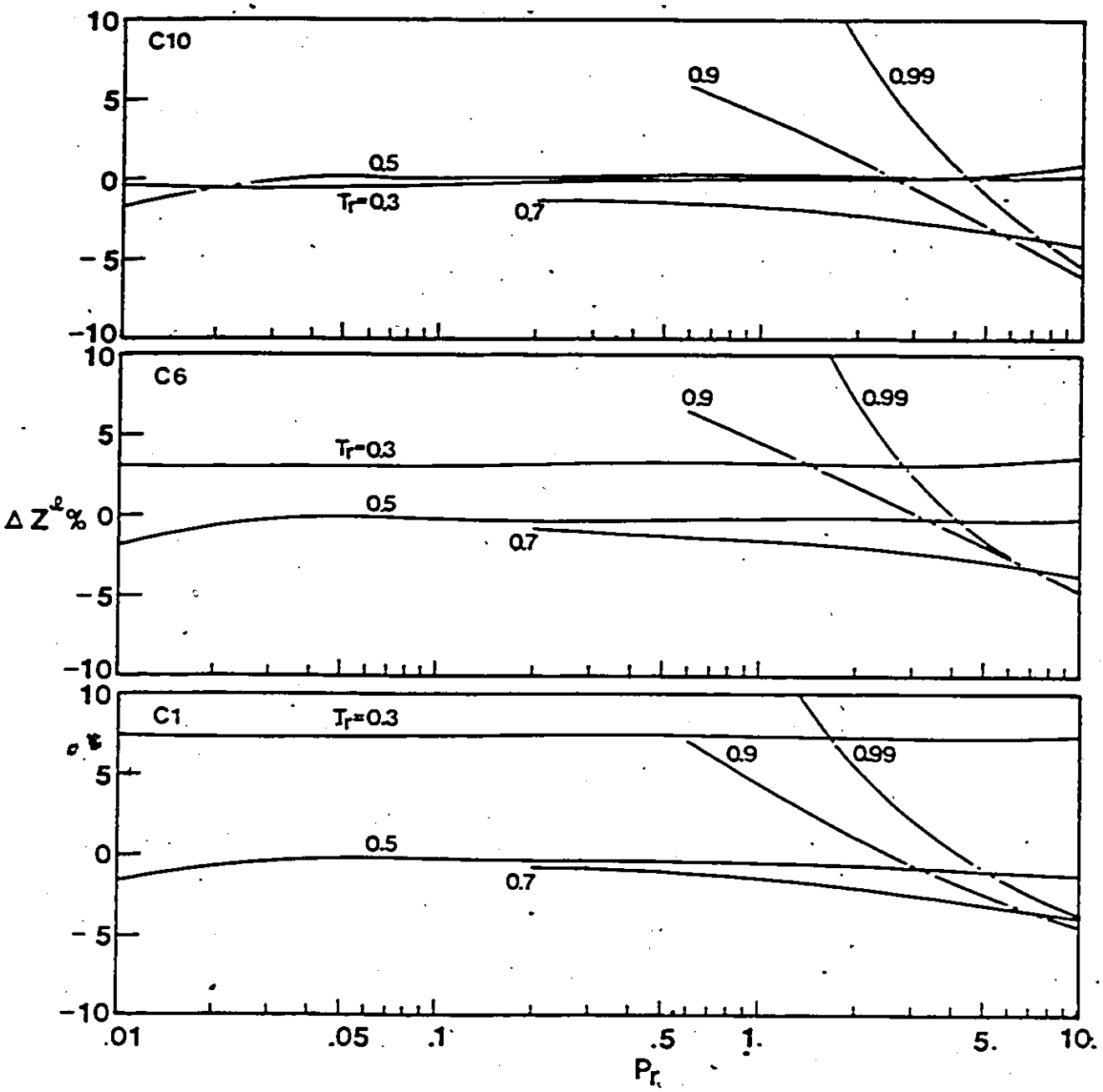

Figure 4.25: The general pattern of error distributions in the liquid compressibility factor.

generate steep isotherms in the liquid region at low temperatures. Consequently, for $T_r < 0.7$ the magnitude of the error associated with the calculated Z^ℓ at any pressure will be the same as that calculated for Z^ℓ at conditions close to the saturation point. Under these conditions the behavior of Eq.(1.3) is mainly affected by β_c. For $T_r > 0.7$, it becomes increasingly difficult for Eq.(1.3) to generate the correct shape of the liquid-phase isotherms with larger errors occuring in the vicinity of the critical point. In fact, as temperatures approach the critical the volumetric behavior of Eq.(1.3) is gradually influenced by ζ_c. In general, if u and w are taken from within the contours shown in Figure 4.24, the resulting equations can represent Z^ℓ within $\pm$ 2.0% for $0.5 \leq T_r \leq 0.7$. In order to have better prediction of Z^ℓ at $T_r < 0.50$, u and w must be taken from the area which is above the locus of the optimum points. However, this would be at the expense of the accuracy in the region near the critical point, since higher critical compressibility factors would be predicted. If the representation of Z^ℓ is to be improved at $T_r > 0.7$, u and w must be taken from the area below the optimum point locus which in turn would sacrifice the accuracy at low temperatures.

The performance of Eq.(1.3) in the representation of Z^ℓ can be improved by determining the temperature dependence of parameter a directly from Z^ℓ instead of P^v. As a result, the optimum values of α must be obtained by minimizing the average absolute deviations in Z^ℓ at each T_r. The typical temperature dependence of the optimum α determined by minimizing deviations in Z^ℓ for C1, C6 and C10 is shown in Figure 4.26. The temperature dependence of α obtained in this manner can be accurately expressed by the following equation

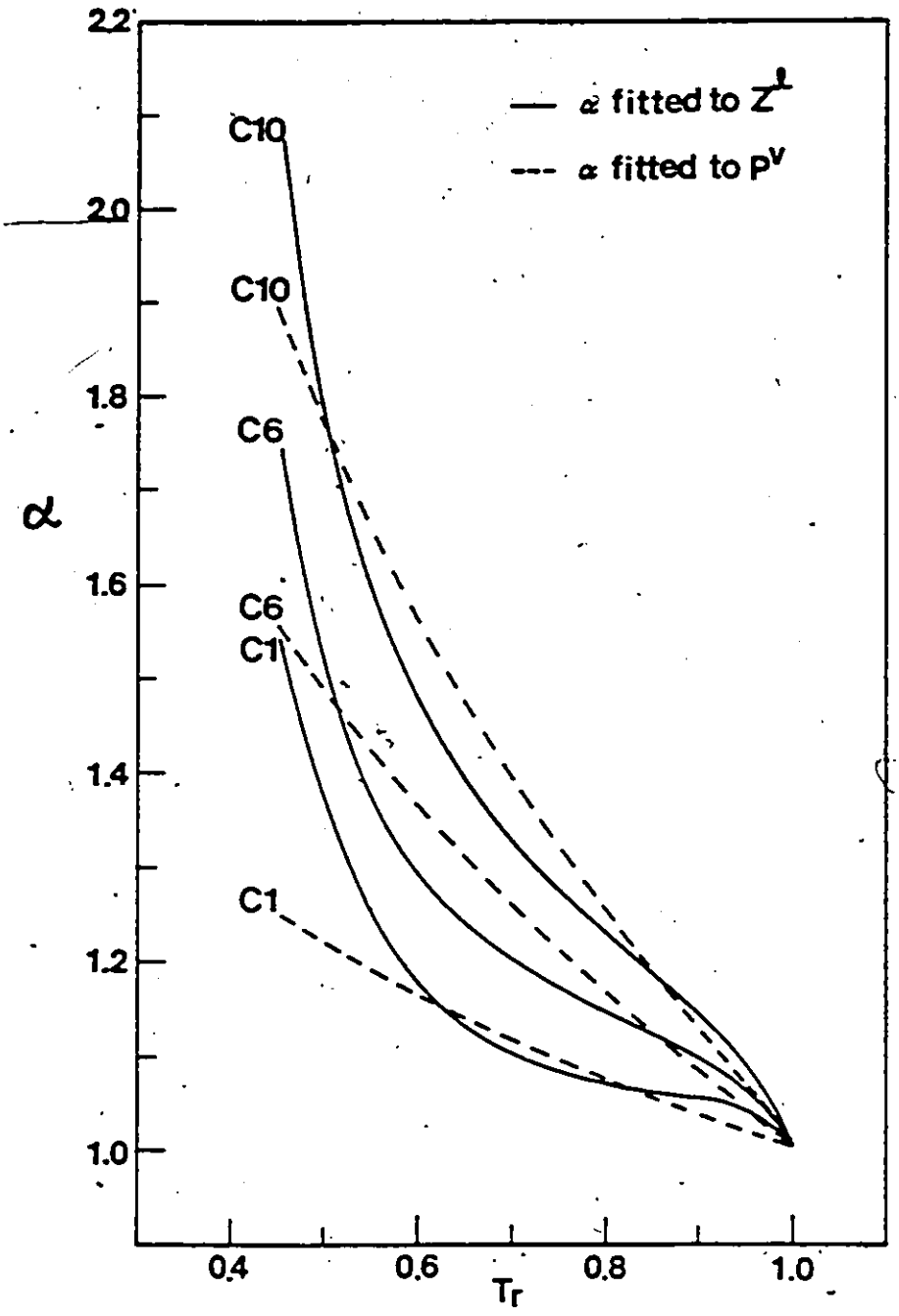

Figure 4.26: Comparison of the temperature dependence of α obtained from vapor pressure and liquid compressibility factor.

$$\alpha = 1 + D_0(1-T_r)^{4/5} + D_1(1-T_r)^{8/5} + D_2(1-T_r)^{12/5} \qquad (4.18)$$

where constants D_0, D_1 and D_2 can be correlated by simple polynomials in the acentric factor. By using Eq.(4.18), deviations in Z^{ℓ} can generally be halved.

Unfortunately, the temperature function determined using Z^{ℓ} values is not suitable for equilibrium calculations since it causes large errors in P^{ν}. This can be seen in Figure 4.26 where the temperature dependence of α determined from Z^{ℓ} and P^{ν} are compared for C1, C6 and C10. As can be seen the two temperature dependences are completely different from one another. As found in this study, the accuracy in the representation of P^{ν} is more sensitive to the value of α than that of Z^{ℓ}. Therefore, it is necessary that the temperature function for α be determined using P^{ν}. Nevertheless, Eq.(4.18) can be employed as the temperature function for α when more accurate representation of Z^{ℓ} is required.

4.1.6 Concluding Remarks

The results of the analyses of the volumetric behavior of Eq.(1.3) indicate that

1. For accurate equilibrium calculations, Eq.(1.3) must be able to reproduce P^{ν} accurately.
2. The temperature dependence of parameter a expressed by Eqs(4.13,16) is suitable for Eq.(1.3) when calculating P^{ν}, v^{ℓ}, v^{ν}, Z^{sup} and Z^{ℓ}.
3. Accurate prediction of P^{ν} ensures similar accuracy in the representation of v^{ν}. Errors in v^{ν} are mirror images of those in P^{ν} along the zero percent line.
4. Parameters u and w have a stronger influence on the overall representation of v^{ℓ} and Z^{ℓ} than on v^{ν} and Z^{sup}.
5. Over the temperature and pressure range studied, the general patterns of the error distributions in v^{ℓ}, Z^{ℓ} and Z^{sup} are the same but the magnitude of errors are dependent on the values of u and w and β_c and ζ_c.
6. There exist a number of (u,w) values for Eq.(1.3) that give similar average deviations in v^{ℓ} and Z^{ℓ}, but result in different local volumetric behavior on the P-V surface.
7. Examination of the deviation contours on a u-w diagram provides information on the quantitative effect of these parameters on the overall performance of Eq.(1.3). Comparison of the predicted β_c and ζ_c with β_c^* and Z_c provides insight into the local volumetric behavior of Eq.(1.3) in the (saturated) liquid phase.

8. In general, for representing v^{ℓ} and Z^{ℓ}, β_c is important at lower reduced temperatures while ζ_c becomes necessary in the critical region. However, both β_c and ζ_c must be adjusted simultaneously so that Eq.(1.3) achieves the desired local volumetric behavior.

9. In order to accurately represent v^{ℓ} and Z^{ℓ} the locus of (u,w) and therefore (β_c,ζ_c) of an EOS should be in the same direction as those for v^{ℓ} and Z^{ℓ} rather that in the direction of (β_c^*, Z_c).

10. The average absolute percent deviations obtained at the optimum points represent the 'best' overall performance of Eq.(1.3) possible.

4.2 Design of Equation of state

With reference to the results of the previous analyses, the main task in designing an equation is to select the appropriate u and w in Eq.(1.3). There are two points that should be taken into consideration when selecting the parameters. First of all, in order to have a balanced representation of v^{ℓ}, Z^{ℓ}, v^{v} and Z^{sup} values of u and w must be in the overlapping areas of the deviation contours in Figures 4.12, 4.13, 4.20 and 4.24. Secondly, for practical purposes emphasis must be placed on the local representation of these properties. In general, it is preferable to accurately represent the more volatile components at higher T_r and the less volatile components at lower T_r. This is especially important in the representation of v^{ℓ} where it is necessary for the equation to predict higher values of β_c and lower values of ζ_c for fluids with smaller molecules and conversely for fluids with larger molecules.

Figure 4.27 presents the areas of overlap between the deviation contours of v^{ℓ}, Z^{ℓ} and Z^{sup} for C1, C6 and C10. The overlapping area of the 1.0 and 2.5% deviation contours of v^{ℓ} for C20 for $0.50 \leq T_r \leq 0.85$ and for $0.50 \leq T_r \leq 0.98$, respectively is also included for reference. The overlapping areas of the normal alkanes other than C1, C6 and C10 fall between those for C1 and C10 by order of their carbon number. The curves in Figure 4.27 represent the loci of the optimum points for C1 to C10, while the v^{ℓ} curves extend to C20. Any line or curve which passes through the overlapping areas will yield the following average absolute deviations for each of the four properties

1. $v^{\ell} \leq 1.0\%$ $(0.50 \leq T_r \leq 0.85)$
2. $v^{\ell} \leq 2.5\%$ $(0.50 \leq T_r \leq 0.98)$
3. $v^{v} \leq 2.5\%$ $(0.50 \leq T_r \leq 0.98)$
4. $Z^{\ell} \leq 4.0\%$ $(0.30 \leq T_r \leq 0.99,\ 0.01 \leq P_r \leq 10.0)$
5. $Z^{sup} \leq 2.5\%$ $(1.01 \leq T_r \leq 4.00,\ 0.01 \leq P_r \leq 10.0)$

It should be noted that although the loci for Z^{sup} and v^{ℓ} for $0.50 \leq T_r \leq 0.98$ can pass through some of the overlapping areas, the actual optimum points are not located in these areas. However all optimum points for v^{ℓ} at $0.50 \leq T_r \leq 0.85$ for C1 to C20 are contained in the overlapping areas thereby satisfying the two conditions mentioned at the beginning of this section. This locus will be used as a basis for the design of equations of state.

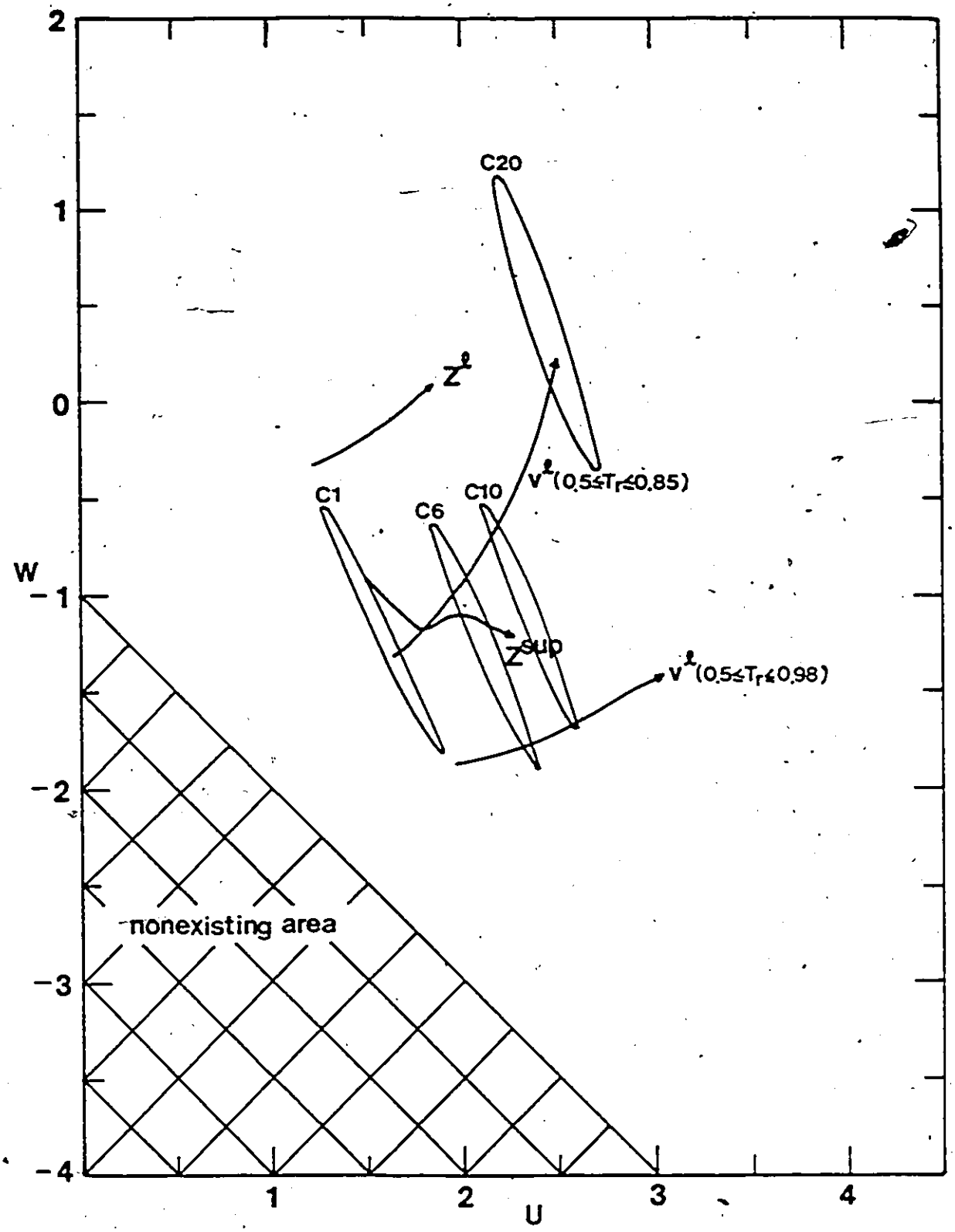

Figure 4.27: Overlapping areas resulted from superimposing deviation contours.

4.2.1 Two Adjustable One Temperature Dependent Parameter Equation

When designing a 2P1T equation the parameters u and w in Eq.(1.3) must remain as constants. Hence each point (u,w) represents a two-parameter equation which has constant β_c and ζ_c. Since not all the overlapping areas for the ten alkanes share a common region on the u-w plane, it is impossible to find a single point (u,w) so that the resulting equation can represent v^{ℓ}, v^{v}, Z^{ℓ} and Z^{sup} of all the ten alkanes within the deviations specified by the overlapping areas. Nevertheless, with proper choice of u and w a 2P1T equation can represent v^{v} and Z^{sup} of the ten alkanes within the accuracy specified by the overlapping areas. This is because the deviation contours for v^{v} and Z^{sup} of the ten alkanes share a common area on the u-w plane. On the other hand, a 2P1T equation can only represent v^{ℓ} and Z^{ℓ} for fluids with similar molecular weights. This is because the deviation contours for v^{ℓ} and Z^{ℓ} only overlap with their immediate neighbors. As a result, a 3P1T or 4P1T equation is required for more accurate representation of v^{ℓ} and Z^{ℓ}.

Notwithstanding the limitations of the 2P1T equations, an attempt is made to find a 'most suitable' 2P1T equation by adjusting u and w to minimize the overall average absolute percent deviation in v^{ℓ} of the ten alkanes for $0.50 \leq T_r \leq 0.85$. It is interesting to note that the optimum values of u and w thus obtained are 2.026 and -1.062, respectively, which are practically the same as those in the PR equation. The point (2,-1) is located in the area shared by the deviation contours for Z^{sup} and v^{v} for C2 to C10. As a result, one may conclude that the PR

equation is one of the 'most suitable' 2P1T equations for representing v^{ℓ}, v^{v}, Z^{ℓ} and Z^{sup} of normal fluids with acentric factors ranging from 0 to 0.5.

4.2.2 Three Adjustable One Temperature Dependent Parameter Equation

As discussed in Chapter III, there are two ways to reduce Eq.(1.3) to a three-parameter equation

1. To assume an algebraic relationship between u and w.
2. To maintain either u or w as a constant.

The first method was used in developing the SW, the HK, the PT equations which are represented by the u*w=1 relationship. The 3P1T equations such as the Clausius, the TSRK and the C1 equations which were developed using the volume-translation technique could also have resulted from the first method. The family of equations represented by w=0, such as the 3RK equation are examples of the second method. When either of these methods are used to develop a new equation care must be taken in order to avoid any shortcomings in the representation of v^{v}, Z^{ℓ}, Z^{sup} and, in particular, v^{ℓ}.

Figure 4.28 shows the loci of several well-known 3P1T equations together with the overlapping areas from Figure 4.27. As can be seen, the family of equations represented by the u*w=1 relation does not give good prediction of v^{ℓ} and Z^{ℓ} especially for alkanes with large molecules. Its locus moves in the opposite direction from those of the optimum points for v^{ℓ}. Moreover the direction of the locus places an

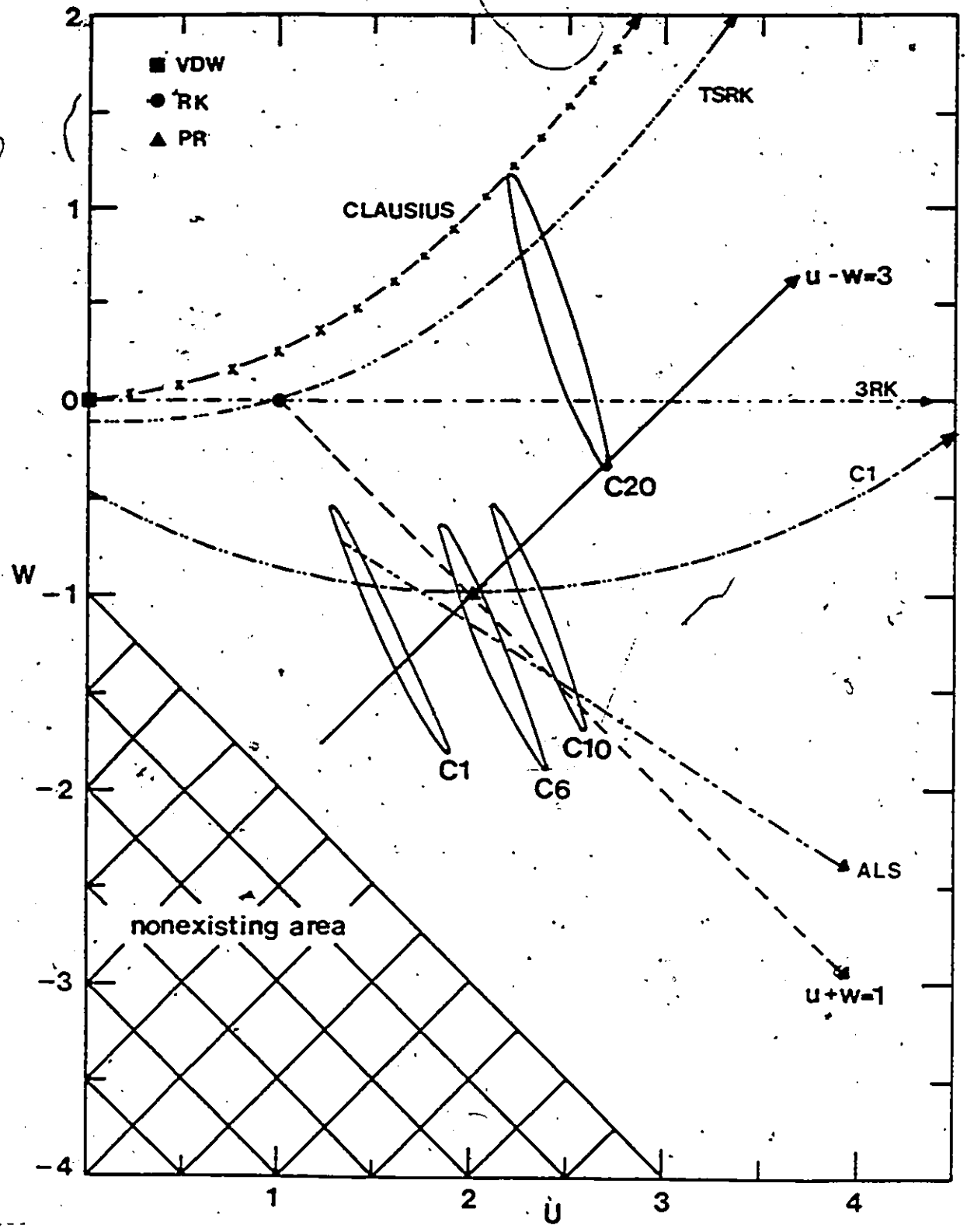

Figure 4.28: Relative positions of several known equations of state and the overlapping areas of the deviations contours.

impractical emphasis in the representation of v^{ℓ} in terms of the range of T_r and the molecular weight of the fluids. For alkanes with small molecules such as methane, which usually appear as volatile components the position of the locus forces the equation to predict large values of ζ_c and small values of β_c when compared to the corresponding values of Z_c and β_c^*. With respect to the effect of β_c and ζ_c on the local error distribution in v^{ℓ}, the error is shifted towards higher T_r. On the other hand, for alkanes with large molecules such as decane, the equation predicts too small a value of ζ_c and too large value of β_c, thus shifting the error towards lower T_r. Consequently, the desired emphasis is reversed which further indicates the limitations of using the forms of the RK and the PR equations as building blocks in the design of a 3P1T equation.

Each of the constant-Ω_{ac} curves on the u-w plane represents a family of 3P1T equations which result from the volume translation of a 2P1T equation with the same Ω_{ac}. Comparing the loci of the Clausius (Ω_{ac}=0.42281), the TSRK (Ω_{ac}= 0.42747), and the C1 (Ω_{ac}=0.45653) equations in Figure 4.28 the C1 equation appears to be the most suitable for representing v^{ℓ}, v^{v}, Z^{ℓ} and Z^{sup} of the first ten alkanes. This is because it passes through the overlapping areas of the first ten normal alkanes. However, when representing v^{ℓ} of alkanes with large molecules such as C20, it would be inferior to the TSRK equation. From the constant-Ω_{ac} curves plotted in Figure 4.1, it appears that the most suitable choice of the value of the constant-Ω_{ac} in a 3P1T equation would be approximately 0.450 since this curve would pass through all the overlapping areas including that of C20. However, in doing so,

the resulting equation would shift the error in the representation of v^{ℓ} for small molecules towards larger T_r similar to that of the u+w=1 family of equations.

When choosing either u or w to be held constant in a 3P1T equation, it is better to maintain the parameter w as a constant in order that the locus of the equation passes through most of the overlapping areas. From the orientation of the contours in Figure 4.27, a suitable value for w would be -1. Thus the resulting equation which is a three-parameter variation of the PR equation, can represent v^{ℓ}, v^{v}, Z^{ℓ} and Z^{sup} of fluids up to C10 within the accuracy specified by the overlapping areas. However, this sacrifices the accuracy in predicting v^{ℓ} for fluids with molecules larger than those of C10, especially at low T_r. On the other hand, the family of 3P1T equations with w=0 (variations of the RK equation) can overcome this problem but would lose accuracy for fluids with small molecules.

To overcome the shortcomings discussed above, the relationship between u and w should be formulated so that the locus of (u,w) is close to that of the optimum points for v^{ℓ} for $0.50 \leq T_r \leq 0.85$. By assuming a linear relationship between u and w the equation can be kept as simple as possible. Comparing Figure 4.27 and Figure 4.28 indicates that the line relating u and w in Eq.(1.3) should have a positive slope. One suitable choice is u - w = 3 since it passes through all the overlapping areas as well as being a good approximation to the locus of v^{ℓ} for $0.50 \leq T_r \leq 0.85$.

4.2.3 Four Adjustable One Temperature Dependent Parameter Equation

The locus of the 4P1T equation proposed by Adachi, Lu and Sugie (ALS)[5] is depicted in Figure 4.28. As can be seen, this locus is similar to that of the u=w=1 family of equations. Therefore, depending on the molecular weight of the fluid, the ALS equation will also have poor representation of v^{ℓ} in the important range of T_r. Since its locus can be closely approximated by a line, the ALS equation can be practically simplified to a 3P1T equation.

In principle, 4P1T equations should be more flexible than the 3P1T equations and therefore better able to represent the volumetric properties. However the complexity of the equation is increased and the 4P1T equation appears to have no great advantage over the 3P1T equation when approximating the locus of the optimum points of v^{ℓ} for $0.50 \leq T_r \leq 0.85$.

4.2.4 New Equation of State

Based on the above discussions, a new 3P1T equation is proposed. The exact mathematical relationship between u and w for the new equation is given by $u - w = 3$. Substituting this expression into Eq.(1.3) gives

$$P = \frac{RT}{v - b} - \frac{a}{v(v+c) + b(3v+c)} \tag{4.19}$$

where $c = wb$, and

$$a = \alpha(T_r)\ \Omega_{ac}(\omega)\ R^2T_c^2/P_c \tag{4.20}$$

$$b = \Omega_{bc}(\omega)\ RT_c/P_c \tag{4.21}$$

$$c = \Omega_{cc}(\omega) \; RT_c/P_c \qquad (4.22)$$

with

$$\Omega_{cc}(\omega) = w\Omega_{bc}(\omega). \qquad (4.23)$$

Values of the parameter w are obtained by minimizing the average absolute percent deviations in v^{ℓ} of the first ten normal alkanes for $0.50 \leq T_r \leq 0.85$. The generalized expressions for Ω_{ac}, Ω_{bc}, α and w in terms of T_r and the acentric factor ω are as follows:

$$\Omega_{ac}(\omega) = 0.471807 - 0.0574699\,\omega + 0.036007\,\omega^2 \qquad (4.24)$$

$$\Omega_{bc}(\omega) = 0.0922390 - 0.052525\,\omega + 0.021904\,\omega^2 \qquad (4.25)$$

$$w = -1.36417 + 1.06662\,\omega + 0.256505\,\omega^2 \qquad (4.26)$$

$$\alpha(T_r) = [1 + \kappa(T_r, \omega)\,(1 - T_r^{\frac{1}{2}})]^2 \qquad (4.27)$$

where

$$\kappa(T_r, \omega) = \frac{\gamma(\omega)}{\gamma_o}\,(A_0 + A_1 T_r + A_2 T_r^{\,2}) \qquad (4.28)$$

Depending on the value of ω, the following expressions are used to evaluate the parameters in Eq.(4.28),

For $\omega \leq 0.4906$,

$$\gamma(\omega) = 0.33262 + 1.8894\omega - 1.04038\,\omega^2 + 1.6634\,\omega^3 \qquad (4.29)$$

$$\gamma_o = 0.89417,\; A_0 = 1.08551,\; A_1 = -0.59744,\; A_2 = 0.44643$$

where n-heptane is the reference fluid.

For $0.4906 \leq \omega \leq 1$,

$$\gamma(\omega) = 0.81262 - 0.18376\ \omega + 1.9727\ \omega^2 - 0.67758\ \omega^3 \qquad (4.30)$$

$$\gamma_0 = 1.5312,\ A_0 = 2.1801,\ A_1 = -2.1085,\ A_2 = 1.6708$$

where n-heptadecane is the reference fluid.

At temperatures above the critical the quantity κ is evaluated at the critical point,

$$\kappa(T_r, \omega) = \kappa(1, \omega),\ T_r > 1 \qquad (4.31)$$

The corresponding expressions for β_c and ζ_c are generalized as follows

$$\beta_c(\omega) = 0.291437 - 0.117453\ \omega \qquad (4.32)$$

$$\zeta_c(\omega) = 0.313639 - 0.011951\ \omega \qquad (4.33)$$

Chapter V

APPLICATION OF THE NEW EQUATION OF STATE TO PURE FLUID CALCULATIONS

The new equation is tested by calculating the vapor pressures, P^v, for 30 substances, the saturated liquid molar volumes, v^ℓ, for 26 substances, the saturated vapor molar volumes, v^v, for 18 substances, the liquid compressibility factors, Z^ℓ, for 18 substances and the supercritical gas compressibility factors, Z^{sup}, for 15 substances and comparing with experimental values. The results are reported in Table 5.1 together with those obtained from the SRK, the PR and the SW equations. A summary of the comparisons between the calculated and experimental values for these five pure-component properties is presented in Table 5.2.

As can be seen in Table 5.2 the new equation yields the lowest overall average absolute percent deviations in the calculated P^v, v^ℓ, Z^ℓ and Z^{sup} values, while the overall deviation in the calculated v^v is slightly higher than that obtained from the SW equation.

In general, the new equation has better overall representation of the five properties than the SW equation which is better than the PR equation which in turn is better than the SRK equation. In the calculation of P^v the new equation has lower deviations than the other three equations, especially for substances with large molecules. With the

Table 5.1: Average absolute percent deviations between calculated and experimental values of five physical properties for normal fluids

$|\Delta P^{vs}|_{ave}$

Substance	ND	SRK	PR	SW	MEW	Tr range	ref.
methane	29	1.50	1.60	0.62	0.74	0.59 - 0.990	17
ethane	27	1.27	1.07	0.67	0.38	0.61 - 0.991	17
propane	31	1.55	1.02	0.66	0.25	0.65 - 0.991	17
n - butane	28	1.62	0.95	0.73	0.42	0.64 - 0.993	17
n - pentane	30	1.00	0.33	0.20	0.43	0.66 - 0.993	17
n - hexane	43	1.44	1.40	1.12	0.83	0.54 - 0.995	17
n - heptane	21	1.58	0.75	0.73	0.48	0.64 - 0.994	143
n - octane	18	1.78	0.93	1.02	0.31	0.69 - 0.990	143
n - nonane	21	1.69	2.31	1.70	1.23	0.52 - 0.859	110
n - decane	27	5.02	10.5	2.29	1.05	0.40 - 0.827	9
n - undecane	27	1.24	0.86	1.00	1.16	0.45 - 0.785	9
n - dodecane	27	3.28	4.13	3.36	2.71	0.56 - 0.800	9
n - tridecane	27	1.59	0.44	0.57	0.91	0.57 - 0.810	9
n - teradecane	27	3.02	2.34	3.15	2.78	0.58 - 0.820	9
n - pentadecane	27	2.24	0.85	0.62	0.44	0.59 - 0.830	9
n - hexadecane	27	2.09	1.17	0.37	0.65	0.59 - 0.840	9
n - heptadecane	27	2.25	0.85	1.13	0.35	0.60 - 0.850	9
n - octadecane	27	1.91	1.44	0.77	0.90	0.61 - 0.850	9
n - nonadecane	27	1.41	1.84	4.52	2.68	0.62 - 0.860	9
n - eicosane	27	0.83	0.78	4.62	1.16	0.63 - 0.870	9
i - butane	29	1.96	1.45	1.20	0.48	0.63 - 0.993	17
ethylene	21	1.54	1.14	0.81	0.99	0.60 - 0.981	17
propylene	26	1.07	0.60	0.71	1.49	0.62 - 0.989	17
butene	26	1.39	0.67	0.52	0.43	0.65 - 0.979	17
acetylene	22	2.11	1.54	1.31	0.93	0.63 - 0.989	17
benzene	47	1.10	0.89	0.61	0.41	0.55 - 0.997	17
carbon monoxide	24	0.77	1.43	1.40	1.34	0.51 - 0.981	17
carbon dioxide	32	0.46	0.67	0.87	1.37	0.71 - 0.995	17
nitrogen	18	1.43	1.39	0.74	0.56	0.61 - 0.991	17
oxygen	14	1.03	0.62	0.43	0.50	0.58 - 0.986	17

Table(5.1) cont'd.

$|\Delta v^{L}_{m}|_{ave}$

Substance	ND	SRK	PR	SW	MEW	Tr range	ref.
methane	29	6.88	7.28	6.20	2.84	*	17
ethane	27	13.7	6.68	9.44	6.23	*	17
propane	31	13.8	5.75	7.39	4.93	*	17
n - butane	28	13.4	4.65	5.23	3.78	*	17
n - pentane	30	15.2	4.71	4.92	4.20	*	17
n - hexane	43	16.4	4.10	4.33	3.84	*	17
n - heptane	21	19.9	6.11	5.46	5.37	*	143
n - octane	18	22.0	7.91	5.67	5.70	*	143
n - nonane	21	16.9	3.41	1.01	1.55	*	110
n - decane	29	19.4	6.54	1.15	0.80	0.41 - 0.85	9
n - undecane	29	20.6	6.92	1.22	1.07	0.43 - 0.85	9
n - dodecane	30	22.8	8.40	1.45	0.82	0.43 - 0.86	9
n - tridecane	28	21.8	7.92	2.49	2.21	0.45 - 0.86	9
n - teradecane	27	25.7	13.6	1.69	0.95	0.43 - 0.80	9
n - heptadecane	29	31.4	16.5	2.21	1.91	0.45 - 0.84	9
n - octadecane	26	37.2	22.2	6.51	6.24	0.43 - 0.77	9
i - butane	29	11.8	5.10	4.64	3.42	*	17
ethylene	21	7.57	6.59	4.12	2.50	*	17
propylene	26	10.4	5.26	4.23	2.90	*	17
1 - butene	26	12.3	4.41	4.32	2.87	*	17
acetylene	22	12.6	5.00	5.07	3.48	*	17
benzene	47	13.3	4.40	4.59	3.24	*	17
carbon monoxide	24	3.88	8.49	3.13	2.18	*	17
carbon dioxide	32	14.6	4.62	5.25	4.13	*	17
nitrogen	18	6.49	8.12	5.08	3.37	*	17
oxygen	14	4.52	7.96	3.64	2.14	*	17

* Same range as indicated in the Table for $|\Delta P^{v}_{m}|_{ave}$

Table(5.1) cont'd.

$|\Delta v^{v}_{z}|_{ave}$

Substance	ND	SRK	PR	SW	NEW	Tr range	ref.
methane	29	2.21	3.23	1.18	1.98	*	17
ethane	27	0.48	2.24	0.82	1.40	*	17
propane	31	0.97	2.45	1.04	1.24	*	17
n - butane	28	1.10	1.49	1.29	1.35	*	17
n - pentane	30	1.36	1.11	0.77	1.06	*	17
n - hexane	43	1.10	1.33	1.16	1.45	*	17
n - heptane	21	1.61	1.04	0.78	0.95	*	17
n - octane	18	1.74	1.04	0.77	1.85	*	17
i - butane	29	1.33	2.32	1.21	1.14	*	17
ethylene	21	2.23	1.60	2.83	2.95	*	17
propylene	26	1.95	1.41	2.15	2.45	*	17
1 - butene	26	1.42	2.02	1.05	1.55	*	17
acetylene	22	0.83	0.97	1.03	1.37	*	17
benzene	47	1.76	2.79	2.31	2.60	*	17
carbon monoxide	24	3.70	2.97	3.52	3.30	*	17
carbon dioxide	32	1.60	1.30	1.46	1.61	*	17
nitrogen	18	2.93	4.33	2.07	3.04	*	17
oxygen	14	3.36	3.95	3.55	3.97	*	17

* Same range as indicated in the Table for $|\Delta P^{v}_{z}|_{ave}$

Table(3.1) cont'd. $|\Delta Z^{sup}|_{ave}$

Substance	ND	SRK	PR	SW	NEW	Tr range	Pr range	ref.
methane	21	6.52	4.62	5.68	1.75	0.80 - 0.95	0.30 - 6.0	137
ethane	125	4.79	6.42	1.86	1.29	0.55 - 0.95	0.30 - 10.0	84
propane	81	-8.40	4.36	2.53	1.19	0.62 - 0.95	0.12 - 4.77	23
n - pentane	78	8.75	3.60	1.65	1.90	0.66 - 0.95	1.02 - 6.13	23
n - hexane	32	12.9	1.72	1.90	1.62	0.74 - 0.93	0.19 - 8.85	62
n - heptane	32	13.2	1.10	0.93	1.04	0.56 - 0.88	0.26 - 8.59	118
n - octane	66	15.7	2.62	1.22	1.48	0.66 - 0.92	0.20 - 8.13	31
n - nonane	91	-14.9	2.24	1.59	2.36	0.52 - 0.86	0.60 - 8.95	110
n - decane	70	18.4	5.33	1.21	1.27	0.50 - 0.83	0.65 - 7.36	110
n - undecane	28	18.9	6.05	2.07	1.95	0.47 - 0.90	0 - 9.40	134
n - tridecane	21	22.2	8.73	2.25	1.92	0.45 - 0.85	0 - 5.30	134
n - heptadecane	18	31.8	16.9	3.21	1.77	0.44 - 0.78	0 - 7.11	134
n - eicosane	15	36.1	21.5	3.03	2.40	0.49 - 0.75	0 - 8.51	134
i - butane	71	6.45	5.42	1.43	1.63	0.72 - 0.93	0.47 - 5.67	23
2 - methyl pentane	26	9.66	3.02	1.93	2.13	0.75 - 0.90	0.19 - 8.73	62
cyclohexane	115	6.56	5.76	2.32	2.55	0.56 - 0.92	0.34 - 8.46	97
carbon dioxide	34	11.1	2.44	2.18	1.43	0.80 - 0.93	0.21 - 5.50	23
nitrogen	33	1.57	9.99	1.44	1.86	0.71 - 0.88	0.15 - 5.34	23

$|\Delta Z^{sup}|_{ave}$ (ref. 17)

Substance	ND	SRK	PR	SW	NEW	Tr range	Pr range
methane	440	0.72	2.65	0.95	0.82	1.05 - 7.75	0 - 21.0
ethane	260	1.52	1.39	1.37	0.75	1.02 - 4.47	0 - 10.0
propane	187	1.75	0.99	1.24	0.84	1.07 - 3.70	0 - 6.5
n - butane	150	2.99	1.37	1.94	1.61	1.06 - 3.20	0 - 5.4
n - pentane	150	3.02	1.09	1.42	1.25	1.02 - 2.91	0 - 6.1
n - hexane	45	2.57	1.07	1.17	1.10	1.03 - 1.16	0 - 1.4
i - butane	150	1.74	1.15	0.97	0.85	1.03 - 3.35	0 - 5.7
ethylene	323	1.28	1.66	1.22	0.84	1.0 - 3.74	0 - 9.5
propylene	220	1.98	1.37	1.37	0.99	1.0 - 4.83	0 - 10
1 - butene	59	1.82	1.47	1.39	1.53	1.06 - 1.24	0 - 1.72
Benzene	324	2.32	1.13	1.51	1.34	1.0 - 2.23	0 - 4.2
carbon monoxide	110	0.44	0.61	0.52	0.36	1.09 - 18.6	0 - 2.0
carbon dioxide	272	1.69	1.02	1.26	1.15	1.24 - 7.0	0 - 2.8
nitrogen	357	0.77	0.84	0.93	0.54	1.76 - 23.2	0 - 2.8
oxygen	391	0.25	0.61	0.43	0.37	1.36 - 19.0	0 - 1.9

exception of n-dodecane, n-teradecane and n-nonadecane the new equation has approximately 1.0% average absolute deviations in P^v. In the representation of v^ℓ and Z^ℓ both the SRK and the PR equations are limited to a small range of substances. In most cases, the new equation shows significant improvement over the SW equation. As expected, the four equations have similar accuracy in the prediction of v^v and Z^{sup}. It should be noted that the overall average absolute percent deviation in v^ℓ given by the new EOS is higher than those in v^v, Z^ℓ and Z^{sup}. This is mainly caused by the large errors in the vicinity of the critical points. Although it has a simpler expression for the temperature function of the parameter a, the new equation can still predict P^v more accurately than the SW equation.

Table 5.2

Summary of overall average absolute percent deviations in five physical properties.

Property	NS	ND	SRK	PR	SW	NEW
P^ℓ	30	806	1.69	1.51	1.28	0.94
v^ℓ	26	707	16.1	7.31	4.28	3.18
v^v	18	496	1.69	2.07	1.59	1.92
Z^ℓ	18	957	11.1	5.11	1.92	1.74
Z^{sup}	15	3438	1.43	1.30	1.13	0.88

ND - no. of data points NS - no. of substances

To illustrate the differences in the error distributions between the new equation (u - w = 3) and the SW equation (u + w = 1) the calculated v^ℓ and P^v values for ethylene and n-heptadecane and the calculated Z^ℓ values for carbon dioxide and n-heptadecane are compared in

Figures 5.1, 5.2, 5.3 and 5.4. For the light substances, ethylene and carbon dioxide, the emphasis of the representation by the new equation is at higher T_r values and lower deviations are obtained as indicated in Figures 5.1 and 5.3. For the heavy substance n-heptadecane, the emphasis of the representation by the new equation is at lower T_r values and lower deviations are obtained as shown in Figures 5.2 and 5.4.

As demonstrated in this chapter, one of the major advantages of the new equation of state is that it gives a balanced overall representation of volumetric properties (v^l, v^v, Z^l and Z^{sup}) compared to the other EOS tested. In addition, the new equation can give accurate predictions of v^l and Z^l, while emphasizing conditions of practical importance. Because of its favorable performance the new equation is extended to mixture calculations, as discussed in the following chapters.

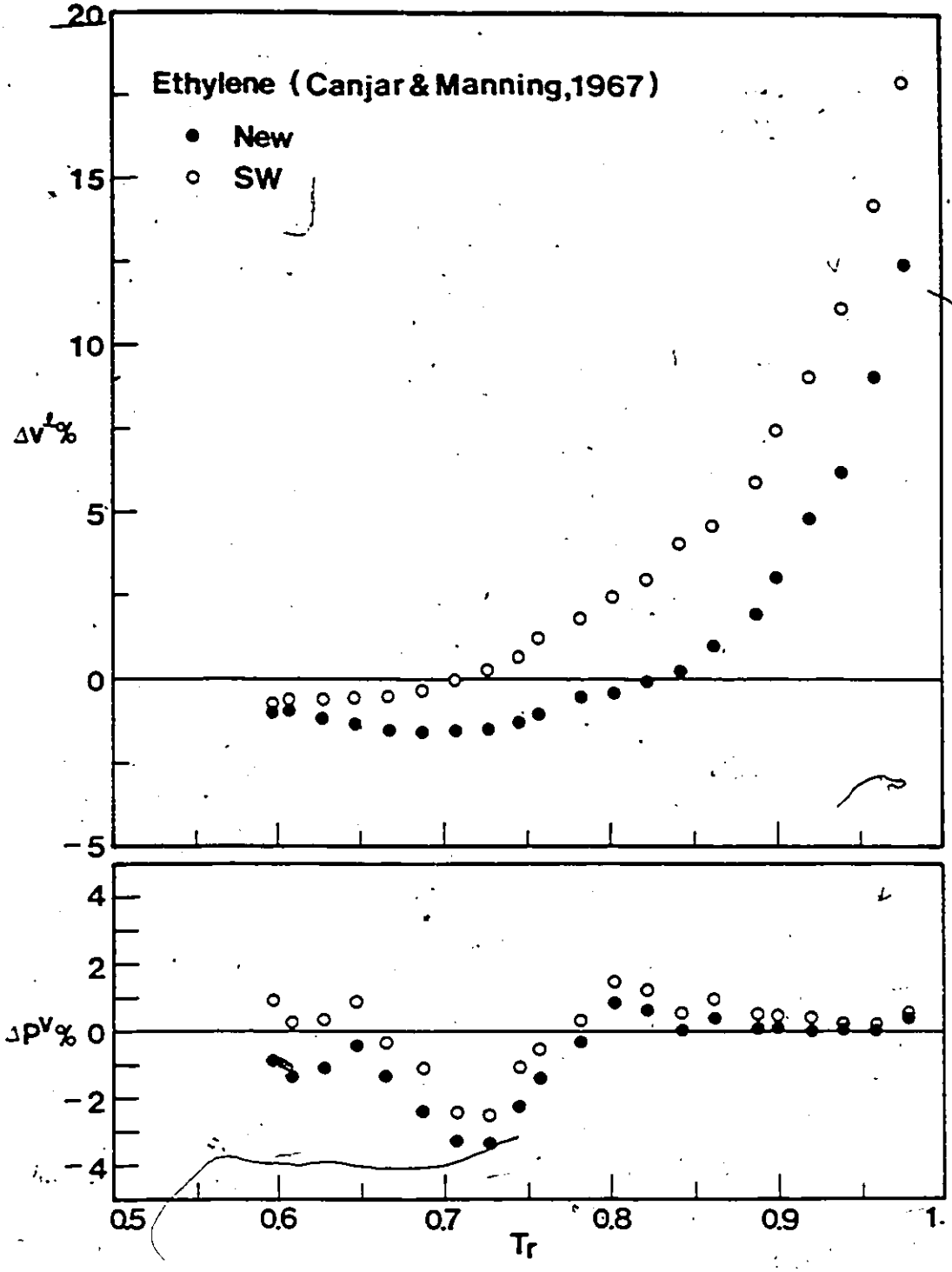

Figure 5.1: Deviations in the saturated liquid molar volumes and vapor pressures for ethylene calculated by the new and the SW EOS.

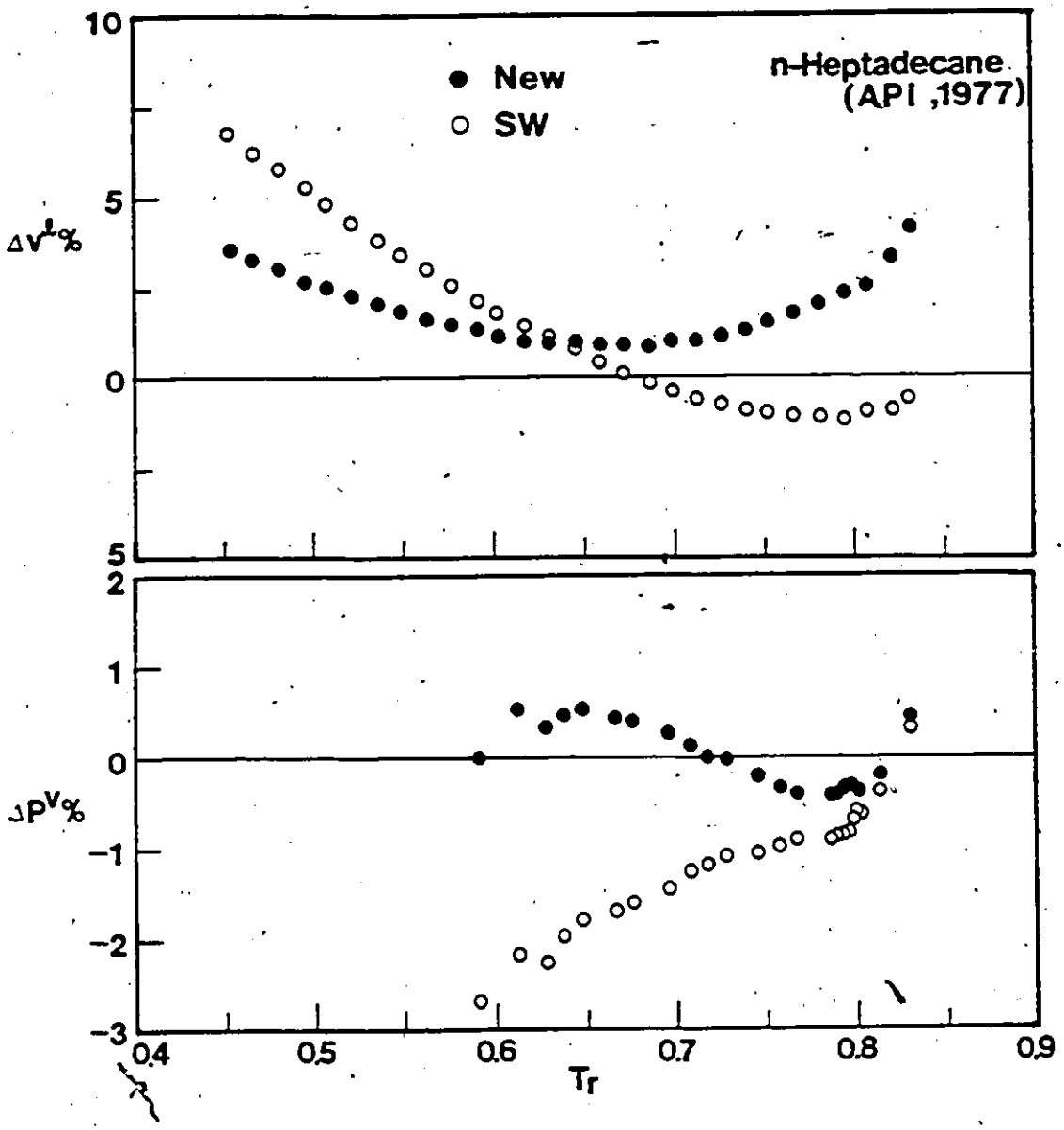

Figure 5.2: Deviations in the saturated liquid molar volumes and vapor pressures for n-heptadecane calculated by the new and the SW EOS.

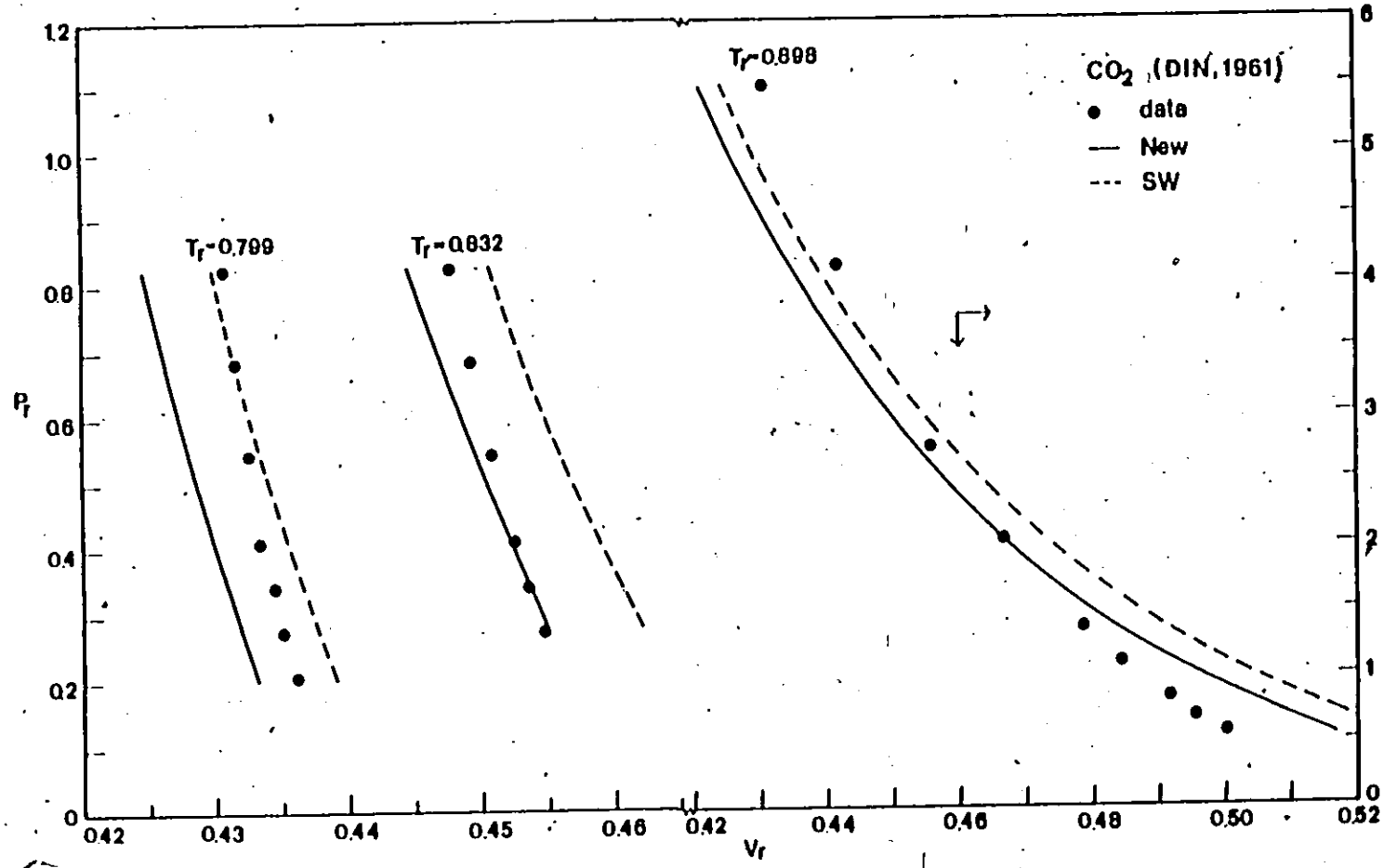

Figure 5.3: Comparison of the liquid volumes for carbon dioxide calculated by the new and the SW EOS.

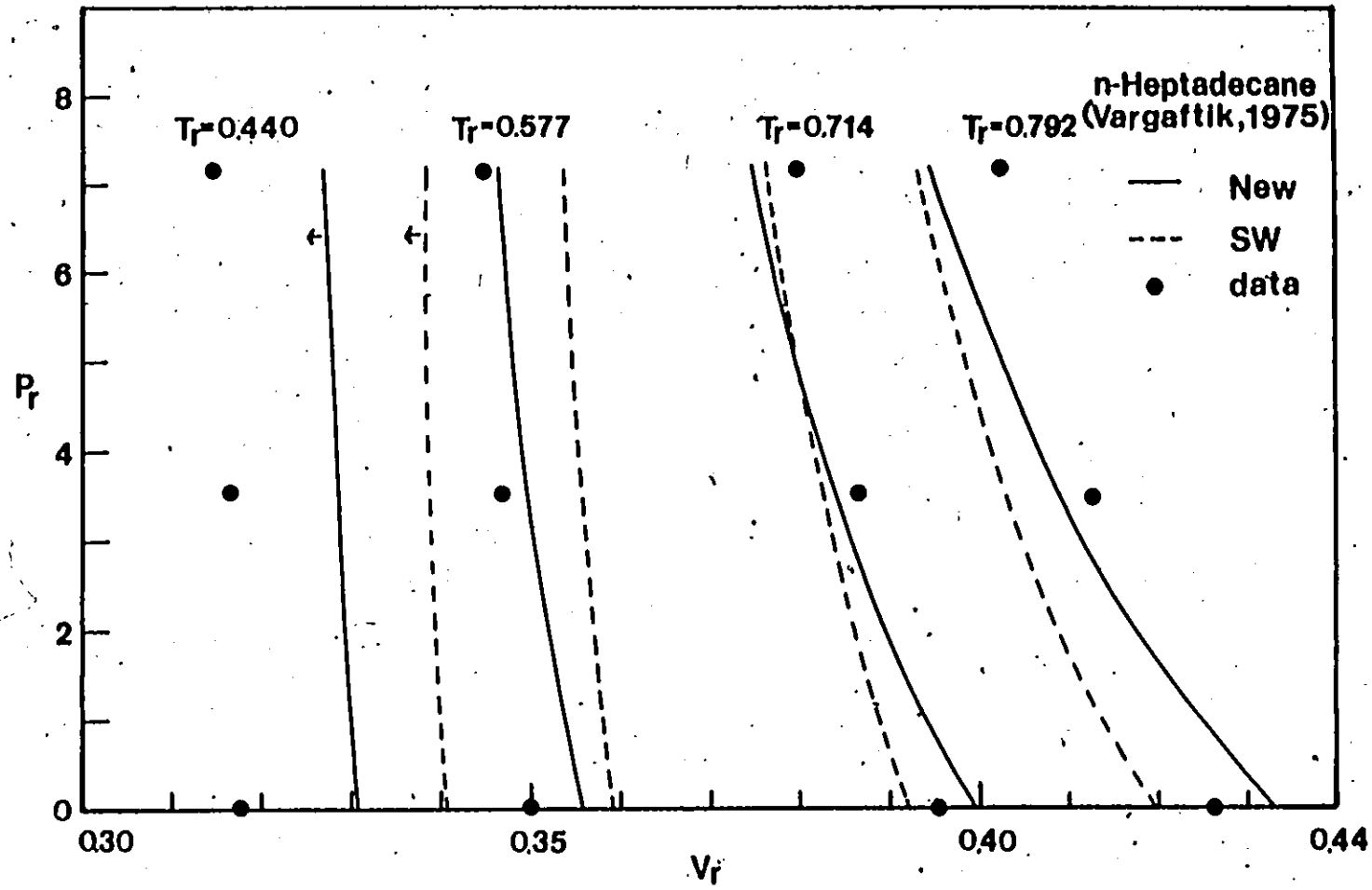

Figure 5.4: Comparison of the liquid volumes for n-heptadecane calculated by the new and the SW EOS.

Chapter VI

THE RANDOM AND LOCAL COMPOSITION MIXING MODELS

The most direct extension of an EOS for pure fluids to mixtures is carried out by replacing its pure fluid parameters with the appropriate mixture parameters. These mixture parameters are determined through the use of mixing rules and are the functions of composition and the pure fluid parameters.

Basically there are two types of mixing rules. The first is the one-fluid random mixing rules which are used primarily for mixtures consisting of nonpolar or slightly polar fluids. For complex mixtures consisting strongly polar and/or hydrogen bonding components, local composition (LC) mixing rules are generally used to obtain the mixture parameters.

6.1 Random Mixing Rules

Observing that just like pure fluids, a mixture has a critical point, van der Waals [133] assumed that a mixture can be treated as a single pure fluid and an EOS for a mixture is the same as that of pure fluids. From a microscopic viewpoint this implies that the molecules in the mixture are randomly mixed. Therefore, rewriting the new EOS (Eq.(4.19)) gives

$$P = RT/(v_m - b_m) - a_m/[v_m(v_m + c_m) + b_m(3v_m + c_m)] \quad (6.1)$$

with $c_m \equiv w_m\, b_m$

where the subscript, m, denotes a mixture property.

Often referred to as the VDW random mixing rules, the following quadratic expressions in composition for the mixture parameters a_m and b_m were first adopted by van der Waals [133] for his equation of state

$$a_m = \sum_i^M \sum_j^M z_i\, z_j\, a_{ij} \quad (6.2)$$

$$b_m = \sum_i^M \sum_j^M z_i\, z_j\, b_{ij} \quad (6.3)$$

in which z_i and z_j are the mole fractions of components i and j in either the liquid or vapor phases. For the cross coefficients a_{ij} and b_{ij} the following combining rules are often used

$$a_{ij} = (a_i a_j)^{\frac{1}{2}}(1-k_{ij}) \quad (6.4a)$$

$$b_{ij} = [(b_i + b_j)/2](1-\ell_{ij}) \quad (6.4b)$$

where $a_i \equiv a_{ii}$ and $b_i \equiv b_{ii}$. The quantities k_{ij} and ℓ_{ij} are the binary interaction coefficients which are empirical parameters determined from binary mixture data. By convention, if i=j, $k_{ij}=\ell_{ij}=0$, and if $i \neq j$, k_{ij} (= k_{ji}) and ℓ_{ij} (= ℓ_{ji}) are usually small positive or negative values. Eqs(6.2,3,4) are the commonly adopted mixing model for such two-parameter equations as the SRK and the PR equations. The empirical coefficient, k_{ij}, was first introduced by Zudkevitch and Joffe in 1970

[144]. Evelein and Moore [30] found that using the second empirical coefficient, ℓ_{ij}, further improved the correlation of VLE (P-T-composition) data for the binary mixtures. However, it is generally observed that only k_{ij} is required for the correlation of the VLE data for normal fluid mixtures.

It should be noted that the quadratic mixing rules for a_m and b_m satisfy the theoretical low-density limit where it requires that the mixture second virial coefficient, B_m, be a quadratic function of mole fraction [104]:

$$B_m = \sum_i^M \sum_j^M y_i\, y_j B_{ij} = a_m - b_m/RT \qquad (6.5)$$

where B_{ij} is the cross coefficient and y_i and y_j are the mole fractions of components i and j in the vapor phase.

The choice of mixing rules for evaluating the third parameter is not obvious. One method used by both Harmens [50] and Schmidt and Wenzel [113] was to replace the pure-fluid acentric factor, ω, in the generalized expressions for the third parameter, c, with the acentric factor of mixture, ω_m. Harmens [50] used a linear mixing rule for ω_m $(=\sum_i^M z_i\omega_i)$ to evaluate c_m. He found [50] that it was useful only for representing VLE values (P-T-composition) of close boiling normal fluid mixtures. Rather large errors occurred in the predicted bubble point pressures and vapor phase compositions for wide boiling mixtures. To evaluate the mixture parameter c_m in the SW equation Schmidt and Wenzel [113] devised the following mixing rule for ω_m

$$\omega_m = [\sum_i^M \omega_i\, z_i\, a_i^{\frac{1}{2}}]/[\sum_j^M z_j\, a_j^{\frac{1}{2}}] \qquad (6.6)$$

Using this mixing rule the SW EOS can calculate the VLE values for a variety of mixtures [40,112,113,138]. However it was found in this study that it is not applicable to hydrogen-containing systems since it gives rise to convergence problems in fugacity calculations due to the unreasonable values of c_m calculated from $c_m=-3\ \omega_m$.

It should be noted that the third parameter, c, in the HK and the SW EOS is a dimensionless quantity which is equivalent to the quantity u or w in Eq.(1.3). However the parameter c_m in the new EOS has the dimension of volume since $c_m=w_m b_m$. Therefore it makes more sense to define mixing rules for quantities which have dimensions rather than choosing arbitrary mixing rules for dimensionless quantities. Since both c_m and b_m have units of volume, the same mixing rule for b_m can be used for c_m

$$c_m = \sum_i^M \sum_j^M z_i\, z_j\, c_{ij} \qquad (6.7a)$$

with

$$c_{ij} = [(c_i+c_j)/2](1-\ell_{ij}). \qquad (6.7b)$$

When $\ell_{ij}=0$, Eqs(6.3,7a) reduce to a linear mixing rule

$$b_m = \sum_j^M z_j\, b_j \qquad (6.8a)$$

$$c_m = \sum_j^M z_j\, c_j \qquad (6.8b)$$

Summarized in Table 6.1 is the mixing model for the new equation. It is designated as the VDW-A and B, where A refers to the use of two empirical binary interaction coefficients (i.e., $\ell_{ij} \neq 0$) and B refers to the use of one coefficient (i.e., $\ell_{ij}=0$).

While theory requires a quadratic mixing rule at low densities, experiment shows that at high densities this rule is not reliable, especially for asymmetric and complex mixtures in which the molecules are not randomly mixed. The use of k_{ij} and ℓ_{ij} in the VDW mixing model can be considered as corrections to the over-simplified assumption that the molecules in mixtures are randomly mixed. By the same token they can also be considered as constants characteristic of the nonideal interaction between a pair of unlike molecules ($i \neq j$). At low densities, molecules are relatively free and do not interfere with one another. These molecules, regardless of their physical and chemical nature can be considered randomly distributed (or mixed) in space. On the other hand, due to the effect of intermolecular forces at high densities, the motion, position and orientation of a specific molecule is strongly affected by its immediate neighbors. Therefore, at such densities, the distribution (or mixing) of molecules is nonrandom so that the quadratic (random) mixing rules may not be adequate. However the random mixing assumption is valid at high densities if the molecular size (or covolume) of the components and the molecular potential (or the internal energy, $u = -\phi/2$) are approximately the same i.e, $b_i=b_j=b_{ij}$ and $u_{ii}=u_{jj}=u_{ij}$ [42,93,114].

Table 6.1: Summary of the random mixing models for the new equation of state.

Model Name

VDW-A

$$a_m = \sum_i^M \sum_j^M z_i z_j a_{ji},\quad a_{ji} = (a_i a_j)^{\frac{1}{2}} (1 - k_{ji})$$

$$b_m = \sum_i^M \sum_j^M z_i z_j b_{ji},\quad b_{ji} = \left(\frac{b_j+b_j}{2}\right)(1 - \ell_{ji})$$

$$c_m = \sum_i^M \sum_j^M z_i z_j c_{ji},\quad c_{ji} = \left(\frac{c_j+c_j}{2}\right)(1 - \ell_{ji})$$

VDW-B

$$a_m = \sum_i^M \sum_j^M z_i z_j a_{ji},\quad a_{ji} = (a_i a_j)^{\frac{1}{2}} (1 - k_{ji})$$

$$b_m = \sum_i^M z_i b_i$$

$$c_m = \sum_i^M z_i c_i$$

6.2 Local Composition (LC) Mixing Rules

For a mixing model to be applicable to a wide variety of mixtures, it should be able to describe in a continuous manner the change in behavior of the complex mixtures from randomness at low densities to nonrandomness at high densities. It should also be able to describe the behavior of the random and quasi-random mixtures in which this transition is not significant. Therefore, the mixing model must be able to

1. reduce to an expression for random mixing at low densities,
2. reduce to an expression for nonrandom mixing at high densities
3. reduce to the same expression as in Condition 1 for the case of (quasi) random mixing at all densities.

The first two conditions indicate that the mixing model be a combination of two models for the low and high density limits. In the low density limit, the model should reduce to a quadratic expression which satisfies the second virial coefficient requirement (Eq.(6.5)), while in the high density limit it should reduce to the nonrandom mixing model. Between the two density limits the model must be able to describe the degree of nonrandomness in the mixture. Condition (3) requires that the model be reduced to a quadratic expression when applying it to a mixture which is randomly mixed.

Several mixing models have been proposed [78,79,136,139,141] which are based on the local composition (LC) concept. The local composition concept is useful for introducing nonrandomness into a model for complex liquid mixtures. This concept was introduced by Wilson in

1964 [140] to describe the degree of segregation among molecules in liquid mixtures. In a mixture of molecules i and j, if the attractive forces between i-i and j-j are larger than those between i-j, molecules of i tend to surround themselves with other molecules i and molecules j tend to surround themselves with other molecules j. On the other hand, if the attractive forces i-j are larger than those for i-i and j-j the molecules mix in such a manner as to form as many i-j nearest neighbors as possible. In general the local composition (mole fraction), z_{ji}, is defined by

$$z_{ji} = \frac{\text{Molecules of j about a central molecule i}}{\text{Total molecules about a central molecule i}}$$

with

$$z_{ji} + z_{ii} = 1 \text{ and } z_{ij} + z_{jj} = 1$$

where $z_{ii} = z_i$, $z_{jj} = z_j$ and $z_{ij} = z_{ji}$.

The method for deriving local composition mixing models for an EOS is to incorporate the local composition excess Gibbs energy (G^E) model into the mixing rule for the attractive parameter a_m in the equation. The reason for using the local composition G^E models is that they can calculate the liquid-liquid equilibria of complex mixtures. Both Vidal and Huron [136] and Mollerup [79] derived LC mixing rules for the parameter a_m based on the nonrandom two-liquid (NRTL) model [106], while Mollerup [78], Whiting and Prausnitz [139] and Won [141] used the UNIQUAC model [4] as the basis. In recent studies both Mollerup

[79] and Mathias and Copeman [71] pointed out that the UNIQUAC-type mixing rule for the parameter a_m could not correlate VLE data for simple hydrocarbon mixtures as accurately as a quadratic mixing rule applied to the same EOS. Therefore, only the NRTL-type mixing rules proposed by Vidal and Huron (designated as NRTL-VH) and by Mollerup (NRTL-M) are considered in this part of the study. It should be noted that the NRTL-M mixing rule is a density dependent local composition (DDLC) mixing rule.

6.2.1 The Density Dependent Local Composition (DDLC) Mixing Rule

The principal assumptions used in deriving the NRTL-M mixing rule are

1. The local composition depends on the overall composition and density of the mixture.
2. The local composition is mainly caused by the attractive forces between molecules and the contribution of the repulsive forces to the nonrandomness is negligible.
3. The expression for the partition function for mixtures can be represented by a generalized VDW partition function for random mixtures.
4. The analytical expression for the attractive term in the EOS, P^a, derived from this partition function remains the same as that for pure fluids while a new expression for the attractive Helmholtz energy, A^a, is derived from the NRTL model.

Because the local composition is assumed to result from the attractive force alone, new mixing rules based on the LC concept will only be for the mixture parameter a_m, since it is directly related to the attractive potential energy. The mixing rules for the parameters b_m and c_m will remain the same as those in the VDW mixing model.

The generalized VDW partition function used by Mollerup [79] has the form

$$Q_m=\prod_i^M \{\frac{1}{Ni!}(V_m/\Lambda_i^3)^{Ni}\}(V_{fm}/V_m)^N[\exp(-\Phi_m/2kT)]^N\prod_i^M(q_{r,v})_i^{Ni} \qquad (6.9)$$

where V_m is the total volume of the mixture, N_i is the number of molecules of component i in a mixture of M components and $N=\sum_i^M N_i$. The analytical expressions for V_{fm} and Φ_m are the same as those for pure fluids. With reference to the new EOS for mixture (Eq.(6.1)) they are

$$V_{fm} = V_m - b_m \qquad (6.10)$$

$$\frac{\Phi}{2}m = - (a_m/ED)\, \ell n[(2v_m + FD + ED)/(2v_m + FD - ED)] \qquad (6.11a)$$

$$ED = (c_m^2 + 2c_mb_m + 9b_m^2)^{\frac{1}{2}} \qquad (6.11b)$$

$$FD = c_m + 3b_m \qquad (6.11c)$$

The contributions of the ideal gas and hard-sphere and attractive molecular interactions to the pressure and molar Helmholtz energy of mixtures can be obtained through Eqs(2.2,3)

$$P = P^{id} + P^{hs} + P^a \qquad (6.12a)$$

where

$$P^{id} = RT/v_m \qquad (6.12b)$$

$$P^{hs} = RTb_m/[v_m (v_m - b_m)] \qquad (6.12c)$$

$$P^{a} = - a_m/[v_m(v_m + c_m) + b_m(3v_m + c_m)] \qquad (6.12d)$$

and

$$A = A^{id} + A^{hs} + A^{a} \qquad (6.13a)$$

where

$$A^{id} = - \sum_{i}^{M} [RTz_i \ln(v_m/N\Lambda_i^3 z_i) + RTz_i + RTz_i \ln(q_{r,v})_i] \qquad (6.13b)$$

$$A^{hs} = - RT\ln[(v_m - b_m)/v_m] \qquad (6.13c)$$

$$A^{a} = Na\, \phi_m/2. \qquad (6.13d)$$

The first step in deriving the DDLC mixing rules is to link an LC excess Gibbs energy model to the attractive term in the new EOS by

$$P^{a} = \frac{1}{RT} \left(\frac{\partial A^{a}}{\partial v_m}\right)_{T,n} \qquad (6.14)$$

where the attractive Helmholtz energy A^a is obtained from an LC excess Gibbs energy model whose parameters are related to those in the EOS. Based on Assumption 4, the analytical expression for P^a obtained from Eq.(6.14) must be the same as that given by Eq.(6.12d). Rearranging Eq.(6.13a) gives the residual Helmholtz energy, A^{RES},

$$A^{RES} = A - A^{id} = A^{hs} + A^{a} \qquad (6.15)$$

where the residual property is defined as the difference between the actual value and the value in the ideal gas state. Therefore A^a is also a residual property due to the attractive forces of molecules. An analytical expression is obtained for A^a by relating it to the residual (attractive) molar internal energy, μ^{RES}, which can be derived from the NRTL model. Since there is no molecular potential in the ideal gas, i.e., $\mu^{id} = 0$, the residual internal energy is equal to the molar internal energy i.e., $\mu^{RES} = \mu$.

The NRTL equation gives an excess Gibbs energy model (G^E) of the form

$$G^E = \sum_i^M z_i \sum_j^M z_{ji} \Delta\mu_{ji} \qquad (6.16a)$$

The quantity $\Delta\mu_{ij}$ is the difference between the molar internal energies of the unlike-pair, μ_{ji} ($=\mu_{ij}$), and the like-pair, μ_{ii},

$$\Delta\mu_{ji} = \mu_{ji} - \mu_{ii} \qquad (6.16b)$$

where the quantity, z_{ji}, is the local composition of molecule j around molecule i which is defined as

$$z_{ji} = (z_j E_{ji}) / [\sum_\ell^M z_\ell E_{\ell i}] \qquad (6.16c)$$

the quantity E_{ji} is the Boltzmann factor defined as

$$E_{ji} = \exp[-(\alpha_{ji}\Delta\mu_{ji})/RT] \qquad (6.16d)$$

where α_{ji} is the nonrandom parameter which accounts for the nonrandomness of the binary mixture α_{ji} should be zero for random mixtures.

In order to find an equivalent expression for A^a Mollerup [78] assumed that

$$G^E = \mu^E = A^E \tag{6.17}$$

where the superscript, E, denotes an excess property which is the difference between an actual property value and the value calculated for an ideal solution. When $G^E=\mu^E$, μ^{RES} (and μ) can easily be related to G^E through the definition of the excess property

$$\mu^E = \mu^{RES} - \sum_i^M z_i \mu_{i\,i}^{RES} = \mu - \sum_i^M z_i \mu_{ii} \tag{6.18}$$

Thus,

$$\mu = \sum_i^M z_i \sum_j^M z_{ji} \mu_{ji} \tag{6.19}$$

If $\mu^E=A^E$ then the residual (attractive) internal energy is equal to the residual attractive Helmholtz energy [78], i.e.,

$$\mu^{RES} = \mu = A^a \tag{6.20a}$$

$$\mu_{i\,i}^{RES} = \mu_{ii} = A_{i\,i}^a \tag{6.20b}$$

Therefore, the expression for A^a should have the same form as that for μ

$$A^a = \sum_i^M z_i \sum_j^M z_{ji} \mu_{ji} \tag{6.21}$$

where the local composition, z_{ji}, is defined by Eqs(6.16c,d). For the complete description of A^a analytical expressions for μ_{ji} and μ_{ii} in terms of the parameters in the equation of state is required. Based on the

method used by Mollerup the following expressions are obtained for μ_{ji} and μ_{ii} in terms of the new EOS parameters

$$\mu_{ji} = -(a_{ji}/ED)\ \ell n[(2v_m+FD+ED)/(2v_m+FD-ED)] \qquad (6.22a)$$

$$\mu_{ii} = -(a_i/ED)\ \ell n[(2v_m+FD+ED)/(2v_m+FD-ED)] \qquad (6.22b)$$

where $a_{ji} = (a_i\ a_j)^{\frac{1}{2}}\ (1-k_{ij})$. Thus both μ_{ji} and μ_{ii} are density dependent. Substituting Eq.(6.22) into Eq.(6.21) yields

$$A^a = -(a_{m0}/ED)\ \ell n[(2v_m+FD+ED)/(2v_m+FD-ED)] \qquad (6.23a)$$

where

$$a_{m0} = \sum_i^M z_i \sum_j^M z_{ji}\ a_{ji} \qquad (6.23b)$$

Substituting Eqs(6.22,23) into Eq.(6.14) yields a new mixing rule for the parameter a_m

$$a_m = a_{m0} + a_{m1} \qquad (6.24a)$$

where

$$a_{m1} = \frac{GD}{RT\ (ED)}\ \ell n[(2v_m+FD+ED)/(2v_m+FD-ED)] \qquad (6.24b)$$

with

$$GD = [\sum_i^M z_i \sum_j^M z_{ji}\ \alpha_{ji}\ (a_{ji} - \sum_k^M z_{ki}\ a_{ki})\ a_{ji}] \qquad (6.24c)$$

A summary of this mixing model (designated as NRTL-M) is presented in Table 6.2. It contains three empirical coefficients α_{ji} $(=\alpha_{ij})$, k_{ij} and ℓ_{ij}. It satisfies the three conditions set out at the beginning.

Table.6.2: Summary of the local composition mixing models for the new equation of state.

Model Name	Mixing and Combining Rules	Notes
NRTL-M	$a_m = a_{mo} + a_{ml}$	$ED = (c_m^2 + 2c_m b_m + 9b_m^2)^{1/2}$
	$a_{mo} = \sum_i^M z_i \sum_j^M z_{ji}\, a_{ji}$, $a_{ji} = (a_i\, a_j)^{1/2}(1 - k_{ji})$	$FD = c_m + 3b_m$
	$a_{ml} = [\sum_i^M z_i \sum_j^M z_{ji}\, \alpha_{ji} (a_{ji} - \sum_k^M z_{ki}\, a_{ki})\, a_{ji}\,]$	$z_{ji} = \dfrac{z_j E_{ji}}{\sum_\ell^M z_\ell E_{\ell i}}$
	$b_m = \sum_i^M \sum_j^M z_i z_j b_{ji}$, $b_{ji} = \dfrac{(b_i + b_j)}{2}(1 - \ell_{ji})$	$E_{ji} = \exp[- \dfrac{\alpha_{ji}\, \Delta u_{ji}}{RT}]$
	$\tau_m = \sum_i^M \sum_j^M z_i z_j c_{ji}$, $c_{ji} = \dfrac{(c_i + c_j)}{2}(1 - \ell_{ji})$	$\Delta u_{ji} = u_{ji} - u_{ii}$
		$u_{ji} = - \dfrac{a_{ji}}{ED} \ln[\dfrac{2V_m + FD + ED}{2V_m + FD - ED}]$
		$u_{ii} = - \dfrac{a_i}{ED} \ln[\dfrac{2V_m + FD + ED}{2V_m + FD - ED}]$
NRTL-VH	$a_m = \{ \sum_i^M z_i [\dfrac{a_i}{ED_i} \ln(\dfrac{2b_i + FD_i + ED_i}{2b_i + FD_i - ED_i}) - \bar{G}_m^E]/ HD$	$HD = [\ln(\dfrac{2b_m + FD + ED}{2b_m + FD - ED})]/ ED$
	$\bar{G}_m^E = \sum_i^M z_i \sum_j^M z_{ji}\, \Delta \bar{u}_{ji}$	$ED_i = (c_i^2 + 2c_i b_i + 9b_i^2)^{1/2}$
	$b_m = \sum_i^M z_i b_i$, $c_m = \sum_i^M z_i c_i$	$FD_i = c_i + 3b_i$
		$z_{ji} = \dfrac{z_j b_j E_{ji}}{\sum_\ell^M z_\ell b_\ell E_{\ell i}}$
		$E_{ji} = \exp[- \dfrac{\alpha_{ji}\, \Delta \bar{u}_{ji}}{RT}]$
		$\bar{u}_{ii} = - \dfrac{a_i}{ED_i} \ln(\dfrac{2b_i + FD_i + ED_i}{2b_i + FD_i - ED_i})$
		$\bar{u}_{ji} = - \dfrac{2 (b_i\, b_j)^{1/2} (\bar{u}_{ii}\, \bar{u}_{jj})^{1/2} (1 - k_{ji})}{(b_i + b_j)}$

6.2.2 The Density Independent Local Composition Mixing Rule

Because it was derived based on the excess Gibbs energy at the infinite pressure limit, the NRTL-type mixing rule of the parameter a_m proposed by Vidal and Huron [136], NRTL-VH, does not depend on density. At infinite pressure, they assumed that the volumes of mixtures and pure components are approximately those of the co-volumes predicted by the EOS

$$v_m = b_m \tag{6.25a}$$

$$v_i = b_i \tag{6.25b}$$

Based on their derivation the first step is to relate the molar excess Gibbs energy G^E to the fugacity coefficients of the mixture, ϕ, and pure components, ϕ_i, using the following thermodynamic relationship

$$\frac{G^E}{RT} = \ln \phi - \sum_i^M z_i \ln \phi_i \tag{6.26}$$

where

$$\ln \phi = \frac{1}{RT} \int_0^P (v_m - \frac{RT}{P})\, dP \tag{6.27a}$$

$$\ln \phi_i = \frac{1}{RT} \int_0^P (v_i - \frac{RT}{P})\, dP \tag{6.27b}$$

Applying Eqs(6.27a,b) to the new equation gives

$$\ln \phi = -\ln \left[\frac{P\,(v_m - b_m)}{RT}\right] + \frac{Pv_m}{RT} - \frac{a_m}{RT\ ED} \ln \left[(2v_m + FD + ED)/(2v_m + FD - ED)\right] - 1 \tag{6.28a}$$

$$\ln \phi_i = -\ln \left[\frac{P(v_i - b_i)}{RT}\right] + \frac{Pv_i}{RT}$$

$$- \frac{a_i}{RT\, EDi} \ln \left[(2v_i FD_i + ED_i)/(2v_i + FD_i - ED_i)\right] - 1 \qquad (6.28b)$$

where

$$ED_i = (c_i^2 + 2c_i b_i + 9b_i^2)^{\frac{1}{2}} \qquad (6.28c)$$

$$FD_i = c_i + 3b_i \qquad (6.28d)$$

At infinite pressure Vidal and Huron assumed that the molar volume of the mixture could be calculated from the molar volumes of pure components using a linear mixing rule

$$v_m = \sum_i^M \bar{z}_i v_i \qquad (6.29)$$

From Eqs(6.25a,b)

$$b_m = \sum_i^M z_i b_i \qquad (6.30)$$

Therefore, at infinite pressure Eq.(6.26) becomes

$$G^E_{\infty} = - \{(a_m/ED) \ln [(2b_m + FD + ED)/(2b_m + FD - ED)]$$

$$- \sum_i^M z_i [(a_i/ED_i) \ln[(2b_i + FD_i + ED_i)/(2b_i + FD_i - ED_i)]\} \qquad (6.31)$$

where the symbol, ∞, denotes a property at infinite pressure. Rearranging Eq.(6.31) gives a new mixing rule for a_m

$$a_m = \{ \sum_i^M z_i (a_i/ED_i) \ln[2b_i + FD_i + ED_i)/(2b_i + FD_i - ED_i)] - G^E_{\infty}\}/HD \qquad (6.32a)$$

where

$$HD = \frac{1}{ED} \ln[(2b_m + FD + ED)/(2b_m + FD - ED)] \qquad (6.32b)$$

$$G^E = \sum_i^M z_i \sum_j^M z_{ji} \Delta\mu_{ji} \qquad (6.32c)$$

with

$$z_{ji} = (z_j b_j E_{ji})/(\sum_\ell^M z_\ell b_\ell E_{\ell i}) \qquad (6.32d)$$

$$E_{ji} = \exp[- (\alpha_{ji} \Delta\mu_{ji})/RT] \qquad (6.32e)$$

Based on their method, the following expressions for μ_{ji} and μ_{ii} are defined in terms of the new EOS parameters

$$\Delta\mu_{ji} = \mu_{ji} - \mu_{ii} \qquad (6.32f)$$

$$\mu_{ji} = - [2(b_i b_j)^{\frac{1}{2}}(\mu_{ii}\mu_{jj})^{\frac{1}{2}}(1-k_{ji})]/(b_i+b_j) \qquad (6.32g)$$

$$\mu_{ii} = - (a_i/ED_i) \ln[(2b_i + FD_i + ED_i)/(2b_i + FD_i - ED_i)] \qquad (6.32h)$$

It should be noted that there is no volume term in any of the above equations. A summary of the NRTL-VH model is presented in Table 6.2.

Two options were suggested by the original authors for selecting the empirical coefficients to be used in the NRTL-VH mixing rule. The first option uses two coefficients k_{ij} ($=k_{ji}$) and α_{ij} ($=\alpha_{ji}$) to fit binary mixture data. However the mixing rule does not satisfy Condition (3), since as shown by Eq.(6.33) it does not reduce to a quadratic expression at $\alpha_{ji}=0$

$$a_m = \{\sum_i^M \sum_j^M z_i z_j a_{ji} [\ln(\frac{2b_i + FD_i + ED_i}{2b_i + FD_i - ED_i}) \ln(\frac{2b_j + FD_j + ED_j}{2b_j + FD_j - ED_j})]$$

$$/\ \ln\left(\frac{2b_m+FD+ED}{2b_m+FD-ED}\right)\Big\} \qquad (6.33)$$

with

$$a_{ji} = (a_i\ a_j)^{\frac{1}{2}}(1-k_{ji}).$$

The second option uses three empirical coefficients, α_{ji}, Δu^{**}_{ji} and Δu^{**}_{ij}. The reason for selecting Δu^{**}_{ji} and Δu^{**}_{ij} rather than k_{ij} is to take into account the differences in molecular interactions when either molecules i or j is the central molecule. However, in this case the value of α_{ij} can never be zero so that Condition (3) can never be satisfied.

Also because the NRTL-VH mixing rule is not density-dependent, it cannot reduce to a quadratic expression as the density approaches zero, thereby not satisfying Condition (3). In principle, this model is unable to describe the degree of nonrandomness in mixtures which are between the two density limits. However, from a computational viewpoint the NRTL-VH mixing rule is advantageous over the DDLC mixing rule since unlike the NRTL-M mixing rule it does not contain volume terms which must be determined iteratively.

In this study, VLE and volumetric data of normal fluid binary mixtures are used to test the new EOS with the VDW-B ($\ell_{ij}=0$) mixing model. Due to the lack of volumetric data for complex mixtures, only VLE (P-T-composition) data is used to test the new EOS using various mixing models (VDW-A and B, NRTL-M and NRTL-VH). It should be

noted that multicomponent mixture calculations are carried out by grouping all components into pairs. Therefore, accurate representation of the properties of each pair is the necessary condition in order to represent the properties of the mixture accurately. In these calculations the maximum number of empirical coefficients is limited to two since using more than two empirical but adjustable coefficients is not practical for routine calculation and correlation. The two empirical coefficients used in the NRTL-M and the NRTL-VH models are α_{ji} and k_{ij}.

Chapter VII

CALCULATION OF MIXTURE VAPOR-LIQUID EQUILIBRIA AND VOLUMETRIC PROPERTIES BY THE NEW EQUATION OF STATE

7.1 General Considerations

At given temperature and pressure the phase equilibrium condition of a mixture in the vapor and liquid phases is that the fugacity of each component in both phases are equal, i.e.,

$$\hat{f}_i^{\ell}(P, T, x_i) = \hat{f}_i^{v}(P, T, y_i) \tag{7.1}$$

where $\hat{f}_i$ is the fugacity of component i in the mixture and x_i and y_i are the mole fractions in the liquid and vapor phases, respectively. When calculating the P-T-x_i-y_i equilibrium relationship by means of an EOS, it is more convenient to use the fugacity coefficient, $\hat{\phi}_i$, which is defined as [132]

$$\hat{\phi}_i^{\ell}(P, T, x_i) = \hat{f}_i^{\ell}/x_i P \tag{7.2a}$$

$$\hat{\phi}_i^{v}(P, T, y_i) = \hat{f}_i^{v}/y_i P \tag{7.2b}$$

Thus Eq.(7.1) becomes

$$x_i\hat{\phi}_i^{\ell} = y_i\hat{\phi}_i^{v} \tag{7.3}$$

which after rearrangement, gives equilibrium ratio, K_i

$$K_i \equiv y_i/x_i = \hat{\phi}_i^{\ell}/\hat{\phi}_i^{v} \qquad (7.4)$$

Eq.(7.4) serves as the key equation for mixture VLE calculations and represents complex expressions of T, P, x_i and y_i. From the phase rule there are M degrees of freedom in an M-component VLE mixture which must be specified. However, there are 2M variables, T, P, x_1, x_2, x_3 ... y_1, y_2, y_3 ... where $\sum_1^M x_i=1$ and $\sum_1^M y_i=1$. Therefore the remaining M variables may be obtained by solving Eq.(7.4) simultaneously for each of the M components. Depending on the variables specified, the VLE calculations can be categorized as

(a) Bubble-point calculation - calculate y_i and either P or T for a given x_i and either T or P,

(b) Dew-point calculation - calculate x_i and either P or T for a given y_i and either T or P,

(c) Flash calculations - calculate x_i and y_i for given T and P and overall composition.

There are many books available (Prausnitz and Chueh [91], Holland [56], Van Ness and Abbott [132]) which provide algorithms to perform the above calculations.

In this study, the new EOS is tested by performing flash calculations for binary mixtures of normal fluids and by calculating the bubble-point pressures of complex mixtures.

7.2 Expressions for the Fugacity Coefficients

The analytical expression for $\hat{\phi}_i$ can be obtained from either one of the following thermodynamic relationships [99]

$$\ell n(\hat{\phi}_i) = \frac{1}{RT}(\partial nA^{RES}/\partial n_i)_{T,\, v_m, n_j} - \ell n(Z_m) \qquad (7.5)$$

$$\ell n(\hat{\phi}_i) = \int_{v_m}^{\infty} [\frac{1}{RT}(\frac{\partial P}{\partial n_i}) - (1/v_m)]\, dv_m - \ell n(Z_m) \qquad (7.6)$$

where $Z_m = P\, v_m/RT$, n_i is the number of moles of component i and $n = \sum_i^M n_i$ is the total number of moles in the mixture. Eq.(7.5) can be rewritten as

$$\ell n(\phi_i) = \frac{1}{RT}\{[\partial nA^{hs}/\partial n_i] + [\partial nA^{a}/\partial n_i]\} - \ell n(Z_m) \qquad (7.7)$$

Eq.(7.7) is used to evaluate $\hat{\phi}_i$ when either the EOS or its mixing rule causes Eq.(7.6) to be cumbersome or impossible to integrate analytically. When the density dependent NRTL-M mixing model is used with an EOS there is no analytical solution for the integration of the attractive part of the EOS in Eq.(7.6). The expressions for $\hat{\phi}_i$ from the new EOS for the three mixing models (VDW, NRTL-VH, NRTL-M) are given below.

(1)the VDW random mixing model

$$\ell n(\hat{\phi}_i) = -\ell n(1 - b_m/v_m) + [2\sum_j^M z_j b_{ji} - b_m]/(v_m - b_m) - (a_m/T)\, F_{ni} - (\frac{F}{T})(2\sum_j^M z_j a_{ji}) + (\frac{F}{T})\, a_m - \ell n(Z_m) \qquad (7.8a)$$

where

$$F = \frac{1}{R\,ED}\,\ell n[(2v_m+FD+ED)/(2v_m+FD-ED)] \qquad (7.8b)$$

$$F_{ni} = F\,[1 - (ED_{ni}/ED)] + \frac{1}{R\,ED}\,\{[(FD_{ni}+ED_{ni})/(2v_m+FD+ED)] - [(FD_{ni}-ED_{ni})/(2v_m+FD-ED)]\} \qquad (7.8c)$$

$$ED_{ni} = \frac{1}{ED}[2\sum_j^M z_j c_{ji}(c_m+b_m) + 2\sum_j^M z_j b_{ji}(c_m+9b_m) - (c_m^2+9b_m^2) - 2b_m c_m] \qquad (7.8d)$$

$$FD_{ni} = 2(\sum_j^M z_j c_{ji} + 3\sum_j^M z_j b_{ji}) - (c_m+3b_m) \qquad (7.8e)$$

(2)the NRTL-VH mixing model

$$\ell n(\hat{\phi}_i) = -\ell n(1-b_m/v_m) + b_i/(v_m-b_m) - (a_m/T)\,F_{ni} - (\frac{F}{T})\,a''_{ni} + (\frac{F}{T})\,a_m - \ell n(Z_m) \qquad (7.9a)$$

where

$$a''_{ni} = \frac{1}{HD^2}\{HD\,[(\sum_i^M z_i(a_i\,HD_i)\,-G^E_{\cdots}) + [a_i\,HD_i - GD''_{ni}] - [\sum_i^M z_i(a_i\,HD_i) - G^E_{\cdots}]\,HD_{ni}\} \qquad (7.9b)$$

$$GD''_{ni} = (D''_i/N''_i) + \sum_k^M (z_k/N''_k)[\mu''_{ik} - (D''_k/N''_k)]\,(b_i E_{ik}) \qquad (7.9c)$$

$$D''_k = \sum_j^M z_j b_j E_{jk} \mu''_{jk} \qquad (7.9d)$$

$$N''_k = \sum_\ell^M z_\ell b_\ell E_{\ell k} \qquad (7.9e)$$

$$HD_{ni} = HD\,(1-ED_{ni}/ED) + \frac{1}{ED}\{[(4\sum_j^M z_j b_{ji} - 2b_m + FD_{ni} + ED_{ni})/(2b_m+FD+ED)] - [(4\sum_j^M z_j b_{ji} - 2b_m + FD_{ni} - ED_{ni})/$$

$$+(2b_m+FD-ED)]\} \qquad (7.9f)$$

(3)the NRTL-M mixing model

$$\ln(\hat{\phi}_i) = -\ln(1-b_m/v_m) + (2\sum_j^M z_j b_{ji}-b'_m)/(v_m-b_m) - (a_{m0}/T)\,F_{ni} - (a_{ni}/T)\,F - \ln(Z_m) \qquad (7.10a)$$

where

$$a_{ni} = (D_i/N_i) + \sum_k^M (z_k/N_k)[a_{ik}-(D_k/N_k)]\,E_{ik} + (F_{ni}/T)\,a_R \qquad (7.10b)$$

$$a_R = \sum_k^M (z_k/N_k)\sum_j^M z_j E_{jk}\alpha_{jk}(a_{jk}-a_k)[a_{jk}-(D_k/N_k)] \qquad (7.10c)$$

$$D_k = \sum_j^M z_j a_{jk} E_{jk} \qquad (7.10d)$$

$$N_k = \sum_\ell^M z_\ell E_{\ell k} \qquad (7.10e)$$

and the quantities F and F_{ni} are given by Eqs(7.8b,c). These expressions are applicable to both liquid and vapor phases.

7.3 Computational Schemes for VLE and Volumetric Calculations

A. VLE Calculations

The algorithms which are used for the flash and bubble-point calculations are presented in Figures 7.1 and 7.2. As shown in Figure 7.1, except when the DDLC mixing rule is used, the flash calculation has

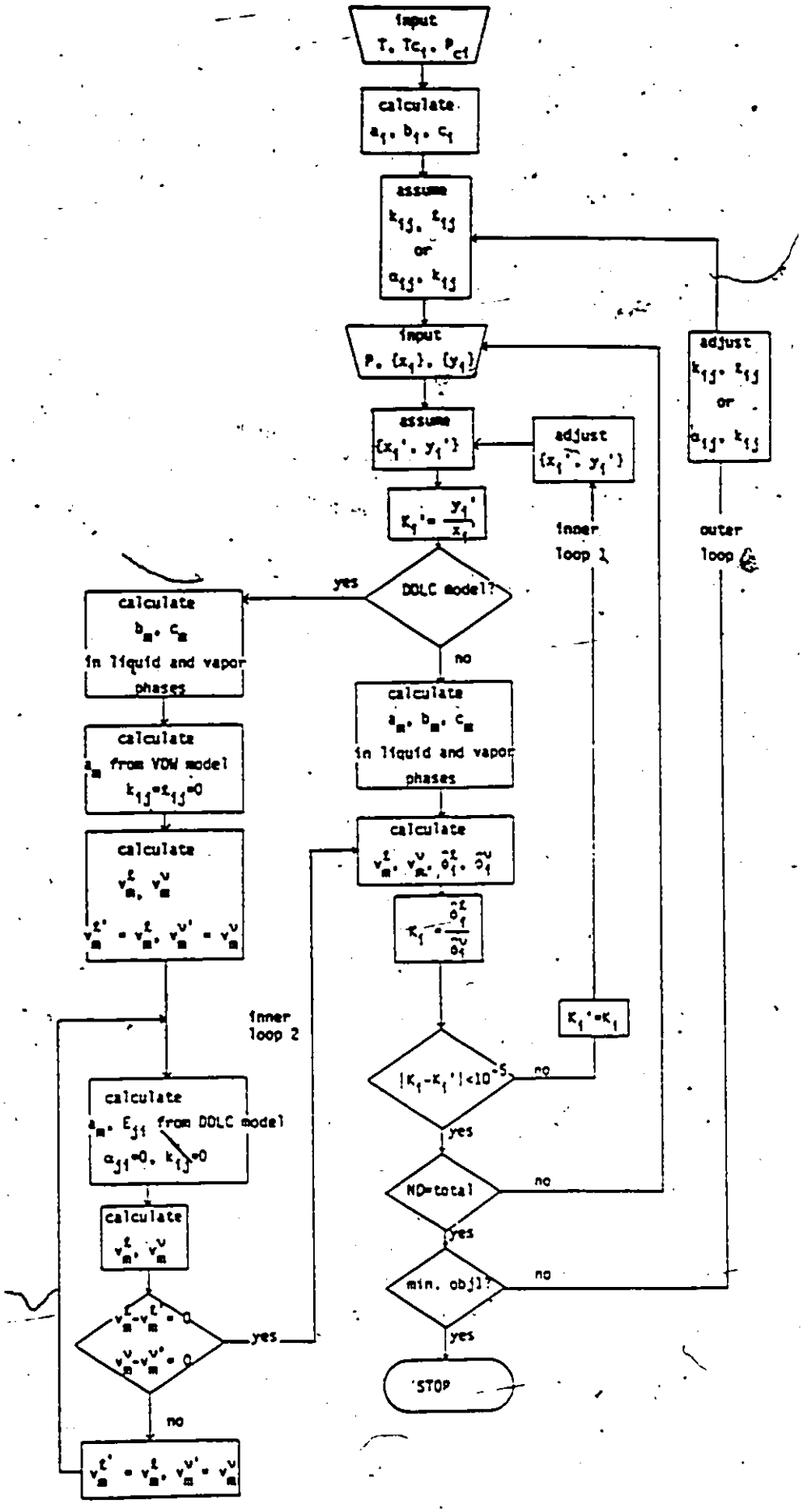

Figure 7.1: Flow diagram for the flash calculation.

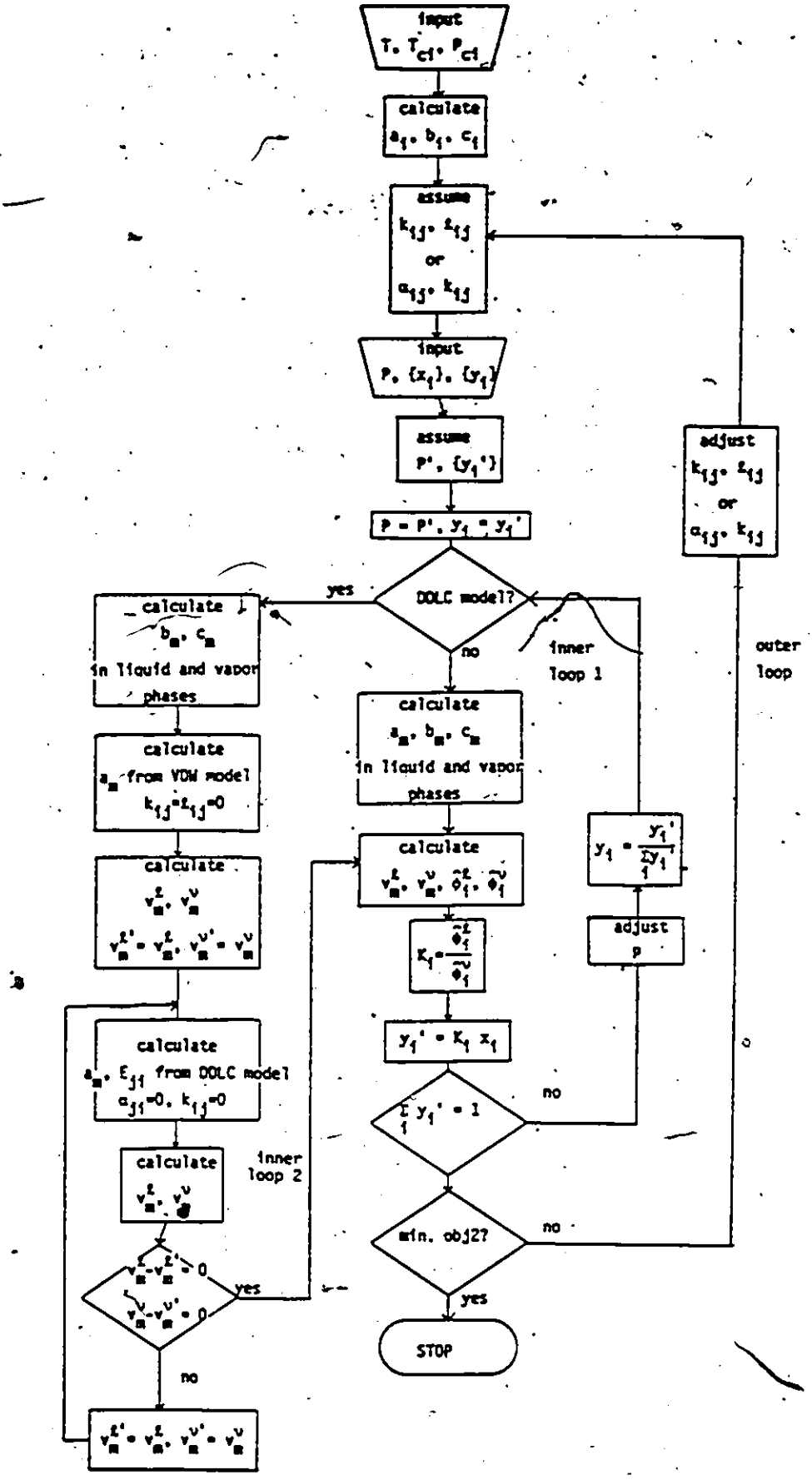

Figure 7.2: Flow diagram for the bubble-point calculation.

two iteration loops. Inner loop 1 calculates the equilibrium ratio, K_i, for each (x_i, y_i) until the value of K_i is constant. The initial guess for K_i is calculated from the experimental x_i and y_i. The outer loop adjusts the binary interaction coefficients (k_{ij} and/or ℓ_{ij}) to minimize the deviations between the calculated and experimental x_i's and y_i's. The objective function, obj1, is

$$obj1 = \{\sum_{1}^{ND} [(x_{i,calc} - x_{i,expt})^2 + (y_{i,calc} - y_{i,expt})^2]\}/ND \qquad (7.11)$$

where the subscripts, calc and expt, represent the calculated and the experimental values, respectively, and ND is the number of data points. The golden-section optimization method [32] is used to adjust the binary interaction coefficients in the mixing model.

When the DDLC mixing rule is used to evaluate the parameter a_m an additional iteration loop (inner loop 2) is required to calculate the Boltzmann factors, E_{ij} and E_{ji}, which contain the mixture molar volumes that must be calculated by trial-and-error. Initial estimates of the mixture molar volumes (v_m^ℓ and v_m^v) are obtained by solving the new EOS coupled with the random mixing model. From these values of v_m^ℓ and v_m^v, the first estimates of E_{ij} and E_{ji} in the liquid and vapor phases are calculated. The new EOS then used with the DDLC model refines the values of v_m^ℓ and v_m^v and E_{ji} and E_{ij}. Generally, it requires four or five iterations until the values of v_m^ℓ and v_m^v are constant.

As can be seen in Figure 7.2 there are three iteration loops for the bubble-point calculation which are basically the same as those in the flash calculation. However, the objective function, obj2, used is

$$obj2 = \{\sum_{1}^{ND} [|(P_{calc} - P_{expt})|/P_{expt}]\}/ND \qquad (7.12).$$

For inner loop 1 the experimental P and y_i are used as initial estimates and P is adjusted by means of the Secant method [63] until $\sum_{1}^{M} y_{i,calc} = 1$.

B. Volumetric Calculations

(1) Saturated liquid and vapor molar volumes of binary mixtures

Two methods are used to calculate the saturated liquid and vapor molar volumes of binary mixtures. In these calculations the VDW-B mixing model was used to evaluate the mixture parameters a_m, b_m and c_m.

Method I: Input pressure, temperature, compositions

In this method the experimental values of P, T, x_i and y_i are used as input data to calculate the saturated liquid and vapor molar volumes (v_m^{ℓ} and v_m^{v}). Because the liquid and vapor compositions are specified equilibrium calculations are not required. The binary interaction coefficient, k_{ij}, is determined by minimizing the objective function, obj3,

$$obj3 = \{\sum_{1}^{ND} [|(v^{\ell}_{m,calc} - v^{\ell}_{m,expt})|/v^{\ell}_{m,expt}] + [|(v^{v}_{m,calc} - v^{v}_{m,expt})|/v^{v}_{m,expt}]\}/ND \qquad (7.13)$$

Method II: Input pressure and temperature only

This method is a flash calculation. The saturated liquid and vapor molar volumes are obtained by solving the cubic equation while satisfying the phase equilibrium condition. The binary interaction coefficient, k_{ij}, is determined by minimizing the objective function, obj2, in Eq.(7.12). It should be noted that in this method the accuracy of the calculated v_m^{ℓ} and v_m^{v} values is affected by the accuracy of the calculated x_i and y_i.

(2) Compressibility factors in the fluid phase

In a fluid mixture the compressibility factor, Z_m, corresponds to the positive root of a volume-cubic EOS. The remaining two roots are either negative or imaginary. The experimental P, T, x_i and y_i are used as input values for the EOS and the binary interaction coefficient, k_{ij}, is obtained by minimizing the objective function, obj4,

$$\text{obj4} = \{\sum_{1}^{ND} [|(Z_{m,calc} - Z_{m,expt})|/Z_{m,expt}]\}/ND \qquad (7.14)$$

7.4 Results and Discussion

7.4.1 Normal Fluid Mixtures

For normal fluid mixture calculations the new EOS with the VDW-B mixing model is tested using a total of 3340 VLE (T-P-x_i-y_i) data points of 37 binary systems at 166 isotherms and 1648 experimental values of saturated liquid and vapor molar volumes of 14 binary systems at 76 isotherms and 3727 experimental values of the fluid phase compressibil-

ity factors of 16 binary systems at 71 isotherms. The binary systems selected can be classified into three sets based on the mixture properties considered. Each set is further divided into several groups in accordance with the chemical nature of the systems. These systems are frequently encountered in the natural gas and petroleum industries.

1. Set 1: Vapor-liquid equilibrium values (P-T-composition)
   - 1-1: Carbon dioxide (CO2)-Hydrocarbon (HC)
   - 1-2: Hydrogen sulfide (H2S)-Hydrocarbon (HC)
   - 1-3: Nitrogen (N2)-Hydrocarbon (HC)
   - 1-4: Hydrocarbon (HC)-Hydrocarbon (HC)
2. Set 2: Saturated liquid and vapor molar volumes
   - 2-1: Hydrocarbon (HC)-Hydrocarbon (HC)
   - 2-2: Carbon dioxide (CO2)-Hydrocarbon (HC)
3. Set 3: Compressibility factors in the fluid phase
   - 3-1: Hydrocarbon (HC)-Hydrocarbon (HC)
   - 3-2: Carbon dioxide (CO2)-Hydrocarbon (HC)
   - 3-3: Nitrogen (N2)-Hydrocarbon (HC)

Comparison between the calculated and experimental values for each of the three sets are presented separately. These results are compared with those obtained from the SRK, the PR and the SW equations. The mixing models that are used in the SRK and the PR equations are those defined by Eqs(6.2,8.a). For the SW equation, the parameters a_m and b_m are also evaluated using Eqs(6.2,8.a), while Eq.(6.6) is used to calculate ω_m from which $c_m(=-3\ \omega_m)$ is obtained. Expressions for $\hat{\phi}_i$ corresponding to the SRK, the PR and the SW equations are given by the original authors [119,88,113].

7.4.1.1 Calculated Vapor-Liquid Equilibrium Compositions

Presented in Table 7.1 are the average absolute deviations in the vapor and liquid equilibrium compositions of the binary systems selected in Set 1, where the average absolute deviation (AAD) is defined as

$$AAD = \{\sum_{1}^{ND} [|(\text{calculated value} - \text{experimental value})|]\}/ND \qquad (7.15)$$

Also reported in Table 7.1 are the values of k_{ij} used in the mixing models of the SRK, the PR, the SW and the new equations.

Summarized in Table 7.2 are the overall average deviations in x_i and y_i for each group in Set 1. As can be seen there is no significant difference between the four equations in the representation of liquid equilibrium compositions for each of the four groups in Set 1. For the 1699 data points the overall average absolute deviations in x_i given by the four equations are between 8.0×10^{-3} and 9.0×10^{-3}. In general, the four EOS have larger errors in x_i for the systems containing H2S and N2 than for the CO2-HC and HC-HC systems.

In the calculation of y_i the performance of the four equations is also similar. For the 1641 data points the overall average absolute deviations in y_i given by the four equations are of the same order of magnitude as those in x_i. Relatively large errors in y_i are predicted by the four equations for systems containing nitrogen.

Examination of Table 7.1 reveals that none of the four equations is consistently better or worse than the others. In general, with the use

Table 7.1: Average absolute deviations in equilibrium compositions calculated by the SRK, the PR, the SW and the new EOS.

CO_2 - SYSTEM	NO	T/K	k_{ij} SRK	k_{ij} PR	k_{ij} SW	k_{ij} NEW	$\lvert\Delta x\rvert_{ave} \times 10^3$ SRK	$\lvert\Delta x\rvert_{ave} \times 10^3$ PR	$\lvert\Delta x\rvert_{ave} \times 10^3$ SW	$\lvert\Delta x\rvert_{ave} \times 10^3$ NEW	$\lvert\Delta y\rvert_{ave} \times 10^3$ SRK	$\lvert\Delta y\rvert_{ave} \times 10^3$ PR	$\lvert\Delta y\rvert_{ave} \times 10^3$ SW	$\lvert\Delta y\rvert_{ave} \times 10^3$ NEW	Ref.
CO_2 -C_1	5	219.26	0.1074	0.1050	0.0865	0.1040	21.5	15.00	34.2	9.88	-	-	-	-	
	12	241.48	0.1064	0.1011	0.0836	0.0989	11.1	11.2	10.9	11.3	-	-	-	-	25
	11	271.48	0.1267	0.1188	0.0991	0.1169	4.59	4.33	4.60	4.23	-	-	-	-	
CO_2 -n-C_2	13	250.00	0.1308	0.1014	0.1296	0.1304	6.82	59.0	7.50	7.67	6.53	43.0	10.1	12.8	22
	16	283.15	0.1803	0.1234	0.1760	0.1704	39.7	15.6	35.2	34.5	40.8	9.74	32.0	31.2	83
	11	293.15	0.1421	0.1320	0.1391	0.1327	14.9	14.5	13.2	12.3	9.18	8.74	7.51	7.10	83
CO_2 -n-C_3	11	277.59	0.1201	0.1160	0.1216	0.1184	5.64	5.64	6.41	7.24	7.29	6.64	5.32	4.29	
	16	294.26	0.1246	0.1177	0.1238	0.1182	2.95	3.29	2.58	2.75	8.63	8.50	6.54	6.06	
	17	310.93	0.1310	0.1202	0.1270	0.1186	6.67	7.01	5.64	5.95	15.0	14.8	11.5	11.1	110
	14	327.59	0.1339	0.1207	0.1296	0.1186	7.02	7.37	5.18	5.98	16.6	16.4	12.4	13.1	
	12	344.26	0.1413	0.1242	0.1370	0.1224	9.87	10.0	8.11	8.74	18.0	18.6	14.9	16.3	
CO_2 -n-C_4	11	255.98	0.1227	0.1191	0.1231	0.1212	14.5	13.6	13.5	13.3	4.00	7.57	6.75	5.45	60
	10	310.93	0.1324	0.1230	0.1261	0.1205	5.49	5.46	5.53	5.55	3.41	4.80	4.17	5.09	110
	10	344.26	0.1456	0.1315	0.1336	0.1255	1.33	2.19	1.71	2.13	6.16	9.47	5.93	7.65	110
	8	377.59	0.1662	0.1462	0.1510	0.1394	2.09	2.47	1.22	1.70	7.50	11.0	4.80	7.47	110
	6	410.93	0.2097	0.1743	0.1898	0.1602	3.21	3.90	3.48	5.02	9.50	8.47	8.04	6.70	110
CO_2 -n-C_5	10	277.65	0.1124	0.1082	0.1118	0.1111	17.7	14.5	12.8	12.1	3.72	3.82	3.91	4.00	
	14	311.04	0.1212	0.1130	0.1139	0.1120	7.93	7.69	7.77	7.84	3.86	5.00	4.64	5.05	13
	15	344.15	0.1379	0.1234	0.1236	0.1209	5.97	4.79	5.71	6.00	7.18	10.3	9.34	10.2	
CO_2 -iso-C_4	12	310.93	0.1270	0.1160	0.1222	0.1134	7.18	5.27	5.75	5.47	3.17	4.67	4.38	5.05	
	7	344.26	0.1473	0.1307	0.1358	0.1253	3.47	4.17	2.84	3.45	9.90	14.1	10.3	13.1	14
	6	377.59	0.1712	0.1338	0.1565	0.1490	9.51	9.60	8.86	9.50	22.8	6.00	21.5	25.5	
CO_2 -n-C_6	10	298.15	0.1100	0.1031	0.1037	0.1051	20.4	19.7	19.0	19.1	5.25	4.36	4.58	4.48	81
	10	313.15	0.0912	0.0842	0.0828	0.0845	16.1	15.8	15.8	16.2	5.24	5.12	5.09	5.17	
CO_2 -n-C_{10}	8	310.93	0.1165	0.1068	0.0955	0.1089	17.5	16.7	13.2	18.9	0.48	0.60	0.54	0.52	
	6	344.26	0.1137	0.1010	0.0846	0.1026	17.9	17.9	13.6	19.6	1.10	2.23	2.08	13.4	
	8	377.59	0.1176	0.1032	0.0827	0.1037	10.3	9.27	4.86	10.8	1.36	3.72	4.21	2.34	100
	8	410.93	0.1212	0.1058	0.0816	0.1050	8.91	6.67	2.83	8.23	3.20	6.62	8.22	4.68	
	8	444.26	0.1272	0.1109	0.0820	0.1086	7.52	3.94	2.39	5.60	3.45	7.70	10.5	5.23	
	7	477.59	0.1310	0.1182	0.0882	0.1123	12.5	6.36	2.03	8.56	9.59	10.6	12.2	9.06	
	4	510.93	0.1633	0.1468	0.1078	0.1390	10.6	5.18	3.32	7.28	16.1	4.18	5.44	6.05	

Table(7.1) cont'd.

			k_{ij}				$\lvert\Delta x\rvert_{ave} \times 10^3$				$\lvert\Delta y\rvert_{ave} \times 10^3$				
	ND	T/K	SRK	PR	SW	NEW	SRK	PR	SW	NEW	SRK	PR	SW	NEW	Ref.
H_2S-SYSTEM															
H_2S-C_1	22	277.59	0.0619	0.0626	0.0535	0.0582	11.3	12.7	9.88	14.1	3.76	5.11	9.95	6.35	110
	21	310.93	0.0600	0.0584	0.0531	0.0469	13.9	13.9	12.5	17.6	6.22	5.23	7.46	7.22	
	12	344.26	0.0880	0.0784	0.0555	0.0745	5.45	6.01	11.8	5.68	23.2	22.1	13.5	18.3	
H_2S-n-C_5	7	277.59	0.0595	0.0532	0.0616	0.0585	12.5	11.7	8.24	7.92	4.90	3.87	3.80	3.97	110
	7	344.26	0.0683	0.0612	0.0691	0.0660	3.26	2.67	4.08	3.88	23.4	23.5	23.2	2.39	
	11	410.93	0.0991	0.0799	0.0897	0.0833	13.2	14.9	12.5	13.5	24.8	26.3	22.4	23.5	
H_2S-n-C_{10}	7	277.59	0.0393	0.0290	0.0335	0.0362	31.5	31.6	24.6	30.3	0.90	0.88	0.91	0.91	110
	7	344.26	0.0345	0.0240	0.0214	0.0340	1.65	2.40	7.81	3.90	0.48	0.38	0.43	0.43	
H_2-SYSTEM	8	410.93	0.0611	0.0461	0.0344	0.0542	13.8	15.0	19.0	13.8	3.06	5.34	5.19	4.33	
H_2-C_1	8	113.71	0.0341	0.0378	0.0424	0.0425	3.12	4.90	9.01	10.4	6.80	2.75	4.44	3.20	122
	15	127.59	0.0300	0.0323	0.0326	0.0339	4.95	4.54	4.96	4.69	4.39	4.92	4.30	3.52	
	8	149.82	0.0350	0.0334	0.0429	0.0295	5.20	3.31	4.84	1.16	4.72	4.46	3.09	2.48	
	8	172.04	0.0413	0.0374	0.0610	0.0350	2.29	2.08	1.22	0.92	7.00	5.22	2.52	2.30	
H_2-n-C_2	14	122.03	0.0439	0.0547	0.0411	0.0539	21.0	21.8	22.3	20.2	1.40	1.27	1.42	1.37	19
	11	149.82	0.0289	0.0395	0.0263	0.0384	12.2	11.7	12.0	14.2	8.15	6.89	7.16	8.06	123
	13	194.26	-0.0082	0.0017	-0.0063	-0.0040	32.2	33.6	31.3	34.9	27.9	22.9	23.7	25.9	123
H_2-n-C_3	6	173.15	0.0797	0.0897	0.0674	0.0874	3.33	4.14	3.27	4.21	3.02	2.40	2.48	2.85	111
	6	223.15	0.0722	0.0814	0.0633	0.0778	9.50	10.0	9.35	10.2	3.98	1.82	2.03	2.03	
	6	273.15	0.0585	0.0674	0.0533	0.0593	4.21	3.77	3.68	3.90	11.9	6.39	9.45	6.96	
H_2-n-C_4	5	310.93	0.0808	0.0915	0.0676	0.0856	17.1	16.1	16.0	16.0	25.4	18.6	19.7	17.8	107
	7	344.26	-0.0143	0.0107	-0.0189	0.0036	36.6	33.6	33.7	33.4	49.4	37.5	41.8	37.3	
	8	377.59	-0.0399	0.0054	-0.0349	-0.0050	40.4	33.7	37.5	33.4	55.8	42.0	47.4	41.4	
C_1-SYSTEM															
C_1-n-C_2	21	131.01	-0.0004	0.0002	-0.0042	0.0024	13.7	16.0	13.5	13.9	4.27	4.93	4.38	4.29	126
	11	158.15	-0.0051	0.0	-0.0038	0.0056	10.3	8.57	5.34	5.29	1.28	1.79	1.42	1.09	
	12	186.11	-0.0025	0.0035	-0.0064	0.0098	2.75	2.58	2.94	3.24	1.09	2.53	2.22	0.97	
	14	189.65	-0.0040	0.0019	-0.0095	0.0079	2.90	2.80	2.93	2.94	1.55	3.14	2.78	1.35	
	11	192.39	-0.0078	-0.0017	-0.0139	0.0044	2.27	2.48	2.46	2.70	2.82	4.20	3.95	2.10	
	12	199.92	-0.0042	0.0013	-0.0102	0.0060	4.73	4.35	5.01	3.81	3.64	3.56	3.82	1.92	

Table(7.1) cont'd.

$n\text{-}C_1$ - SYSTEM	ND	T/K	k_{ij} SRK	PR	SW	NEW	$\lvert\Delta x\rvert_{ave} \times 10^3$ SRK	PR	SW	NEW	$\lvert\Delta y\rvert_{ave} \times 10^3$ SRK	PR	SW	NEW	Ref.
C_1 -n-C_3	4	130.37	0.0093	0.0107	0.0004	0.0118	10.9	13.9	10.7	11.2	0	0.0	0	0	126
	9	158.15	0.0155	0.0222	0.0133	0.0276	16.2	12.4	6.04	6.01	0	0.16	0	0	126
	9	172.04	0.0055	0.0135	0.0026	0.0204	14.8	11.2	6.63	5.70	0.47	0.21	0.35	0.41	126
	10	187.43	0.0067	0.0148	-0.0021	0.0205	6.77	6.07	6.43	6.05	1.04	0.58	0.73	0.83	126
	12	192.26	0.0048	0.0130	-0.0055	0.0184	5.70	4.61	5.00	4.24	1.55	0.74	0.89	1.12	126
	12	213.71	0.0003	0.0076	-0.0095	0.0107	9.45	9.68	7.03	11.8	2.98	3.34	3.13	2.58	126
	27	277.59	0.0095	0.0115	0.0060	0.0110	2.48	3.13	4.54	4.73	11.6	13.9	13.4	12.8	109
	25	294.26	0.0062	0.0129	0.0235	0.0065	4.02	2.96	1.82	5.30	20.6	26.7	22.4	24.2	109
	24	310.93	0.0170	0.0184	0.0094	0.0166	2.45	1.85	1.95	1.55	23.9	29.3	22.6	25.5	109
	19	327.59	0.0314	0.0390	0.0250	0.0330	2.54	3.39	1.88	1.66	21.3	27.1	18.3	22.8	109
	13	344.26	0.0282	0.0206	0.0245	0.0300	4.31	5.10	3.36	3.01	16.4	20.3	13.5	18.1	109
	6	360.93	-0.1153	-0.1507	-0.1148	-0.1356	9.99	12.5	9.60	12.1	21.1	20.5	20.0	19.9	109
C_1 -n-C_4	21	310.93	0.0096	0.0144	-0.0006	0.0147	10.1	9.42	6.82	10.6	9.12	8.74	7.53	7.57	109
	18	327.59	0.0235	0.0281	0.0130	0.0278	5.55	4.08	3.72	4.94	11.8	10.1	8.49	8.89	
	16	344.26	0.0370	0.0469	0.0280	0.0410	4.96	1.89	4.48	3.61	15.6	9.30	7.37	7.81	
	13	360.93	0.0600	0.0565	0.0530	0.0681	3.51	3.95	3.44	3.26	16.0	14.9	9.64	10.1	
	12	377.59	0.0965	0.1013	0.0886	0.1041	4.08	4.32	4.53	5.29	20.7	16.3	15.9	13.0	
	8	394.26	0.1414	0.1450	0.1306	0.1470	3.29	5.54	4.23	5.60	23.1	29.3	20.2	22.7	
C_1 -n-C_5	6	177.59	0.0116	0.0210	-0.0057	0.0270	38.5	32.1	27.7	24.2	0	0	0	0	59
	6	283.15	0.0078	0.0127	-0.0133	0.0169	0.93	10.1	4.67	11.9	3.07	1.62	2.18	2.03	59
	17	310.93	0.0127	0.0172	-0.0097	0.0222	4.85	4.84	3.01	5.55	9.69	6.28	5.78	6.78	109
	15	344.26	0.0087	0.0141	-0.0113	0.0187	8.75	7.76	5.31	8.46	11.3	6.41	6.28	5.58	109
	12	377.59	0.0227	0.0304	0.0047	0.0342	6.78	4.37	3.31	4.97	13.5	6.69	6.32	5.52	109
	8	410.93	0.0459	0.0530	0.0238	0.0557	6.11	3.74	4.01	4.06	15.1	9.90	8.22	7.26	109
C_1 -n-C_6	7	183.15	0.0367	0.0430	0.0090	0.0457	13.3	12.9	11.9	11.9	-	-	-	-	117
	10	273.15	0.0325	0.0375	-0.0023	0.0441	2.52	3.27	1.32	3.92	-	-	-	-	
	13	323.15	0.0355	0.0379	0.0011	0.0454	1.03	0.98	3.60	1.21	-	-	-	-	
C_1 -n-C_7	10	210.93	0.0231	0.0286	-0.0151	0.0313	38.2	39.7	34.6	40.0	5.61	6.12	6.79	5.40	126
	12	233.15	0.0167	0.0221	-0.0215	0.0261	32.2	33.7	26.9	34.4	4.69	5.25	6.41	4.51	126
	14	255.37	0.0193	0.0241	-0.0189	0.0291	15.9	17.0	10.0	18.0	2.59	2.77	2.72	2.67	126
	13	277.59	0.0289	0.0327	-0.0113	0.0389	6.61	7.44	3.14	8.48	4.03	2.86	1.73	3.33	107
	14	310.93	0.0173	0.0219	-0.0192	0.0298	8.76	8.40	2.98	9.74	7.07	4.48	2.07	5.05	107
	14	344.26	0.0142	0.0194	-0.0204	0.0288	10.6	9.07	3.57	10.4	7.56	4.00	2.89	4.45	107
	13	377.59	0.0243	0.0287	-0.0145	0.0391	6.35	4.46	2.94	5.47	6.76	4.02	3.53	4.23	107
	12	410.93	0.0416	0.0459	-0.0032	0.0565	7.66	4.99	4.29	5.59	11.5	6.02	5.62	6.28	107
	10	444.26	0.0677	0.0715	0.0273	0.0815	6.67	4.35	5.05	4.44	16.9	8.39	7.31	9.29	107
	8	477.59	0.0560	0.0738	0.0282	0.0819	9.56	4.33	2.57	5.17	20.7	13.8	12.4	12.4	107
	4	510.93	0.1057	0.1296	0.0779	0.1303	1.04	6.67	6.69	4.92	31.1	37.3	36.3	33.3	107

Table(7.1) cont'd.

			k_{ij}				$\lvert\Delta x\rvert_{ave} \times 10^3$				$\lvert\Delta y\rvert_{ave} \times 10^3$				
	ND	T/K	SRK	PR	SW	NEW	SRK	PR	SW	NEW	SRK	PR	SW	NEW	Ref.
C_1 -n-C_8	7	298.15	0.0431	0.0471	-0.0149	0.0562	1.22	1.32	1.30	1.43	0.53	0.77	0.75	0.68	64
	6	348.15	0.0467	0.0474	-0.0187	0.0606	1.91	1.97	1.31	2.16	2.14	2.78	3.00	2.73	
	6	423.15	0.0781	0.0680	-0.0016	0.0848	1.33	1.28	1.13	1.40	5.49	8.80	10.3	8.33	
C_1 -n-C_{10}	18	310.93	0.0400	0.0432	-0.0225	0.0482	11.3	10.1	8.21	11.2	5.02	3.53	1.97	4.16	109
	17	344.26	0.0356	0.0394	-0.0267	0.0470	9.31	7.68	7.71	8.82	4.03	2.70	3.42	3.13	
	16	377.59	0.0329	0.0375	-0.0285	0.0479	10.6	8.19	7.95	9.62	4.88	2.93	4.58	3.38	
	15	410.93	0.0303	0.0365	-0.0284	0.0492	12.9	9.16	7.89	11.1	7.90	5.16	5.79	5.63	
	13	444.26	0.0327	0.0444	-0.0325	0.0588	10.7	5.77	5.01	7.90	9.72	4.89	5.79	5.44	
n-C_2 - SYSTEM	11	477.59	0.0382	0.0490	-0.0380	0.0644	16.6	10.8	6.45	12.7	14.2	5.63	5.12	6.55	
	8	510.93	0.0647	0.0746	0.0014	0.0903	14.9	10.4	9.40	11.3	19.3	7.13	5.68	9.22	
n-C_2 -n-C_3	7	172.04	-0.0092	-0.0223	-0.0149	-0.0080	11.8	22.8	20.4	16.6	17.2	6.39	19.4	24.6	24
	7	199.82	-0.0139	-0.0200	-0.0114	-0.0184	13.8	15.7	15.2	11.4	7.27	6.66	5.62	5.67	24
	6	227.59	-0.0504	-0.0498	-0.0496	-0.0413	12.5	14.0	13.2	11.6	29.2	33.4	33.0	30.3	24
	9	255.37	-0.0283	-0.0239	-0.0232	-0.0165	15.2	13.2	11.6	10.4	14.2	13.4	13.4	12.4	24
	12	310.93	-0.0115	-0.0075	-0.0081	-0.0032	7.26	5.92	4.92	3.84	10.9	8.15	6.71	5.17	73
	10	333.15	0.0001	0.0004	0.0027	0.0021	9.77	8.56	7.04	7.38	9.72	8.92	7.09	6.85	73
	9	355.37	-0.0094	-0.0099	-0.0053	-0.0080	7.98	7.76	6.67	7.28	8.93	8.21	6.92	6.98	73
n_2 -C_2 - propene	5	260.93	0.0007	0.0052	0.0071	0.0132	17.1	12.6	9.36	10.5	9.78	7.90	6.88	7.21	110
	7	277.59	0.0020	0.0060	0.0072	0.0137	3.67	2.06	1.99	3.52	5.94	4.23	4.99	5.94	
	10	310.93	0.0067	0.0097	0.0096	0.0135	6.24	4.80	4.04	4.23	8.30	6.31	4.59	4.76	
	5	344.26	0.0079	0.0088	0.0126	0.0115	6.12	5.29	3.96	3.94	15.0	12.9	11.2	10.2	
n-C_2 -n-C_4	6	338.71	0.0310	0.0275	0.0247	0.0253	17.2	16.2	16.9	14.7	10.1	12.3	10.6	10.7	76
	8	366.48	0.0396	0.0337	0.0336	0.0323	11.6	11.7	11.2	10.3	12.2	14.4	11.5	12.5	
	5	394.26	0.0441	0.0350	0.0399	0.0357	12.7	13.5	11.4	12.0	17.8	19.3	16.0	17.2	
n-C_2 -n-C_5	5	277.59	0.0053	0.0094	0.0035	0.0158	1.38	4.12	6.15	7.73	3.78	3.47	3.45	3.38	98
	7	344.26	0.0118	0.0120	0.0006	0.0133	13.5	12.4	13.3	10.9	6.87	6.14	6.24	5.62	
	7	377.59	0.0165	0.0138	0.0045	0.0129	6.08	5.00	5.92	3.75	7.55	8.04	7.17	8.32	
	6	444.26	0.0777	0.0642	0.0641	0.0670	9.61	9.35	8.66	8.36	23.6	25.0	21.7	2.22	
n-C_2 -i-C_4	12	311.26	-0.0249	-0.0208	-0.0258	-0.0169	2.06	2.33	2.02	2.47	5.06	5.45	4.71	4.97	15
	10	344.48	-0.0147	-0.0142	-0.0149	-0.0126	9.62	10.4	8.81	9.49	18.1	17.4	15.0	14.6	
	9	377.43	0.0031	-0.0013	0.0040	0.0008	10.6	11.3	10.2	10.7	14.3	15.0	13.8	14.4	

Table(7.1) cont'd.

	NO	T/K	k_{ij} SRK	PR	SW	MEW	$\lvert\Delta x\rvert_{ave} \times 10^3$ SRK	PR	SW	MEW	$\lvert\Delta y\rvert_{ave} \times 10^3$ SRK	PR	SW	MEW	Ref.
$n\text{-}C_2$ -$n\text{-}C_{10}$	5	277.59	0.0215	0.0237	-0.0017	0.0291	4.76	4.07	4.72	5.13	0.17	0.20	0.21	0.21	
	5	310.93	0.0155	0.0170	-0.0154	0.0216	4.85	4.79	4.40	4.32	0.56	0.46	0.52	0.53	
	9	344.26	0.0109	0.0110	-0.0229	0.0141	3.23	3.32	1.81	5.56	2.16	2.61	2.67	2.27	
	13	377.59	0.0120	0.0094	-0.0248	0.0119	2.58	1.46	6.57	1.55	5.49	6.27	7.08	5.94	99
	14	410.93	0.0196	0.0172	-0.0150	0.0186	5.96	6.78	14.0	4.19	5.53	8.78	11.2	7.01	
	15	444.26	0.0226	0.0210	-0.0130	0.0211	6.05	6.86	13.2	5.25	12.5	15.7	20.1	1.48	
	14	477.59	0.0355	0.0332	0.0024	0.0329	3.36	6.37	14.0	3.95	10.4	15.8	20.7	13.4	
$n\text{-}C_3$ - SYSTEM	9	510.93	0.0566	0.0524	0.0175	0.0514	1.90	5.19	10.7	3.24	6.40	8.26	14.5	4.91	
$n\text{-}C_3$ -$n\text{-}C_4$	5	344.26	-0.0048	0.0017	0.0037	0.0085	13.9	14.4	14.5	14.7	18.2	17.5	16.7	16.2	
	8	377.59	0.0003	0.0032	0.0038	0.0063	23.0	19.8	19.6	19.9	24.4	20.8	20.4	21.3	80
	4	410.93	0.0052	0.0049	0.0078	0.0065	12.1	12.4	11.9	12.2	11.3	11.1	10.4	10.4	
$n\text{-}C_3$ -$n\text{-}C_5$	9	344.26	0.0142	0.0180	0.0160	0.0231	3.00	1.78	1.56	2.17	10.9	11.8	11.4	12.4	
	12	377.59	0.0206	0.0226	0.0186	0.0252	5.52	4.97	4.67	4.21	9.09	9.16	8.78	9.64	109
	10	410.93	0.0299	0.0273	0.0255	0.0284	7.29	7.23	5.94	5.85	10.6	10.8	9.67	9.70	
$n\text{-}C_3$ -iso-C_4	11	266.54	-0.0147	-0.0148	-0.0143	-0.0087	9.00	8.77	7.89	4.01	6.30	8.58	8.26	5.20	
	11	299.82	0.0022	0.0068	0.0093	0.0144	3.22	5.39	7.51	10.4	4.64	5.45	5.88	8.64	55
	15	338.71	-0.0140	-0.0073	-0.0040	0.0	9.77	8.81	8.65	9.47	6.99	6.67	7.47	9.57	
$n\text{-}C_3$ -$n\text{-}C_{10}$	4	344.26	-0.0037	-0.0006	-0.0180	0.0054	8.55	6.00	4.37	3.33	0.72	0.55	0.63	0.67	
	5	377.59	-0.0109	-0.0086	-0.0314	-0.0040	2.07	1.90	1.67	1.60	1.15	0.52	0.65	0.98	102
	6	410.93	-0.0074	-0.0066	-0.0320	-0.0038	2.68	2.55	3.75	2.44	2.30	0.97	0.96	1.78	
	6	444.26	0.0007	-0.0011	-0.0285	0.0010	3.98	3.73	5.27	2.53	2.22	0.80	1.39	1.76	
$n\text{-}C_3$ - benzene	7	310.93	0.0276	0.0325	0.0293	0.0362	17.1	14.7	13.5	12.2	5.47	3.58	4.55	4.96	
	10	377.59	0.0132	0.0183	0.0107	0.0197	6.32	5.96	6.09	6.41	8.50	7.93	7.87	9.69	37
	9	444.26	0.0256	0.0250	0.0189	0.0198	10.4	9.69	10.0	10.3	12.9	10.6	9.76	8.03	
	8	477.59	0.0288	0.0268	0.0225	0.0217	3.41	2.59	3.42	3.46	12.7	9.70	9.96	10.1	
propene-$n\text{-}C_3$	9	260.93	0.0063	0.0071	0.0083	0.0129	5.06	5.19	4.29	8.31	5.84	7.02	7.63	10.9	
	9	310.93	-0.0025	0.0040	0.0083	0.0099	19.2	10.9	12.4	12.0	18.9	11.0	12.5	8.51	110
	9	360.93	0.0019	0.0026	0.0044	0.0041	0.76	1.72	0.80	1.23	0.71	1.46	0.94	0.90	
propene-1 -butene	8	277.59	0.0010	0.0023	0.0031	0.0082	3.89	4.29	5.60	9.38	6.25	4.82	4.85	6.10	
	7	310.93	-0.0063	-0.0010	0.0009	0.0059	5.08	2.34	2.99	4.22	4.85	4.29	4.79	3.95	110
	7	344.26	-0.0103	-0.0042	-0.0022	0.0022	4.92	2.77	1.36	0.81	7.17	3.54	2.26	0.63	
	6	377.59	-0.0091	-0.0062	-0.0051	-0.0355	6.83	4.21	2.60	1.95	9.08	5.08	3.20	2.56	
	5	419.93	-0.0144	-0.0144	-0.0117	-0.0134	7.91	8.21	7.95	8.21	9.29	9.11	8.62	8.77	
$n\text{-}C_4$ -$n\text{-}C_{10}$	7	377.59	0.0002	0.0048	-0.0051	0.0112	10.2	5.83	3.90	2.44	0.58	0.20	0.27	0.46	
	7	410.93	-0.0003	0.0032	-0.0099	0.0088	1.68	1.97	2.43	3.09	0.61	0.70	0.70	0.46	102
	10	444.26	0.0031	0.0040	-0.0147	0.0071	3.12	3.00	2.55	2.35	3.66	5.13	5.49	3.90	
	11	477.59	0.0122	0.0098	-0.0138	0.0115	6.12	5.49	4.87	3.92	1.76	4.31	5.12	1.91	
	11	510.93	0.0253	0.0169	-0.0108	0.0203	10.0	9.56	9.70	7.77	11.7	13.2	14.4	11.1	

Table 7.2: Overall average absolute deviations in equilibrium compositions calculated by the SRK, the PR, the SW and the new EOS.

	No. of Isotherms	Data Points	Average Absolute Deviations of $\Delta x \cdot 10^3$ SRK	PR	SW	NEW
CO_2-HC	31	316	10.7	10.9	9.17	9.73
H_2S-HC	9	102	11.8	12.4	12.0	13.0
N_2-HC	13	115	15.4	15.1	15.3	15.3
HC-HC	113	1166	8.04	7.43	6.77	7.30
		Overall Average	9.26	8.90	8.11	8.64
			Average Absolute Deviations of $\Delta y \cdot 10^3$			
CO_2-HC	28	288	9.62	10.4	9.03	9.09
H_2S-HC	9	102	9.46	9.98	8.74	9.89
N_2-HC	13	115	14.9	11.5	12.2	11.4
HC-HC	110	1136	9.31	8.82	8.24	8.15
		Overall Average	9.78	9.36	8.69	8.66

of k_{ij} in their mixing models all four equations can satisfactorily represent VLE of the binary mixtures of normal fluids below the critical point. In the critical point region, all equations tend to predict too large a two-phase coexisting region. This becomes particularly obvious for systems in which the molecular size of the components is quite different. As examples, plotted in Figures 7.3, 7.4 and 7.5 are the vapor-liquid equilibria calculated by the new EOS for the N2-C1, CO2-C10 and C1-C10 mixtures at several selected isotherms. As can be seen for the N2-C1 system in which molecular size of the two components are similar, the new EOS with the VDW-B mixing model can calculate VLE values which are in good agreement with the experimental below and including the critical point region. However, it can only give good account of the VLE for the CO2-C10 and C1-C10 systems below the critical point. Similar behavior is also exhibited by the SRK, the PR and the SW equations.

With reference to Table 7.1, several additional points concerning the prediction of VLE values by the four equations are:

1. For most systems, the equations tend to have larger errors in the liquid composition at lower temperatures and in the vapor composition at higher temperatures.
2. The values of k_{ij} for the HC-HC systems are of the order of magnitude of 10^{-2}. For most of the systems containing CO2, N2 and H2S the values of k_{ij} are larger, especially for the CO2-containing systems, which are of the order of magnitude of 10^{-1}.

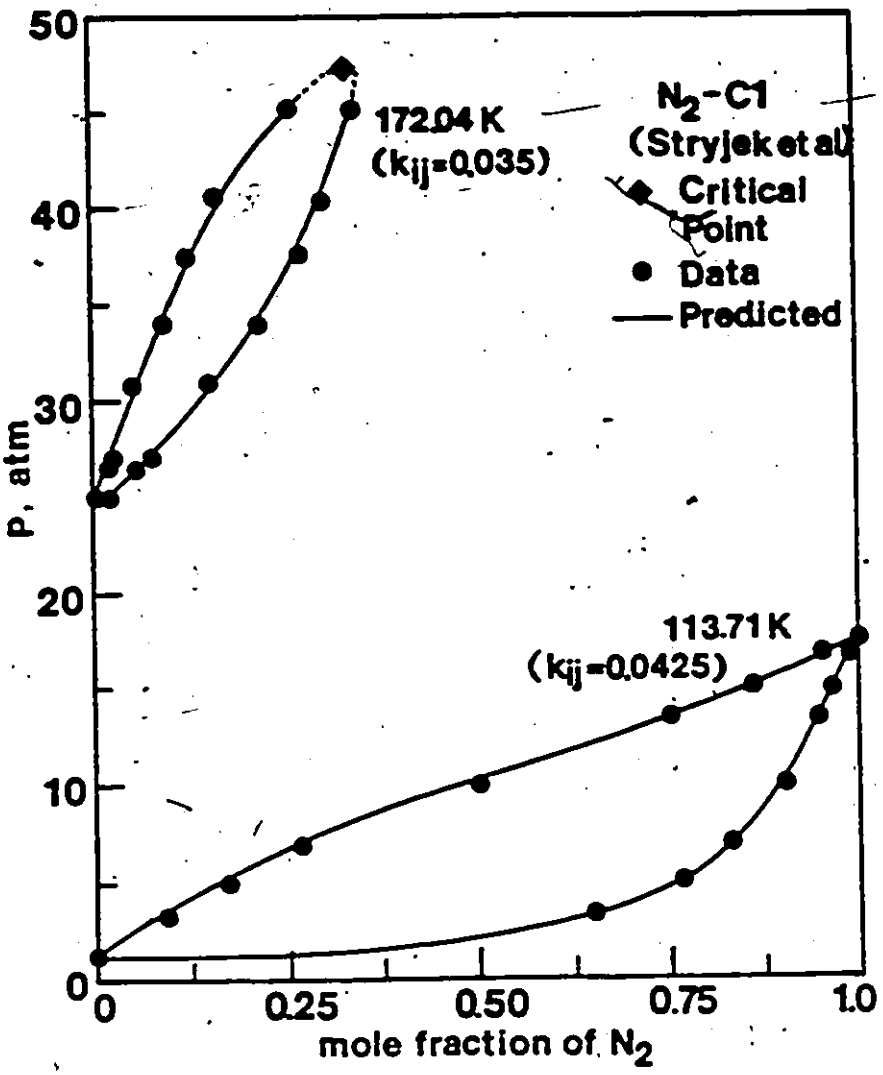

Figure 7.3: Comparison of experimental and calculated VLE values for the N2-C1 system at 113.71 and 172.04 K.

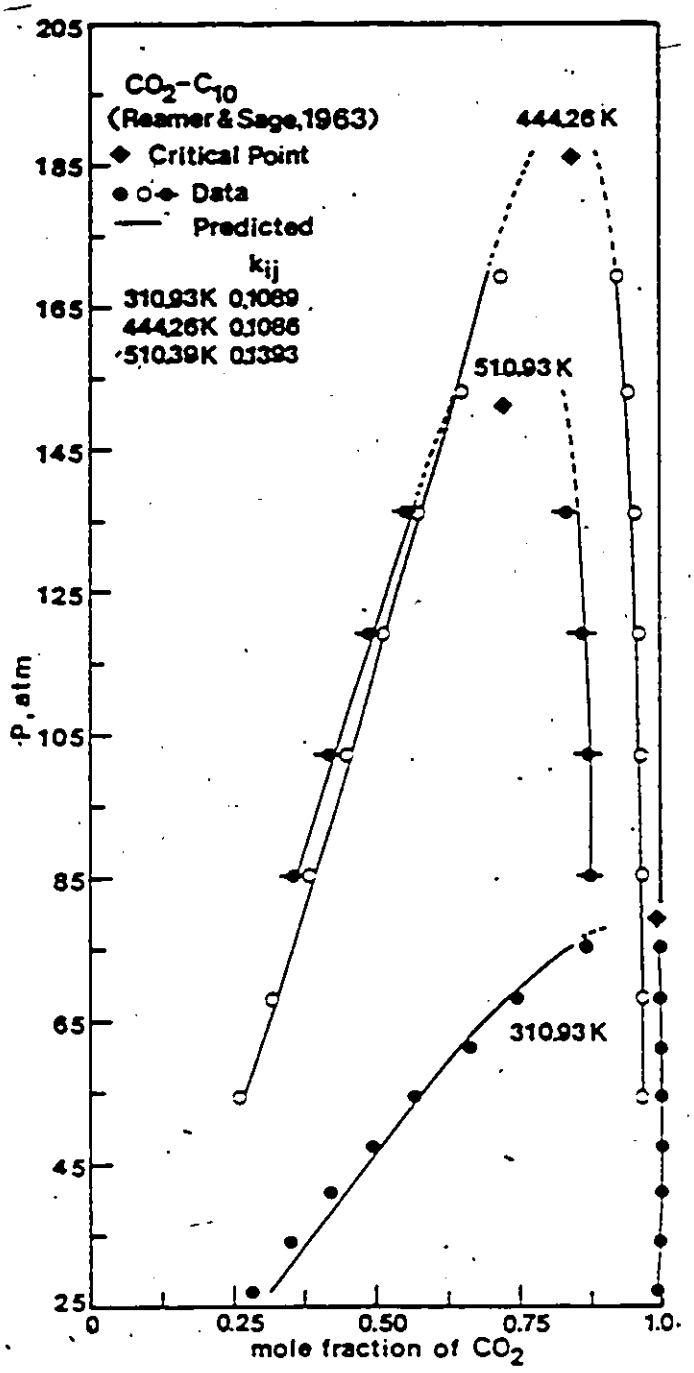

Figure 7.4: Comparison of experimental and calculated VLE values for the CO2-C10 system at 310.93, 444.26 and 510.93 K.

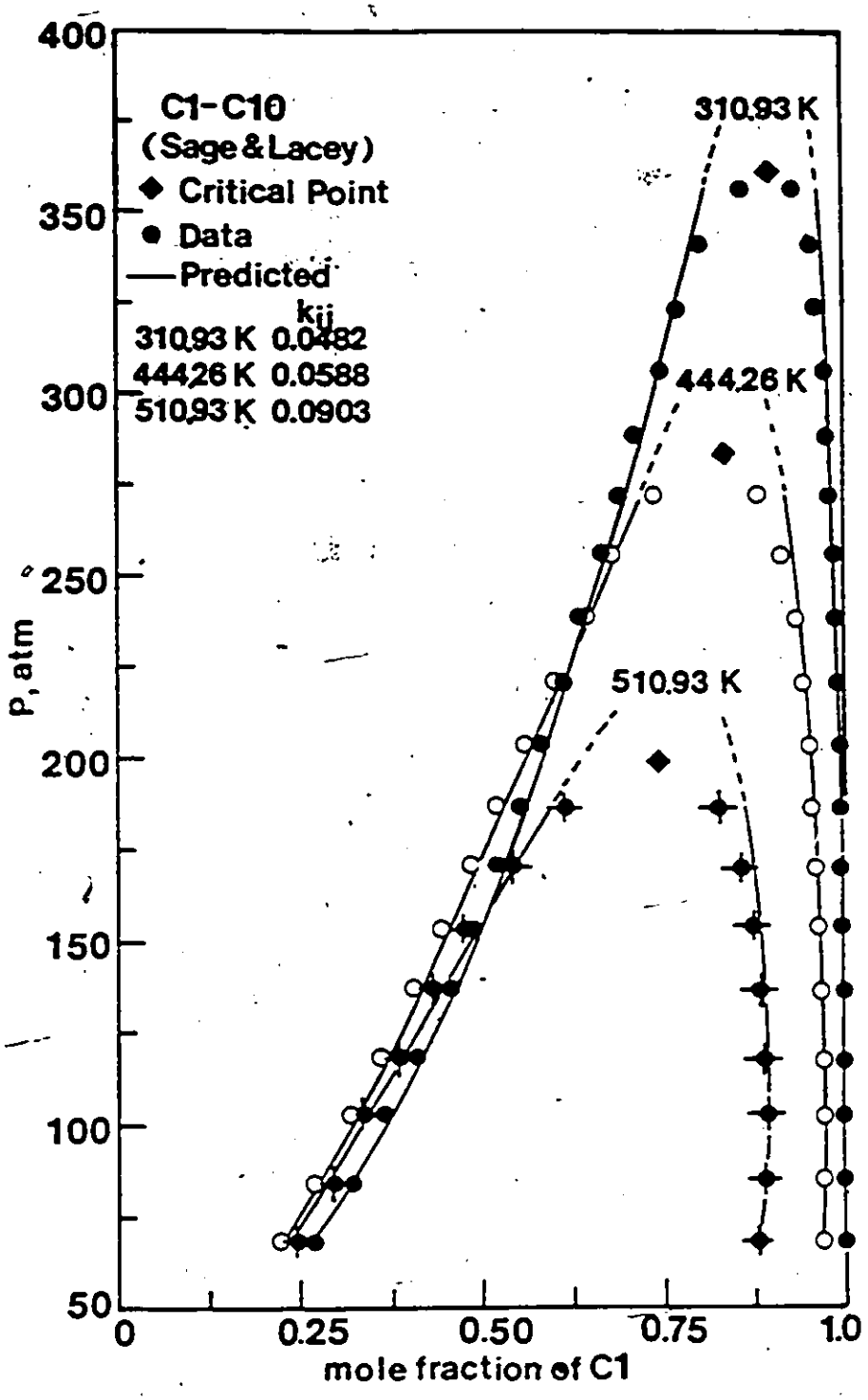

Figure 7.5: Comparison of experimental and calculated VLE values for the C1-C10 system at 310.93, 444.26 and 510.93 K.

3. The SW EOS can represent the VLE for the C1-C10 system slightly better than the other three equations while the new EOS is better for the C2-C10, C3-C10 and C4-C10 systems.

4. It is more difficult for an EOS to represent the VLE of binary systems containing CO2, H2S and N2 than for the HC-HC systems.

Based on the above observations although the four equations did not give comparable results for pure component calculations they do give similar results when calculating VLE of normal fluid mixtures. This may be partly due to the use of k_{ij} in the mixing model which compensates for the inadequacies in the EOS as well as in the mixing models. On the other hand, several authors [33,35,119] have pointed out that the most important factor which influences the prediction of VLE is the accuracy of predicting the pure component vapor pressures. Since all four equations have similar accuracy in predicting vapor pressures they should therefore have similar accuracy when predicting VLE.

7.4.1.2 Calculated Saturated Liquid and Vapor Mixture Molar Volumes

Presented in Tables 7.3 and 7.4 are the average absolute percent deviations in v_m^ℓ and v_m^v at each isotherm predicted by the four equations using Methods I and II, respectively. Also included are the values of k_{ij} that were used in the mixing models for the equations. It should be noted that the average absolute percent deviations in v_m^ℓ and v_m^v calculated from Method II are, in general, higher than those calculated based on Method I. This is because in Method I deviations in v_m^ℓ

Table 7.3: Average absolute percent deviations in the saturated liquid and vapor molar volumes calculated based on Method I.

SYSTEM	ND	T/K	k_{ij}				$\lvert\Delta v_m^{\ell}\%\rvert_{ave}$				$\lvert\Delta v_m^{v}\%\rvert_{ave}$				Ref.
			SRK	PR	SW	NEW	SRK	PR	SW	NEW	SRK	PR	SW	NEW	
C_1 -n-C_3	27	277.59	-0.0901	0.0514	-0.0710	-0.0045	4.95	6.55	3.59	3.76	1.40	2.29	1.52	2.36	
	25	294.26	-0.0714	0.0569	-0.0453	0.0030	4.44	3.80	2.38	1.94	2.77	2.14	2.55	2.58	
	24	310.93	-0.0682	0.0282	-0.0464	-0.0180	7.77	0.76	3.72	1.79	1.52	1.54	1.48	1.97	109
	19	327.59	-0.0752	0.0093	-0.0555	-0.0221	8.03	0.77	3.63	1.39	2.11	1.70	2.00	2.25	
	13	344.26	-0.1110	-0.0218	-0.0731	-0.0386	8.91	0.85	4.81	2.44	2.31	1.19	1.49	1.23	
	6	360.93	-0.2637	-0.1693	-0.2356	-0.1702	9.65	9.33	9.32	8.94	4.74	2.52	3.30	2.52	
C_1 -n-C_4	21	310.93	-0.0649	0.0814	-0.0412	0.0149	7.09	1.54	1.93	0.97	1.89	1.64	1.72	1.56	
	18	327.59	-0.1072	0.0609	-0.0706	0.0012	7.14	1.00	2.31	1.42	2.94	1.93	2.59	1.88	
	16	344.26	-0.1169	0.0375	-0.0738	-0.0157	7.73	0.64	2.88	1.73	3.43	2.49	2.97	2.37	
	13	360.93	-0.1618	0.0033	-0.0861	-0.0471	8.37	0.72	3.86	2.25	4.79	3.20	3.73	3.41	109
	12	377.59	-0.1427	-0.0204	-0.0964	-0.0438	9.31	1.58	4.48	3.13	4.93	3.84	4.31	3.67	
	8	394.26	-0.1485	-0.0207	-0.0786	-0.0343	9.25	2.76	5.03	3.71	5.75	4.76	5.09	4.47	
C_1 -n-C_5	17	310.93	-0.1104	0.1539	-0.0622	0.0258	8.20	1.96	0.39	0.53	1.42	1.70	1.35	1.69	
	15	344.26	-0.0638	0.1152	-0.0243	0.0451	8.95	1.46	1.18	0.89	0.58	0.92	0.59	0.95	109
	12	377.59	-0.0766	0.0899	-0.0273	0.0353	10.2	1.03	2.51	1.55	1.59	1.37	1.36	1.49	
	8	410.93	-0.1927	0.0383	-0.0730	0.0012	11.4	2.37	4.26	3.20	2.91	1.31	1.72	1.54	
C_1 -n-C_7	13	277.59	-0.6111	0.0961	-0.1751	-0.0718	8.66	1.02	0.83	0.56	2.26	2.01	1.49	1.89	
	14	310.93	-0.1816	0.1117	-0.0911	0.0824	10.4	0.83	0.78	1.30	1.31	2.62	1.13	1.18	
	14	344.26	-0.2196	0.1257	-0.0947	0.0219	9.65	0.87	0.59	0.53	1.19	1.36	0.80	1.04	96
	13	377.59	-0.2000	0.0540	-0.0778	0.0448	10.9	1.16	1.34	1.41	1.41	2.08	1.04	1.17	
	12	410.93	-0.3360	-0.0359	-0.2126	-0.0908	9.82	1.00	0.78	0.51	1.09	0.90	0.97	0.95	
	10	444.26	-0.2911	-0.0580	-0.1973	-0.0831	11.6	1.71	1.35	1.01	0.92	0.87	0.93	0.96	
	8	477.59	-0.1094	0.0840	-0.0132	0.0815	14.5	5.24	4.81	4.48	1.11	0.92	0.90	0.88	
	4	510.93	-0.2865	-0.0586	-0.1241	-0.0197	20.4	12.4	12.3	11.9	2.89	2.21	1.97	1.93	
C_1 -n-C_{10}	18	310.93	-0.9031	0.0902	-0.3098	-0.1497	11.8	5.23	1.69	1.22	3.38	1.61	1.85	1.04	
	17	344.26	-0.7604	0.0324	-0.2177	-0.1147	11.7	4.59	1.21	0.79	2.85	1.70	1.47	0.78	
	16	377.59	-0.6709	0.0079	-0.2414	-0.0729	11.6	4.23	1.04	0.73	2.32	1.67	1.00	0.46	
	15	410.93	-0.5731	-0.0084	-0.2246	-0.0353	11.5	4.07	0.94	0.83	2.13	1.68	0.89	0.38	109
	13	444.26	-0.4291	0.0155	-0.1894	-0.0353	14.0	6.03	2.46	2.29	1.15	1.16	0.53	0.72	
	11	477.59	-0.3426	0.0352	-0.1715	-0.0074	12.6	4.96	1.34	1.29	0.48	0.35	0.35	0.32	
	8	510.93	-0.2988	0.0069	-0.1486	0.0066	13.9	5.83	2.47	2.42	0.21	0.35	0.32	0.32	

Table(7.3) cont'd.

SYSTEM	NO	T/K	k_{ij}				$\lvert\Delta v_m^E x\rvert_{ave}$				$\lvert\Delta v_m^V x\rvert_{ave}$				Ref.
			SRK	PR	SW	MEW	SRK	PR	SW	MEW	SRK	PR	SW	MEW	
n-C_2 -n-C_5	5	277.59	-0.5180	0.1144	-0.0708	0.0118	5.67	2.79	4.07	2.86	0.72	0.61	0.55	0.72	98
	7	344.26	-0.1404	0.0002	-0.0585	0.0228	7.95	0.72	2.21	1.48	3.07	0.85	2.08	1.02	
	7	377.59	-0.1398	-0.0387	-0.0896	-0.0550	10.1	1.29	3.08	2.17	2.44	0.38	0.99	0.44	
	6	444.26	-0.1353	-0.0334	-0.1134	-0.0503	12.3	4.40	5.67	4.65	6.00	4.15	4.27	4.02	
n-C_2 -nC_{10}	5	310.93	-1.786	-0.1067	-0.1980	-0.1409	7.99	2.56	0.46	0.51	3.14	3.14	4.71	3.31	99
	9	344.26	-0.8383	-0.1499	-0.2175	-0.1579	8.20	2.63	0.41	0.33	0.95	1.89	1.17	1.56	
	13	377.59	-0.4731	-0.1524	-0.2358	-0.1493	9.88	3.19	1.01	0.89	1.42	1.47	0.85	1.19	
	14	410.93	-0.4461	-0.1430	-0.2126	-0.1232	10.6	3.19	0.69	0.95	2.64	2.43	0.69	1.18	
	15	444.26	-0.3014	-0.0726	-0.1970	-0.1099	12.3	4.61	1.09	1.32	1.60	1.48	1.22	1.43	
	16	477.59	-0.2276	-0.0606	-0.1353	-0.0704	12.6	4.21	1.21	1.34	1.16	1.15	0.72	1.00	
	9	510.93	-0.1868	-0.0219	-0.0917	-0.0210	11.8	4.99	2.58	2.80	1.27	0.32	0.32	0.29	
n-C_2 - propene	5	260.93	-0.3093	0.0955	-0.1182	-0.0377	5.28	1.49	3.75	2.42	1.83	2.82	2.40	1.98	110
	7	277.59	-0.2406	0.0384	-0.0880	-0.0269	5.01	3.14	3.27	2.39	1.52	1.48	0.73	1.14	
	10	310.93	-0.0062	0.0013	-0.0055	-0.0016	14.0	3.69	8.93	5.31	2.08	1.49	0.86	1.55	
	5	344.26	-0.0102	0.0025	-0.0036	0.0014	15.9	8.09	11.9	9.49	7.49	5.67	6.53	5.37	
propene-1-butene	8	277.59	-0.4399	0.1795	-0.0459	0.0154	2.42	2.01	0.32	0.19	0.89	1.05	0.66	0.56	110
	7	310.93	-0.3055	0.0897	-0.0696	-0.0112	3.20	1.41	0.92	0.48	1.36	1.32	0.63	0.47	
	7	344.26	-0.2489	-0.0152	-0.0960	-0.0497	5.34	2.07	2.58	1.50	3.57	0.48	0.84	0.43	
	6	377.59	-0.0172	-0.0136	-0.0166	-0.0146	15.6	3.55	8.41	5.64	3.40	2.95	2.99	2.70	
	5	410.93	-0.0271	-0.008	-0.0205	-0.0116	19.5	12.8	14.5	13.3	5.68	1.32	3.64	1.50	
n-C_3 -n-C_{10}	4	344.26	-2.145	-0.0089	-0.0784	-0.0355	8.34	2.56	2.56	1.57	1.90	0.76	1.35	0.72	102
	5	377.59	-0.2495	0.0433	-0.0303	0.0247	11.6	4.08	1.30	1.46	1.94	3.22	2.12	3.15	
	6	410.93	-0.1780	-0.0189	-0.0752	-0.0299	12.5	3.83	0.94	0.97	2.28	2.33	1.48	2.10	
	6	444.26	-0.3670	-0.0813	-0.1116	-0.0712	17.0	8.64	5.47	5.52	4.08	2.38	1.46	1.98	
n-C_4 -n-C_{10}	7	377.59	-0.8655	-0.0476	-0.0943	-0.0627	5.20	1.68	1.55	1.03	2.77	1.95	2.25	1.90	102
	7	410.93	-0.8124	-0.1026	-0.1366	-0.0924	7.49	2.76	2.97	2.18	2.65	2.78	3.28	2.78	
	11	444.26	-0.1754	-0.0891	-0.1184	-0.0886	11.6	2.43	0.65	0.85	3.77	5.62	2.84	0.56	
	10	477.59	-0.3410	-0.0834	-0.1206	-0.0873	7.49	3.01	0.79	0.93	7.53	2.73	6.29	2.78	
	11	510.93	-0.0502	0.0045	-0.0257	0.0085	16.5	7.67	5.01	5.56	5.43	5.12	5.11	5.45	

Table(7.3) cont'd.

SYSTEM	NO	T/K	k_{ij} SRK	k_{ij} PR	k_{ij} SW	k_{ij} NEW	$\lvert\Delta v_m^{\ell}\%\rvert_{ave}$ SRK	$\lvert\Delta v_m^{\ell}\%\rvert_{ave}$ PR	$\lvert\Delta v_m^{\ell}\%\rvert_{ave}$ SW	$\lvert\Delta v_m^{\ell}\%\rvert_{ave}$ NEW	$\lvert\Delta v_m^{v}\%\rvert_{ave}$ SRK	$\lvert\Delta v_m^{v}\%\rvert_{ave}$ PR	$\lvert\Delta v_m^{v}\%\rvert_{ave}$ SW	$\lvert\Delta v_m^{v}\%\rvert_{ave}$ NEW	Ref.
CO_2 -n-C_3	11	277.59	-0.0692	0.1590	0.0782	0.1155	4.09	4.39	2.01	2.40	3.21	1.75	2.03	2.08	
	16	294.26	0.0015	0.1093	0.0712	0.0931	6.58	5.52	3.08	3.74	5.32	3.56	4.19	4.12	
	17	310.93	0.1071	0.1172	0.1156	0.1096	11.7	5.53	7.02	4.80	2.39	1.70	1.64	2.08	110
	14	327.59	0.1005	0.1216	0.1137	0.1146	11.7	3.46	7.04	5.27	2.98	1.40	1.80	1.42	
	12	344.26	0.0877	0.1013	0.0873	0.0919	11.9	2.64	6.12	4.41	6.67	4.40	6.07	4.38	
CO_2 -n-C_4	10	310.93	0.0327	0.0993	0.0337	0.0714	7.96	3.72	0.48	1.53	2.99	2.80	4.52	3.56	
	10	344.26	0.1073	0.1271	0.1105	0.1098	11.7	2.67	4.82	3.28	0.30	1.48	1.26	1.81	110
	8	377.59	0.1026	0.1286	0.1154	0.1151	13.9	3.72	7.18	5.42	0.41	1.36	0.84	1.47	
	6	410.93	0.0779	0.1281	0.1132	0.1145	15.3	7.57	10.3	8.67	2.08	0.53	0.60	0.59	
CO_2 -n-C_{10}	8	310.92	-0.0420	-0.6113	-0.0912	-0.1760	9.54	5.44	2.45	1.90	8.80	12.0.	13.9	12.9	
	6	344.26	-0.3412	0.0249	-0.0127	0.0332	13.8	5.95	2.65	2.21	4.15	1.18	1.55	1.21	
	8	377.59	-0.4769	-0.3139	-0.1256	-0.0854	12.6	4.04	1.40	1.03	1.72	3.82	2.17	3.31	100
	8	410.93	-0.3230	-0.1021	-0.1026	-0.0393	13.5	4.29	1.38	1.31	2.16	3.08	1.17	1.51	
	8	444.26	-0.2876	-0.1151	-0.1081	-0.0422	13.9	4.19	1.41	1.42	1.30	2.40	0.55	0.73	
	7	477.59	-0.2650	-0.0635	-0.1004	-0.0311	12.2	4.40	1.51	1.61	1.99	1.56	0.87	0.81	
	4	510.93	-0.1127	0.0557	-0.0091	0.0554	15.0	7.50	3.90	3.96	0.27	0.18	0.20	0.20	

Table 7.4: Average absolute percent deviations in the saturated liquid and vapor molar volumes calculated based on Method II.

SYSTEM	NO	T/K	k_{ij}				$\lvert\Delta v_m^l x\rvert_{ave}$				$\lvert\Delta v_m^v x\rvert_{ave}$			
			SRK	PR	SW	NEW	SRK	PR	SW	NEW	SRK	PR	SW	NEW
C_1 -n-C_3	27	277.59	0.0095	0.0115	0.0060	0.0110	7.84	7.79	5.61	3.80	2.51	3.48	2.04	2.50
	25	294.26	0.0062	0.0129	0.0024	0.0065	6.84	5.10	3.68	2.23	1.78	4.80	2.49	4.01
	24	310.93	0.0170	0.0184	0.0094	0.0166	10.8	0.85	5.78	2.90	1.44	4.87	2.01	4.02
	19	327.59	0.0314	0.0390	0.0250	0.0330	11.9	1.44	6.57	3.53	1.70	4.08	1.98	3.36
	13	344.26	0.0282	0.0207	0.0245	0.0300	14.5	3.39	8.82	5.81	4.71	2.93	3.16	1.40
	6	360.93	-0.1153	-0.1507	-0.1148	-0.1356	9.40	0.76	4.44	2.17	1.96	6.66	0.68	4.97
C_1 -n-C_4	21	310.93	0.0096	0.0144	-0.0006	0.0147	8.48	3.35	2.87	1.80	3.85	2.80	2.12	2.28
	18	327.59	0.0235	0.0281	0.0130	0.0278	9.89	1.69	3.97	2.06	5.33	2.08	3.37	1.92
	16	344.26	0.0370	0.0469	0.0280	0.0410	11.7	0.81	5.57	3.47	7.32	1.91	4.55	2.58
	13	360.93	0.0600	0.0565	0.0530	0.0680	14.0	2.46	7.38	5.20	7.99	2.46	5.60	3.65
	12	377.59	0.0965	0.1013	0.0886	0.1041	16.5	5.12	9.97	7.68	10.8	4.38	8.16	5.94
	8	394.26	0.1414	0.1450	0.1306	0.1470	17.5	6.35	10.8	8.60	12.7	6.63	9.79	8.17
C_1 -n-C_5	17	310.93	0.0127	0.0172	-0.0097	0.0222	9.01	3.22	0.59	0.67	2.93	2.01	1.80	1.62
	15	344.26	0.0087	0.0141	-0.0113	0.0187	9.48	2.61	1.38	0.94	2.34	1.40	0.85	1.13
	12	377.59	0.0227	0.0304	0.0047	0.0342	11.4	0.97	2.86	1.75	2.66	1.46	1.26	1.21
	8	410.93	0.0459	0.0530	0.0238	0.0557	15.0	2.86	5.94	4.33	4.88	1.11	2.24	1.37
C_1 -n-C_7	13	277.59	0.0289	0.0327	-0.0113	0.0389	12.4	0.72	1.65	0.94	3.86	1.88	2.50	2.46
	14	310.93	0.0173	0.0219	-0.0192	0.0298	11.7	0.59	1.40	0.75	2.17	2.82	0.57	1.03
	14	344.36	0.0142	0.0194	-0.0204	0.0288	11.2	0.78	1.02	0.37	3.11	2.16	1.03	1.36
	13	377.59	0.0243	0.0287	-0.0145	0.0391	12.8	0.86	1.95	1.25	3.06	2.25	1.15	1.60
	12	410.93	0.0416	0.0459	0.0032	0.0565	13.1	1.30	2.20	1.33	5.76	1.89	3.20	2.68
	10	444.26	0.0677	0.0715	0.0273	0.0815	15.0	3.18	3.69	2.90	6.61	2.51	3.51	3.11
	8	477.59	0.0560	0.0738	0.0282	0.0819	16.9	5.31	5.47	4.76	4.04	0.97	1.03	1.14
	4	510.93	0.1057	0.1296	0.0779	0.1303	26.4	14.5	14.2	13.7	3.29	4.36	4.01	4.11
C_1 -n-C_{10}	18	310.93	0.0400	0.0432	-0.0225	0.0482	16.6	4.46	2.99	1.84	4.22	2.16	2.45	1.60
	17	344.26	0.0356	0.0394	-0.0267	0.0470	16.5	4.43	2.84	1.54	3.98	1.80	1.88	1.22
	16	377.59	0.0329	0.0375	-0.0285	0.0479	16.1	4.25	2.60	1.29	3.76	1.58	1.36	0.96
	15	410.93	0.0303	0.0365	-0.0284	0.0492	15.6	4.14	2.56	1.22	3.61	1.43	0.88	0.65
	13	444.26	0.0372	0.0444	-0.0225	0.0588	17.5	6.09	4.20	2.98	3.92	0.97	0.88	0.85
	11	477.59	0.0382	0.0490	-0.0180	0.0644	15.6	4.82	2.89	1.79	4.69	0.67	1.06	1.19
	8	510.93	0.0647	0.0746	0.0014	0.0903	17.2	6.55	4.12	3.35	5.67	1.20	1.40	1.66

Table(7.4) cont'd.

SYSTEM	ND	T/K	k_{ij}				$\lvert\Delta v_m^L x\rvert_{ave}$				$\lvert\Delta v_m^V x\rvert_{ave}$			
			SRK	PR	SW	MEW	SRK	PR	SW	MEW	SRK	PR	SW	MEW
$n\text{-}C_2$ -$n\text{-}C_5$	5	277.59	0.0053	0.0094	0.0035	0.0158	9.56	2.99	2.78	1.66	1.50	0.39	0.92	0.39
	7	344.26	0.0118	0.0120	0.0006	0.0133	15.4	3.29	7.55	5.19	5.66	1.76	3.94	2.56
	7	377.59	0.0165	0.0138	0.0045	0.0129	16.4	3.89	7.46	5.49	5.16	1.54	3.31	2.16
	6	444.26	0.0777	0.0642	0.0641	0.0670	22.0	9.98	12.4	10.6	8.80	2.70	5.11	3.76
$n\text{-}C_2$ -nC_{10}	5	310.93	0.0155	0.0170	-0.0154	0.0216	17.5	4.56	4.46	3.69	5.90	3.24	5.08	3.50
	9	344.26	0.0109	0.0110	-0.0229	0.0141	18.2	5.36	4.60	3.68	1.65	3.48	1.94	2.19
	13	377.59	0.0120	0.0094	-0.0248	0.0119	18.3	5.63	4.46	3.64	2.25	2.87	1.10	1.68
	14	410.93	0.0196	0.0172	-0.0150	0.0186	19.4	6.80	5.47	4.18	2.68	2.26	0.78	1.46
	15	444.26	0.0226	0.0210	-0.0131	0.0211	19.1	7.03	5.30	4.22	2.92	2.43	1.53	1.95
	14	477.59	0.0355	0.0332	0.0024	0.0329	18.5	6.65	4.55	3.58	3.98	1.54	0.78	1.19
	9	510.93	0.0556	0.0524	0.0175	0.0514	18.2	7.05	4.79	4.13	6.75	1.02	0.98	1.75
$n\text{-}C_2$ - propene	5	260.93	0.0007	0.0052	0.0071	0.0132	9.19	3.55	4.55	2.34	3.65	2.22	3.15	2.25
	7	277.59	0.0010	0.0060	0.0077	0.0137	9.32	3.66	4.27	1.89	2.47	1.20	1.86	1.24
	10	310.93	0.0087	0.0096	0.0096	0.0135	16.8	5.36	11.9	8.04	3.99	1.13	2.59	1.09
	5	344.26	0.0079	0.0088	0.0126	0.0115	23.1	10.3	17.0	13.0	6.80	1.62	4.87	2.24
propene-1-hutene	8	277.59	0.0010	0.0023	0.0031	0.0082	7.68	4.94	0.87	0.26	11.3	6.46	0.88	0.65
	7	310.93	-0.0063	-0.0010	0.0009	0.0059	8.84	3.90	1.94	0.38	1.68	0.57	1.10	0.59
	7	344.26	-0.0103	-0.0042	-0.0022	0.0022	12.4	1.48	5.39	2.94	3.04	0.75	1.87	0.85
	6	377.59	-0.0091	-0.0062	-0.0051	-0.0036	18.1	5.72	11.3	8.27	3.07	2.31	1.94	2.22
	5	410.93	-0.0144	-0.1435	-0.0117	-0.0134	29.5	17.2	22.4	19.4	30.0	4.09	0.61	3.06
$n\text{-}C_3$ -$n\text{-}C_{10}$	4	344.26	-0.0037	-0.0006	-0.0180	0.0054	15.0	2.05	2.73	1.67	2.45	0.71	1.34	0.67
	5	377.59	-0.0109	-0.0086	-0.0314	-0.0040	15.5	3.89	1.45	1.30	1.27	3.18	1.85	2.94
	6	410.93	-0.0074	-0.0066	-0.0320	-0.0038	17.2	4.29	2.43	1.72	2.23	1.65	1.60	1.79
	6	444.26	0.0007	-0.0011	-0.0285	0.0010	24.8	10.8	7.70	7.41	1.87	1.36	0.57	0.88
$n\text{-}C_4$ -$n\text{-}C_{10}$	7	377.59	0.0002	0.0048	0.0051	0.0112	15.9	2.58	2.71	2.05	3.42	2.16	2.69	2.12
	7	410.93	-0.0003	0.0032	-0.0099	0.0088	17.8	4.53	4.77	4.05	5.94	3.13	4.05	3.16
	11	444.26	0.0031	0.0040	-0.0147	0.0071	19.4	6.52	5.95	5.29	10.9	6.80	8.27	7.37
	10	477.59	0.0122	0.0098	-0.0138	0.0115	21.5	8.39	6.47	6.20	6.65	3.99	4.68	4.49
	11	510.93	0.0253	0.0169	-0.0108	0.0203	22.8	10.0	7.84	7.49	4.73	7.02	6.57	6.62

Table(7.4) cont'd.

SYSTEM	ND	T/K	k_{ij}				$\lvert\Delta v_m^{\ell}x\rvert_{ave}$				$\lvert\Delta v_m^{v}x\rvert_{ave}$			
			SRK	PR	SW	NEW	SRK	PR	SW	NEW	SRK	PR	SW	NEW
CO_2 -n-C_3	11	277.59	0.1201	0.1160	0.1216	0.1184	8.69	4.56	2.25	2.10	1.41	2.23	1.89	2.17
	16	294.26	0.1246	0.1177	0.1238	0.1182	11.9	4.91	5.05	3.73	1.86	3.78	2.93	3.62
	17	310.93	0.1310	0.1202	0.1270	0.1186	16.4	7.03	9.81	7.22	1.81	2.60	0.99	2.15
	14	327.59	0.1339	0.1207	0.1296	0.1186	16.1	4.36	9.46	6.50	1.59	3.03	0.67	2.31
	12	344.26	0.1413	0.1242	0.1370	0.1224	19.6	7.83	13.1	10.1	3.65	2.47	2.20	1.49
CO_2 -n-C_4	10	310.93	0.1324	0.1230	0.1261	0.1205	14.3	5.47	6.41	5.00	1.30	3.53	2.40	3.32
	10	344.26	0.1456	0.1315	0.1336	0.1255	14.1	3.10	6.21	4.31	1.48	2.73	0.91	2.20
	8	377.59	0.1662	0.1462	0.1510	0.1394	17.0	4.97	9.04	6.88	3.02	2.09	0.90	1.47
	6	410.93	0.2097	0.1743	0.1898	0.1602	23.1	12.1	15.6	13.6	8.33	2.65	4.67	2.39
CO_2 -n-C_{10}	8	310.92	0.1165	0.1068	0.0955	0.1089	19.8	6.76	3.17	2.47	16.1	12.0	13.4	12.5
	6	344.26	0.1137	0.1010	0.0846	0.1026	19.6	6.63	3.03	2.45	4.19	0.81	1.29	1.13
	8	377.59	0.1176	0.1032	0.0827	0.1037	19.9	7.22	3.65	2.90	5.25	4.23	3.17	3.78
	8	410.93	0.1212	0.1058	0.0816	0.1050	20.0	7.75	4.43	3.66	3.44	1.54	0.74	1.17
	8	444.26	0.1272	0.1109	0.0820	0.1086	19.9	7.98	4.65	3.91	4.78	8.86	0.89	1.10
	7	477.59	0.1310	0.1182	0.0802	0.1125	18.9	8.02	5.22	4.27	6.70	1.38	1.77	1.96
	4	510.93	0.1633	0.1468	0.1078	0.1393	20.0	9.44	6.34	5.71	7.50	2.06	1.89	2.41

and v_m^v are minimized whereas in Method II deviations in x_i and y_i are minimized and v_m^ℓ and v_m^v are then calculated based on these results. As can be seen the new equation has the smallest average absolute percent deviations in v_m^ℓ for most binary systems especially those whose molecules are of different sizes i.e., C1 and C10 and CO2 and C10.

Summarized in Table 7.5 are the overall average absolute percent deviations in v_m^ℓ and v_m^v calculated based on Methods I and II. It should be noted that the new equation has the best overall performance of the four equations when calculating v_m^ℓ based on either method. For Method I, the new equation has an overall average absolute percent deviation of 2.31% compared to 2.92% for the SW equation, 3.37% for the PR equation and 9.91% for the SRK equation. For Method II, 3.77% is predicted by the new equation compared to 4.69% for the PR equation, 5.23% for the SW equation and 14.7% for the SRK equation. In both methods, the SRK equation is the least accurate of the four equations and its results are not acceptable for engineering applications.

As shown in Tables 7.3 and 7.4, the four equations have comparable deviations in v_m^v for most systems tested. All four equations have a tendency to predict larger errors at higher temperatures. However, the results shown in Table 7.5 indicate that the new EOS gives slightly better overall performance than the PR and the SW equations which are better than the SRK equation. For Method I, the new equation has an average absolute deviation of 1.94% compared to 2.02% for the SW equation, 2.09% for the PR equation and 2.54% for the SRK equation. For

Table 7.5: Overall average absolute percent deviations in the saturated liquid and vapor molar volumes based on Methods I and II.

	No. of Isotherms	Data Points	Saturated Liquid Molar Volume, V_m^l							
			Method I				Method II			
			SRK	PR	SW	NEW	SRK	PR	SW	NEW
CO_2-HC	16	153	11.0	4.51	4.12	3.42	16.7	6.36	6.94	5.35
HC-HC	60	671	9.67	3.11	2.64	2.05	14.3	4.30	4.84	3.41
		Overall Average	9.91	3.37	2.92	2.31	14.7	4.69	5.23	3.77

	No. of Isotherms	Data Points	Saturated Vapor Molar Volume, V_m^v							
			Method I				Method II			
			SRK	PR	SW	NEW	SRK	PR	SW	NEW
CO_2-HC	16	153	3.16	2.77	3.33	2.79	3.81	3.06	2.36	2.80
HC-HC	60	671	2.39	1.94	1.81	1.75	4.06	2.61	2.48	2.37
		Overall Average	2.54	2.09	2.02	1.94	4.01	2.69	2.46	2.45

Method II, 2.45% is predicted by the new equation compared to 2.46% for the SW equation, 2.69% for the PR equation and 4.01% for the SRK equation.

When calculating both liquid and vapor molar volumes larger errors are predicted when approaching the critical point, especially in the liquid phase. These errors are severe for the SRK and the PR equations. Experimental and calculated saturated liquid and vapor molar volumes for the CO2-C10 system at 444.26 and 510.93 K using the new equation and the VDW-B model are compared in Figure 7.6. As can be seen it becomes increasingly difficult to represent the saturated molar volumes at higher temperatures and in the critical point region, especially in the liquid phase. However, at both temperatures the results obtained from Method I are better than those from Method II.

It should be noted that the values of k_{ij} obtained based on Methods I and II (Tables 7.3 and 7.4, respectively) are different not only in numerical value but also in sign. Those from Method I are negative for most isotherms, whereas those from Method II are positive under the same conditions. For both methods the values of k_{ij} are not constant but are temperature dependent.

The magnitude of k_{ij} can be considered as a measure of the correction that is required in order for the EOS and its mixing model to accurately represent mixture properties. The values of k_{ij} in the new EOS with the VDW-B model are usually smaller than those in the SRK, the PR and the SW equations with their respective mixing models. The

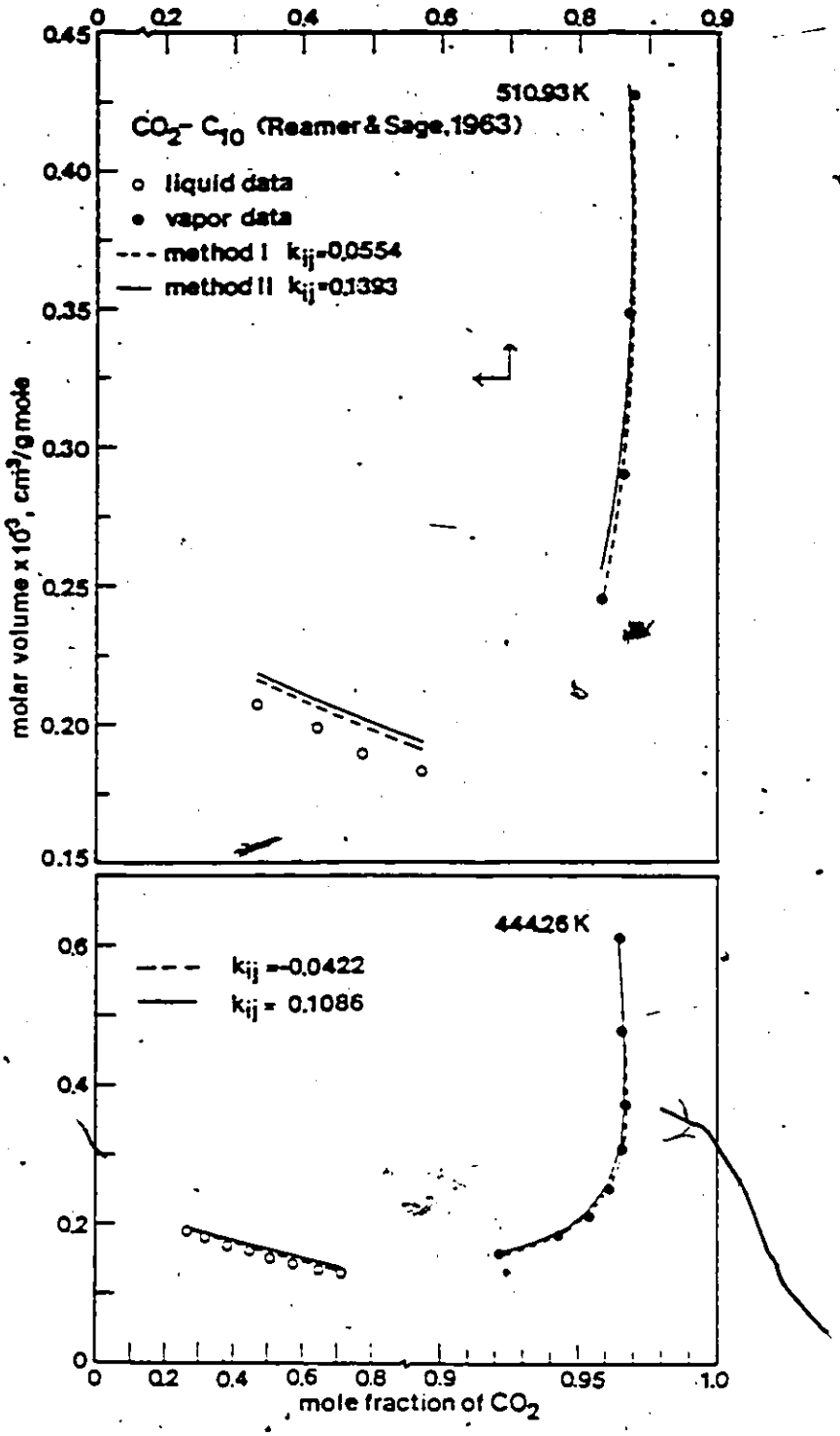

Figure 7.6: Comparison of experimental and calculated saturated molar volumes of the CO2-C10 system at 444.26 and 510.93 K.

SRK equation with its mixing model requires the largest values of k_{ij}. Therefore one may assume that of the four equations the new EOS with the VDW-B mixing model requires the least correction while the SRK equation and its mixing model requires the most in order to represent v_m^ℓ and v_m^v for most systems. One of the reasons why the new EOS requires the smallest k_{ij} values for the four equations for calculating v_m^ℓ and v_m^v is that it was best able to represent v^ℓ and v^v for pure component. It should be noted that the new EOS which has the smallest k_{ij} values also has the best overall performance when calculating v_m^ℓ and v_m^v. On the other hand, the SRK which has the largest values of k_{ij} has the poorest overall performance of the four equations. By the same token, having obtained similar values of k_{ij} for the four equations (see Table 7.1) the overall performance of the equations in calculating VLE values does not differ very much.

7.4.1.3 Calculated Compressibility Factors of Fluid Mixtures

Shown in Table 7.6 are the average absolute percent deviations in the mixture compressibility factors, Z_m, calculated by the PR, the SW and the new equations. Due to its poor performance in calculating saturated liquid mixture molar volumes, the SRK equation is not included in the comparison. Also included are the values of k_{ij} used in their respective mixing models. As can be seen the SW and the new equations give comparable results for most mixtures. Both equations have average absolute deviations of about 1.5% for most systems. All three equations predicted larger errors in Z_m at high pressures. Experimen-

Table 7.6: Average absolute percent deviations in the compressibility factors of fluid mixtures

SYSTEM	ND	T/K	k_{ij} PR	k_{ij} SW	k_{ij} NEW	$\lvert\Delta Z_m\%\rvert_{ave}$ PR	$\lvert\Delta Z_m\%\rvert_{ave}$ SW	$\lvert\Delta Z_m\%\rvert_{ave}$ NEW	Ref.
C_1 -nC_2	43	294.26	0.0350	-0.0544	0.0009	2.89	2.67	2.77	109
	45	327.59	0.0382	-0.1019	-0.0451	1.44	1.34	1.67	
	45	360.93	0.0086	-0.1575	-0.0860	0.95	0.82	1.25	
	45	394.26	0.0230	-0.1780	-0.0838	0.65	0.51	0.88	
C_1 -n-C_3	52	277.59	0.1283	-0.0625	0.0146	5.81	1.94	2.02	109
	66	344.26	0.0973	-0.0533	0.0120	3.49	1.56	1.63	
	70	410.92	0.1070	-0.0802	-0.0090	2.39	1.13	1.17	
	70	444.26	0.1132	-0.0970	-0.0097	2.51	1.55	1.50	
	70	510.93	0.1594	-0.1142	-0.0152	1.47	0.82	0.72	
C_1 -n-C_4	57	310.92	0.1492	-0.0861	-0.0063	3.54	1.16	0.90	109
	59	344.26	0.1038	-0.0918	-0.0334	3.44	1.48	1.15	
	68	377.59	0.0322	-0.1105	-0.0496	3.24	1.83	1.44	
	45	410.93	0.1439	-0.0960	-0.0404	3.29	1.29	1.19	
	45	444.26	0.0952	-0.0993	-0.0352	2.94	1.31	1.19	
	44	510.93	0.1218	-0.1187	-0.0407	2.37	1.32	1.14	
C_1 -n-C_5	35	310.93	0.1850	-0.0712	0.0148	2.42	0.65	0.70	109
	40	377.59	0.1407	-0.0600	0.0129	1.73	0.84	0.91	
	57	444.26	0.0925	-0.0645	0.0010	1.78	1.33	1.42	
	60	510.93	0.1084	-0.0755	0.0117	1.38	1.23	1.25	
C_1 -n-C_{10}	39	310.93	-0.6616	-0.5798	-0.3750	6.65	2.89	1.51	109
	39	377.59	-0.2758	-0.2758	-0.1108	5.11	1.48	0.65	
	38	444.26	-0.1390	-0.1390	-0.0123	4.05	1.61	2.15	
	45	510.93	-0.1988	-0.1989	-0.0431	2.70	1.12	1.49	

Table(7.6) cont'd.

SYSTEM	ND	T/K	k_{ij} PR	k_{ij} SW	k_{ij} NEW	$\overline{\lvert\Delta Z_m\%\rvert}_{ave}$ PR	$\overline{\lvert\Delta Z_m\%\rvert}_{ave}$ SW	$\overline{\lvert\Delta Z_m\%\rvert}_{ave}$ NEW	Ref.
n-C_2 -propene	64	277.59	0.1730	-0.0372	0.0297	4.74	1.66	1.33	
	60	344.26	0.0032	-0.0615	-0.0336	4.63	2.48	2.35	110
	65	410.93	0.0347	-0.0774	-0.0349	3.18	1.97	2.20	
	65	477.59	0.0778	-0.0952	-0.0569	2.25	1.31	1.51	
n-C_2 -n-C_5	63	277.59	0.2200	-0.0474	0.0103	2.84	0.95	0.65	
	60	310.93	0.1240	-0.0630	-0.0047	3.40	1.19	1.04	
	50	377.59	0.0014	-0.0990	-0.0644	3.98	1.83	1.80	98
	46	444.26	-0.0126	-0.0928	-0.0697	3.52	2.29	2.11	
	41	510.93	-0.0091	-0.1371	-0.1023	3.44	2.22	2.10	
n-C_2 -n-C_{10}	63	277.59	-0.3388	-0.2877	-0.2322	5.53	2.25	1.27	
	59	310.93	-0.2230	-0.2296	-0.1595	4.77	1.52	0.60	
	37	377.59	-0.1738	-0.1847	-0.1098	2.92	0.42	0.57	99
	45	444.26	-0.1414	-0.1987	-0.1352	4.04	1.82	2.34	
	45	510.93	-0.1308	-0.1736	-0.1037	2.39	1.52	1.95	
n-C_3 -n-C_5	13	344.26	-0.0236	-0.0757	-0.0199	0.18	0.19	0.18	
	27	377.59	0.0656	0.0288	0.0647	0.90	0.85	0.90	109
	12	410.93	-0.1084	-0.1532	-0.1038	0.52	0.54	0.51	
	18	444.26	-0.0420	-0.0792	-0.0425	0.50	0.43	0.50	
propene-n-C_3	34	260.93	0.3523	0.0735	0.1386	3.21	1.20	0.88	
	37	310.93	0.1632	0.0010	0.0622	3.36	1.53	1.37	
	30	360.93	-0.0271	-0.0681	-0.0377	2.67	1.58	1.63	110
	38	410.93	0.0052	-0.0366	-0.0185	2.89	1.72	1.87	
	38	477.59	0.0349	-0.0752	-0.0536	1.96	1.20	1.40	

Table(7.6) cont'd.

SYSTEM	ND	T/K	k_{ij} PR	k_{ij} SW	k_{ij} NEW	$\lvert\Delta Z_m\%\rvert_{ave}$ PR	$\lvert\Delta Z_m\%\rvert_{ave}$ SW	$\lvert\Delta Z_m\%\rvert_{ave}$ NEW	Ref.
propene-1-butene	64	277.59	0.3178	0.0051	0.0556	3.05	0.74	0.47	110
	63	344.26	0.0718	-0.0697	-0.0121	4.28	1.89	1.71	
	65	410.93	-0.0310	-0.0532	-0.0381	4.29	2.87	2.77	
propene-benzene	65	310.93	0.3532	0.0792	0.1246	2.92	1.71	1.71	110
	56	377.59	0.1341	0.0071	0.0641	4.69	1.70	1.58	
	50	444.26	0.0679	-0.0459	-0.0089	4.46	1.92	1.91	
	43	510.93	0.0068	-0.0600	-0.0417	4.79	3.29	3.15	
CO_2 -n-C_2	63	310.93	0.1333	0.0489	0.0774	3.96	2.83	2.80	110
	65	377.59	0.1383	0.0472	0.0701	2.43	1.63	1.83	
	65	444.26	0.1724	0.0095	0.0464	1.48	0.96	1.06	
	65	510.93	0.1925	-0.0429	0.0164	1.10	0.73	0.74	
CO_2 -n-C_3	62	277.59	0.2084	0.0858	0.1289	4.67	1.87	1.82	110
	61	310.93	0.1288	0.0523	0.0779	4.60	2.39	2.38	
	65	377.59	0.1228	0.0451	0.0575	3.32	2.39	2.46	
	65	444.26	0.1735	0.0320	0.0650	2.12	1.58	1.66	
	65	510.93	0.1618	-0.0025	0.0318	1.32	1.01	1.06	
CO_2 -n-C_4	54	310.93	0.1698	0.0618	0.0977	4.30	1.88	1.92	110
	59	377.59	0.1129	0.0463	0.0690	3.27	2.24	2.23	
	65	444.26	0.1114	0.0330	0.0527	2.41	1.87	1.94	
	65	510.93	0.1157	-0.0320	0.0154	1.76	1.44	1.47	
N_2 -n-C_2	56	277.59	0.1584	-0.0041	0.0158	3.36	1.25	1.18	110
	64	344.26	0.2474	-0.0655	0.0266	2.24	1.22	1.25	
	65	410.93	0.3405	-0.0563	0.0347	1.42	0.76	0.72	
	65	477.59	0.5001	-0.0872	0.0094	1.01	0.51	0.44	
	65	510.93	0.5804	-0.0889	0.0248	1.06	0.60	0.51	

tal Z_m values are compared in Figure 7.7 with those calculated by the new equation for an equimolar mixture of CO2 and propane at 313.93, 444.26 and 510.93 K. As can be seen, relatively larger deviations in Z_m are predicted at presures above 400 atmospheres.

Values of k_{ij} used for the PR, the SW and the new equations can be either positive or negative, depending on the system and temperature. In general, the new equation requires smaller values of k_{ij} than the PR and the SW equations. The magnitude of k_{ij} for the new equation is usually between 10^{-3} and 10^{-2}, except for the C1-C10 and C2-C10 systems.

In summary, the results of the three mixture calculations indicate that the VDW-B mixing model is suitable for extending the new EOS for pure fluids to normal fluid mixtures. This mixing model enables the new EOS to give comparable or better results than those obtained from the SRK, the PR and the SW equations with their respective mixing models. The new EOS is superior particularly in the representation of v_m^{ℓ}. For systems in which the molecular size of the components is quite different, the new EOS, just as any other volume-cubic equation, has difficulties in describing the critical region. This is probably due to the inability of volume-cubic equations to accurately describe the behavior of pure fluids in the vicinity of the critical point.

Summarized in Table 7.7 are the overall average absolute percent deviations in the calculated Z_m for each individual groups in Set 3. As can be seen for the three groups studied, the new equation is slightly

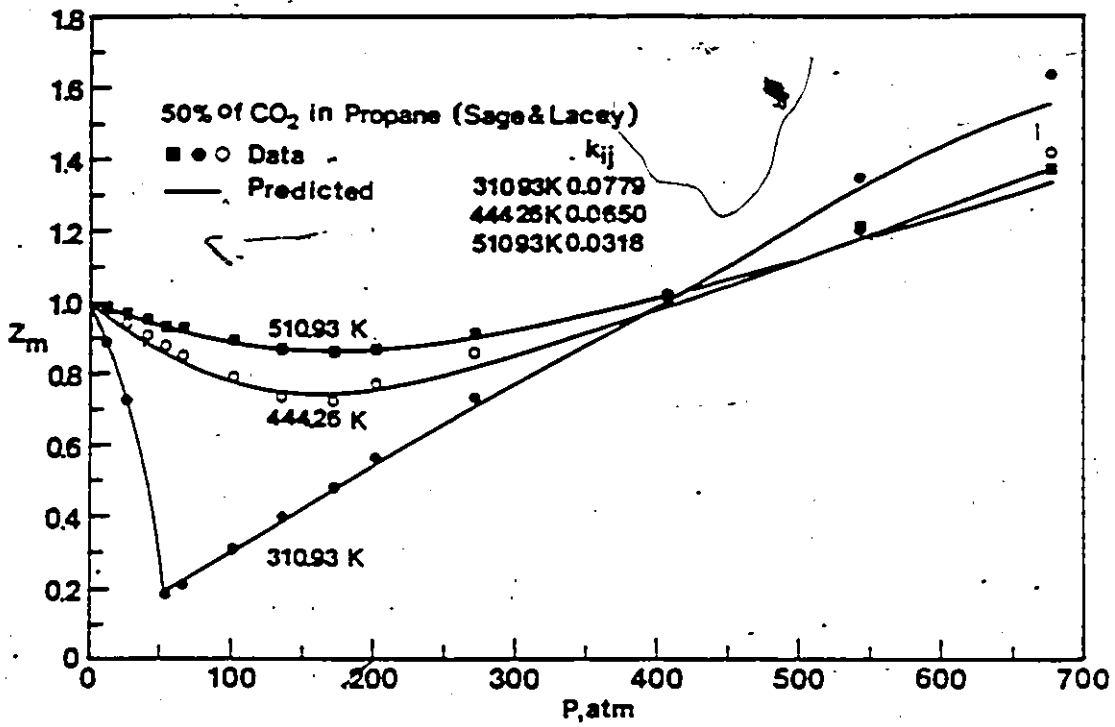

Figure 7.7: Comparison of experimental and calculated compressibility factors of an equimolar mixture of CO2 and propane.

better than the SW equation which is better than the PR equation in the overall representation of Z_m. The overall average absolute deviations given by the new, the SW and the PR equations are 1.48%, 1.53% and 2.99%, respectively.

Table 7.7: Overall average absolute percent deviations in the compressibility factors of fluid mixtures

	Data Points	PR	SW	NEW
CO_2-HC	819	2.78	1.75	1.79
N_2-HC	315	1.77	0.86	0.82
HC-HC	2593	3.21	1.54	1.46
	Overall Average	2.99	1.53	1.48

7.4.2 Complex Mixtures

The results of several bubble-point calculations for mixtures containing either alcohols or water are compared in order to choose one of the following mixing models (VDW-A, VDW-B, NRTL-VH, NRTL-M) to be used with the new EOS for calculating the VLE of complex mixtures. The 311 data points from 25 binary VLE systems together with their literature source are listed in Table 7.8. The systems chosen are frequently encounted in industry.

Presented in Table 7.8 are the calculated results of the bubble-point pressure and vapor phase equilibrium composition obtained using four mixing models. Deviations in the bubble-point pressure are average absolute percent deviations while those in the vapor phase equilibrium

Table 7.8: Average absolute deviations in bubble-point pressures and vapor compositions.

SYSTEM	NO	T/K	VDW-B k_{ij}	VDW-A k_{ij}	VDW-A ℓ_{ij}	MRTL-VH k_{ij}	MRTL-VH α_{ij}	MRTL-M k_{ij}	MRTL-M α_{ij}	$\lvert\Delta P\rvert_{ave}$ VDW-B	VDW-A	MRTL-VH	MRTL-M	$\lvert\Delta y_1\rvert_{ave} \times 10^3$ VDW-B	VDW-A	MRTL-VH	MRTL-M	ref
carbon dioxide(1) - methanol(2)	8	298.15	0.0387	0.0689	0.0295	0.07495	0.05692	0.07238	0.01719	5.86	2.97	2.30	2.26	1.68	1.60	1.56	1.61	81
	9	313.15	0.0568	0.0719	0.0152	0.06977	0.03739	0.07246	0.00895	3.34	2.24	2.21	2.18	9.97	9.66	9.66	9.63	
ethane(1) - methanol(2)	5	298.15	0.0190	0.0060	-0.0129	-0.02520	0.01031	0.00500	-0.01647	4.46	3.01	3.15	3.03	2.38	2.36	2.11	2.13	81
ethane(1) - acetone(2)	8	298.15	0.1356	0.1555	0.0204	0.1597	0.04290	0.1532	0.00977	3.71	1.39	1.55	1.57	0.78	0.84	0.82	0.81	81
ethane(1) - methylacetate(2)	10	298.15	0.1206	0.1498	0.0319	0.1559	0.06071	0.1472	0.01598	5.49	1.46	1.30	1.32	1.70	0.85	0.81	0.84	81
ethane(1) - ethyl ether(2)	6	298.15	0.0210	0.0342	0.0172	0.04433	0.06343	0.03448	0.01159	0.83	0.59	0.495	0.508	4.77	6.18	4.47	4.43	81
ethane(1) - benzene(2)	7	298.15	0.0477	0.0249	-0.0246	0.01405	-0.03687	0.02443	-0.01207	3.20	1.24	1.04	1.01	0.29	0.57	0.57	0.58	81
propane(1) - ethanol(2)	16	325.0	0.0251	0.0436	0.0184	0.02154	0.06716	0.04384	0.04316	4.97	4.31	4.29	4.12	12.2	12.9	12.9	13.0	
	12	350.0	0.0212	0.0358	0.0161	0.01474	0.07589	0.03564	0.04689	3.38	3.28	3.32	3.23	11.2	12.5	12.5	12.7	
	11	375.0	0.0262	0.0448	0.0222	0.02474	0.1024	0.04240	0.06928	2.50	2.27	2.31	2.21	23.5	23.6	23.4	23.6	39
	12	400.0	0.0286	0.0616	0.0434	0.04300	0.1737	0.05410	0.1454	2.72	1.08	1.02	0.90	28.2	30.5	28.0	30.0	
	11	425.0	0.0218	0.0529	0.0435	0.03861	0.2158	0.04444	0.1725	2.38	1.27	1.20	1.30	47.0	52.1	46.7	51.3	
acetone(1) - benzene(2)	11	298.15	0.0309	0.0655	0.0403	0.03567	0.2534	0.03802	0.2623	0.98	0.96	0.99	1.01	5.85	5.84	6.93	7.74	125
acetone(1) - cyclohexane(2)	23	298.15	0.1212	-0.1729	-0.3523	0.08611	-0.5903	0.09443	-0.1638	4.77	0.38	1.02	1.69	32.7	8.32	9.51	13.9	125
acetone(1) - water(2)	22	373.15	-0.2127	0.0589	0.2330	-0.1209	0.2578	-0.1496	0.05140	11.5	3.41	3.10	6.35	58.5	14.4	13.0	20.6	
	17	423.15	-0.1761	0.1248	0.2729	-0.06976	0.2835	-0.07789	0.1241	8.91	1.95	1.18	4.08	35.8	12.8	12.1	16.5	
	25	473.15	-0.1499	0.1473	0.2835	-0.04378	0.2931	0.09607	0.5026	6.98	1.08	0.696	1.25	29.0	7.53	4.37	10.4	41
	8	523.15	-0.1141	0.1115	0.2363	-0.02906	0.2698	0.07592	0.5504	3.96	0.80	0.657	1.11	35.3	4.90	6.64	6.96	
methanol(1) - water(2)	16	373.15	-0.0749	-0.0814	-0.0065	-0.06086	-0.1431	-0.07723	-0.00799	1.55	1.52	1.53	1.50	23.1	22.9	23.0	23.0	
	14	423.15	-0.0692	-0.0410	0.0306	-0.03895	-0.00297	-0.06225	0.04241	1.26	0.99	1.00	1.06	13.4	13.0	12.7	12.8	
	15	473.15	-0.0683	-0.0406	0.0316	-0.03708	-0.00518	-0.05764	0.07799	0.67	0.51	0.52	0.552	9.74	9.52	9.12	10.2	41
	6	523.15	-0.0737	-0.0140	0.0726	-0.02513	0.1114	-0.05455	0.3463	1.03	0.35	0.35	0.241	10.0	8.23	4.75	7.43	
acetone(1) - methanol	14	373.15	0.0090	0.1610	0.1898	-0.0025	0.7301	0.00679	0.04064	1.56	0.49	0.56	0.948	12.4	13.8	14.1	11.7	
	15	423.15	0.0142	0.4364	0.5194	0.1047	1.906	0.004850	-0.09057	1.40	0.90	0.42	1.40	16.5	15.8	18.1	16.5	41
	10	473.15	0.0110	0.3749	0.4748	0.8888	1.027	0.003307	-0.08450	2.47	2.14	2.04	2.47	30.1	27.8	39.5	30.2	

composition are average absolute deviations. Also included are the values of the empirical coefficients associated with the four mixing models. It should be noted that with the VDW-B model the new EOS cannot satisfactorily represent the bubble-point pressures and vapor phase equilibrium compositions of most systems. The deviations in the predicted bubble-point pressures and vapor phase equilibrium compositions are about two to three times higher than those obtained with the VDW-A, the NRTL-VH and the NRTL-M models. Besides it has a strong tendency for the EOS to predict a false phase-splitting behavior. This clearly indicates that one empirical binary coefficient in the VDW mixing model is not sufficient to represent the vapor-liquid equilibria of complex mixtures. As an example, in Figure 7.8 the predicted VLE for acetone-water system at 473.15 K by the new EOS with the VDW-B model is compared with the experimental result. As can be seen with the VDW-B model the new equation tends to predict a false phase split at low acetone concentration.

On the other hand, when both the k_{ij} and ℓ_{ij} are used in the VDW model (VDW-A) the calculated results are comparable with those given by the NRTL-VH and the NRTL-M models. As can be seen in Figure 7.8 the model did not lead the new equation to the prediction of a false phase-splitting. In fact, with this model the new EOS can represent the VLE of this mixture reasonably well. It should be noted that both NRTL models contain two adjustable binary coefficients. For most systems, the more theoretical NRTL-M model fails to show any superiority over the other two models. It is rather surprising that the built-in

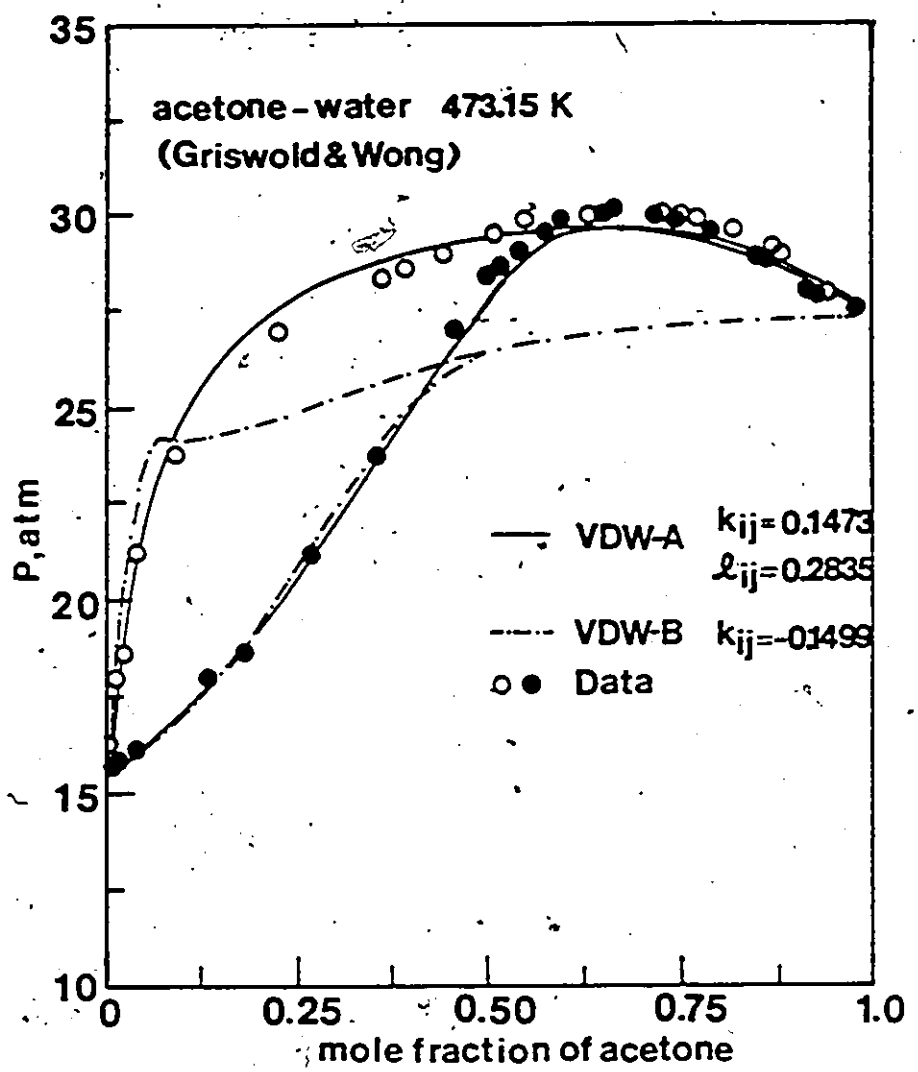

Figure 7.8: Comparison of experimental and calculated VLE for acetone-water system at 473.15 K.

density dependence of this model does not result in any significant improvement over the other two density independent mixing models. Also there is an additional iteration loop required by this model (see Figure 7.2) which can result in computation times which are two to three times that of the VDW-A model. For routine VLE calculations, long computation times are not practical as demonstrated by Boston and Mathias [16] and Mathias and Copeman [71]. Due to the exponential terms in the local composition expressions, both the NRTL-type LC models are sensitive to changes in the coefficients, k_{ij} and α_{ij}. This often results in convergence problems if the initial values of k_{ij} and α_{ij} are not properly chosen. However, the VDW-A mixing model does not have this problem as its coefficients, k_{ij} and ℓ_{ij} can be determined after only a few iterations.

The main reason why the VDW-A model gives results which are comparable to those given by the local composition models is because in the development of these models repulsive forces, thus the free volumes, were assumed to have no significant contribution to the occurrence of local composition in a complex mixture. In effect, this assumption leads to the use of a linear mixing rule for b_m and therefore c_m in the new equation. However, the main reason that the VDW-B model did not give good results and the VDW-A model did is because the VDW-B model uses a linear mixing rule for b_m while the VDW-A model uses a quadratic mixing rule. Therefore the local composition models could be improved if quadratic rather than linear mixing rules were used for b_m and c_m. However this would also introduce a third adjustable coefficient

which would eliminate the large practical advantage of a two-coefficient mixing model such as the VDW-A model as well as making the computation even more difficult.

Based on the above discussion the simple, yet accurate VDW-A model appears to be the most suitable model to be used with the new EOS.

Chapter VIII

CONCLUSIONS

Fourteen well-known volume-cubic equations of state were evaluated by calculating eight physical properties of normal alkane. It was found that three-parameter equations with one temperature dependent parameter give the best overall performance.

Using a new design procedure based on deviation contours it was found that the parameters u and w have a greater influence on the overall representation of v^{ℓ} and Z^{ℓ} than of v^{v} and Z^{sup}. It was also shown the importance of the quantities β_c and ζ_c predicted by an equation of state; β_c influencing the representation of v^{ℓ} and Z^{ℓ} at low temperatures while ζ_c is important in the critical point region.

Based on these results a new three-parameter equation of state containing only one temperature dependent parameter was proposed which utilizes the relationship u-w=3 as it was found to provide a balanced representation of the volumetric properties of pure normal fluids while emphasizing state conditions of practical importance. The new equation was tested by calculating the vapor pressures and volumetric properties of pure normal fluids and comparing the results with those obtained from the Soave-Redlich-Kwong, the Peng-Robinson and the Schmidt-Wenzel equations. The new equation was found to give better overall

performance, especially in the calculation of saturated liquid molar volumes and liquid compressibility factors.

The new equation of state was extended to normal fluid mixtures using a random mixing model for the parameters. When compared with the Soave-Redlich-Kwong, the Peng-Robinson and the Schmidt-Wenzel equations the new equation gave comparable results for vapor-liquid equilibrium calculations. However, it had better overall representation of the volumetric properties of normal fluid mixtures, especially in the liquid phase.

In the calculation of the vapor-liquid equilibria of complex mixtures, both random and local composition mixing rules were used for the parameters in the new equation. It was found that random mixing rules containing two adjustable empirical coefficients are the most suitable when the new equation is applied to complex mixtures.

Appendix A

VOLUME TRANSLATION OF TWO-PARAMETER EQUATION OF STATE OF THE VAN DER WAALS TYPE

Any two-parameter volume-cubic EOS of the VDW-type can be represented by a single point on a u-w diagram. Application of the volume-translation technique to any two-parameter equation yields a curve on such a diagram, representing a family of equations having an identical Ω_{ac} value. In other words, the value of Ω_a at the critical point of the two-parameter equation prior to the volume-translation would not at all be affected. Furthermore, the u and w values are related to those of the original equation prior to the volume translation by an exact mathematical relation. This relation is derived as follows.

Let the original equation be represented by

$$P = \frac{RT}{(v - b)} - \frac{a}{v^2 + ubv + wb^2} \qquad (A.1)$$

Translating the quantities b and v of Eq.(A.1) by volume c

$$v' = v - c \qquad (A.2)$$

$$b' = b - c \qquad (A.3)$$

and substituting these expressions into Eq.(A.1) yields

$$P = \frac{RT}{(v - b)} - \frac{a}{v'^2 + u'bv' + w'b^2} \qquad (A.4)$$

with

$$u' = u + 2c/b + uc/b \qquad (A.5)$$

and

$$w' = w + (u + 2w)c/b + (1 + u + w)c^2/b^2 \qquad (A.6)$$

It can be readily shown that

$$w' = w + \left[\frac{4w - u^2}{(2 + u)^2}\right] u' + \left[\frac{1 + u + w}{(2 + u)^2}\right] u'^2 - \left[\frac{u + 2w}{(2 + u)}\right] u + \left[\frac{1 + u + w}{(2 + u)^2}\right] u^2 \qquad (A.7)$$

Schmidt and Wenzel [112] demonstrated that u and w (or u' and w') must satisfy the two constrains,

for $u \geq -2$,

$$w > -u - 1, \qquad (A.8a)$$

for $u \leq -2$,

$$w > u^2/4. \qquad (A.8b)$$

to avoid the situation that $v^2 + ubv + wb^2 = 0$ for $v \geq b$. Therefore the ration b/c of Eqs(A.5, A.6) cannot be equal to -1. In addition, the condition $u \neq -2$ should be imposed to Eq.(A.7).

Appendix B

SELECTED TEMPERATURES AND PRESSURES FOR CALCULATING SUPERCRITICAL GAS COMPRESSIBILITY FACTORS

Substance	ND	Temperatures °F	Pressures psia
Methane	440	-100.0 -80.0 -60.0 0.0 40.0 100.0 140.0 200.0 300.0 400.0 500.0 600.0 700.0 800.0 900.0 1000.0 1200.0 1400.0 1600.0 1800.0 2000.0 2200.0	1 14.696 50.0 100.0 200.0 300.0 400.0 500.0 600.0 800.0 1000.0 1500.0 2000.0 3000.0 4000.0 6000.0 8000.0 10000.0 12000.0 14000.0
Ethane	260	100.0 140.0 200.0 300.0 400.0 500.0 600.0 800.0 1000.0 1200.0 1400.0 1600.0 2000.0	1 14.695 50.0 100.0 200.0 300.0 400.0 500.0 600.0 800.0 1000.0 1200.0 1400.0 1600.0 2000.0 3000.0 4000.0 5000.0 6000.0 7000.0
Propane	187	250.0 300.0 400.0 500.0 600.0 800.0 1000.0 1200.0	1 14.696 50.0 100.0 200.0 300.0 400.0 500.0

		1400.0 1600.0 2000.0	600.0 800.0 1000.0 1200.0 1400.0 1600.0 2000.0 3000.0 4000.0
n-Butane	150	350.0 400.0 500.0 600.0 800.0 1000.0 1200.0 1400.0 1600.0 2000.0	1 14.696 100.0 200.0 300.0 400.0 500.0 600.0 800.0 1000.0 1200.0 1400.0 1600.0 2000.0 3000.0
n-Pentane	150	400.0 500.0 600.0 800.0 1000.0 1200.0 1400.0 1600.0 1800.0 2000.0	1 14696 100.0 200.0 300.0 400.0 500.0 600.0 800.0 1000.0 1200.0 1400.0 1600.0 2000.0 3000.0
N-Hexane	45	480.0 500.0 520.0 560.0 600.0	1 14696 50.0 100.0 200.0 300.0 400.0 500.0 600.0
i-Butane	150	300.0 400.0 500.0 600.0 800.0 1000.0 1200.0 1400.0 1600.0 2000.0	1 14.696 100.0 200.0 300.0 400.0 500.0 600.0 800.0 1000.0 1200.0 1400.0 1600.0 2000.0 3000.0
Ethylene	323	50.0 100.0 140.0 200.0 240.0 300.0 340.0 400.0 440.0 500.0 600.0 700.0 800.0 900.0 1000.0 1400.0	1 14696 50.0 100.0 200.0 300.0 400.0 500.0 600.0 700.0 800.0 900.0 1000.0 2000.0 3000.0

		2000.0	4000.0 5000.0 6000.0 7000.0
Propylene	220	200.0 300.0 400.0 500.0 600.0 800.0 1000.0 1200.0 1400.0 1600.0 1800.0	1 14.696 50.0 100.0 200.0 300.0 400.0 500.0 600.0 800.0 1000.0 1200.0 1400.0 1600.0 2000.0 3000.0 4000.0 5000.0 6000.0 7000.0
1-Butene	60	340.0 360.0 380.0 400.0 440.0 480.0	1 14.696 100.0 200.0 300.0 400.0 500.0 600.0 800.0 1000.0
Benzene	324	560.0 600.0 640.0 700.0 740.0 800.0 840.0 900.0 940.0 1000.0 1100.0 1200.0 1300.0 1400.0 1500.0	1 14.696 40.0 100.0 150.0 200.0 250.0 300.0 400.0 500.0 600.0 700.0 800.0 1000.0 1500.0 2000.0 2500.0 3000.0 1600.0 1700.0 1800.0
Carbon oxide	110	-200.0 -100.0 0.0 100.0 200.0 400.0 600.0 800.0 1000.0 2000.0 4000.0	1 14.696 100.0 200.0 300.0 400.0 500.0 600.0 800.0 1000.0
carbon dioxide	272	220.0 260.0 300.0 400.0 500.0 600.0 800.0 1000.0 1200.0 1400.0 1600.0	1 14.696 50.0 100.0 200.0 300.0 400.0 500.0 600.0 800.0 1000.0

		1800.0 2000.0 2400.0	1200.0 1400.0 1600.0
		3000.0 3400.0	1800.0 2000.0 3000.0
Nitrogen	357	-60.0 -20.0 0.0 40.0	1 14.696 50.0 100.0
		300.0 400.0 600.0 800.0	500.0 600.0 700.0
		1000.0 1400.0 2000.0	800.0 900.0 1000.0
		2400.0 3000.0 3400.0	1100.0 1200.0 1300.0
		4000.0 4400.0 4800.0	1400.0
Oxygen	391	-80.0 -40.0 0.0 40.0 100.0	1 14.696 50.0
		140.0 200.0 240.0 300.0	100.0 200.0 300.0
		340.0 400.0 500.0 600.0	400.0 500.0 600.0
		800.0 1000.0 1400.0 2000.0	700.0 800.0 900.0
		2400.0 300.0 3400.0	1000.0 1100.0 1200.0
		4000.0 4400.0 4800.0	1300.0 1400.0

Taken from Canjar and Manning [17].

REFERENCES

1. Abbott, M.M., AIChE J. 19 596 (1973).
2. Abbott, M.M., "Equations of State in Engineering and Research" Eds. Chao, K.C.; Robinson, R.L. Jr., (1977), Chapter 3.
3. Abbott, M.M., ACS 182, 72, Am. Chem. Soc. Washington, D.C., (1979).
4. Abrams, D.S.; Prausnitz, J.M., AIChE J. 21 116 (1975).
5. Adachi, Y.; Lu, B.C.-Y.; Sugie, H., Fluid Phase Equilibria 11 29 (1982).
6. Adachi, Y.; Lu, B.C.-Y., Fluid Phase Equilibria 13 133 (1983).
7. Adachi, Y.; Chung, W.K.; Yu, J.-M.; Lu, B.C.-Y., Adv. Cryog. Eng. 29 973 (1984).
8. Alder, B.J.; Hoover, W.G.; Young, S., J. Chem. Phys., 49 3693 (1968).
9. American Petroleum Institute, Proj. 44, "Selected Values of Properties of Hydrocarbons and Related Compounds" Washington, D.C., (1977).
10. Asselineau, L.; Bogdanic, G.; Vidal, J., Fluid Phase Equilibria 3 273 (1979).
11. Banner, H.E.; Quinlan, C.W.; Ind. Eng. Chem. Process Des. Dev., 8 407 (1969).
12. Barile, R.G.; Thodos, G., Can. J. Chem. Eng. 43 137 (1965).

13. Besserer, G.J.; Robinson, D.B., J. Chem. Eng. Data 18 416 (1973).

14. Besserer, G.J.; Robinson, D.B., J. Chem. Eng. Data 18 298 (1973).

15. Besserer, G.J.; Robinson, D.B., J. Chem. Eng. Data 18 301 (1973).

16. Boston, J.F.; Mathias, P.M., Proc. 2nd Int. Conf. on Phase Equilibria and Fluid Properties in the Chemical Industry, 823 (1980), DECHEMA, Frankfurt/Main.

17. Canjar, L.N.; Manning, F.S., "Thermodynamic Properties and Reduced Correlations for Gases" Gulf Publishing Company, Huston, (1967).

18. Carnahan, N.F.; Starling, K.E., J. Chem. Phys., 51 635 (1969).

19. Chang, S.D.; Lu, B.C.-Y., Chem. Eng. Progr. Symp. Ser. 63, 18 (1967).

20. Chaudron J.; Asselineau, L.; Renon, H., Chem. Eng. Sci. 28 839 (1973).

21. Clausius, R., Ann. Phys. Chem. IX 337 (1880).

22. Davalos, J.; Anderson, R.E.; Phelps, R.E.; Kidnay, A.J., J. Chem. Eng. Data 21 81 (1976).

23. Din, F., "Thermodynamic Functions of Gases" Butterworth, London, (1961).

24. Djordjevich, L.; Budenholzer, R.A., J. Chem. Eng. Data 15 10 (1970).

25. Donnelly, H.G.; Katz, D.L., Ind. Eng. Chem. 46 511 (1954).

26. Donohue, M.D. and Prausnitz, J.M., AIChE J. 24 849 (1978).

27. Doring, R.; Knapp, H., Proc. 2nd Int. Conf. on Phase Equilibria and Fluid Properties in the Chemical Industry, 34 (1980), DECHEMA, Frankfurt/Main.

28. Edmister, W.C., Hydro. Proc. 47 239 (1968).

29. El-Twaty, A.I.; Prausnitz, J.M., Chem. Eng. Sci. 35 1765 (1980).

30. Evelein, K.; Moore, G., Ind. Eng. Chem. Process Des. Dev. 18 618 (1979).

31. Felsing, W.A.; Watson, G.M.; J. Am. Chem. Soc. 64 1822 (1942).

32. Forsythe,G.E.; Malcolm, M.A.; Moler, C.B., "Computer Methods for Mathematical Computations" Prentice-Hall, New Jersey, (1977), Chapter 8.

33. Freze, R.; Chevalier, J.-L.; Peneloux, A.; Rauzy, E., Fluid Phase Equilibria 15 33 (1983).

34. Fuller, G.G., Ind. Eng. Chem. Fundam. 15 254 (1976).

35. Gibbons, R.M.; Laughton, A.P., J Chem. Soc., Faraday Trans. 80 1019 (1984).

36. Gibbs, J.W., "The scientific Papers of J. W. Gibbs" Dover, New York, (1961) volume 1.

37. Glanville, J.W.; Sage, B.H.; Lacey, W.N., Ind. Eng. Chem. 42 508 (1950).

38. Gomez-Nieto, M.; Thodos, G., Ind. Eng. Chem. Fundam. 17 45 (1978).

39. Gomez-Nieto, M.; Thodos, G., AIChE J. 24 672 (1978).

40. Goral, M.; Maczynski, A.; Schmidt, G.; Wenzel, H., Ind. Eng. Chem. Fundam. 20 267 (1981).

41. Griswold, J.; Wong, S.Y., Chem. Eng. Progr. Symp. Ser. 48, 18 (1952).

42. Guggenheim, E.A., J. Chem. Phys. 13 253 (1945).

43. Guggenheim, E.A., "Mixtures" Oxford University Press, London, (1952).

44. Guggenheim, E.A., Mol. Phys. 9 199 (1965).

45. Hamam, S.E.M.; Chung, W.K.; Elshayal, I.M.; Lu, B.C.-Y., Ind. Eng. Chem. Process Des. Dev. 16 51 (1977).

46. Harmens, A., Cryogenics 15 217 (1975).

47. Harmens, A., Cryogenics 17 519 (1977).

48. Harmens, A., Ph.D. Dissertation, The Technical University of Berlin (1980).

49. Harmens, A.; Knapp, H., Ind. Eng. Chem. Fundam. 19 291 (1980).

50. Harmens, A., Proc. 7th Int. Congr. of Chemical Engineering, Chemical Equipment Design and Automation, Prague, Czechoslovakia, (1981), Paper D1.32.

51. Heidmann, R.A., Fluid Phase Equilibria 14 55 (1983).

52. Helfand, E.; Frisch, H.L., J. Chem. Phys. 34 1037 (1961).

53. Heyen, G., "Chemical Engineering Thermodynamics" Ed. Newman, S.A., Ann Arbor Science Publishers, MI (1983), Chapter 15.

54. Hill, T.L., "Introduction to Statistical Thermodynamics" Addison-Wesley, Mass. (1960).

55. Hipkin, H., AIChE. J. 12 484 (1966).

56. Holland, C.D., "Fundamentals of Multicomponent Distillation" McGraw-Hill, New York, (1981).

57. Horvath, A.L., Chem. Eng. Sci. 29 1334 (1972)

58. Hsu, Y.-Y.; Graham, R.W., "Transport Processes in Boiling and Two-Phase System" McGraw-Hill, New York, (1976), pp.457-460.

59. Kahre, L.C., J. Chem. Eng. Data 20 363 (1975).

60. Kalra, H.; Krishnana, D.B.; Robinson, D.B., J. Chem. Eng. Data 21 222 (1976).

61. Kamerlingh Onnes, H., Comm. Phys. Lab Leiden 71 (1901).

62. Kelso, E.A.; Felsing W.A., J. Am. Chem. Soc. 62 3132 (1940).

63. King, C.J., "Separation Processes" McGraw-Hill, New York, (1980).

64. Kohn, J.P.; Bradish, W.F., J. Chem. Eng. Data 9 5 (1964)

65. Kubic, W.L., Fluid Phase Equilibria 9 79 (1982).

66. Lee, B.I.; Kesler, M.G., AIChE J. 21 510 (1975).

67. Starling, K.E.; Han, M.S., Hydrocarbon Processing 51 129 (1972).

68. Lira, R.; Malo, J.M.; Leiva, M.A.; Chapela, G., "Chemical Engineering Thermodynamics" Ed. Newman, S.A., Ann Arhor Science Publisher, MI. (1983), Chapter 14.

69. Martin, J.J., Ind. Eng. Chem. 59 34 (1967).

70. Martin, J.J., Ind. Eng. Chem. Fundam. 18 81 (1979).

71. Mathias, P.M.; Copeman, T.W., Fluid Phase Equilibria 13 91 (1983).

72. Mathias, P.M, Ind. Eng. Chem. Process Des. Dev. 22 385 (1983).

73. Matschke, D.E.; Thodos, G., J. Chem. Eng. Data 7 232 (1962).

74. McDermott, C.; Ashton, N., Fluid Phase Equilibria 1 33 (1977).

75. Michelsen, M.L., Fluid Phase Equilibria 4 1 (1980).

76. Mehra, V.S.; Thodos, G., J. Chem. Eng. Data 10 307 (1965).

77. Mollerup, J., Adv. Cryog. Eng. 20(E-2) 172 (1975).

78. Mollerup, J., Fluid Phase Equilibria, 7 121 (1981).

79. Mollerup, J., Fluid Phase Equilibria, 15 189 (1983).

80. Nysewander, C.N.; Sage, B.H.; Lacey, W.N., Ind. Eng. Chem. 32 118 (1940).

81. Ohgaki, K.; Katayama, T., J. Chem. Eng. Data 21 53 (1976).

82. Ohgaki, K.; Suno, F.; Katayama, T., J. Chem. Eng. Data 21 55 (1976).

83. Ohgaki, K.; Katayama, T., Fluid Phase Equilibria 1 27 (1977).

84. Pal, A.K.; Pope, G.A.; Arai, Y.; Carnahan, N.F.; Kobayashi, R., J. Chem. Eng. Data 21 394 (1976).

85. Passut, C.A.; Danner, R.P., Ind. Eng. Chem. Process Des. Dev. 12 365 (1973).

86. Patel, N.C.; Teja, A.S., Chem. Eng. Sci. 37 463 (1982).

87. Peneloux, A.; Rauzy, E.; Freze, R., Fluid Phase Equilibria 8 7 (1982).

88. Peng, D.Y.; Robinson, D.B., Ind. Eng. Chem. Fundam. 15 59 (1976); The Peng-Robinson equation of state, DB Robinson & Associates Ltd.

89. Pitzer, K.S.; Lippmann, D.Z.; Curl, R.F. Jr.; Huggins, C.M.; Petersen, D.E., J. Am. Chem. Soc. 77 3433 (1955).

90. Plocker, U.; Knapp, H.; Prausnitz, J.M., Ind. Eng. Chem. Process Des. Dev. 17 324 (1977).

91. Prausnitz, J.M.; Chueh P.L., "Computer Calculations for High-Pressure Vapor-Liquid Equilibria" Prentice-Hall, New Jersey, (1967).

92. Prausnitz, J.M., "Molecular Thermodynamics of Fluid-Phase Equilibria" Prentice-Hall, New Jersey, (1969).

93. Prigogine, I. and Bellemans, A., J. Chem. Phys. 15 80 (1953).

94. Prigogine, I., "Chemical Thermodynamics" Longmans, Green and Co. London, (1954).

95. Quayle, O.R., Chem. Rev. 53 439 (1953).

96. Reamer, H.H.; Sage B.H.; Lacey, W.N., Ind. Eng. Chem. 1 29. (1956).

97. Reamer, H.H.; Sage, B.H., Ind. Eng. Chem. 2 9 (1957).

98. Reamer, H.H.; Sage, B.H.; Lacey, W.N., J Chem. Eng. Data 5 44 (1960).

99. Reamer, H.H.; Sage, B.H., J. Chem. Eng. Data 7 161 (1962).

100. Reamer, H.H.; Sage, B.H., J. Chem. Eng. Data 8 508 (1963).

101. Reamer, H.H.; Sage, B.H., J Chem. Eng. Data 9 24 (1964).

102. Reamer, H.H.; Sage, B.H., J. Chem. Eng. Data 11 17 (1966).

103. Redlich, O.; Kwong, J.N.S., Chem. Rev. 44 239 (1949).

104. Reed, T.M.; Gubbins, K.E., "Applied Statistical Mechanics" McGraw-Hill, New York, (1973), Chapter 7.

105. Reid, R.C.; Prausnitz, J.M.; Sherwood, T.K., "The Properties of Gases and Liquids" 3rd ed. McGraw-Hill, New York, (1977).

106. Renon, H.; prausnitz, J.M., AIChE J., 14 135 (1968).

107. Roberts, L.R.; McKetta, J.J., AIChE J. 7 173 (1961).

108. Rowlinson, J.S.; Swinton, F.L., "Liquids and Liquid Mixtures" 3rd ed., Butterworth, London, (1982).

109. Sage, B.H.; Lacey, W.N., "Thermodynamic Properties of the Higher Paraffin Hydrocarbons and Nitrogen" American Petroleum Institute, New York (1950).

110. Sage, B.H.; Lacey, W.N., "Some Properties of the Light Hydrocarbons, Hydrogen Sulfide, and Carbon Dioxide" American Petroleum Institute, New York (1955).

111. Schindler, D.L.; Swift, G.W.; Kurata, F., Hydrocarbon process., Special report, 45 205 (1966).

112. Schmidt, G.; Wenzel, H., Chem. Eng. Sci. 35 35 1503 (1980).

113. Schmidt G.; Wenzel, H., Can. J. Chem. Eng., 59 532 (1981).

114. Scott, R.L., J. Chem. Phys. 25 193 (1956).

115. Scott, R.L., "Physical Chemistry, An Advanced Treatise" Ed. Henderson, D., Vol. 8A, (1971), Chapter 1.

116. Sengers, J.V.; Levelt Sengers, J.M.H., "Progress in Liquid Physics: Critical Phenomena in Classical Fluids" (1978), Chapter

117. Shim, J.; Kohn J.P., J.Chem. Eng. Data 7 3 (1962).

118. Smith, L.B.; Beattie, J.A.; Kay, W.C, J. Am. Chem. Soc. 59 1587 (1937).

119. Soave, G., Chem. Eng. Sci. 27 1197 (1972); 3rd Int. Chem. Eng. Conf., Portugal, April 20-24, (1981), pp.1.1-1.3.

120. Spencer, C.F.; Alder, S.B., J. Chem. Eng. Data 43 137 (1978).

121. Starling, K.E.; Lee, T.J.; Lee, L.L., ACS 187, American Chemical Society, Washington, D.C., (1979), Chapter 7.

122. Stryjek, R.; Chappelear, P.S.; Kobayashi, R., J. Chem. Eng. Data, 19 334 (1974).

123. Stryjek, R.; Chappelear, P.S.; Kobayashi, R., J. Chem. Eng. Data, 19 340 (1974).

124. Tarakad, R.R.; Spencer, C.F.; Adler, S.B., Ind. Eng. Chem. Process Des. Dev. 18 728 (1979).

125. Tasic, A.; Djordjevic, B.; Grozdonic, D., Chem. Eng. Sci. 33 189 (1978).

126. Technical Publication TP-4 "Low Temperature Data from Rice University for Vapor-Liquid and P-V-T Behavior" Gas Processing Association, Tulsa, Oklahoma, (1974).

127. Temperley, H.N.V.; Rowlinson, J.S.; Rushbrooke, G.S., "Physics of Simple Liquids" Interscience, New York, (1968).

128. Thiele, E.T., J. Chem. Phys. 39 474 (1963).

129. Tsonopoulos, C., AIChE J. 20 263 (1974).

131. Usdin, E.; McAuliffe, J.C., Chem. Eng. Sci. 31 1077 (1976).

132. Van Ness, H.C.; Abbott, M.M., "Classical Thermodynamics of Non Electrolyte Solutions" McGraw-Hill, New York, (1982), Chapter 4.

133. van der Waals, J.D., Doctoral Dissertation, Leiden, Holland (1873).

134. Vargaftik, N.B., "Tables on the Thermodynamical Properties of Liquids and Gases" 2nd Ed., Hemisphere Publishing Co., Washington, D.C., (1975).

135. Vera, J.H.; Prausnitz, J.M., Chem. Eng. J. 3 1 (1972).

136. Vidal, J.; Huron M.-J., Fluid Phase Equilibria, 3 255 (1979).

137. Vennix, A.J.; Leland, T.W. Jr.; Kobayashi, R., J. Chem. Eng. Data 15 238 (1970).

138. Wenzel, H.; Moorwood, R.A.S; Baumgartner, M., Fluid Phase Equilibria 9 225 (1982).

139. Whiting, W.B. and Prausnitz, J.M., Fluid Phase Equilibria, 9 119 (1982).

140. Wilson, G.M., J. Am.Chem. Soc., 86 127 (1964).

141. Won, K.W., Fluid Phase Equilibria, 10 191 (1983).

142. Wong, D.S.H.; Sandler, S.I.; Teja, A.S., Ind. Eng. Chem. Fundam. 23 38 (1984).

143. Young, S., Sci. Proc. Roy. Dublin Soc. 12 374 (1910).

144. Zudkevitch, D.,; Joffe, J., AIChE J. 16 112 (1970).